

NASA TECHNICAL
MEMORANDUM

NASA TM X-62,107

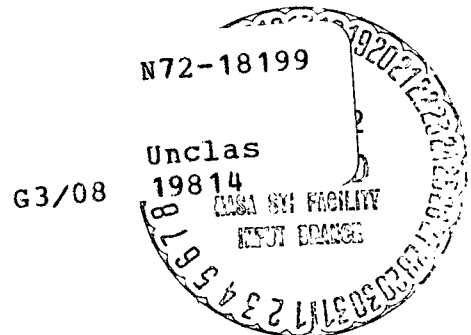
NASA TM X-62,107

DATA ACQUISITION SYSTEMS FOR OPERATIONAL EARTH
OBSERVATION MISSIONS

J. M. Deerwester, D. Alexander, R. D. Arno, L. E. Edsinger, S. M. Norman
K. F. Sinclair, E. L. Tindle, and R. D. Wood

Office of Aeronautics & Space Technology
Advanced Concepts & Missions Division
Moffett Field, California 94035

FACILITY FORM 602
(NASA-TM-X-62107) DATA ACQUISITION SYSTEM
FOR OPERATIONAL EARTH OBSERVATION MISSIONS
J. M. Deerwester, et al (NASA) Feb. 1972
253 p
CSCL 05B
(CATEGORY)



NATIONAL AERONAUTICS AND SPACE ADMINISTRATION
WASHINGTON, D. C. FEBRUARY 1972

SUMMARY AND CONCLUSIONS

This report identifies the data acquisition system capabilities expected to be available in the 1980 time period as part of operational Earth observation missions. By data acquisition system is meant the sensor platform (spacecraft or aircraft), the sensors themselves and the communication system. The acquisition system, together with the data handling system (not analyzed in detail here), would comprise the total observation system.

In addition to the projections of future operational capabilities this study has two other objectives. The first is to identify the technology efforts needed to bring the presumed capabilities for the most promising options to fruition. Second, it is hoped that the study of future operational capabilities together with the actual performance of the intervening development programs (ERTS, Skylab, and the Earth Resources Aircraft Program) can act as a catalyst to the iterative process that will eventually lead to the proper balance between capabilities and user requirements.

Future capabilities and support requirements are projected for the following sensors:

- Film Camera; on board processing per Lunar Orbiter.
- Return beam vidicon; of the type to be aboard ERTS A and B.
- Multispectral scanner; of the type to be aboard ERTS A; five bands in the visual through the near IR.
- Infrared scanner; one band in the thermal IR; also a sixth band of a multispectral scanner of the type to be aboard ERTS B.
- Infrared radiometer.
- Microwave scanner.
- Microwave radiometer.
- Coherent side-looking radar.
- Scatterometer.

Results of the study are presented for the most part in parametric form. For each sensor class, charts are shown that depict swath width and spatial resolution (and, as appropriate, temperature resolution) as functions of the sensor design parameters; projected technology boundaries are also shown. Companion charts of data acquisition rates and spacecraft weights are included.

In addition to these sensor-related results, parametric analyses were also conducted in the following areas:

Spacecraft Orbit Selection. A wide variety of orbit inclinations, eccentricities and altitudes were investigated. It is concluded that eccentric orbits offer no advantages for sensors that depend on proper solar illumination; the circular sun-synchronous orbit is the most desirable. For sensors that operate in the thermal IR or microwave portions of the spectrum, however, one particular eccentric orbit seems attractive, namely the stationary perigee orbit. At inclinations of 63 degrees and 117 degrees the location of perigee remains fixed in the orbit plane. Thus perigee can be located over any desired latitude (the continental United States, for example) and it will remain there indefinitely. The corresponding low altitude enhances the performance of this particular group of sensors.

Certain user needs may best be fulfilled by a very frequent (one day or less) coverage interval. Such frequencies can be readily attained from geosynchronous orbits. If the resolution capability is adequate from such an altitude, this orbit class will also be attractive.

Cloud cover effects. Cloud cover statistics have been assembled for all resource regions within the continental United States, Alaska and nearby waters. For each region, summary curves are shown that relate expected cumulative surface coverage to the actual and desired coverage frequency. These charts also

implicitly contain information concerning the effect of multiple satellites. It is concluded that for the United States as a whole, for instance, if at least 90 percent of the country is to be viewed during a given interval, up to four properly located satellites will be needed.

Aircraft coverage capabilities. The role of aircraft-borne sensor platforms as part of an operational Earth observation system would most likely be that of an adjunct, rather than as a competitor, to satellite-borne sensors. However, since the proper mix of aircraft and satellites cannot be specified at this time, the aircraft coverage analysis is predicated on coverage of the continental United States solely by aircraft. This study approach thus ensures the inclusion of data appropriate to the reduced coverage requirements of aircraft when used in conjunction with satellites.

Two distinct aircraft usage concepts were investigated. The first is the use of a special purpose fleet of aircraft to cover the resource areas of interest. The second is the use of commercial air carriers that already overfly much of the country. The results show that the flexibility of scheduling and logistics associated with a special fleet make it superior to the commercial air carriers in both coverage capability and number of planes (or payloads) required. For instance, twelve twin engine turbojets can adequately cover all resource areas investigated in the span of two weeks--only a fraction of the commercial airliners that would have to be equipped to obtain similar coverage. The use of a special fleet would also avoid the complexity of determining appropriate subsidies, obviate the need for FAA re-certification, and so forth.

Communications system. Communication system capabilities and limitations are defined in terms of real time data transmission, the contribution of onboard data storage, and the potential

benefits of advanced (millimeter wave and laser) systems. This investigation shows that several alternatives exist which provide a satisfactory means of telemetering the sensor data to the ground for processing. These range from improved ground capability, to the use of non real-time transmission modes, to the development of data relay satellites or advanced communications systems. Any particular approach to be followed in actual operations would be determined by the sensors employed on the data acquisition system and their corresponding data generation rates, coverage, and operational constraints.

In addition to the parametric analyses, the study also includes about 35 specific examples of spaceborne and airborne data acquisition systems. These were arrived at by employing user requirements established in prior studies as design goals for the data acquisition systems. Since it was suggested earlier than an iteration between requirements and capabilities is essential, one might infer that the requirements documented to date (including those used in this study) do not necessarily reflect the real needs of the user community; this inference is correct. Nevertheless, they represent the best information at our disposal and, through the example acquisition systems, do provide a focus for the more promising systems and their associated technology requirements. Based, then, on the sample acquisition systems thus defined, certain other conclusions evolve:

- Not all of the user requirements (or, more precisely, requirements as we understand them) can be met by 1980. Nevertheless, a rather advanced level of acquisition system performance could be achieved by that time period.
- Aircraft or satellites will be limited because of weight to one primary sensor, plus perhaps the small lightweight radiometers, unless the largest launch vehicles (Titan III D/SCS or shuttle) are employed. This is not to imply, however, that a multipurpose satellite design compatible with various sensors would not be desirable.

- Many technology requirements exist in the realm of sensors and communications systems. Ultimately, of course, it will be the judgment of those responsible for the technology developments per se that will dictate those to be pursued. But this study has uncovered certain critical technologies (i.e., essential for the sensor to possess the capabilities and/or support requirements ascribed it here) that should be mentioned. These critical technologies are listed below:

Film Camera. Thin base film anti-ferrotyping; laser communications system.

RBV. Larger format and more lines/mm.

Scanning Devices. Lightweight mirror technology; larger detector arrays; long life, lightweight, low temperature IR cooling systems.

Microwave Sensors. Large, lightweight, high tolerance antennas.

Spectral resolution and coverage capabilities are not included in this study primarily because the associated requirements are even more nebulous than those associated with spatial resolution and coverage. Consideration of this added dimension would, however, likely add to this list of critical technologies.

To conclude this summary on a less ambiguous note, it is our judgment that an operational system will require spatial resolution better than that which can be achieved from ERTS. Because of the wide-spread feeling that multispectral data will yield information of great utility to large segments of the user community, it seems apparent that furtherance of the scanner technologies mentioned above will prove to be most fruitful. But as contingency against the possibility that unambiguous multispectral signature analysis will not be realized, a portion of the available resources should be devoted toward the appropriate film camera technologies.

CONTENTS

	Page
SUMMARY AND CONCLUSIONS	i
INTRODUCTION	1
ORBIT ANALYSIS	7
LAUNCH VEHICLE CAPABILITIES	31
AIRCRAFT COVERAGE AND PERFORMANCE	41
SIGNIFICANCE OF CLOUD COVER	63
SENSOR CAPABILITIES	69
SENSOR SUPPORT REQUIREMENTS	117
COMMUNICATIONS SYSTEMS ANALYSIS	143
REPRESENTATIVE ACQUISITION SYSTEMS	167
DATA HANDLING	189
TECHNOLOGY IMPLICATIONS	197
APPENDIX A - INTEGER ORBITS	203
APPENDIX B - CLOUD COVER DISTRIBUTION	205
APPENDIX C - GENERALIZED USER REQUIREMENTS	211
APPENDIX D - METRIC ACCURACY REQUIREMENTS	215
APPENDIX E - RADIATION SHIELDING CONSIDERATIONS FOR FILM	217
APPENDIX F - MODULATION TRANSFER FUNCTION ANALYSIS FOR FILM CAMERA AND TELEVISION	223
APPENDIX G - MULTISPECTRAL SCANNER SIGNAL AND NOISE CONSIDERATIONS	225
APPENDIX H - IR SCANNER/RADIOMETER SIGNAL AND NOISE CONSIDERATIONS	227
APPENDIX I - THERMAL IR CAPABILITY FOR MSS	229
APPENDIX J - FILM CAMERA AND TELEVISION EXPOSURE AND IMAGE MOTION CONSIDERATIONS	231
REFERENCES	235

LIST OF ILLUSTRATIONS

Figure		Page
2-1	Effect of Latitude on Swath Width Requirements	12
2-2	Effect of Swath Width on Coverage Interval	12
2-3	Swath Width Requirements for Incomplete Coverage at 40 Degree Latitude	14
	(a) 50 Degree Inclination	
	(b) 64 and 116 Degree Inclination	
	(c) 97 Degree Inclination	
2-4	Effect of Coverage Interval on Semi-Major Axis	15
2-5	Minimum Altitudes for One Year Satellite Lifetime	17
2-6	Ground Trace for Orbit No. 2	19
2-7	Ground Trace for Orbit No. 3	19
2-8	Characteristics of Orbit No. 5	21
	(a) Solar Elevation Angle; 1 Satellite	
	(b) Solar Elevation Angle; 2 Satellites	
	(c) Altitude Variation	
	(d) Perigee Location and Lighting Conditions	
2-9	Characteristics of Orbit No. 6	23
	(a) Solar Elevation Angle; 1 Satellite	
	(b) Solar Elevation Angle; 2 Satellites	
2-10	Characteristics of Orbit No. 9	25
	(a) Solar Elevation Angle at Noon	
	(b) Altitude Variation at 40 Degree N. Latitude	
	(c) Perigee Location & Lighting Conditions	
2-11	Drag Make-up Requirements for Orbit No. 10	27

Figure		Page
2-12	Characteristics of Orbit No. 11	27
	(a) Solar Elevation Angle; 1 Satellite	
	(b) Solar Elevation Angle; 2 Satellites	
2-13	Errors in Orbit Plane Orientation Due to Variations in Insertion Parameters	28
4-1	Swath Width and Aircraft Altitude Relationship for 90 Degree Field of View	42
4-2	Resource Areas and Possible Base Locations	44
4-3	Distance Between Bases and Maximum Aircraft Range Required	46
4-4	Relationship Between Coverage Efficiency and Flight Flexibility	48
4-5	Coverage Efficiency as Affected by Number of Bases (Cloud Free)	48
4-6	Coverage Efficiency as Affected by Number of Bases (With Cloud Cover)	48
4-7	Aircraft Required as Affected by Number of Bases	48
4-8	Observation Schedule for Selected Earth Resources	50
4-9	Resource Area Coverage Rate	50
4-10	Aircraft Coverage Geometry	52
4-11	Special Fleet Aircraft Required	52
4-12	Effective Swath Width Covered from Mean High Altitude Jet Airways and Corresponding Resource Coverage	56
4-13	Probability of Covering Various Numbers of Air Route Legs	58
4-14	Fractional Coverage of Random Area	61
4-15	Contribution of Directed Air Routes	61
4-16	Expected Coverage of Resource Areas from Commercial Air Carriers	61

Figure		Page
5-1	Observation Coverage as Influenced by Cloud Cover	66
	(a) Continental United States	
	(b) Alaska	
	(c) Mineral Resources	
	(d) Iceberg	
6-1	Measured MTF of Typical Camera Lens for a Heterochromatic Source	76
6-2	Flying Spot Scanner Performance	79
	(a) Modulation Transfer	
	(b) Required Spot Size	
6-3	Film Modulation Transfer Function	79
6-4	Film System Geometry	81
6-5	Film Camera System Swath Width	81
6-6	Film Camera System Spatial Resolution	83
6-7	Sine Wave Modulation Transfer Functions of Television Camera Components	85
6-8	4.5" RBV Modulation Transfer Function (Without Lens)	85
6-9	RBV Spatial Resolution	88
6-10	Multispectral Scanner for ERTS	91
6-11	Spectral Response of Photomultipliers	91
6-12	Effect of Dwell Time on the Performance of Multispectral and Infrared Scanners	94
6-13	Infrared Specific Detectivities	96
6-14	Infrared Radiometer Swath Width	98
6-15	Effects of Dwell Time on the Performance of Infrared Scanners and Radiometers	98
6-16	Maximum Antenna Size for Microwave Systems	101

Figure		Page
6-17	Attainable Angular Resolution for Parabolic Antennas	101
6-18	Limiting Aperture Size for Parabolic and Linear Antennas	101
6-19	Amplifier Noise Temperature	103
6-20	Atmospheric Attenuation in the Microwave and Millimeter Spectrum	103
6-21	Temperature Resolution of Microwave Scanners and Radiometers	105
6-22	Microwave Scanner and Radiometer Spatial Resolution	105
6-23	Effect of Dwell Time on the Performance of Microwave Scanners	107
6-24	Radar System Noise	110
6-25	Focused Synthetic Aperture Radar Geometry	110
6-26	Coherent Side Looking Radar Swath Width	113
6-27	Scatterometer Geometry	113
7-1	Image Motion Geometry	118
7-2	9.5" Film System Weight with IMC and Processing (No Shielding)	123
7-3	Radiation Shield Weight for 9.5" Film Magazine	125
7-4	TV Tube Lengths	127
7-5	4.5" Vidicon System Weight (With IMC)	129
7-6	Cassegranian Telescope Weight	132
7-7	Antenna Weights for Active and Passive Microwave Systems	135
7-8	Radar Total Input Power	138
7-9	Radar Transmitter Weight	140
8-1	Nominal Station Coverage for Data Acquisition System Altitude of 590 km	144

Figure		Page
8-2	Data Link Performance and Limitations	149
8-3	Data Acquisition Rate Over U. S. with Constant 50 Mbps Telemetry Rate Throughout Orbit	153
8-4	Effects of Ground Station Access Time on Transmitter Power	160
9-1	Film Camera Characteristics	180
	(a) Coverage Summary	
	(b) Data Production	
	(c) Satellite Weight	
9-2	Return Beam Vidicon Characteristics	181
	(a) Capability Summary	
	(b) Data Production	
	(c) Satellite Weight	
9-3	Multispectral Scanner Characteristics (5 Channels)	182
	(a) Capability Summary	
	(b) Data Production	
	(c) Satellite Weight	
9-4	Infrared Scanner Characteristics	183
	(a) Capability Summary	
	(b) Data Production	
	(c) Satellite Weight	
9-5	Infrared Radiometer Characteristics	184
	(a) Capability Summary	
	(b) Data Production	
	(c) Satellite Weight	
9-6	Microwave Scanner Characteristics	185

Figure		Page
	(a) Capability Summary	185
	(b) Data Production	
	(c) Satellite Weight	
9-7	Microwave Radiometer Characteristics	186
	(a) Capability Summary	
	(b) Data Production	
	(c) Satellite Weight	
9-8	Coherent Side-Looking Radar Characteristics	187
	(a) Capability Summary	
	(b) Data Production	
	(c) Satellite Weight	
9-9	Scatterometer Characteristics	188
	(a) Capability Summary	
	(b) Data Production	
	(c) Satellite Weight	
10-1	Basic Information Diffusion Model	192
B-1	Global Cloud Cover Regions	209
B-2	Ten Degree Latitude/Longitude Regions	209
E-1	Trapped Radiation Dose	218
E-2	Radiation Shield Effectiveness	218
E-3	Solar Proton Dose in Earth Orbit	220
E-4	Total Radiation Dosage	220

LIST OF TABLES

Table		Page
2-1	Orbit Characteristics	11
2-2	Minimum Orbit Altitudes for Two Year Lifetime	16
3-1	Launch Vehicle Performance Summary	32
3-2	Representative Shuttle Payload Capabilities	39
4-1	Possible Groups of Air Bases	45
4-2	Selected Earth Resource Characteristics	49
4-3	Candidate Earth Resource Aircraft Characteristics	53
4-4	Domestic Trunkline Traffic (1968)	55
4-5	Airline and Air Traffic Characteristics	57
5-1	Average Annual Cloud Cover	65
6-1	Projected Technology Limits	70
8-1	Downlink Telemetry Power Budget at S-Band, Altitude 590 km	146
8-2	MSFN Comparative Telemetry Performance	147
8-3	Summary of Maximum Data Rate Capability for Various Communications Systems	147
8-4	Communications Parameters for Representative Orbits	152
8-5	Maximum Sensor Rate for 50 Mbps Telemetry Through a Data Relay Satellite	152
8-6	Possible Bands for High Data Rate Telemetry	155
8-7	Acquisition System RF Power for 1 Gbps Through Relay Satellite	156
8-8	Power Budget for 1 Gbps Spacecraft-to-Ground Telemetry at 35 GHz	157
8-9	Comparison of Direct Transmission Modes for a Data Rate of 1 Gbps	158

Table		Page
8-10	Laser Direct Link Power Budget	163
8-11	Laser Relay Link Power Budget	165
9-1	Normalized Error Functions	175
9-2	Representative Satellite Borne Acquisition Systems	177
9-3	Representative Aircraft Borne Acquisition Systems	179
B-1	Resource Distribution (% Total Area by Global Cloud Region)	206
B-2	Resource Distribution (% Total Area by Aircraft 10° Latitude/Longitude Sectors)	207
B-3	Continental United States Cloud Cover Statistics	208
C-1	User Requirement Summary	212
D-1	Map Accuracy Requirements	216

1. INTRODUCTION

In the past, most studies that dealt with Earth observations had as their objective an identification of the requirements of the user community and, in some cases, estimates of the benefits that would accrue if such requirements could be met. This study concentrates instead on the other aspect of Earth observations, namely the logistic and technological capabilities. However, in order to ensure that the study is undertaken in the proper context, this introduction is expanded to include a brief discussion of the important user requirement parameters that must be considered when examining system capabilities.

Purpose and Scope

A consequence of focusing past attention on requirements is that there is now a paucity of data concerning operational capabilities of space-borne and air-borne observation systems. To help fill this void was the original purpose of this study. As the study progressed, and also as additional discussions were held with individuals who have had a continuing association with Earth survey missions in general, a potentially more important reason for a study such as this has emerged. And this has to do with using projected operational capabilities as a catalyst to an iterative process that will hopefully result in a better approximation of the performance acceptable to the users. The feeling in various quarters is that not all of the requirements set forth thus far represent the needs of the user community that will ultimately emerge from the compromises between perceived requirements and evolving capabilities. To the extent this feeling is warranted it has important consequences, particularly in those cases in which the stated requirements are of minor importance to the user but which nevertheless impose stringent technological or operational demands on the acquisition system. The thought has emerged, then, that perhaps requirements (acceptable performance) can only realistically be defined in light of actual capabilities. Initially these capabilities might be simply as projected by a study such as this, but ultimately, as some have suggested, meaningful statements of requirements may have to await a demonstrated pre-operational capability.

With the foregoing as a prelude the objectives of this study can therefore be summarized as follows:

- (1) postulate future operational capabilities for Earth observation data acquisition systems;
- (2) identify critical technology items;
- (3) in so doing, provide the impetus for an iteration between requirements and capabilities.

Capabilities are expressed in this report in terms of spatial and temperature resolutions, swath width and frequency of coverage. In some cases the capabilities are constrained by communication system limitations; in other cases by launch vehicle performance capabilities; and in still others, of course, by projected sensor technologies themselves. A broad range of sensor classes is investigated, from the small light-weight radiometers, through film cameras and multispectral scanners to coherent side-looking radars.

As used in this study an "acquisition system" consists of the sensor(s); the subsystems necessary to provide functional support for the sensor; a communication system including, as appropriate, data relay satellites; and, of course, the carrier vehicle itself. This latter category includes both satellites and aircraft.

Specifically not analyzed in detail is the ground data reduction, analysis and distribution system. This aspect of the total system was not considered in detail primarily because of time and manpower limitations - certainly not because it is of secondary importance. (One could argue, of course, that a study of the ground data handling system conducted before the ranges of data rates and the information content associated with operational acquisitions are established would be premature.) Certain data handling system concepts, however, are discussed later in the report. This discussion, together with the results of the main effort, could form the basis of a separate study that addresses this nebulous, but vitally important, question of how data becomes information.

The time period assumed in this study for the operational Earth observation program is between the late 1970s and early 1980s; the technology projections are made accordingly. It would seem likely that

even during this operational phase, developmental missions for even more advanced systems would be carried out but these are not considered here.

A final comment, dealing with intervening development programs between now and the late 1970's, is necessary to properly introduce this report. In brief, it is assumed without exception that such programs will affirm the feasibility of obtaining and handling data in a manner consistent with useful Earth resources surveys. For instance it is assumed (not unreasonably) that the ERTS satellites will function more or less as intended and that the experience gained in handling ERTS data will point the way toward promising techniques for handling the larger amount of data that will emanate from operational systems. Several other examples of good outcomes from the development programs could be cited but one more will hopefully make the point that needs to be made: Aircraft test flights of a 24 channel multispectral scanner will soon begin. The question here is not whether the resolution expected in each spectral region will be realized. Rather, the important questions are (1) will the art of multispectral signature analysis be advanced to the point where useful information can be extracted from the data by (or for) the agricultural/forestry community and (2) will the results of the test program enable us to build scanners having far fewer channels and that yet provide unambiguous signatures. We assume affirmative answers in each case.

These kinds of assumptions are a necessary foundation for the analysis carried out in this type of study.

User Requirement Considerations

The results contained herein are predominately in parametric form and are independent of user requirements. Specific examples of data acquisition systems were extracted from the parametric results, however, and were arrived at by considering the requirements as we understand them. Where it is of importance, only the requirements associated with terrain observations of the continental United States, Alaska and nearby waters are included. Again, the primary reason for this restriction was the manpower limitations.

User requirements are originally formulated in terms of data needed, but subsequently must be transformed into system operational or performance

requirements. These are generally specified in terms of spectral resolution and coverage, spatial resolution and coverage, and area coverage frequency. With all observation systems (aircraft, satellite, or whatever), resolution, area coverage, and frequency of coverage are all interrelated, and in some cases impose very demanding constraints. Care must be exercised in attempting to satisfy such constraints, particularly over an extended period of time (assumed in this study to be one year), for such simultaneous diverse constraints can result in the unwitting specification of requirements that are inordinately severe and in some cases even physically impossible to meet. For example, it is impossible to obtain solar elevation angles greater than 50 deg in Alaska due to its high latitude, and values this high occur only during the summer.

Discussed below are some of the operational parameters which, in addition to the sensor design parameters, are important considerations in the specification of an Earth observation system. As a first illustration a situation can be envisioned in which it may be possible to simultaneously meet some specified coverage frequency and resolution but only by employing such a narrow field of view (swath width) that incomplete surface coverage exists after the coverage interval. If a further requirement of 100 percent coverage is imposed then the only recourse is multiple satellites (or additional aircraft).

The sensor platform altitude is an important operational parameter since it affects resolution and swath width (the width of the area that can be viewed at any one time). The higher the platform the more area that can be viewed but with a corresponding decrease in resolution. Resolution can theoretically be regained by reducing the field of view, but all things being equal, it is not the best approach since higher altitudes require more sophisticated sensors, better stabilization, and more energy to achieve the higher position. All things are, of course, not equal. Reducing the altitude necessitates smaller swath widths and, in the case of satellites, shorter times over the data readout centers, and if low enough, orbit perturbations due to atmospheric drag.

Although aircraft offer high resolution from their relatively low altitudes their swath width restrictions are quite severe, being limited to a side view of about 45 deg from the nadir since this angle yields about the maximum tolerable resolution deterioration and spatial distortion. From satellites orthogonality is rarely a consideration since most of the viewing is of features essentially directly below. Equatorial orbits are an exception, however, since the United States is centered at about 40 deg N. latitude.

Perhaps the most stringent constraints come from lighting requirements (or solar elevation angles) since most of the viewing, at least for visible and near IR observations, should be made with the sun no lower than 30 deg above the horizon--a condition which exists only eight hours per day. Furthermore certain requirements may dictate that not only must the observations be made during daylight but that they be made at a constant local time. This further restricts the choice of orbits for satellites and limits the utility of aircraft.

Obviously no single observation system can satisfy all operating constraints. The analysis of these constraints (and the attendant limitations on physical capabilities), as presented in this report, is intended as a guide for the future specification of operational criteria. This is so that the unintentional specification of operational inconsistencies can be avoided and the resultant technological requirements will be stated as realistically as possible.

2. ORBIT ANALYSIS

The process of orbit selection for an Earth observation satellite consists of attempting to obtain the desired viewing conditions on the surface while satisfying the operational limitations imposed by orbital dynamics. The orbit analysis presented here attempts to clarify these limitations; it is not intended to relate user requirements to sensor capabilities from differing orbits. Instead, this section considers only the effects of different orbits on the various user defined parameters and is specifically intended to help those readers not familiar with orbit mechanics understand orbit imposed constraints. Included are analyses of eccentric orbits and multiple satellites, as are the effects of atmospheric drag on the orbit selection process. The section concludes with a discussion of some long term effects of orbit insertion errors.

Integer Orbits

The general class of orbits considered are those which have (approximately) an integral number of revolutions per day*. Since it is desirable to obtain complete coverage of the Earth's surface, the orbits are defined so that the drift, or distance, between adjacent orbit traces covers the Earth's surface in a contiguous manner. The Earth's oblateness which causes this drift can be used to advantage in order to obtain complete surface coverage. The apparent daily drift of the orbit trace (or, equivalently, regression of the node) can be selected so as to nearly compensate for the Earth's daily rotation. Therefore these orbits have approximately an integral number of revolutions per day. It is important to understand that at a specified latitude the first orbit of each day is displaced from the first orbit of the previous day by a constant distance. If 100 percent coverage is to be achieved, this distance (the ground trace distance) must be smaller than the swath width capability of the sensor; if the swath width is too small, complete coverage can never be obtained.

In the discussion that follows, the number of orbits per day is denoted by N while the number of days until the ground track would be repeated is denoted by T . Note that T defines the coverage interval so

* A more complete discussion of integer orbits can be found in Appendix A and Ref. 1.

that any particular surface area will be covered twice in T days, once from the north to south pass and once from the south to north pass.

It may appear that the definition of T is ambiguous because of the double coverage after T days. But such a definition is necessary since T is the minimum time for complete surface coverage. The orbit traces on the north to south passes will leave gaps in the coverage for any time less than T days; similarly for the south to north passes. These gaps do not totally complement each other since the orbit traces criss cross and hence leave diamond shaped gaps in any time less than T days.

Special Cases of Integer Orbits

Two special cases are discussed. The first case is the class of sun synchronous orbits. These orbits result in optimum lighting conditions. The second case is the class of stationary perigee orbits. These orbits result in minimum altitudes above the area to be observed.

Sun Synchronous Orbits - The sun synchronous orbits require a balance between the regression of the node and the apparent solar motion due to the Earth's movement about the sun. The Earth's orbital motion is about 1 deg. per day and the regression of the node (in radians per day) is given by

$$-3 \pi N \frac{J_2 R^2}{a^2 (1-e^2)} \cos I$$

where R is the Earth's radius, $J_2 = 0.001082$, a is the semi major axis, e is eccentricity, I is inclination, and N is the number of orbits per day. For the values of a and e considered here the inclinations for the sun synchronous orbit are about 97 deg. It should be emphasized that the solar elevation angle is not constant throughout the year nor throughout the orbit; instead the spacecraft will always pass over the same latitude on the Earth's surface at the same local time. Due to the tilt of the Earth's axis it is not possible to obtain constant solar elevation angles.

Stationary Perigee Orbits - The stationary perigee orbit is important since, in general, perigee can precess as much as 180 deg. in one year. Therefore, for eccentric orbits, the variation in altitude over a particular observation area could be significant.

The Magnitude of this precession of perigee (in radians per day) is given by

$$+3 \pi N \frac{J_2 R^2}{a^2 (1-e^2)^2} (2 - 5/2 \sin^2 I)$$

For the critical inclinations of 63.4 deg. and 116.6 deg. the precession rate is identically zero and perigee is stationary above a specified latitude. For other values of I perigee may either advance or regress in the orbit plane. As will be illustrated later, for any given inclination, the change in latitude of perigee can be either northerly or southerly depending on the initial location of perigee.

General Considerations

The time of day for the launch is an important parameter since the local sunlight conditions (or equivalently time of day) at launch define the pattern of lighting for the entire year after launch. For example in the sun synchronous case a launch at local noon will place the sun at its maximum possible elevation, i.e. Earth-Sun line will remain in the orbit plane. A launch six hours later, however, will yield minimum solar elevation angles since the Earth will have rotated 90 deg. and all orbit traces will lie approximately along the terminator. It should be noted that a midnight launch will also yield maximum elevation angles but they will occur on the other side of the Earth from the launch point.

For the analysis of all orbits considered here the launch time of day was assumed to occur so that the best sunlight conditions over the United States would occur during the summer months since the preponderance of applications require observations during that time of year. Obviously, the effect of missing this optimum launch time (the daily launch window) would be significant. However, such effects were not studied in detail since this would involve an analysis of factors that might cause launch delays and is outside the scope of this study.

The time of year of the launch also affects the observational capability. A launch date in the late summer, for example, would not allow sufficient time to obtain data pertaining to crops. Therefore this study is predicated on a launch which is early enough in the year to obtain sufficient summer coverage. A March 21 launch was assumed and,

as indicated above, the orbit was oriented to obtain optimum sunlight conditions and, for eccentric orbits, low altitudes over the United States.

Selection of Orbit Parameters

In total, eleven specific orbit classes have been investigated and their important parameters are summarized in Table 2-1. Most of the orbits are special cases as discussed previously; however examples of other orbits are also included. A detailed discussion of each orbit class follows later but first some preliminary remarks concerning possible variations in orbit parameters is warranted. Many of the orbit parameters in Table 2-1 are independent and could be given an infinite number of numerically different values. To limit the data it is thus necessary to determine which orbit parameters have the most significant effect on the system capabilities.

First, it is obvious that the required swath width is an important parameter. This requirement is, of course, greatest at the equator where the orbit traces are furthest apart. Figure 2-1 illustrates the decrease in swath required for increasing latitudes. Since the United States is approximately centered about 40 deg. N. latitude, the required swath width is measured at this latitude. As illustrated in the figure, however, the requirement will decrease for higher latitudes, particularly those which include Alaska (about 65 deg.) Figure 2-1 is based on an eccentric sun synchronous orbit with a perigee altitude of 285 km. The results for other orbit eccentricities are essentially identical. It should be noted that for a given latitude the lower inclination orbits will result in smaller swath width requirements.

Figure 2-2 shows the required swath at 40 deg N latitude as a function of T for the various orbits. Figure 2-2 is appropriate for all eccentricities of interest ($e < 0.05$). Note that the effects of inclination, however, are quite pronounced; for a given swath width the time required for total coverage from a sun synchronous orbit is about double that of a 50 deg. inclined orbit.

Table 2-1 Orbit Characteristics

Orbit Code	Incl. (deg)	No. Orbits Per Day	Time to Cover (days)	Perigee Altitude (km)	Apogee Altitude (km)	Semi-Major Axis (km)	Eccentricity	Period (hours)	Apse Rate (deg/day)	Nodal Regression Rate (deg/day)	Solar Drift Rate (deg/day)	Swath Width Required at 40° (km)
1	0	1	--	35,800	35,800	42,107	0.	23.93	--	0.0	--	--
2	50	1	--	35,800	35,800	42,107	0.	23.93	--	0.0	--	--
3	50	1	--	6,380	65,100	42,107	.7	23.93	0.	-0.03	--	--
4	50	15	13	520	520	6,880	0.	1.58	--	-4.66	5.65	91
5	50	15	13	400	1,000	6,888	.03	1.58	.56	-4.67	5.66	91
6	63.4	15	13	380	692	6,903	.04	1.62	0.	-3.34	4.33	127
7	97.6	14	13	920	920	7,282	0.	1.72	--	-0.99	0.	167
8	97.6	15	13	587	587	6,954	0.	1.61	--	-0.99	0.	156
9	97.6	15	13	345	829	6,954	.04	1.61	-.54	-0.99	0.	156
10*	97.6	16	13	148	445	6,662	.02	1.51	-.63	-0.99	0.	147
11	116.6	15	13	330	910	6,987	.05	1.72	0.	-3.27	-2.28	129

* Drag makeup required

Figure 2-1 Effect of Latitude on Swath Width Requirements

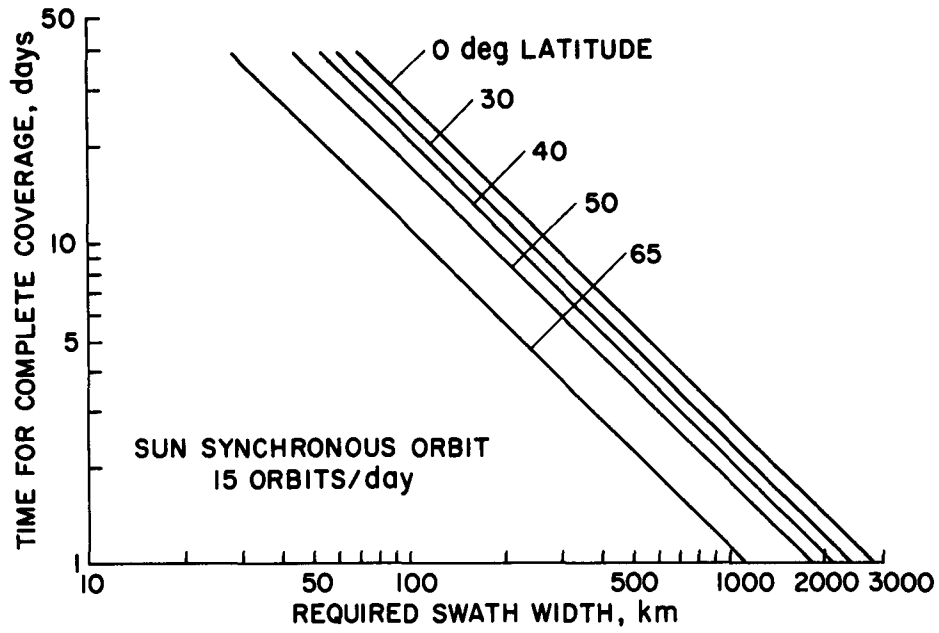
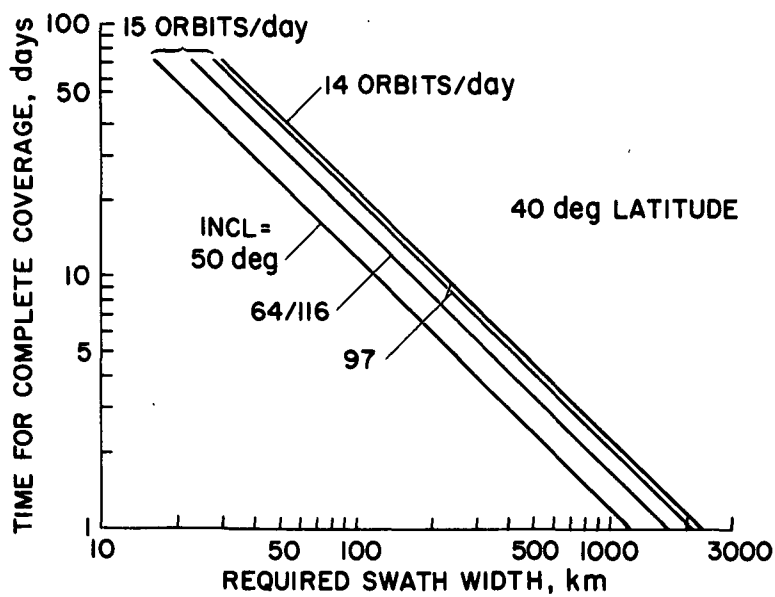


Figure 2-2 Effect of Swath Width on Coverage Interval



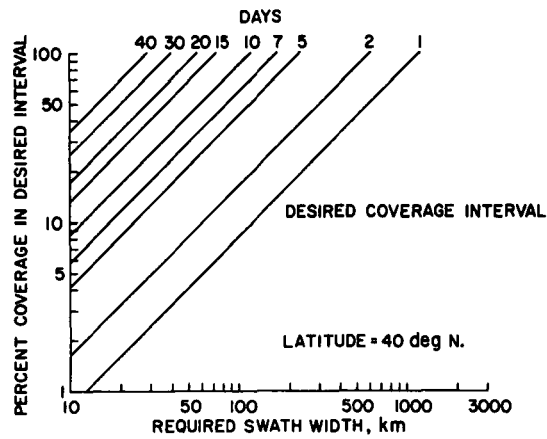
For some applications, incomplete coverage may be tolerable. For others complete coverage may be desired but the large swath width required may degrade the spatial resolution to unacceptable values. Data appropriate to such situations are shown in Figure 2-3 which indicate, for a given swath width capability of the sensor and a desired coverage interval, the percentage of the area that will in fact be observed during the desired interval.

T has been shown to strongly affect the required swath width. But an examination of the actual orbits reveals that T does not materially affect the orbital parameters. The effect of T on the semi-major axis is shown in Figure 2-4 for two orbit inclinations. Note that the value of the semi-major axis tends to asymptotically approach a fixed value as T is increased above about 1 week. Therefore, it is possible to select a particular value of T with the full assurance that although it would be happenstance if the selected value were appropriate for an actual mission, the results of the orbit analysis will be appropriate for a wide range of T; T = 13 was selected as representative for all I and N. It is for this reason that throughout the remainder of this report all orbits are referred to only by the code numbers of Table 2-1; it is unnecessary to belabor the point that actual altitudes will vary by a few kilometers as the coverage interval changes.

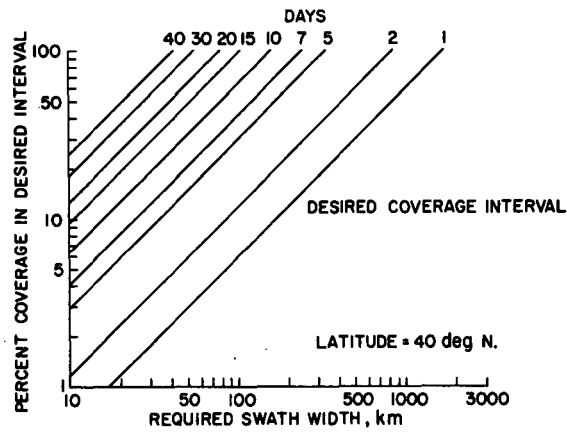
In a similar manner the eccentricity approaches an asymptotic value as T is increased for elliptical orbits. This is not illustrated, however, since the eccentricities are essentially constant for values of T greater than about 5 days. In fact, the values of eccentricities are so small that the effect on orbital parameters, other than altitude, is negligible.

The final consideration relevant to orbit selection concerns the effects of atmospheric drag on the minimum acceptable altitude. In order to rigorously determine the orbits that are compatible with a one year lifetime, it is necessary to have at hand the actual ballistic parameter and this, of course, is known with certainty only after a specific spacecraft configuration has been established. By making certain assumptions, it is possible, however, to determine the compatible orbits, and by conservatively selecting altitudes somewhat higher than the computed values, to assure with reasonable certainty that lifetimes of at least

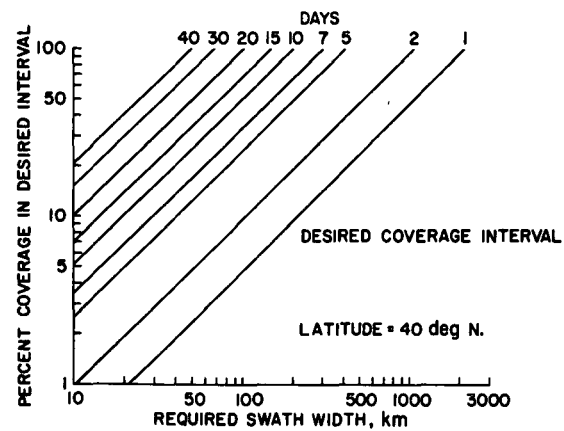
Figure 2-3 Swath Width Requirements for Incomplete Coverage at 40 Degree Latitude



a. 50 Degree Inclination

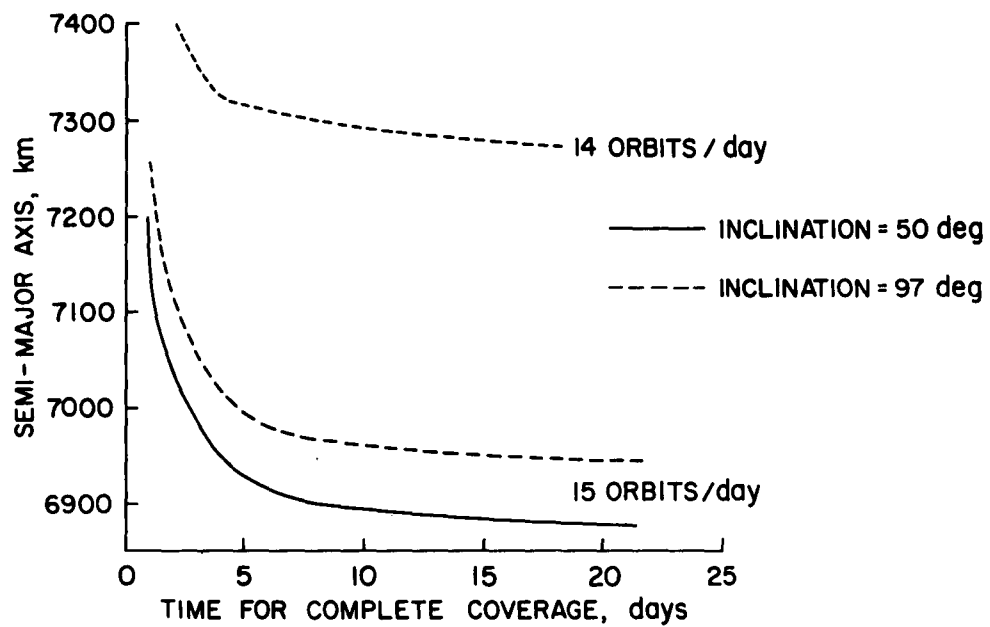


b. 64 and 116 Degree Inclination



c. 97 Degree Inclination

Figure 2-4 Effect of Coverage Interval on Semi-Major Axis



one year can be achieved for all satellites appropriate to the Earth observations missions.

The assumption is made that the spacecraft has no drag makeup system and a power requirement of 500 watts requiring a sun-oriented solar array of 14 m². The end-on cross sectional area of the spacecraft is assumed to be 1.8 m² and the drag coefficient for the spacecraft is taken as 2. The array drag coefficient, averaged over one orbit and referenced to the total surface area is, from Ref. 3.

$$\bar{C}_D = \frac{1}{\pi} \int_0^\pi (0.1 + 1.9 \sin \alpha) d\alpha = 1.31$$

where α is the angle of attack.

The total effective ballistic parameter is subsequently found to be 0.045 W (kg/m²) where W is the spacecraft weight.

With the ballistic parameter thus determined, orbits that satisfy the one year lifetime requirement can be found from the data of Ref. 3. Figure 2-5 shows some possible orbits for several values of satellite weight. For comparative purposes the circular orbit altitudes required for a 2 year lifetime are listed below in Table 2-2.

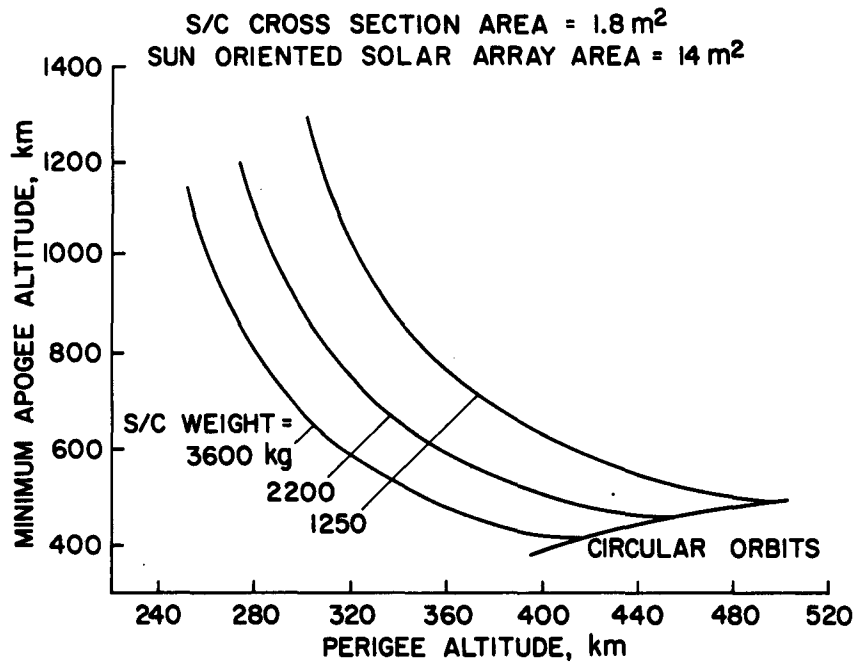
Table 2-2
Minimum Orbit Altitudes for Two Year Lifetime

<u>Spacecraft Weight (kg)</u>	<u>Circular Orbit Altitude (km)</u>
1250	537
2200	496
3600	463

Orbit Descriptions

Specific characteristics of the orbits shown earlier in Table 2-1 are summarized in the following paragraphs. These characteristics include information regarding ground coverage, solar elevation angle, altitude variations for eccentric orbits and the location and lighting conditions at perigee.

Figure 2-5 Minimum Altitudes for One Year Satellite Lifetime



Orbit No. 1

The geostationary (or 24 hour period) orbit is included here since it alone offers the possibility of continuous coverage. While the need for continuous coverage itself is questionable, this capability can be used to yield the coverage intervals of one or two days that may be required for certain applications. The swath area capability of the sensor can readily be chosen to encompass at least the continental United States. The price paid for these capabilities, of course, is degraded spatial resolution compared to the lower altitude orbits, and none of the viewing is vertical. The geostationary orbit is also one of the most demanding missions from the standpoint of launch vehicle energy.

Orbit No. 2

The 50 deg. inclined 24 hour orbit is included because, although it does not yield continuous U.S. coverage, it does permit daily coverage and a sizeable increase in the payload capability for a given launch vehicle over orbit no. 1. Figure 2-6 shows the northern hemisphere ground trace for this orbit, the trace in the southern hemisphere being a mirror image. It is seen that a near-vertical viewing angle of the continental United States is available for about 4 hours each day.

Orbit No. 3

This is the final 24-hour period orbit investigated. This is a highly eccentric orbit allowing a further increase in payload over orbit no. 2. The orbit parameters were selected so that the spacecraft would not penetrate the outer Van Allen belts too deeply at perigee. The ground trace of this orbit is shown in Figure 2-7. The wide variation in satellite velocity together with the Earth's surface velocity results in the teardrop shaped trace. Note that although a one day coverage interval of the continental United States from "low" altitude is possible, the time over the United States is only about 15 minutes.

Orbit No. 4

Because of launch azimuth restrictions the orbit inclination of 50 deg. represents the maximum attainable from Cape Kennedy without recourse to a dog leg maneuver. Such an inclination permits coverage of the continental United States but not of Alaska. This being a circular orbit,

Figure 2-6 Ground Trace for Orbit No. 2

50 deg CIRCULAR ORBIT
PERIOD = 23.93 hr

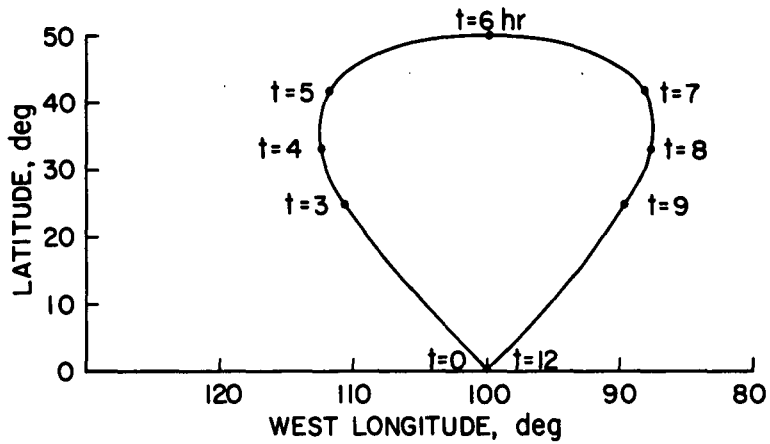
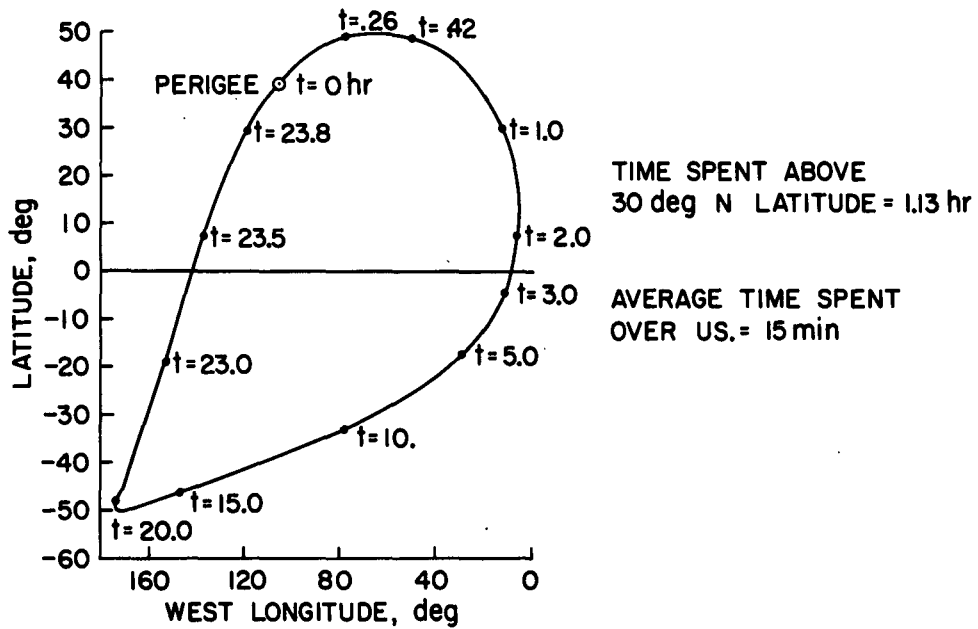


Figure 2-7 Ground Trace for Orbit No. 3

INCLINATION = 50 deg
PERIGEE ALT = 6380 km
PERIOD = 23.93 hr



it is but a special case of Orbit No. 5 and, because eccentricities of interest are quite low, the description that follows is also relevant to this orbit--with the obvious exception that the altitude is constant.

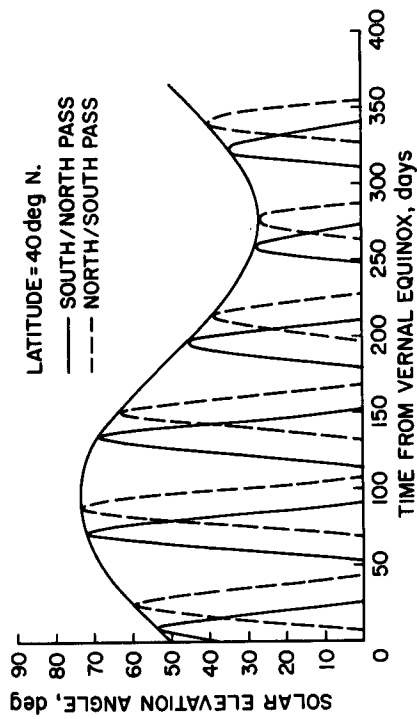
Orbit No. 5

Figure 2-8 illustrates the coverage capabilities of this orbit. The variation in solar elevation angle throughout the year is shown in Figure 2-8a, based on a launch date arbitrarily selected as March 21, or equivalently the date of the Vernal Equinox. It should be noted that a different launch date will yield significantly different lighting patterns and it is not correct to assume, for example, that a launch 30 days after March 21 would result in the same solar elevation angles shown in Figure 2-8a with a 30 day displacement. Inherent in the variation is the nodal regression, affecting the orientation of the orbit plane with respect to the sun and, hence, the solar elevation angle. The general conclusions are, however, applicable regardless of launch date.

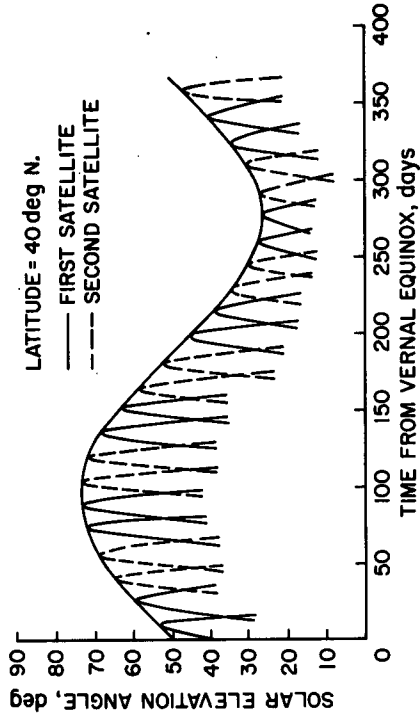
The orientation of the orbit plane was selected so as to obtain adequate summertime lighting. The upper boundary represents the variation in the maximum solar elevation angle throughout the year. A negative solar elevation angle corresponds to a nighttime pass so it is seen that there are six distinct periods throughout the year, totalling about 75 days, when the satellite will pass 40 deg. N latitude in darkness. For about 150 days of the year the solar elevation angle is less than 20 deg. which is less than minimum requirements for visual and near IR sensors. The lighting conditions can be significantly improved, however, by the use of two satellites placed in similar orbits but separated by 12 hours in launch time (i.e., the longitude of the ascending nodes differ by 180 deg.). The lighting conditions, if two such optimally positioned satellites are used, are illustrated in Figure 2-8b. Note that the elevation angles are almost always greater than 20 deg. (For clarity in the figure no distinction is made between south-to-north and north-to-south passes.)

In addition to the lighting conditions the altitude variation, shown in Figure 2-8c, is also of interest. Both the north to south and south to north passes are shown; the curves are not continuous since only daylight passes are indicated. The altitude for the equivalent circular orbit is

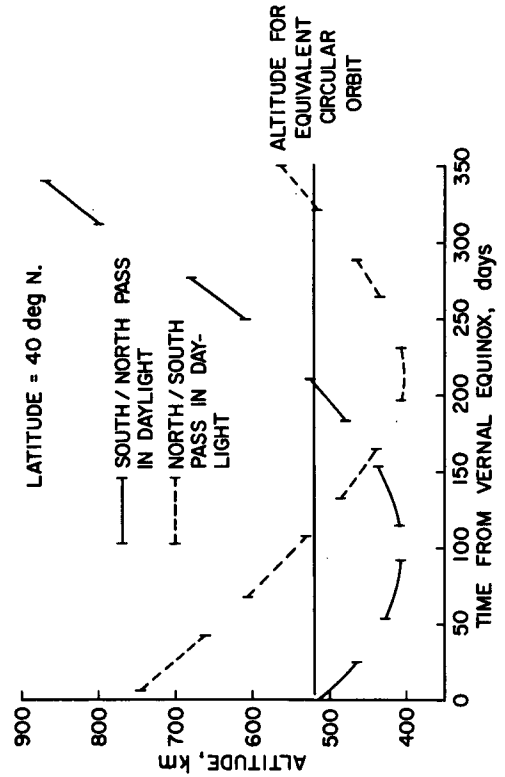
Figure 2-8 Characteristics of Orbit No. 5



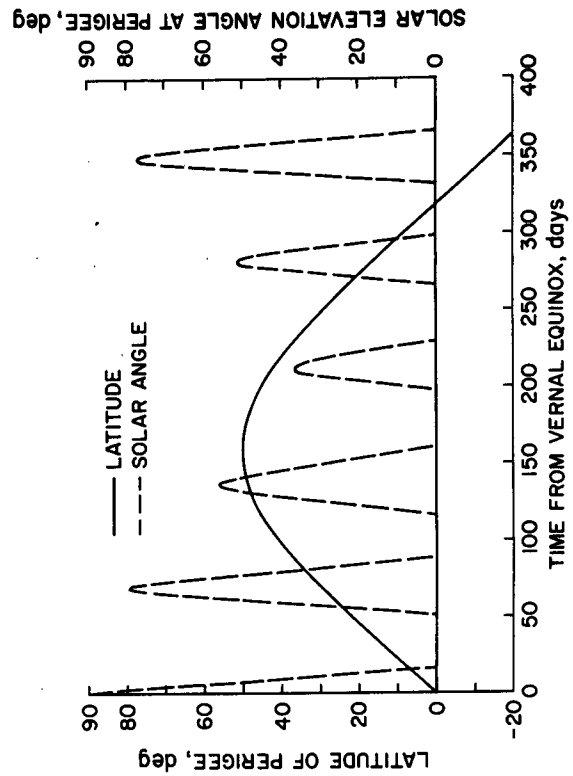
a. Solar Elevation Angle; 1 Satellite



b. Solar Elevation Angle; 2 Satellites



c. Altitude Variation



d. Perigee Location and Lighting Conditions

indicated and it should be noted that at least one pass is always below this altitude.

Since the altitude variation is significant, the location, or more specifically, the latitude of perigee is important since the highest spatial resolution will occur at perigee. Figure 2-8d indicates the variation in both latitude and lighting at perigee. The initial location of perigee is arbitrary and was selected to obtain the best conditions during the summer months. Note that the solar elevation angle at perigee varies quite drastically and is negative during about one-half of the year.

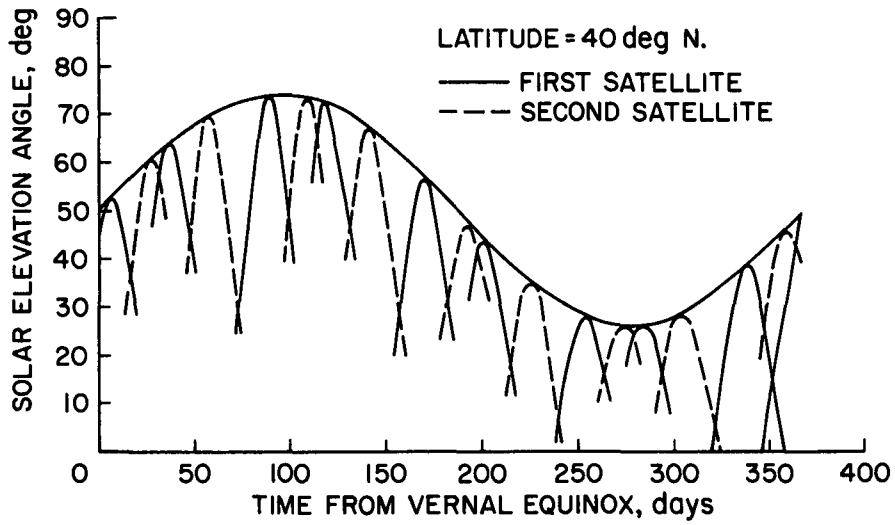
Orbit No. 6

This inclination of 63.4 deg. represents the highest inclination considered in this study for launches from Cape Kennedy. A substantial launch vehicle payload degradation nevertheless results due to the required yaw maneuvers. Since the location of perigee is stationary, it is placed at 40 deg N latitude to obtain the best coverage of the United States. Figure 2-9a illustrates the variation in solar elevation angle throughout the year for a single satellite. Figure 2-9b shows the sun angle variation for two satellites in similar orbits except that one is launched six hours later (i.e. the longitudes of the ascending node differ by 90 deg). It is not desirable to use a 180 deg difference in ascending nodes as was the case for the 50 deg orbits since this value will not allow sufficient nodal regression to fill the large gap that exists about 65 days after launch.

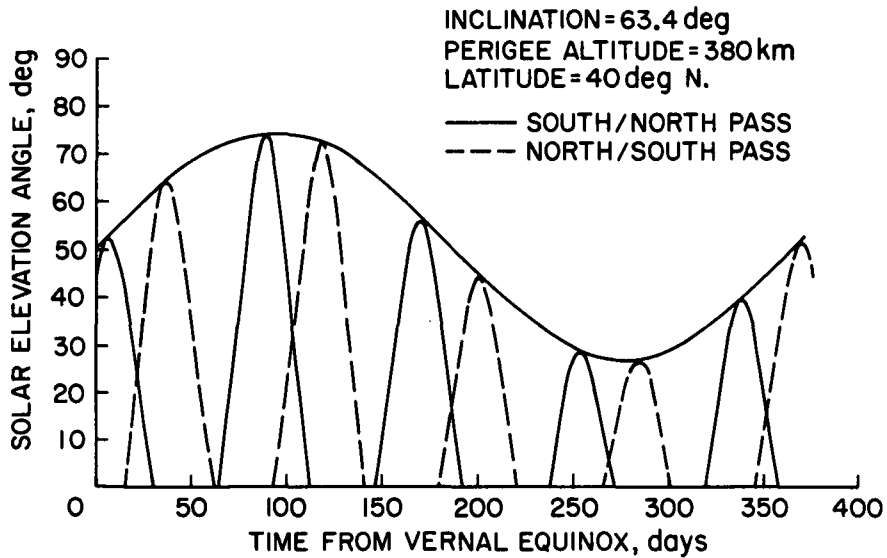
Orbit No. 7

The planned orbits for the ERTS satellites are members of this particular class of circular sun synchronous orbits. The detailed discussion of such orbits is presented for the more general eccentric orbit, i.e. Orbit No. 9. It should be mentioned that the altitude of this orbit is rather high, yielding approximately 14 orbits per day. This has the effect of slightly increasing the coverage interval for a given swath width (see Figure 2-2) and somewhat degrading the spatial resolution capability of certain sensors. On the other hand the higher altitude increases the time available for direct data transmission to any given readout station. It could be presumed, however, that an operational

Figure 2-9 Characteristics of Orbit No. 6



a. Solar Elevation Angle; 1 Satellite



b. Solar Elevation Angle; 2 Satellites

Earth observation system would contain either a sufficient number of properly located stations or would include data relay satellites.

Orbit No. 8

This orbit is similar to Orbit No. 7 except that its altitude is about 330 km lower, resulting in approximately 15 orbit passes per day. The general features of this orbit are discussed next.

Orbit No. 9

Coverage capabilities for this orbit are illustrated in Figure 2-10. The solar elevation angle is shown in Figure 2-10a for noon lighting at 40 deg and 65 deg latitudes; note the wide variation throughout the year even for this optimal condition. Figure 2-10b indicates the altitude variation at 40 deg N. latitude for both the daytime and nighttime passes. The altitude of the equivalent circular orbit (Orbit No. 8) is also shown. The spacecraft remains below this altitude in sunlight over the continental United States for approximately 260 days. Low altitude passes continue but occur in darkness.

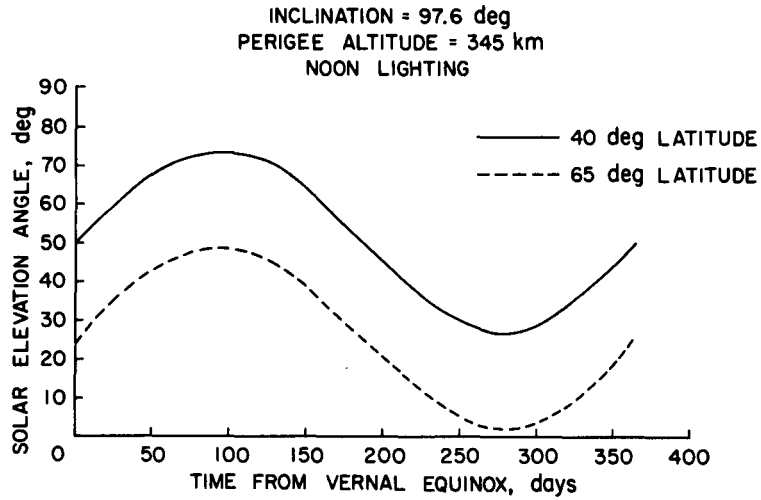
The initial latitude of perigee for this orbit was chosen to yield sunlit perigee passes over the United States during midsummer as shown in Figure 2-10c. Perigee remains in the northern hemisphere essentially throughout the first year but is only in sunlight during the first 200 days.

Orbit No. 10

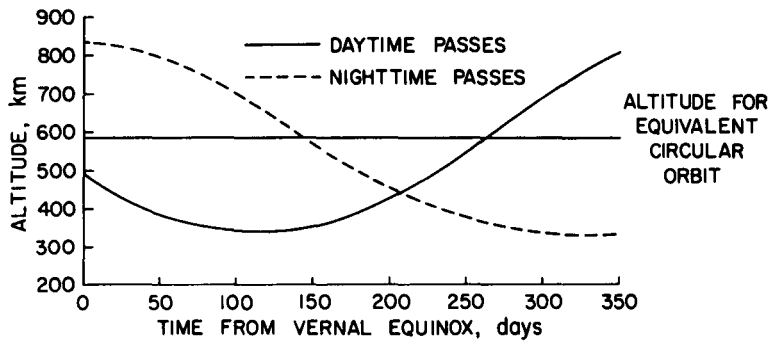
As noted earlier in Table 2-1 this orbit is characterized by 16 orbits per day. The corresponding altitudes are so low that an onboard drag makeup system is necessary. Consequently the lifetime of the system will be dependent on the amount of propellant that can be carried aboard the spacecraft. This orbit is included here only as an alternative to aircraft for applications that might require high spatial resolution for short duration missions such as disaster assessment. Such a use would, of course, dictate that the system be continuously on standby status at the launch site.

To compute the drag makeup velocity requirements, the assumptions made for the earlier lifetime analysis apply except that no solar arrays

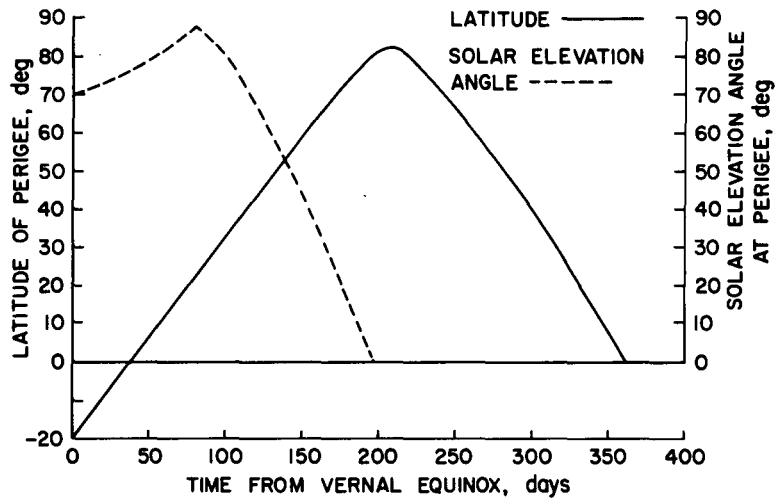
Figure 2-10 Characteristics of Orbit No. 9



a. Solar Elevation Angle at Noon



b. Altitude Variation at 40 Degree N. Latitude



c. Perigee Location & Lighting Conditions

are employed. In this case the ballistic parameter is approximately $0.275 W$ (kg/m^2) where W is the spacecraft weight. Results are shown in Figure 2-11 for a spacecraft weight of 3600 kg and are based on data from Ref. 4. Note that the figure may be used for other spacecraft weights since the drag makeup velocity varies inversely with weight.

Orbit No. 11

Having a stationary perigee location, this orbit is similar to Orbit No. 6. The inclination of 116 deg, however, can be readily achieved from WTR without the performance penalties associated with Orbit No. 6 launches from Cape Kennedy. Since this inclination is nearer that of the sun synchronous orbits the solar elevation angle does not vary as rapidly as it does for the previous non-synchronous orbits. This is illustrated in Figure 2-12a. The lighting conditions for two satellites launched 6 hours apart are shown in Figure 2-12b.

Error Analysis

Deviations from the nominal orbits will occur because of orbit insertion errors and perturbations caused by the higher order gravitational harmonics. The effects of the higher order harmonics are not considered here but can be included in analyses of the satellite orbits requiring sufficient detail for actual mission operations.

The long term effects of insertion errors can be significant even though the absolute magnitude of the error may be small and for this reason, the ERTS satellites will employ an orbit adjust propulsion system. For example a change in the nodal regression rate of about 0.1 deg per day will change the orientation of the orbit by about 30 deg at the end of one year. Since the regression rate is a function of orbit inclination, an insertion error in inclination will change this rate. Such errors can have pronounced effects on the lighting conditions, as shown in Figure 2-13 for Orbit No. 8. The change after one year in the angle between the orbit plane and Earth-sun vector is shown as a function of the initial orbit inclination. Of course, for this sun synchronous orbit the nominal variation is zero. However an initial one-half degree error in inclination, for example, will result in a shift of 30 deg in the orbit plane away from the Earth-sun line after one year.

Figure 2-11 Drag Make-up Requirements for Orbit No. 10

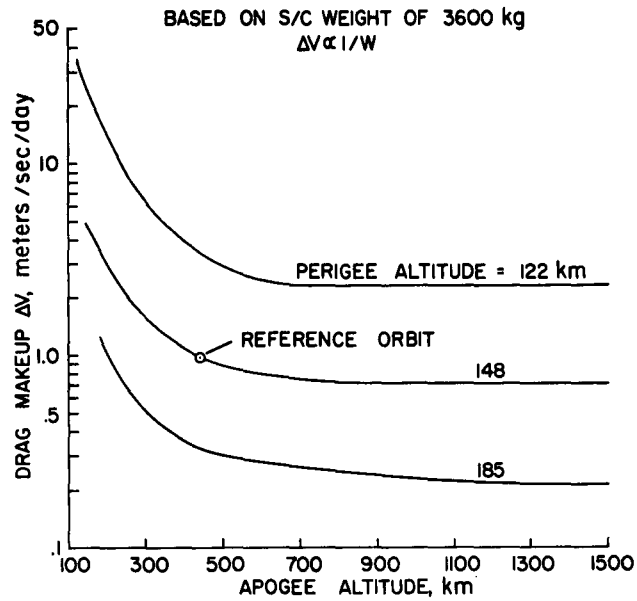
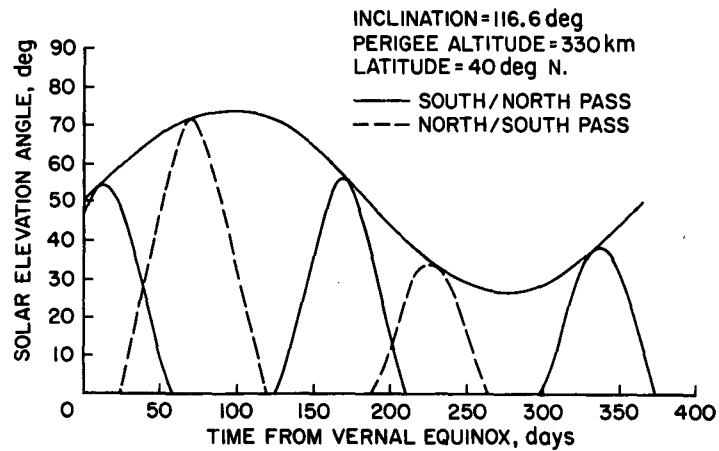
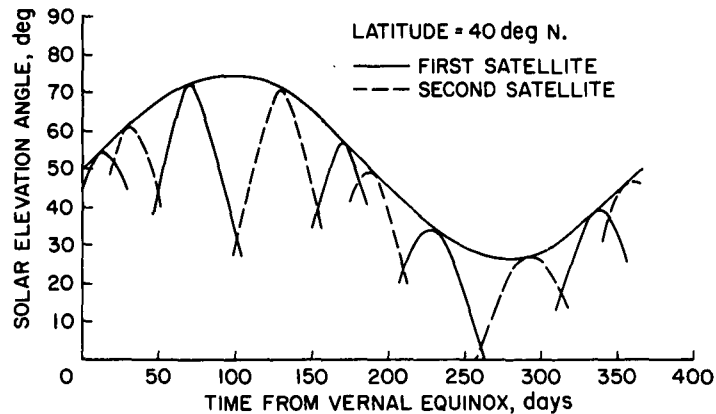


Figure 2-12 Characteristics of Orbit No. 11

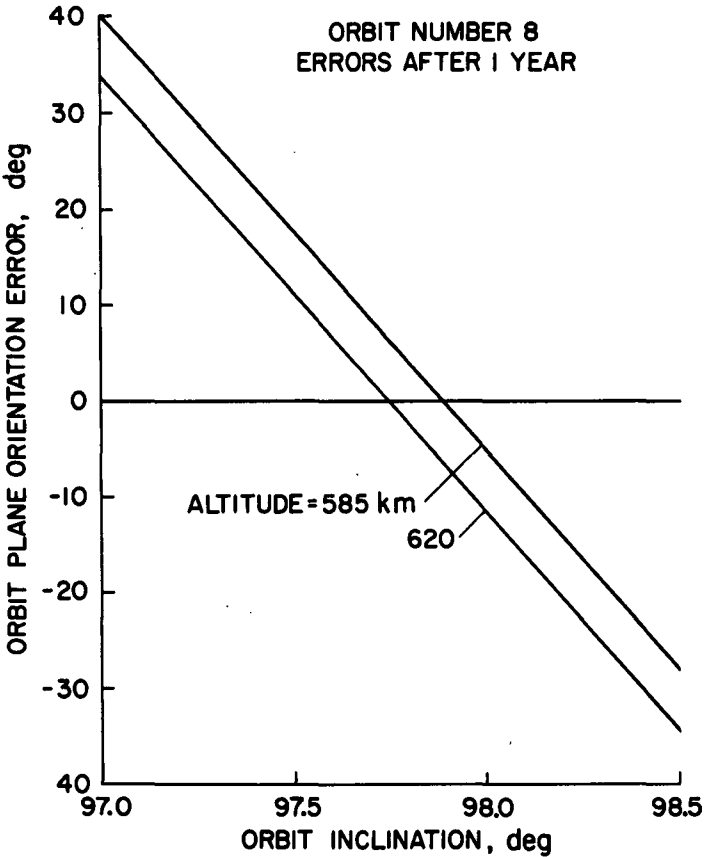


a. Solar Elevation Angle; 1 Satellite



b. Solar Elevation Angle; 2 Satellites

Figure 2-13 Errors in Orbit Plane Orientation Due to Variations in Insertion Parameters



Since the nodal regression rate is also a function of semi-major axis, altitude errors would also be expected to result in orbit orientation errors. As seen, however, the effects are minor. A 35 km altitude error causes only a 5 deg orientation error at the end of one year.

3. LAUNCH VEHICLE CAPABILITIES

The United States has developed a number of fully integrated launch vehicle-upper stage combinations. This section summarizes the performance capabilities of those systems that seem appropriate for unmanned Earth observation satellites. The salient features of each of the systems are also discussed. Only systems that are in operation today or are expected to have been in operation several years prior to their possible use in an Earth observation program are considered. Moreover, although future events may indicate this to be an incorrect assumption, it is assumed here that no new launch facilities for existing vehicles will be constructed. This, of course, limits certain systems to a particular launch site (e.g. Atlas/Centaur launched only from Cape Kennedy; Titan/Agna launched only from WTR).

Performance Summary

Generalized payload-velocity data are available for all systems considered except the shuttle. To avoid reproducing this data only the payload weight capability for each of the 11 orbits defined in the previous section are listed here. These capabilities are summarized in Table 3-1 and are based primarily on information from References 5-7. Only those items that are felt to need clarification are discussed here. For the most part these are the footnoted items. The various vehicles are described later in this section in order to identify the particular vehicle configurations being considered and to provide some background of interest to those readers who are not a part of the aerospace community.

Consider first the need in some instances for a solid propellant third stage (assumed to be the TE-364-4) and a payload insertion motor for the high energy missions using the Delta vehicle. The third stage is needed to place the payload on the proper coast ellipse to the higher altitude. A final burn is then needed to perform the plane change and/or circularization maneuver (Orbit Nos. 1 and 2) or to increase the velocity at apogee of the transfer ellipse (perigee of the final ellipse for Orbit No. 3). This final maneuver is assumed to be performed by a

Table 3-1 Launch Vehicle Performance Summary

Orbit Code	Incl. (deg)	Perigee (km)	Apogee (km)	Launch Site	Payload Weight Capability - kg											
					Scout	Delta w 3 SRM (TE-364-4)	Delta w 6 SRM (TE-364-4)	Delta w 9 SRM (TE-364-4)	Thor w 3 SRM/ Agena D	Titan IIIB/ Agena D	Atlas/Centaur (TE-364-4)	Titan IIIC	Titan IIID/ SCS	Titan IIID/ Centaur		
1	0	35,800	35,800	KSC	0	(260) ^a	(330) ^a	(405) ^a	-	b	-	(990)	1,180	-	b	3,540 ^a
2	50	35,800	35,800	KSC	0	(265) ^a	(345) ^a	(430) ^a	-	-	-	(1,045)	1,500	-	-	4,190 ^a
3	50	6,380	65,100	KSC	0	(265) ^a	(315) ^a	(365) ^a	-	-	-	(1,280)	1,590	-	-	4,320 ^a
4	50	520	520	KSC	130	1,050	1,410	1,770	-	-	5,000	11,400	-	-	-	14,100
5	50	400	1,000	KSC	130	1,050	1,410	1,770	-	-	5,000	11,400	-	-	-	14,100
6 ^d	63.4	380	692	KSC	0	180	410	635	-	-	2,640	5,920	-	-	-	8,900
7	97	920	920	WTR	110	635	910	1,180	910	2,680	-	b	-	b	8,100	-
8	97	587	587	WTR	120	865	1,140	1,410	1,050	3,000	-	-	-	-	8,850	-
9	97	345	829	WTR	110	820	1,090	1,360	1,000	2,910	-	-	-	-	8,750	-
10	97	148	445	WTR	Drag Makeup	Spacecraft Required	1,275 ^e	1,275 ^e	1,275 ^e	3,230 ^e	Drag Makeup Req.	9,400 ^f	Drag Makeup	9,400 ^f	Drag Makeup	-
11	116.6	330	910	WTR	110	635	910	1,180	910	2,680	-	-	-	-	8,150	-

- a. Based on employing separate payload insertion motor or stage.
- b. Indicates facilities not available at required launch site.
- c. Increase in Centaur coast time to one hour assumed.
- d. Forty-five degree launch azimuth with plane change at orbit insertion.
- e. Orbit lifetime limited to three months with drag makeup.
- f. Orbit lifetime limited to seven months with drag makeup.

solid rocket motor designed into the payload itself as was done, for example, in the Intelsat program.

Insertion motors are also required for the high energy missions if the Centaur is employed. Unlike the Delta vehicle the Centaur can place the payload on the proper coast ellipse. It does not, however, possess sufficient lifetime to remain operative at apogee of the coast ellipse. Thus a final insertion stage is required. It is assumed that this stage is the TE-364-4 if the Atlas/Centaur is employed. Payloads will be larger, both in terms of weight and size, if the Titan III-D/Centaur is used and a correspondingly larger liquid propulsion system payload insertion stage was assumed.

For all other missions using Centaur no additional stage will be required. Based on the assumed increase in Centaur coast time to about one hour, sufficient lifetime exists for the Centaur to perform the final maneuver.

Another factor involving the performance calculations concerns Orbit No. 6. Range safety constraints at Cape Kennedy limit the orbit inclinations to not more than about 50 degrees. Thus some form of yaw maneuver is necessary to enter the 63 deg. orbit. A complete simulation of the ascent trajectory would have been required to consider the effects of yaw steering of the boosters. The simpler approach adopted here considered an in-plane ascent at the range safety azimuth limit followed by an orbital plane change. This yields payload weights somewhat less than those associated with an optimal ascent profile.

The final note concerning Table 3-1 deals with Orbit No. 10. Recall that this orbit is deliberately chosen with a low perigee altitude to maximize spatial resolution but that the large atmospheric drag requires on-orbit propulsion to prevent orbit decay. The integration of a propulsion system having such a capability with the payload represents a rather specialized vehicle. Moreover such a mission, if desirable at all, would likely be flown on a rather sporadic basis. Thus it would seem undesirable to develop a special purpose vehicle for such limited use. A version of the Agena spacecraft, however, is equipped with a secondary propulsion system for such missions. The Satellite Control

Section (SCS) discussed later has been developed for similar use atop the Titan III-D. These spacecraft are assumed here to be appropriate if a need arises for a very low altitude orbit in any Earth observation program although such orbits are not considered further in this report.

Vehicle Descriptions

Generally speaking the systems are discussed in order of increasing payload weight capability. Typical capabilities lie within the range of 700-3000 kg delivered to intermediate altitudes. Systems with capabilities outside this range, however, are also considered. Smaller vehicles might be appropriate, for instance, if a payload consisted only of a radiometer. Conversely the larger vehicles, with payloads of about 10,000 kg, are included since they would be needed to take fuller advantage of side-looking radar, to permit several of the larger sensors to be carried aboard a single satellite, or to deliver relatively large data relay satellites to geosynchronous orbit should such systems be needed.

It might also be mentioned that this rather wide spectrum of launch vehicle capabilities is considered here not only for the reasons just given but also in keeping with a plausible philosophy of intentionally choosing a launch vehicle whose payload weight capability is discernably greater than the payload weight requirement. History shows that the cost of a payload is several fold greater than the cost of its launch vehicle. Many have asserted (although not necessarily proven) that a major reason for this is the sizable effort that must be undertaken after payload development has been initiated in order to reduce the weight (which had increased over initial estimates) to make it compatible with the capability of the selected launch vehicle. An intentionally over-designed launch vehicle might thus result in lower total program costs.

Scout

At the outset of this study the Scout was not felt to be appropriate for Earth observation missions. Subsequent analysis has indicated however, that its payload capability may be adequate if the payload consists only of radiometers. Although such a system by itself would not appear to be of much utility the Scout is included here for completeness.

The Scout is a small (and inexpensive) vehicle that employs solid propellants throughout. The standard configuration is a four stage vehicle although a fifth stage is available for higher energy missions. Over 50 Scout launches have been performed in support of such programs as Explorer, ESRO and other international programs. Launch facilities exist at WTR, Wallops Island and San Marco Island in the Indian Ocean.

Delta

The versions of the Delta currently in operation are two or three stage vehicles consisting of a long tank Thor booster with thrust augmentation supplied by three strap-on solid rocket motors as the first stage; a vehicle approximately 1.4 m in diameter, 5 m in length and containing about 5000 kg of liquid propellant as the second stage; and, as mission requirements dictate, a small solid rocket third stage. Because the second stage engine of the current Delta vehicle is restricted to a single firing, the payload capability diminishes rapidly with altitude for Earth orbital missions. Therefore the third stage is used not only for high energy missions but for most orbital missions as well. The Delta has been the mainstay of NASA's stable of launch vehicles. Over 70 launches of its various versions have been made in support of such programs as Explorer, Biosatellite, ESSA, and Pioneer. This vehicle will also be used to launch the ERTS satellites. The inclusion of an additional solid rocket motor into the payload has also enabled the Delta vehicle to launch the Intelsat satellites into geostationary orbit. Delta launch facilities exist both at Cape Kennedy and at WTR.

Substantial modifications to the Delta are currently underway. Perhaps the most significant is the incorporation of the Titan Transtage propulsion system (discussed later) into the second stage. This system, being capable of multiple starts, will obviate the need for the solid third stage for most Earth orbits of interest. Higher energy orbits can also be more easily accommodated by employing a larger third stage, e.g. TE 364-4. Modifications to the Thor booster are also being carried out, the most noteworthy being the provision to strap on three, six or nine Castor II solid rocket motors. The version of the Delta described here will be available in the not-too-distant future. Consequently the Delta

performance data shown in Table 3-1 are predicated on the availability of this improved system.

Thor/Agena D

This is a two stage vehicle with the Thor first stage being essentially as described above. The Agena D is comparable in size to the second stage of the Delta vehicle. The propulsion system, however, is capable of multiple starts thus making a third stage unnecessary for orbital missions. Thor/Agena launch facilities exist only at WTR, thus limiting possible orbit inclinations to at least 90 degrees.

The Agena was developed by DoD as a combination upper stage propulsion system and spacecraft. To date, approximately 300 Agena vehicles have been launched; over 200 of these have been in the spacecraft configuration. As a three-axis stabilized spacecraft, the Agena provides functional support to various integrated payloads. The on-orbit lifetime of the earliest vehicles was several days. With the incorporation of such items as large solar arrays, control moment gyros, and with the normal evolution of the various subsystems, the lifetime has increased considerably. Several vehicles have remained in operation for about one year in orbit.

Among the functions performed by the Agena spacecraft are on-orbit maneuvering from either the main engine or a secondary propulsion system, initiation of payload recovery from orbit, launch of subsatellites, wide band data transmission to ground stations, and various sequencing operations based on both preprogrammed and transmitted commands.

With the exception of its use as the Gemini Target Vehicle and in the SERTS program, NASA usage of the Agena has been limited to that of an ascent propulsion stage. Thor/Agenas have been used, for example, to launch OGO and Nimbus satellites. It is assumed here that, with the exception of its possible use as a low altitude spacecraft where drag makeup would be needed, its role in any Earth observation program will also be that of an ascent propulsion stage only.

Titan IIIB/Agena D

Three versions of the Titan III launch vehicle exist. The Titan IIIB is the basic vehicle from which the others are derived. It is a

two stage vehicle, the stages having the designations Core I and Core II. The Titan IIIB/Agena D is in current operation at WTR. All launches have been in support of DoD programs.

Atlas/Centaur

This vehicle is NASA's largest launch vehicle in current operation that was designed exclusively for unmanned missions. Although launch facilities exist only at Cape Kennedy, thereby limiting the orbit inclinations to intermediate values, the Atlas/Centaur is considered here because it does permit heavy payloads to be orbited without recourse to vehicles developed primarily for military applications. This vehicle was used to place the Surveyor and Mariner spacecraft on their respective trajectories and to orbit the OAO. It has also been used to deliver the ATS and, recently, the Intelsat IV satellites to geosynchronous orbit. To date approximately 20 Atlas/Centaur launches have occurred.

The Centaur stage itself is about 3 m in diameter, 9 m in length and has a gross weight of about 13,500 kg. Although the two Centaur engines are restartable the payload capability of the current Atlas/Centaur nevertheless diminishes rapidly with increasing orbit altitude. The most efficient manner of injection into orbit is to coast from a low altitude parking orbit (typically 180 km altitude) to the desired altitude, followed by the final injection maneuver. The optimal coast length is about one half of an orbit and, depending on the final altitude, is of at least 45 minutes duration. The current Centaur, however, is restricted to coast times of about 25 minutes because of the need to settle the liquid hydrogen at the aft end of the propellant tank by means of small hydrogen peroxide thrusters. Space limitations constrain the amount of peroxide to the equivalent of 25 minutes of operation. Nonetheless it is assumed here that the coast time could be extended to about 60 minutes if mission requirements dictate. All payload weight values shown in Table 3-1 are based on this assumption. Because the time required to coast to geosynchronous altitude, however, is several hours, a third stage will be needed to perform the final maneuver for any such missions.

Titan IIIC

The core of this vehicle is the Titan IIIB; thrust augmentation is

provided by two five-segment 120" solid rocket motors. The upper stage of the Titan IIIC is designated Transtage (sometimes referred to as Core III), and was designed expressly to meet the requirements of injecting separable payloads into geosynchronous orbit. The Transtage is 3 m in diameter and about 4.5 m in length. About ten flights of the Titan IIIC have been made in support of DoD programs. Launch facilities exist only at Cape Kennedy.

Titan IIID/SCS

The Titan IIID is basically the Titan IIIC without the Transtage being employed. The Titan IIID/SCS was developed for use at WTR and is currently in operation. Since the engine of Core II is not restartable the payload weight of the Titan IIID alone, although sizable at low altitudes, diminishes rapidly with increasing altitude. For this reason, among others, the SCS (Satellite Control Section) was developed to perform the insertion maneuvers into higher orbits. The SCS is about 3 m in diameter and 2 m in length and employs monopropellant hydrazine. Similar to the Agena spacecraft, the SCS can also provide functional support for the payload and perform orbit adjust maneuvers, including drag makeup, via the hydrazine propulsion system. Its usage here is assumed to be limited to that of an orbit insertion stage except for any Earth observation mission for which drag makeup would be needed.

Titan IIID/Centaur

This vehicle system is being developed to launch the Viking spacecraft to Mars in 1975. Ground facilities will exist only at Cape Kennedy. The Titan IIID/Centaur is used to best advantage for high energy missions. Its use in any Earth observation program is assumed here to be limited to geosynchronous missions where payload weights greater than those afforded by the Atlas/Centaur or Titan IIIC might be desirable.

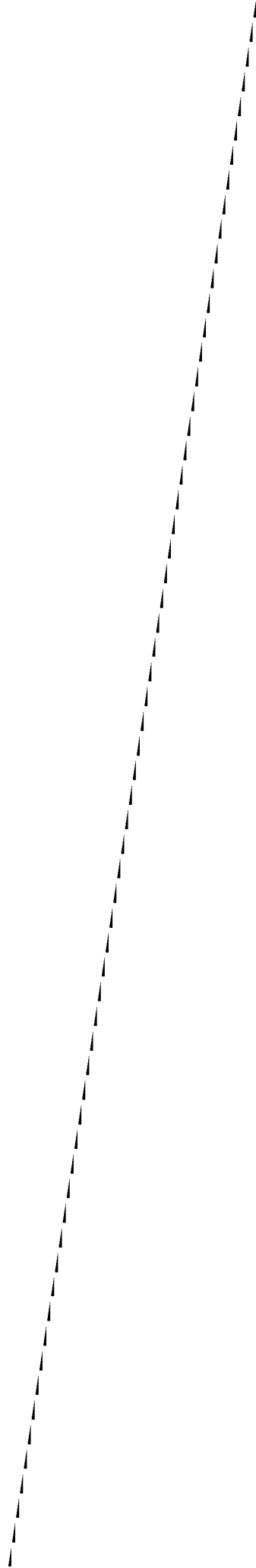
Shuttle

This is a manned, reusable system currently in the preliminary design phase. It is expected to be in operation in the late 1970's. Typical shuttle performance capabilities are shown in Table 3-2.

Table 3-2
Representative Shuttle Payload Capabilities

<u>Incl. (deg)</u>	<u>Alt. (km)</u>	<u>Payload (kg)</u>	<u>Airbreathing Engines</u>
28	185	29,500	out
55	500	11,300	in
90	185	18,200	out

In addition to its obvious use as a means of delivering heavy systems (or a number of smaller satellites) to orbit the shuttle would offer other unique capabilities in an operational Earth observation program. It could be used, for example, to replenish the film supply of a camera-bearing satellite or to replenish the refrigerant of an active cooling system for an infrared detector. Other basic uses of the shuttle that would be appropriate to all sensor types include replenishment of attitude control gas, orbit adjust propellant and modification or repair (either in orbit or on Earth) of the satellite system. An important example of the repair function would be the replacement of any on-board data storage systems which, commonly, are shorter-lived than many other spacecraft systems.



4. AIRCRAFT COVERAGE AND PERFORMANCE

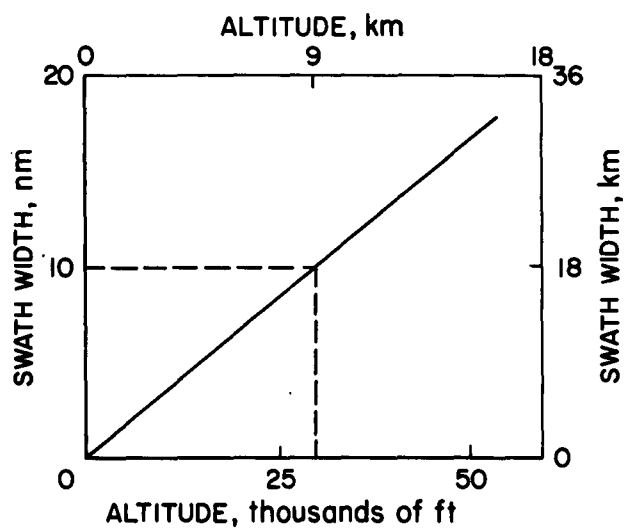
A complete investigation of Earth resource survey methods should naturally include consideration of aircraft as well as satellite borne surveillance. Aircraft could be used exclusively or in conjunction with satellites. One possibility is the use of a special fleet of aircraft to cover the areas of resource interest. Another possibility is the use of commercial air carriers which already overfly much of the continental U.S. This section explores these two possibilities.

Many of the figures and much of the data of this section retain English units for the convenience of those who are accustomed to these more familiar aeronautics units.

Special Purpose Fleet

All of the United States (of which only the traditional "continental" portion is considered here) is of resource or inventory interest. Much of the country has two or more resource features of interest, each having its own frequency of coverage and resolution requirements. (See Ref. 8 for details,) Frequency of coverage requirements are met by controlling the number of aircraft or satellites deployed. Resolution and swath width are functions of the sensor design parameters and flight altitude. If it is reasonable to assume that resolution requirements can be met from aircraft, the only criteria in aircraft surveillance, then, is to overfly the required ground area with a minimum of effort or at a reasonable cost. Generally, higher altitudes are more desirable because of increased coverage capability. Figure 4-1 shows the swath width versus altitude for a 90 deg. angle of acceptance. For this condition the spatial resolution at the edge of the swath is about half as good as at the nadir and is thus considered to represent the maximum field of view. For example, an aircraft flying at 30,000 feet (9 km) altitude would sweep out a 10 n.m. (18 km) wide swath if the field of view was 90°. As an illustration, if the 2,280,000 n.m.² (7,800,000 km²) area of the coterminous United States is divided by the ten mile (18 km) swath width, it would take 228,000 air miles (422,000 km) to cover the country under ideal circumstances. Or, in other words, it would take

Figure 4-1 Swath Width and Aircraft Altitude Relationship for 90 Degree Field of View



452 hours to cover the country at a ground speed of 500 knots (930 km/hr). If one plane were flown five hours per day it would take 90 days to cover the United States, or it could be done with ten aircraft in nine working days.

In reality there are many factors which change these performance numbers. There will certainly be cloud cover to contend with, and due to aircraft range and base locations it may be necessary to overfly certain areas more frequently than required for adequate resource observation. Certain points seem obvious: first, the longer the range of the plane the better, because it allows more versatile flight patterns; second, the more bases (and aircraft) the better, so that less time need be wasted getting to the areas requiring observation; third, bases should be located where observations are required most frequently; and fourth, minimizing the number of bases is desirable to simplify data collection. Ultimately, then, it is desirable to trade off the number of aircraft and their characteristics with the number of bases and their location with respect to resource areas.

The most obvious measure of efficiency in aircraft usage is the proficiency with which they cover a designated area. Figure 4-2 shows the continental U.S., four observation categories of interest, and 24 arbitrarily selected base locations. Table 4-1 lists possible groups of bases as a function of the number of bases. As a function of the number of bases, then, a visual estimate of the distance between bases can be made. And a similar estimate can be made of the aircraft range required assuming that they return to the same base. These results are shown in Figure 4-3.

Meanwhile, graphical plots of aircraft flight patterns have been used to determine how efficiently an aircraft might cover different size areas. Coverage efficiency is defined as the ratio of theoretical coverage miles (i.e. with non-overlapping coverage) to the actual number of miles flown. These exercises indicate that the coverage efficiency varies from zero to one as a function of the aircraft range and the size of the area to be covered. More precisely, if "flight flexibility" is defined as the ratio of twice the furthest linear excursion distance

Figure 4-2 Resource Areas and Possible Base Locations

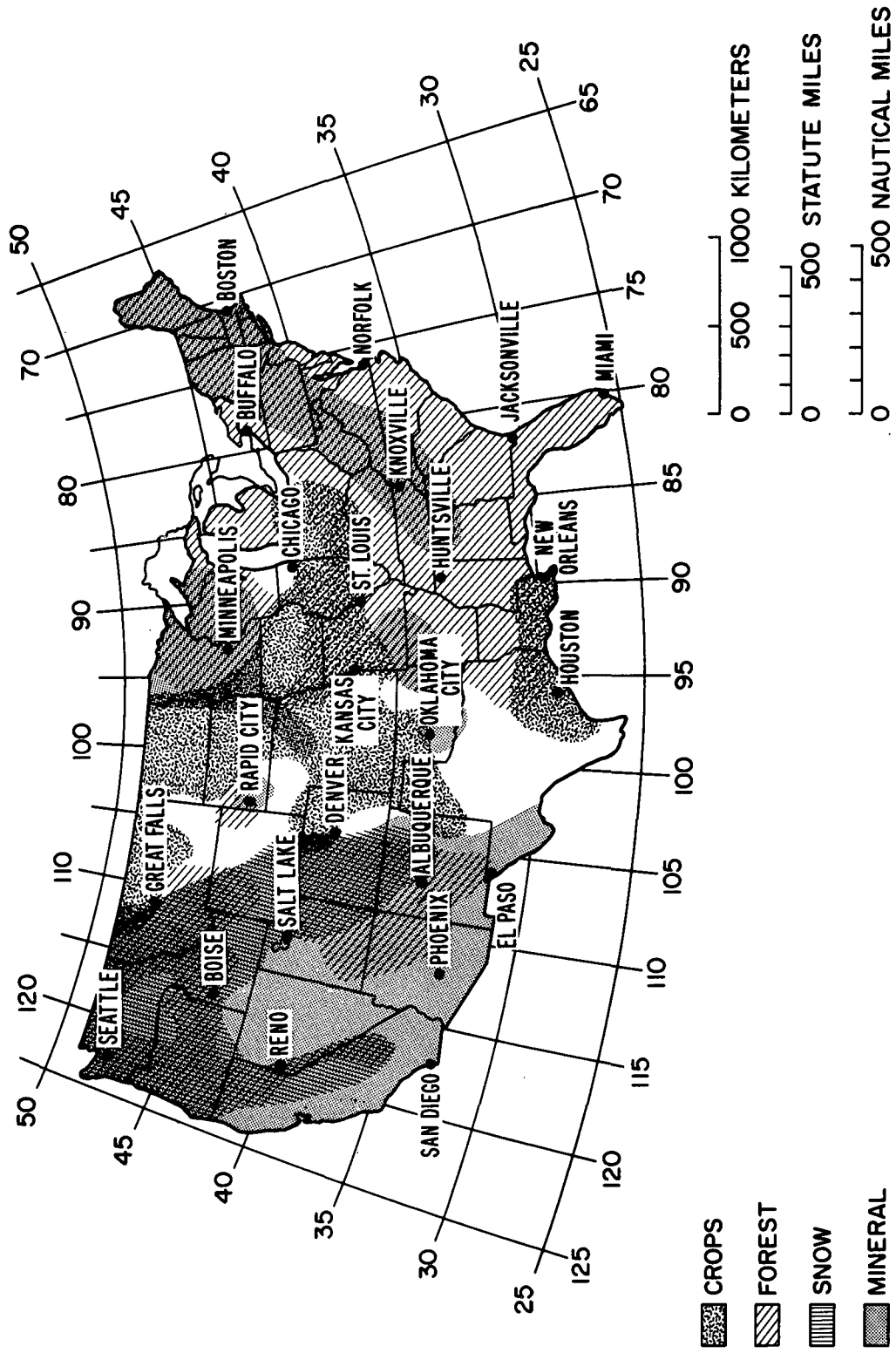
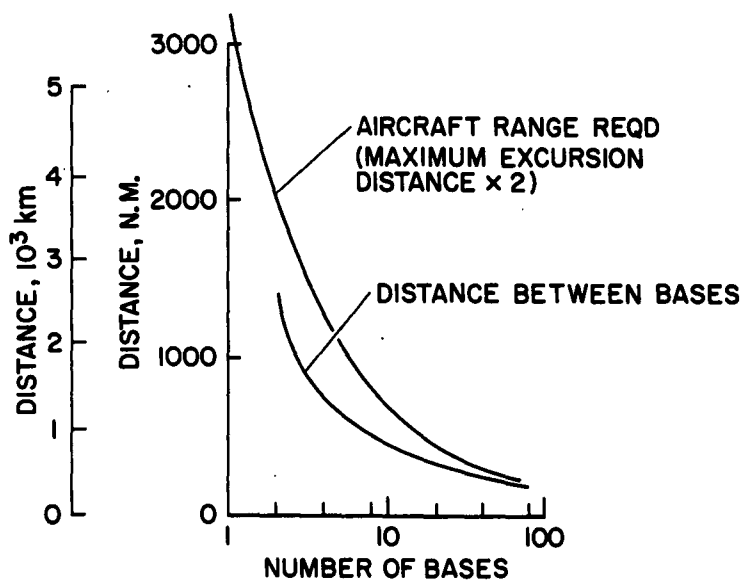


TABLE 4-1

POSSIBLE GROUPS OF AIR BASES

Number of bases			
1	Kansas City		
2	Salt Lake City Knoxville		
3	Salt Lake City Kansas City Norfolk		
4	Reno Denver St. Louis Norfolk	Boise Albuquerque Minneapolis Knoxville	Reno Denver Huntsville Buffalo
5	Seattle Salt Lake City Oklahoma City Chicago Norfolk	Seattle Salt Lake City Kansas City Knoxville Boston	Boise Albuquerque Minneapolis New Orleans Boston
6	Seattle San Diego Denver Minneapolis New Orleans Norfolk	Reno Albuquerque Rapid City St. Louis Jacksonville Boston	Reno Albuquerque Rapid City Kansas City Knoxville Buffalo
10	Seattle San Diego Salt Lake City Albuquerque Rapid City Oklahoma City Chicago New Orleans Knoxville Boston		
24	Seattle Reno San Diego Boise Salt Lake City Great Falls Phoenix Rapid City Denver	Albuquerque El Paso Minneapolis Kansas City Oklahoma City Houston Chicago St. Louis Huntsville	New Orleans Buffalo Knoxville Jacksonville Norfolk Boston

Figure 4-3 Distance Between Bases and Maximum Aircraft Range Required



and the aircraft range, then coverage efficiency is found to be a function of flight flexibility as shown in Figure 4-4. Since "flight flexibility" is a function of maximum excursion distance, and maximum excursion distance is a function of the distance between bases, it is possible to plot coverage efficiency versus number of bases and aircraft range. This is done in Figure 4-5, where, for example, it is seen that a fleet of aircraft with 1000 n.m. (1800 km) range, operating from ten bases can be expected to have a coverage efficiency of about 85%. Figure 4-5, however, represents an ideal situation because cloud cover was not considered. Since the overall integrated yearly U.S. cloud cover is about 54% (see Section 5), it is obvious that not all flights will be able to avoid dilution of the above performance numbers. Cloud cover will hamper operations and decrease coverage efficiency by interfering with the optimum flight patterns. This effect will, however, be minimized as the number of bases is increased since only those aircraft in the cloud free areas need be operated. This advantage could be further enhanced with cloud cover data from satellites. With the assumption that cloud deterioration of coverage efficiency is proportional to flight flexibility, it is readily possible to incorporate the effects of cloud cover. Figure 4-6 shows that the fleet of planes with 1000 n.m. (1850 km) range operated from ten bases will have a coverage efficiency of 55% as opposed to the 85% of Figure 4-5.

Using the data from Figure 4-6 it is possible to get a more reasonable estimate of the number of aircraft required than was calculated in the arbitrary example cited earlier. As shown in Figure 4-7, coverage of the entire 2,280,000 n.m.² of the United States from ten bases with aircraft traveling at 500 knots and making a complete survey in nine five-hour days, for example, would require 18 aircraft of 1000 n.m. (1850 km) range, 13 aircraft of 1500 n.m. (2780 km) range, or 12 aircraft of 2000 n.m. (3700 km) range. The numbers from Figure 4-7 can be proportionally changed to account for differences in speed, area requirement, time to cover, or swath width.

A better estimate of the number of aircraft required can be made by examining further specific resource areas alluded to earlier, i.e. snow cover, mineral deposits, forest mapping, and crop inventory. These four

Figure 4-4 Relationship Between Coverage Efficiency & Flight Flexibility

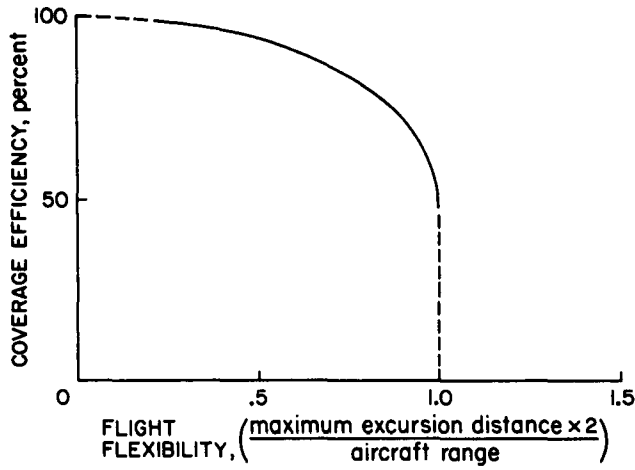


Figure 4-5 Coverage Efficiency as Affected by Number of Bases (Cloud Free)

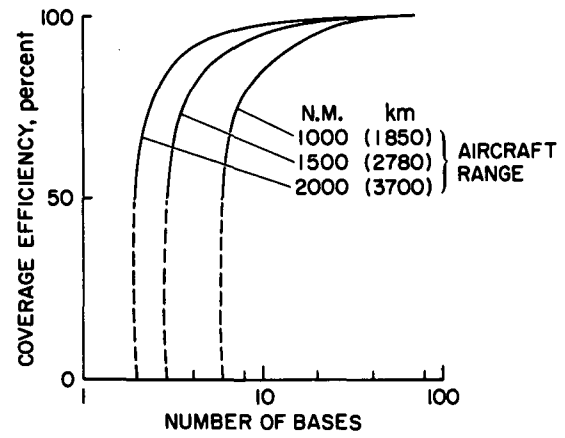


Figure 4-6 Coverage Efficiency as Affected by Number of Bases (With Cloud Cover)

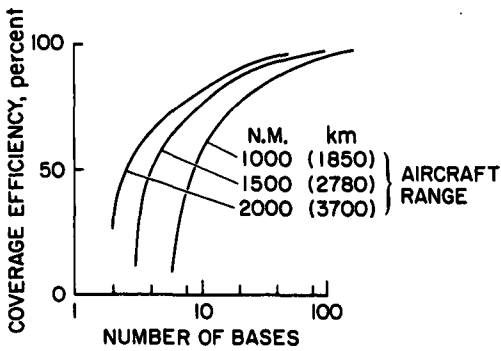
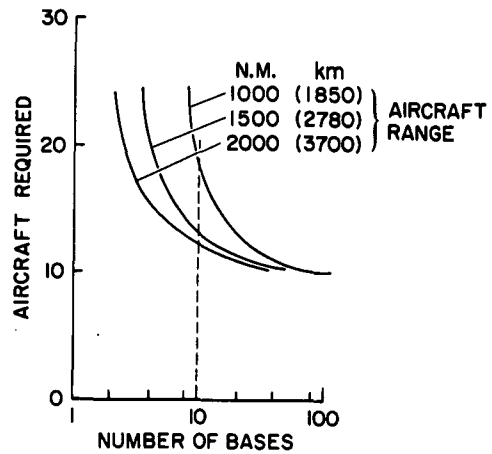


Figure 4-7 Aircraft Required as Affected by Number of Bases



20

were selected for this analysis because they cover all regions of the country, have disparate observation schedules, and require a wide variety of sensors. Table 4-2 lists some of their requirements and characteristics.

Table 4-2
Selected Earth Resource Characteristics

<u>Name</u>		<u>Observation Schedule</u>	<u>Area nm² (km²)</u>
Snow Cover		Every two weeks Dec. 1 - June 30	422,000 (1,450,000)
Mineral Deposits	West	Twice, Sept. & Oct.	800,000 (2,740,000)
	East	Twice, Sept. & Oct.	445,000 (1,520,000)
Forest Mapping	West	20% Coverage, Once/week March-May; Sept.-Nov.	468,000 (1,600,000)
	East	20% Coverage, Once/week March-May; Sept.-Nov.	830,000 (2,840,000)
Crop Inventory	North Wheat	Every two weeks	104,000 (356,000)
	South Wheat	See Figure 4-8	98,000 (336,000)
	Corn, Belt		256,000 (878,000)
	Texas/ Louisiana		60,000 (206,000)

The observation schedule is illustrated in Figure 4-8 and the cumulative area coverage rates are shown in Figure 4-9. As Figure 4-8 shows, however, there is some duplication in coverage between resource features. Consequently, the peak coverage rates of Figure 4-9 are unrealistically high. Furthermore, it would appear that some minor rescheduling could also reduce the peak coverage rate.

Figure 4-9 indicates that the average coverage rate is about 400,000 n.m.² (1,370,000 km²) per week. With judicious scheduling a maximum coverage rate of 50,000 n.m.² (172,000 km²) per day in the months of November

Figure 4-8 Observation Schedule for Selected Earth Resources

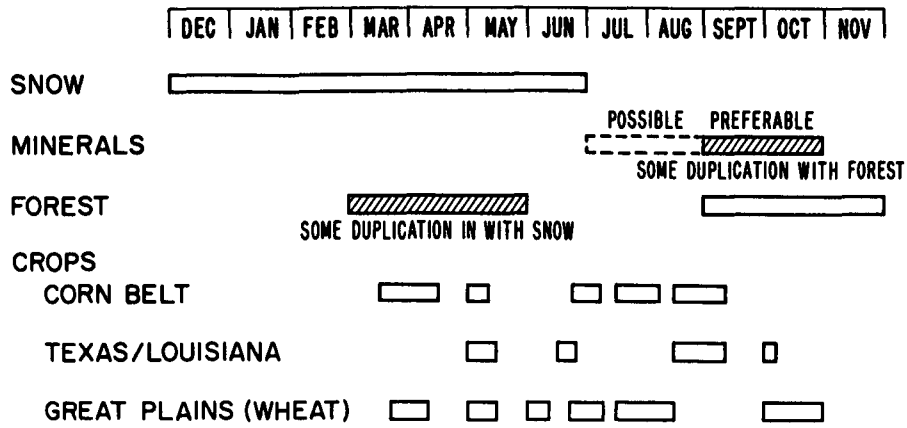
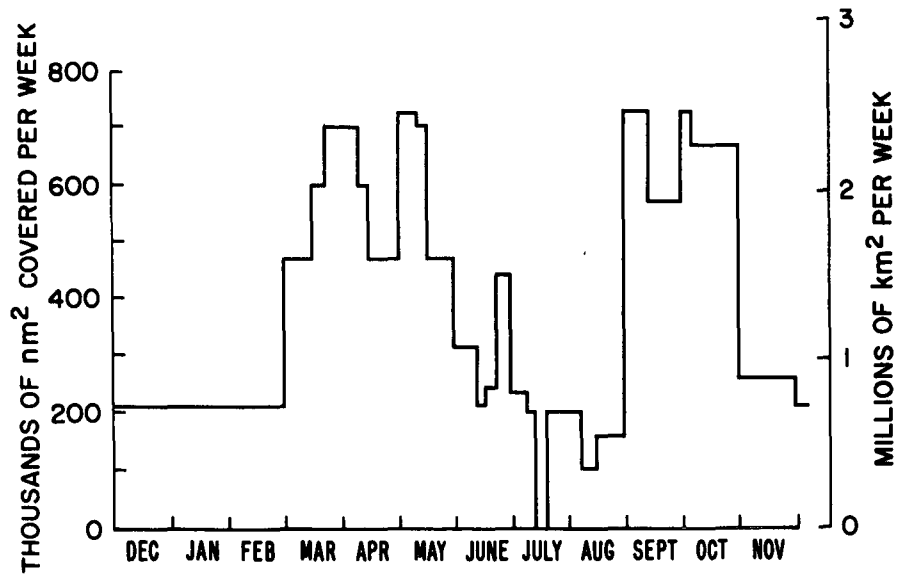


Figure 4-9 Resource Area Coverage Rate



through February and 100,000 n.m.² (343,000 km²) per day March through October should be obtainable, based on a five day week. An approximation of the number of planes required, N, can be estimated with the following formula and referring to Figure 4-10.

$$N = \frac{\text{Coverage rate required}}{\text{Coverage rate/plane}}$$

Plane coverage rate;

$$R = 2 a v E h$$

a = altitude

v = block speed

E = coverage efficiency

h = hours flown (block)/per day

Assuming that the resultant variation in lighting conditions can be tolerated by using h = 5 hr/day, and using a required coverage rate of 100 K n.m.²/day (343 K km²/day), the formula reduces to:

$$N = \frac{60,800,000}{a v E}$$

a = altitude, ft.

v = velocity, knots

E = coverage efficiency, decimal

There are a number of aircraft in each of several categories which appear to satisfy all the requirements of payload, range, speed, and altitude for earth observation missions. Strictly speaking, the only requirements are the ability to carry about 800 lb (360 kg) of payload plus a crew of perhaps another 500 lb (230 kg). (See Section 9) The categories of aircraft which could be used to satisfy these requirements range from twin piston engine to four engine jet and are described in Table 4-3. Data for this table was taken from Refs. 9 and 10 and various industry literature.

The above formula, along with the aircraft data of Table 4-3 and the coverage efficiency of Figure 4-6, was used to construct the aircraft requirements of Figure 4-11. This figure, which gives the number of various types of planes required versus number of bases, shows the advantage jets and turbo prop planes have over piston engine planes due to their greater speed and range.

Figure 4-10 Aircraft Coverage Geometry

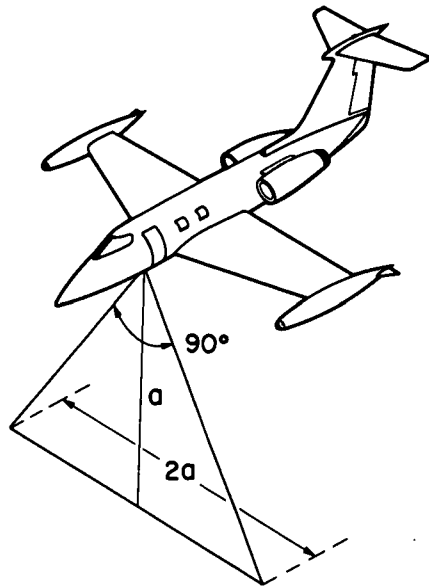


Figure 4-11 Special Fleet Aircraft Required

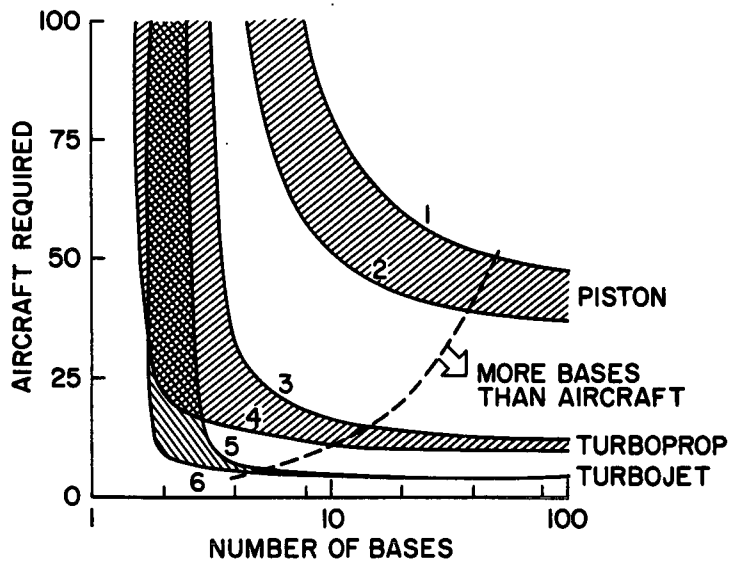


Table 4-3

Candidate Earth Resource Aircraft Characteristics (with crew)

	Piston Multiengine		Turboprop		Jet	
	light (1)	heavy (2)	small (3)	large (4)	Two-engine (5)	Four engine (6)
Typical Example	Twin Comm AE 500U	BE S18	MO MU2	Gulf I	Lear Jet	Jetstar
Purchase Price - F.A.F. \$ Equipped \$	99,950 110,000	179,500 190,000	311,000 320,000	1,119,000 1,300,000	649,000 650,000	1,650,000 1,700,000
Passenger Seats	6	9	5	24	6	10
Fuel Consumption, gal/hr	22	45	60	205	220	535
Block Speed, sm/hr-nm/hr	185-160	195-170	250-220	300-260	450-390	450-390
Range w/1500 lb - nm	1,000	1,300	1,400	2,200	1,700	2,150
Cruise altitude - ft.	8,500	10,000	23,000	25,000	40,000	40,000

Air Carriers

Commercial air carriers would seem to offer an untapped potential for observation of earth resources based on the diverse route schedule that is maintained. A quick glimpse of airway routes (Ref. 11) shows that a great portion of the coterminous United States is covered by high altitude (i.e. above 18,000 foot altitude) commercial traffic.

Most cross-country commercial jets fly between 30 and 40,000 feet (9 and 12 km) altitude which yields a ten to thirteen n.m. (18-24 km) swath width at 90 deg. field of view. The most conservative evaluation of commercial air carrier coverage of the United States would thus be obtained by assuming 5 n.m. (9 km) coverage to each side of the high altitude airways. In reality the effective swath width is much greater because multiple aircraft tracing the same airway will randomly track different ground paths. This is due to the fact that radar and inertial guidance permits ease of navigation off established routes. In addition, flight controllers space planes to provide proper separation distances and vector direct flights to avoid bad weather. A five mile (9 km) random lateral displacement of several aircraft will increase the effective side view to perhaps 10 miles (18 km), resulting in a total effective swath width of 20 n.m. (37 km). Similarly, a 15 n.m. (28 km) displacement will increase the effective swath width to 40 n.m. (74 km).

Graphical solutions of coverage were made which show the degree of coverage to be very high in certain parts of the country even for just the 20 n.m. swath width. Rhode Island is covered completely by a 20 n.m. swath from commercial airways. Other states have coverages varying from 26% in Montana to 92% for Massachusetts; the overall national average is 47%. At an effective 40 n.m. swath width 21 states have a coverage of 90% or better and the national average is increased to 80%. Complete coverage is not easy to obtain, however, because total effective swath widths averaging 100 n.m. (185 km) and as much as 260 n.m. (480 km) would be required. Great lakes coverage averages about 30% for a 20 n.m. swath and 50% for a 40 n.m. swath. Ocean shoreline coverage for 20 n.m. was 59% and for 40 n.m. is 82%.

Resource features are, of course, the primary concern. Commercial airway coverage of these features is generally good - being 75-90%

complete for all areas at 40 n.m. swath width (except northern wheat which is about 50% complete). Figure 4-12 summarizes coverage of the resource features as a function of swath width.

The results given in Figure 4-12 are based on the existence of airways rather than aircraft. Therefore the more important question regarding the use of commercial air carriers to cover the coterminous United States concerns the number of aircraft required, i.e. the number of commercial aircraft that would have to be equipped with observation payloads to provide adequate coverage. Table 4-4, constructed from data from Ref. 12, lists the domestic trunk airlines and an approximation of the number of aircraft held in 1968.

Table 4-4
Domestic Trunkline Aircraft (1968)

American	235
Braniff	73
Continental	54
Delta	122
Eastern	260
National	53
Northeast	39
Northwest	100
PanAm	152
TWA	198
United	342
Western	64
<hr/>	
TOTAL	1692

The aircraft totals of Table 4-4 include all types of aircraft held but are primarily three and four engine jets. Each air carrier generally schedules the aircraft at random over their designated routes, hence any one aircraft will fly an unpredictable path within the carrier's route system. Those air routes in the coterminous United States are regulated by the FAA through 21 Air Route Traffic Control Centers. The general characteristics of these centers and the air traffic within them is summarized in Table 4-5. This information was taken directly or indirectly from Refs. 13-15 and various issues of Aviation Week and Space Technology.

Figure 4-12 Effective Swath Width Covered from Mean High Altitude Jet Airways and Corresponding Resource Coverage

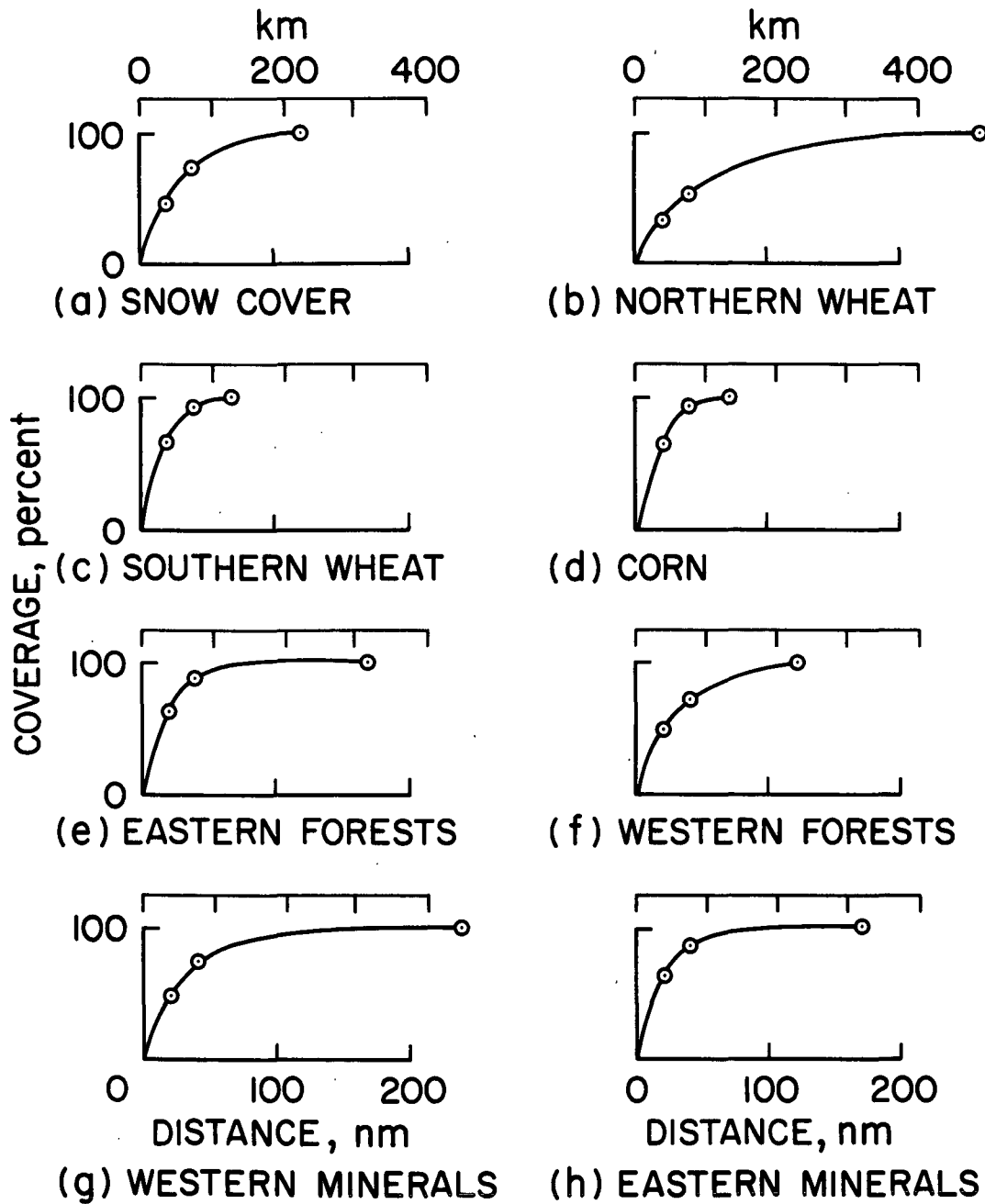


Table 4-5
Airline and Air Traffic Characteristics

Number of Air Route Traffic Control Centers (ARTCC) in Coterminous U.S.	21
Approx no. of air route miles per ARTCC	4500 n.m. (8350 km)
Approx no. of air route legs (between beacons) per ARTCC	30
Approx avg. leg length.	150 n.m. (280 km)
Average aircraft airtime/day	7 hr/day
Average aircraft speed	450 n.m./hr (835 km/hr)
Average aircraft miles/day	3000 n.m./day (5600 km/day)
Average total aircraft miles/day	4.5 x 10 ⁶ n.m./day (8.3 x 10 ⁶ km/day)
No. of aircraft in service	1500
Total airline legs.	630
Legs covered/day by average aircraft	20
Total leg mileage	95,000 n.m. (175,000 km)

Not all airways bear the same traffic. However, to a first approximation it can be assumed that the coverage of the various air route legs is random. If it is assumed that the average commercial aircraft flies twenty 150 n.m. (280 km) air route legs per day for a total of 3000 n.m. (5600 km) per day, it is possible to calculate the probability of covering any number of the 630 total air route legs versus the number of planes equipped. The probability, P_q , of covering q particular air route legs

$$P_q = (P_h)^q$$

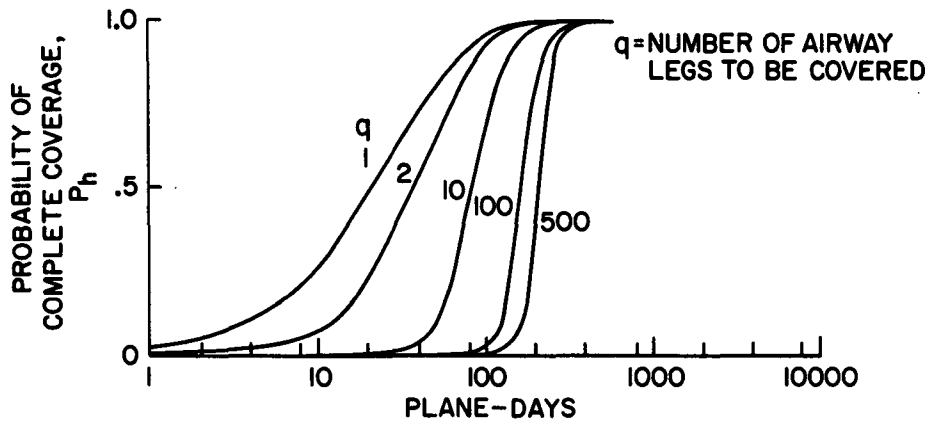
where P_h is the probability of covering any particular air route leg and is given by:

$$P_h = 1.0 - \left(\frac{629}{630}\right)^{20n}$$

In the above expression n is the number of plane days flown and $20n$ represents the number of legs randomly covered by n plane days.

Figure 4-13 shows the probability of covering various numbers of air route legs versus plane-days, i.e. versus the product of the number of planes equipped with sensor packages and the number of days they are flown.

Figure 4-13 Probability of Covering Various Numbers of Air Route Legs



(The latter merely states that since the flying patterns are random, one plane flying ten days produces the same result as ten planes flying one day, exclusive of cloud cover considerations.) The curve for $q = 1$ in Figure 4-12 also represents the fractional coverage that is expected in any area of any size since the expected coverage is equal to the probability of coverage of any particular element.

The fractional coverage curve is probably the most informative, but more refinements are appropriate. Commercial air carriers are frequently directed to fly other than the established airways and the airway and directed coverage must be included in the analysis of expected resource coverage. The Department of Transportation, through the FAA, collects and compiles a great deal of statistical information concerning commercial, military, and general aviation. This data is primarily intended for planning aviation facilities and services, and therefore lacks the statistics that would be most useful in planning Earth resources coverage. Certain general conclusions can nevertheless be drawn from such sources as the Enroute IFR Peak Day Charts (Ref. 13) which show a facsimile of the actual traffic pattern for the busiest day of the year within each of the Air Route Traffic Control Centers (ARTCC). These charts show a significant number of high altitude flights (above 18,000 feet) in other than the established jet airways. In most traffic control areas there were as many directed routes carrying five or more aircraft on the busiest day as there are established airways. This would seem to imply a reasonable confidence that additional areas are and will be covered as a matter of course. Unfortunately, the random nature of these directed flights, the failure of most centers to distinguish between commercial, military, and general aviation flights, the omission of time of day, and manner of chart preparation precludes any definitive statement of the exact coverage that can be expected. The following formulae were used to calculate the fractional coverage of an arbitrary area that can be expected as a function of plane days. The assumptions used to construct these formulae are 1) that there are as many directed routes as established air routes, making a total of 1260; 2) that for each seven airway flights there are three directed flights; and 3) only one out of two flights will have both proper lighting conditions and an absence of cloud cover.

The fractional coverage of an area with half airway legs and half directed legs is equal to the average coverage, or:

$$F_q = \frac{1}{2} F_{\text{airway}} + \frac{1}{2} F_{\text{directed}}$$

Since the fractional coverage of an area is equal to the average cumulative probability of overflying any single element within the area

$$F_q = \frac{1}{2} \left[1.0 - \left(\frac{629}{630} \right)^{7n} \right] + \frac{1}{2} \left[1.0 - \left(\frac{629}{630} \right)^{3n} \right]$$

where n = the number of plane.days.

Figure 4-14 shows this fractional coverage plotted against plane.days. For example, 100 planes would achieve 50% fractional coverage in 1 day or 75% coverage in two days, or virtually 100% coverage in 10 days. Note that this coverage is only a measure of air route coverage. Actual resource or area coverage is a function of swath width as well. That is, even with an infinite number of plane-days coverage can only be as good as was indicated in Figure 4-12. Figure 4-12 however, only includes airway coverage; it does not include the contribution of directed flights. Figure 4-15 is an approximation of the effect of these extra flights. It is assumed that an additional increment of coverage is possible as a function of the maximum coverage that can be obtained from the established airways.

Using Figures 4-11, 4-13, and 4-14, then, it is possible to determine the fractional coverage of the various resource areas as a function of plane days as shown in Figure 4-15. An effective swath width of 30 n.m. (56 km) or 15 n.m. lateral coverage is assumed, based on a reasonable combination of 10 n.m. swath width and 10 n.m. displacement. Figure 4-16 indicates that not all resource areas can be completely covered by air carriers with an effective 30 n.m. swath width. About 95% of the best coverage that can be expected for all resource areas can be achieved in 500 plane days. If coverage is required every two weeks on the average, then 36 planes would be required.

Special Fleet/Air Carrier Comparisons

Although any final comparison between data gathering methods must be on an economic basis, the relatively small number of planes

Figure 4-14 Fractional Coverage of Random Area

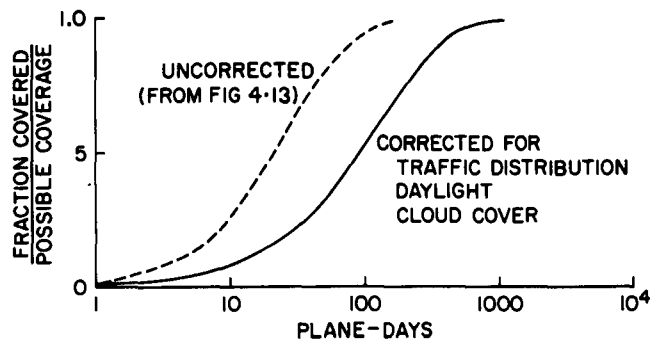


Figure 4-15 Contribution of Directed Air Routes

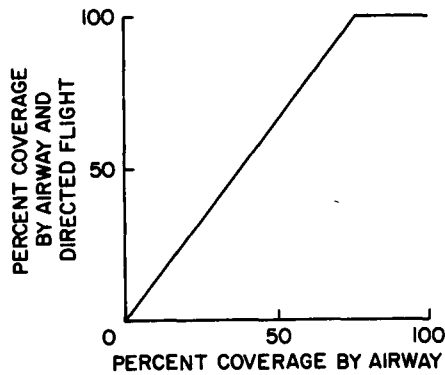
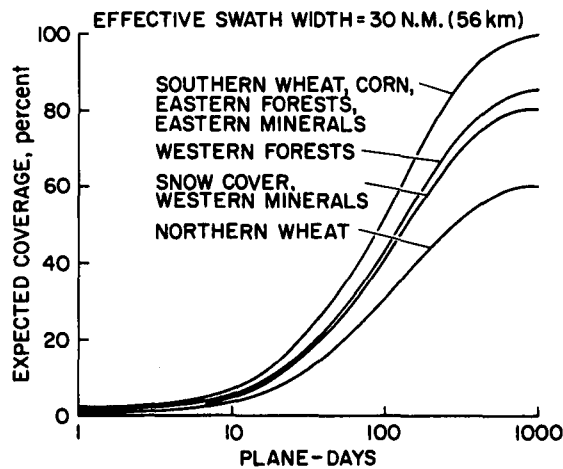


Figure 4-16 Expected Coverage of Resource Areas from Commercial Air Carriers



required in either case would seem to imply that data handling rather than data gathering will be the driving cost factor. In the meantime, it is not too unreasonable to speculate that the advantages provided by the special fleet (i.e., better potential coverage, more flexibility in scheduling, fewer interfaces with FAA and commercial interests, etc.) make it a more reasonable approach to Earth resource observations. In a broader sense, it appears that aircraft can and will play an important role in future Earth resource observation programs, at least for the coterminous United States.

5. SIGNIFICANCE OF CLOUD COVER

The objective of this analysis is to determine the effect of cloud cover on the number of satellite passes and the number of satellites necessary to observe a given portion of each primary Earth resource area of the continental United States and Alaska. Interpreted properly, the results apply to aircraft borne acquisition systems as well.

Cloud Cover Data

Actual global cloud cover data acquired from Nimbus and ESSA satellites were used in conjunction with a cloud cover simulation computer program (Refs. 16, 17) to provide an approximation of cloud cover encountered. Using the expected cloud cover data (which include persistence, spatial, and temporal probabilities) applicable to the seasonal time period of each application, it is possible to calculate the number of identical ground track satellite passes required to observe a given portion of each resource area.

As an independent verification of the cloud cover simulation technique, use was also made of aircraft cloud cover data derived from USAF pilot observations (Ref. 18) on clear lines-of-sight. The statistical sample was not as large as that from which the satellite data was derived. Further, to avoid subjective judgment on the extent of cloud cover, the pilot observers were instructed to report only either clear (no obstruction) or not-clear (100% obstructed) vision. Thus the 'extent' of cloud cover is statistically inferred for each sector observed, and the data may tend to show greater cloud cover than actually existed. For most cloud regions over the resource areas of continental United States, however, the cloud cover predicted by simulation of the satellite data and the observer reports from high altitude aircraft are quite similar, varying no more than 10%. Only data obtained from high altitude aircraft (35,000 to 45,000 foot altitude) were used in this comparison. Since virtually no clouds exist at higher levels the data should be expected to provide the best agreement with the satellite derived data. Second, of course, to maximize swath width of aircraft borne sensors, the aircraft would also operate within this altitude range. Operations from lower

altitudes would minimize the effects of cloud cover but would result in an overall reduction in coverage capability.

During this study, Mr. V. J. Oliver, National Environmental Service Center, was most helpful in providing additional information about some current Earth resource survey projects and cautioned against a too literal interpretation of their results. As an example, the Air Force spent about one year mapping roughly one-third of Africa with high-altitude aircraft. But with the assistance of APT satellite cloud pictures, they were able to map the remaining two-thirds of Africa in about nine months because the aircraft could be directed in advance to cloud-free areas. Mr. Oliver also pointed out that if we were to use the global region cloud cover data derived from ESSA and Nimbus, which were taken daily at 1300 hours local standard time, the resultant conclusions may not represent reality. As a guide in photographing the resources of Florida, for example, we would obtain very poor results. Florida is a small area in global cloud region 19. The probability of cloud cover over region 19 is normally about 50%, yet at 1300 hours most of Florida usually is completely covered by scattered clouds and local thunder storms; whereas at 0800 hours, Florida is usually free of cloud cover.

The persistence of cloud cover over a specific geographic region is a function of many factors, including season, location (latitude/longitude), local terrain (mountains, valleys, etc.), time of day, wind patterns, predominant barometric pressures, etc. However, because the actual data were collected for large geographic regions, statistically they tend to compensate.

Results

The Monte Carlo procedure for determining the statistical variability of the Earth's cloud cover formed the basis for the results that follow. Each resource area was apportioned by cloud region and expressed as a percent of total area. The summation of the products of each resource area percent and expected average cloud cover percent provided the weighted average percent cloud cover (C) for each resource area during the relevant observation period. (See Figure 4-8 for observation schedule.) The cloud cover data is summarized in Table 5-1. For Alaska and the continental

United States the entries represent average annual values. (See Appendix B for details.)

Table 5-1
Average Annual Cloud Cover

<u>Observation Region</u>	<u>Percent Cloud Cover</u>
Minerals	38.4
Continental United States	53.9
Forests, Wheat, Corn & Delta Crops	58.8
Gulf Fishing	60.7
Snow Cover	62.7
Alaska	69.1
Pacific Fishing	73.7
Icebergs	79.8

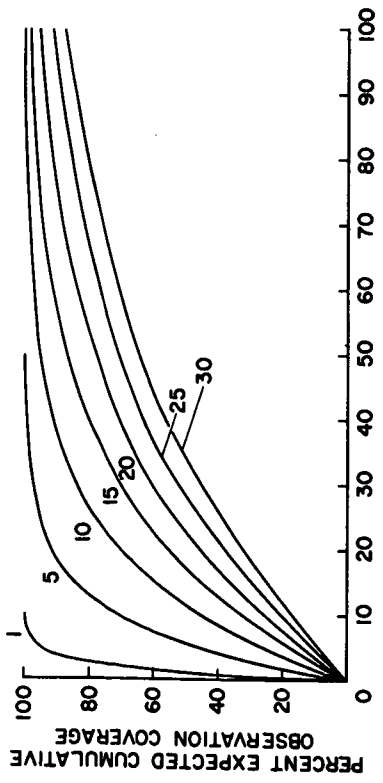
The fraction of an area or resource that can be observed (B_n) is, then, a function of the weighted average cloud cover (C), the total time allotted for coverage (T_0), and the length of time between repetitive satellite passes (T). The fractional coverage, B_n , is found from the equation

$$B_n = 1 - C T_0 / T$$

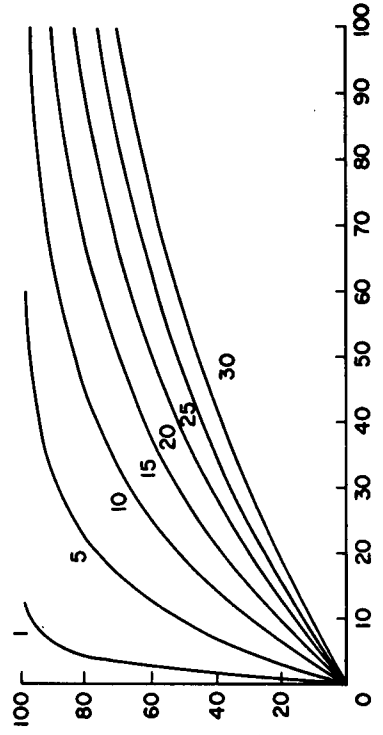
in which case the ratio T_0/T represents the number of identical ground traces over a given area in time T_0 . Figure 5-1 was prepared using this equation. The fractional coverage, B_n , is found on the ordinate, the time allowed for coverage, T_0 , is found on the abscissa, and shown parametrically on the face of the graph is a series of curves representing different values of T , the actual coverage interval.

Parts (a) and (b) relate to the continental United States and Alaska respectively. Results for the minerals and icebergs regions are shown, in parts (c) and (d), since they represent the two extremes.

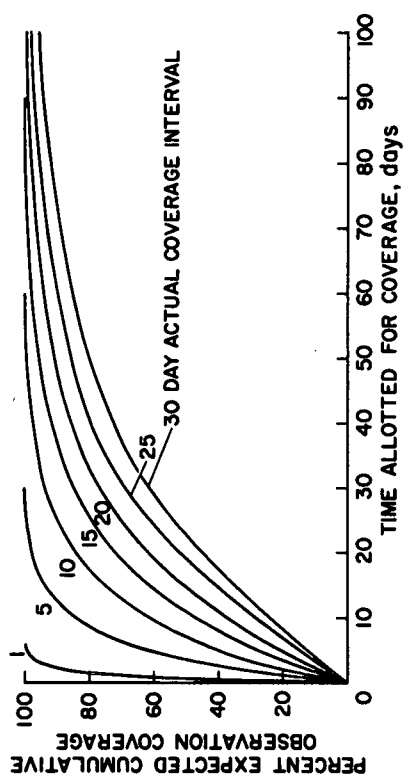
Figure 5-1 Observation Coverage as Influenced by Cloud Cover



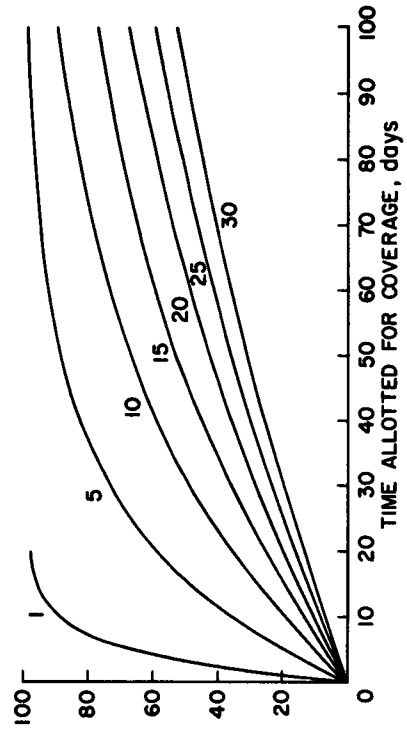
a. Continental United States



b. Alaska



c. Mineral Resources



d. Iceberg

It should be noted that for cloud cover over a given geographic area to assume random distribution (a primary condition for this statistical variability computation), viewing frequencies between identical ground-tracks must be at least a day apart. As suggested by Oliver, most cloud systems change pattern significantly on a one to three day period, whereas little change is noted in a shorter time scale.

The results of this analysis indicate that 95 percent of the selected Earth resources of the continental United States and Alaska, including off-shore fish and iceberg flow, can be observed by satellites or aircraft in no more than ten identical ground track passes as a consequence of random cloud cover over each resource region. In order to better describe the uses of the figures, several examples of various satellite systems are cited using Figure 5-1 (a).

Example 1: Assume a requirement to observe the continental United States in the visual or IR spectrum every 20 days. From Figure 5-1 (a) it is seen that if the satellite altitude and sensor swath width are chosen accordingly (i.e., the actual coverage time is, in fact, 20 days) only 46 percent of the area will have been observed.

Example 2: Assume that a 20 day coverage interval remains as a requirement but, in addition, at least 90 percent of the country must be viewed during the 20 days. In this case the actual coverage interval must be about 5 days, necessitating either more satellites or a wider swath width.

Example 3: Now assume that the swath width associated with the 5 day coverage interval (which is therefore about four times as wide as that associated with a 20 day coverage interval) degrades the spatial resolution of the sensor to unacceptable values. If the requirements are firm then three additional satellites will be required, each of which will cover the country every 20 days. The orientation of the orbit planes of each satellite must be such

that their ground tracks overlap but are separated in time by about one day. (Recall that major cloud patterns are essentially stationary for shorter time periods.)

Example 4: Finally assume that it is really only necessary to overfly the country every 60 days. Then the single satellite of Example 1 will observe, on the average, 85 percent of the area during the 60 day period.

6. SENSOR CAPABILITIES

The generalized user requirements discussed in Appendix C define the general characteristics of the data acquisition systems needed. Factors such as spatial resolution, spectral range, temperature sensitivity, etc., serve to identify the applicable sensing techniques and to set the pertinent performance limits for these systems. Flexible sensors, in the form of scaling laws, can then be developed for techniques that appear to have feasibility. Application of these scaling laws over the range of possible operational conditions will define the extent to which the requirements can be met and also permit the selection of the best mix of operational conditions and point design sensors. This section of the report deals with the development of these scaling laws.

Two major factors influence the development of a useful scaling relation for a sensor type. The first consists of the physical laws that govern the operation of the particular device being considered and the second involves the state of the technology in each of the component areas which, when combined, form the sensor. Since this study is being performed in the context of operational Earth observation missions circa 1980, all required technology in support of these missions must essentially be available in practical form by the 1976-77 period. This will allow four to five years for translation of a rough experimental model verifying basic feasibility to a developmental status sufficiently advanced to warrant inclusion in a prospective payload. The projected technology limits used in the study are summarized in Table 6-1. These limits are not necessarily physical in nature but, in certain instances, reflect our judgment of what appears to be practical. For instance, the maximum aperture diameter of one meter seems reasonable based on weight and cost considerations but, of course, is not an absolute limit.

The relationships presented here are in the context of the platforms considered in the study. For spacecraft, a typical velocity of 7.8 km/sec is used since the variation over the range of useful

TABLE 6-1

PROJECTED TECHNOLOGY LIMITS

	<u>Film</u>	<u>Vidicon</u>	<u>MSS</u>	<u>IR</u>	<u>μ Wave</u>	<u>Radar</u>	<u>Scatt</u>
Aperture Size (cm)	100	100	100	100	300 λ	1000 λ	1000 λ
Focal Length (cm)	635	635	635	635	--	--	--
IFOV (per line pr)	2.2	5.3	32	32	8000	19 ⁽¹⁾	2400
Detector Performance	72 1/mm	30	See Fig. 6-11	See Fig. 6-13	--	--	--
Flying Spot Scanner	5 μm	--	--	--	--	--	--
Geometric Fidelity	Metric ⁽²⁾	Non-metric	--	--	--	--	--
Radiation	Shield Req ⁽³⁾	No Shield	--	--	--	--	--
Format Size (mm)	228	51	--	--	--	--	--
Receiver Noise	--	--	--	--	See Fig. 6-19	See Fig. 6-24	See Fig. 6-24
Receiver Bandwidth	--	--	--	--	0.1 f ₀	--	--
Pulse Duration	--	--	--	--	--	10 ⁻⁹	10 ⁻⁹
Compression Factor	--	--	--	--	--	400	--
Peak Power	--	--	--	--	--	4X10 ⁸ λ	4X10 ⁸ λ
Pulse Rate	--	--	--	--	--	10 ⁶	10 ⁶

(1) Based on arbitrary power limit of 10 KW, 590 Km altitude, 45 degree depression angle.

(2) See Appendix D.

(3) See Appendix E.

altitudes is small. For aircraft, a typical velocity of 215 m/sec (485 mph) is used.

In defining the sensor environment, a worst case approach was used throughout. That is, the lighting and contrast conditions considered were those representative of the most difficult anticipated. Better conditions will, of course, result in better performance. Throughout the paper, a line pair convention has been used for resolution since, for all imaging devices, a change in the imaged field requires two adjacent resolution elements to be discernible. This just permits detection of a contrast change, not identification of objects or shapes. More line pairs, varying with the type of object, lighting conditions, etc., are required for identification. Many sources were used in the development of this material but the primary sources were Refs. 19 and 20.

Sensing techniques potentially useful for Earth resources missions have been identified in previous studies and experimental programs. These sensors, in the order of presentation in the following material, are: Film camera, television, multispectral scanner, infra-red scanner/radiometer, microwave scanner/radiometer, radar and scatterometer. Two sections which apply generally, one covering nomenclature and the other optical components, precede the sensor discussion.

Nomenclature

<u>Symbol</u>	<u>Description</u>	<u>Units</u>
A	Collector Area	cm ²
A _c	Coverage Area	km ²
A _d	Detector Area	mm ²
A _f	Film Spool Area	cm ²
B	Instantaneous Field of View (IFOV)	rad

<u>Symbol</u>	<u>Description</u>	<u>Units</u>
B_r	Real Antenna Beamwidth	rad
B_s	Synthetic Aperture Beamwidth	rad
C	Compression Factor	- - -
C_m	Radiometer Constant	$^{\circ}\text{K sec}^{1/2}$
D	Image Plane Format Dimension	mm
D^*	Specific Detectivity	$\text{cm Hz}^{1/2} \text{W}^{-1}$
D_c	Aperture Diameter	cm
D_s	Scanning Spot Diameter	μm
D_R	Data Acquisition Rate	bps
D_{SA}	Synthetic Aperture Length	m
D_T	TV Tube Diameter	cm
F	Focal Length	cm
F_R	Effective System Noise Figure	- - -
G	Grey Scale	- - -
H	Altitude	km
L	Total Lines Per Frame Height	- - -
L_a	Antenna Aperture (Azimuth)	m
L_f	Film Length	m
L_t	TV Tube Length	cm
L_v	Antenna Aperture (Elevation)	m
M	System Weight	kg
M_A	Antenna Weight	kg
M_C	Primary Mirror Mass	kg
M_M	Structure Mass	kg

<u>Symbol</u>	<u>Description</u>	<u>Units</u>
M_s	Secondary Mirror Mass	kg
M_{sh}	Shielding Mass	kg
M_{sm}	Scan Mirror Mass	kg
N	Number of Cells	- - -
N_λ	Spectral Radiance	$Wcm^{-2}ster^{-1}$
P	Average Power	W
P_t	Peak Power	W
R	Resolution (pixel pair)	m
R_s	Film roll outer radius	cm
S	Swath Width or Ground Size	km
S_n	Signal-to-noise Ratio	- - -
T	Temperature	$^{\circ}K$
ΔT	Change in Temperature	$^{\circ}K$
V_a	Antenna Volume	m^3
V_s	Platform Velocity	km/sec
c	Speed of Light	3×10^5 km/sec
d	Detector Size	mm
d_c	Duty Cycle	- - -
f	Aperture Ratio (f/stop)	- - -
Δf	Bandwidth	Hz
f_o	Operating Frequency	Hz
g	Fractional overlap	- - -
l	Resolution	lines/mm
m_p	Pitch Motion	mm
m_r	Roll Motion	mm

<u>Symbol</u>	<u>Description</u>	<u>Units</u>
m_t	Total Motion	mm
m_y	Yaw Motion	mm
n	Number of Detectors	- - -
p	Pulse Repetition Rate	sec^{-1}
r	Slant Range	km
t	Transmittance of Optical System	- - -
t_c	Cycle Time	sec
t_e	Data Collection Period	sec
w	Film Thickness	cm
α	Scan Angle	rad
$\dot{\alpha}$	Image Motion Rate	rad/sec
ϵ	Quantum Efficiency	- - -
θ	Depression Angle	rad
$\dot{\theta}$	Yaw Rate	rad/sec
λ	Wavelength (optical)	μm
λ_r	Wavelength (radio)	m
ρ	Reflectance	- - -
$\Delta\rho$	Change in Reflectance	- - -
τ	Dwell Time or Time Constant	sec
τ_a	Pulse Duration	sec
τ_c	Compressed Pulse Duration	sec
$\dot{\phi}$	Pitch and Roll Rate	rad/sec
ω	Rotational Speed	rad/sec

Optical Component State-of-the-Art

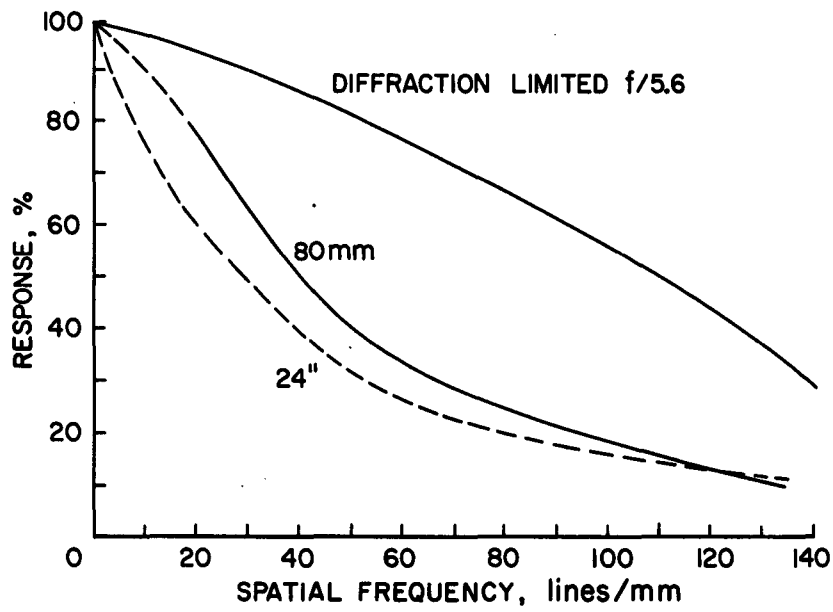
In this paper, the size of the collecting aperture in optical systems has been arbitrarily limited to one meter diameter. As mentioned earlier, one meter has been chosen not as a real state-of-the-art limit but rather as a practical economic limit for a spacecraft in the time frame of interest in this report. Near diffraction limited apertures on the order of five or six meters in diameter are not out of the question (although maintaining near diffraction limited performance in space for such large apertures poses many extremely serious structural and thermal problems, perhaps requiring active optics). However, the cost and complexity associated with apertures of this size, the demanding stabilization and control problems required to make effective use of such resolving power potential and the enormous weight of such large apertures all seem to rule out serious consideration of such systems except, possibly, for a large observatory dedicated to astronomical observations. While the one meter size restriction is clearly an arbitrary limit, it nonetheless represents a very significant undertaking for space flight.*

The performance of a good present day lens, as typified by the lenses used in the Lunar Orbiter camera system (Ref. 21), is shown in Figure 6-1. Overlaid on the same figure is the performance of a diffraction limited $f/5.6$ lens. Throughout this analysis it has been assumed that diffraction limited performance can be attained and, as this figure shows, improvement over present practice is not insignificant. However, once all of the other elements involved in computing the overall modulation transfer function (MTF) of the camera system are taken into account, the effect of the lens on performance is minimized. Consequently, the gain is not nearly as dramatic as one might expect.

Focal lengths as large as 635 cm have been used in this study. With a singly folded system, the optics will then somewhat exceed

* Spaceborne telescopes as large as 91.4 cm (36 inches) have been built (OAO-B) but not with near diffraction limited performance. However, heavy balloon suspended systems (Stratoscope II) of the same size having such capability have been flown.

Figure 6-1 Measured MTF of Typical Camera Lenses for a Heterochromatic Source



320 cm (over ten feet). Since a reasonable focal ratio (f stop) is required to achieve good spatial frequency response, apertures in the range of one meter will be required with such long focal lengths. For example, at the 635 cm focal length, an aperture of one meter results in an f/6.3 focal ratio. A stop of about this size or smaller is required for most of the applications discussed.

Film Camera Systems

The frame camera is the most highly developed visual imaging device available. It is capable of high spatial resolution and excellent geometric fidelity. The principle disadvantages of this system are the non-reusable and radiation sensitive nature of film and the processing required before the recorded image can be utilized. For long lifetime spacecraft, these considerations pose serious problems, primarily from the standpoints of size and weight.

In this section of the report, component state-of-the-art will be discussed and scaling laws useful for estimating the performance of film cameras will be developed.

Camera System Component State-of-the-Art

Because of the long history of the art, camera system components are highly sophisticated at this time. Barring totally unforeseen breakthroughs, relatively small progress can be anticipated in any of the component areas in the next five to ten years. The status of each of the major components is discussed briefly below.

Geometric Fidelity. Precision film cameras can satisfy the metric accuracy requirements outlined in Appendix D (assuming hard copy return). With the flying spot readout, however, non-linearities can be introduced by the scan system. These can be minimized by restricting the scan amplitude during readout and by the use of an accurate pre-exposed pattern on the film. These measures should permit meeting the metric standards even when electronic readout and ground reconstruction is employed.

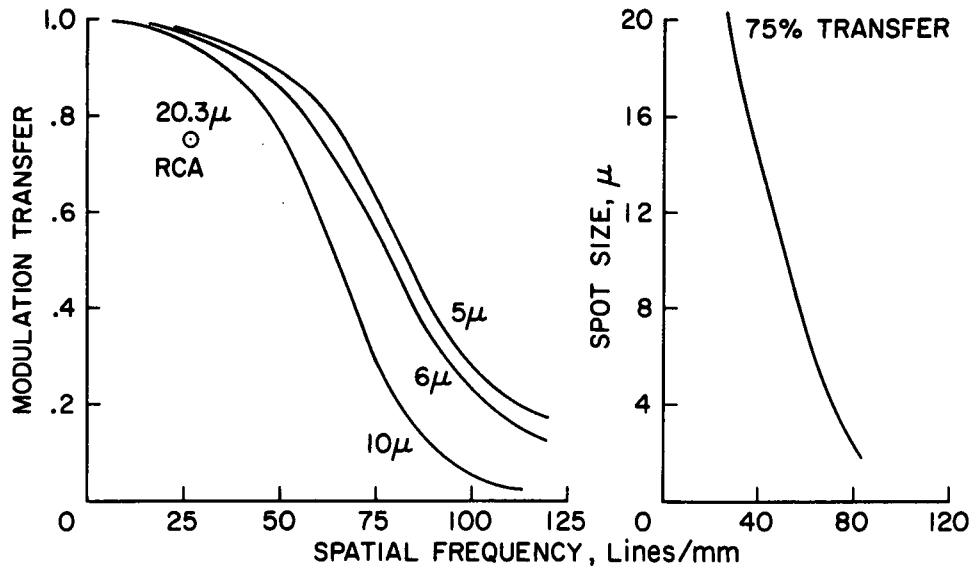
Flying Spot Scanners. The performance of current flying spot scanners of the type required for film readout (Ref. 22) is shown in Figure 6-2(a). The scanner spot size for a modulation transfer of 0.75 as a function of spatial frequency can be specified as shown in Figure 6-2(b). The use of lasers and light emitting diodes should make improvement in this area by a factor of 2 or more feasible. The theoretical limit on the size of the spot diameter is a function of the wavelength of the light used and the F number of the minifying optical lens assuming that the light source illumination is sufficient.

Film. The present performance of some typical aerial films (Ref. 23) is shown in Figure 6-3. Film performance seems to be quite adequate when considered in the context of the other system elements. Major improvements in the near future do not seem likely nor necessary. There are problems with film, however, not related to resolution performance. The more significant of these in the context of Earth orbital operations are radiation sensitivity and onboard processing.

The bimat system used for Lunar Orbiter onboard processing has a life of about 60 days. It appears likely that this can be significantly extended although to date insufficient work has been done to justify great confidence. Another onboard processing technique, known as Poromat, has demonstrated a life expectancy of about one year under laboratory conditions. But again, insufficient work has been done to justify great confidence. However, it appears that no real technological barrier prevents achievement of long-life onboard processing systems of this general type.

The radiation sensitivity of film primarily impacts the support requirements for film systems (shielding weight) which are discussed in the following section. A general discussion of film radiation sensitivity is provided in Appendix E.

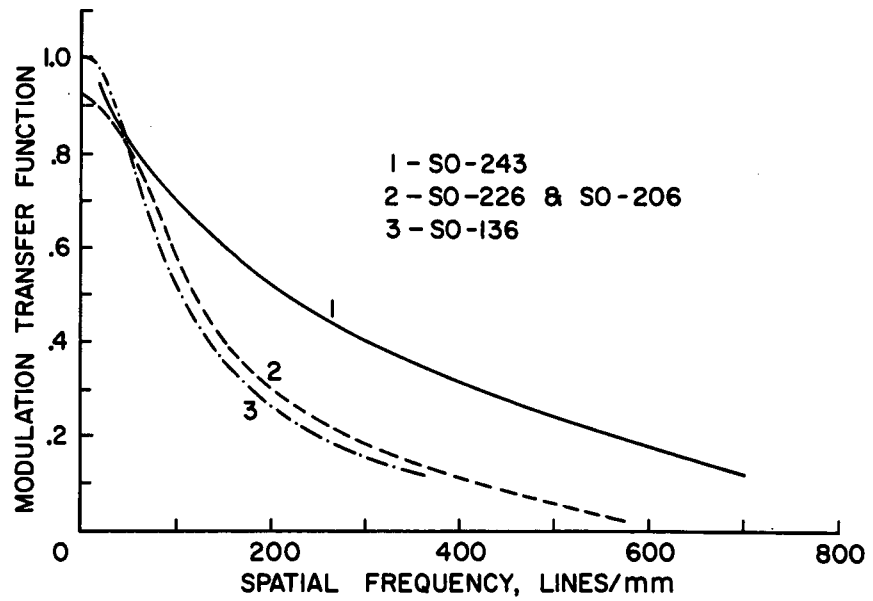
Figure 6-2 Flying Spot Scanner Performance



a. Modulation Transfer

b. Required Spot Size

Figure 6-3 Film Modulation Transfer Function



Camera System Scaling Laws

The overall performance of a film camera system is determined by a number of factors including scene brightness, contrast and content, atmospheric transmission and scattering, the camera lens, image motion, the film, processing, the readout system, and finally, ground reconstruction. All of these factors are most conveniently related by means of modulation transfer functions (MTF). With this approach, the fidelity of spatial frequency transfer for each element of the system can be determined or estimated and the transfer of the overall system defined by multiplying together the individual responses. For typical low contrast scenes observed from space, a transfer of about 75 percent at the spatial frequency corresponding to the desired resolution is required from the lens, image motion, film and the readout system (See Appendix F). It is assumed here that one line pair, or spatial frequency cycle, corresponds to one resolution element. Referring to Figure 6-3, which shows the modulation transfer as a function of spatial frequency for special high definition aerial film (S0-243), it is seen that 75 percent response corresponds to a spatial frequency of about 72 lines per millimeter. Taking this as the ultimate capability of film systems in operational situations, some very simple relationships portraying the performance of film systems can be developed.

Figure 6-4 illustrates the geometrical relationships pertinent for a frame type imaging system. Since the two triangles shown are similar, the ratio of the spacecraft altitude, H, to the focal length of the camera, F, is the same as the ratio of the ground size (swath width), S, to the format size of the camera, D. Thus, the swath width can be expressed as

$$S = 0.1 D \frac{H}{F}$$

This expression is plotted in Figure 6-5 for $F \leq 635$ cm.

Figure 6-5 Film Camera Swath Width

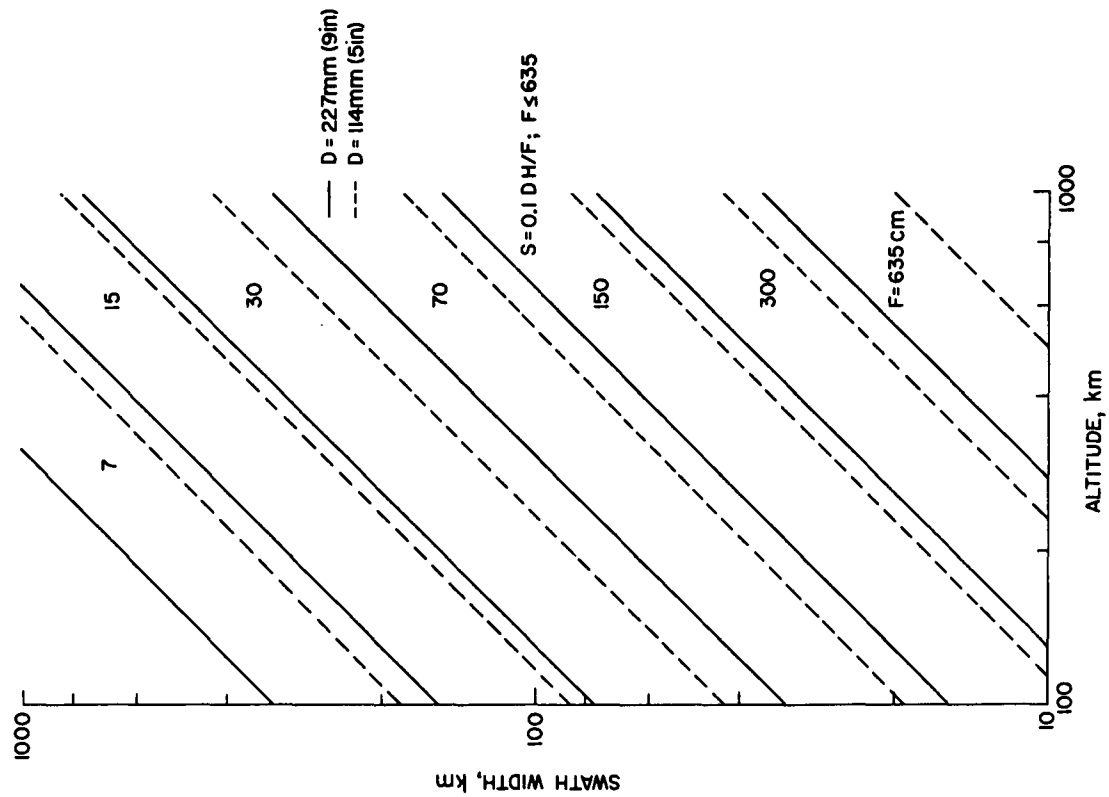
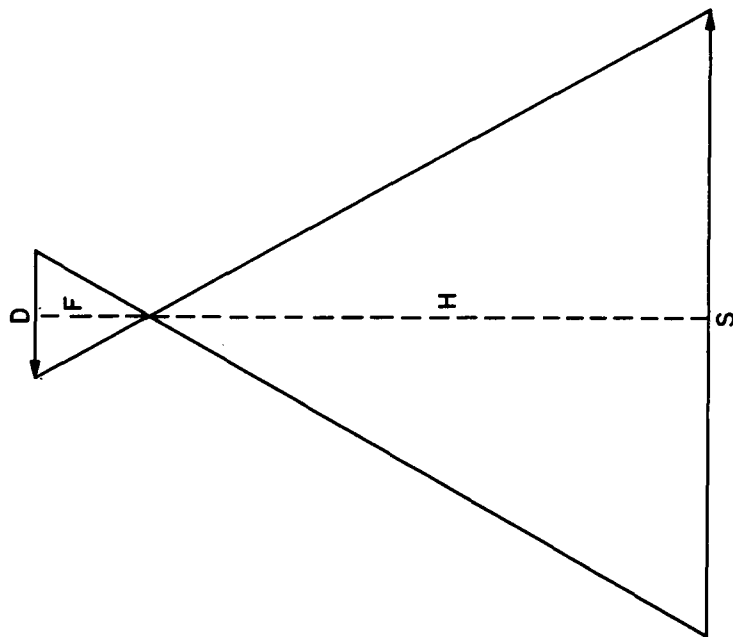


Figure 6-4 Film System Geometry



The resolution of the system is simply the ground size divided by the total number of line pairs available. Consequently,

$$R = \frac{S \times 10^3}{72D}$$

or, substituting for S,

$$R = 1.38 \frac{H}{F}$$

This relationship is shown in Figure 6-6.

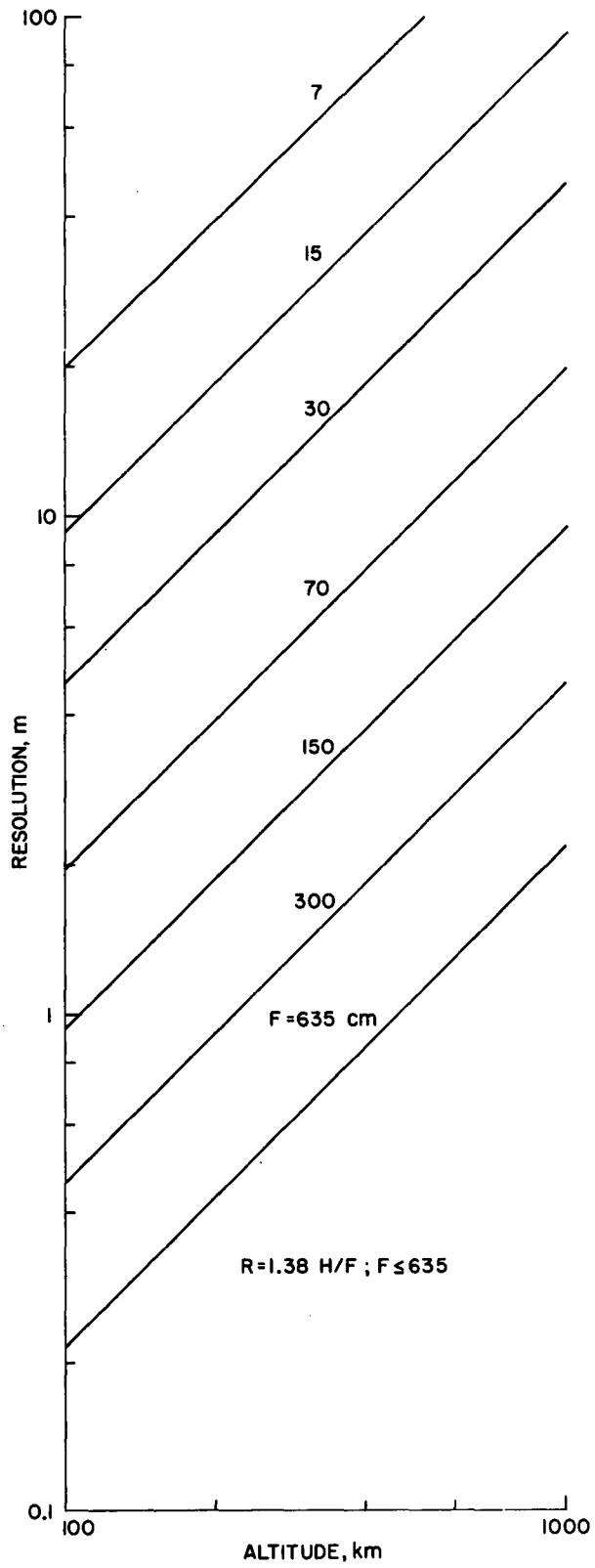
A given technology level limits the attainable resolution of spacecraft film camera systems under low contrast conditions to the value set by the smallest attainable ground size and the total number of line pairs available. Thus,

$$R_{\max} = \frac{S_{\min}}{LD} = \frac{36H}{16400} = 2.2 \times 10^{-3}H$$

Television

Television systems are all electronic analogs of the film camera discussed previously. While in many ways these two systems are designed to do essentially the same job, there are a number of important differences, especially in processing and readout. Clearly, other factors being equal, television systems are preferred to standard photographic methods for spacecraft applications because of the difficulty in handling and processing the film. In addition, some types of aerial film have a rather limited unshielded life in Earth orbit because of radiation sensitivity. Nonetheless, it is feasible to safely store a large quantity of photographic film aboard a spacecraft, to process that film aboard the vehicle, and to read it out electronically. These competing circumstances make it necessary to examine the role of both film and electro-optical sensor systems in future Earth observations spacecraft.

Figure 6-6 Film Camera System Spatial Resolution



The state-of-the-art of current television sensors will be examined and scaling laws for estimating the performance of TV systems will be developed in this section.

Television System Component State-of-the-Art

The only component unique to television systems that must be covered is the image tube itself. It combines the functions of the film processor and the flying spot scanner used in film systems. Typical state-of-the-art MTF data for high quality television components are shown in Figure 6-7. The effect of reading beam sharpness on tube performance can be readily appreciated from the figure. The performance of a current laboratory model (Ref. 24) return beam vidicon (without lens) is shown in Figure 6-8. While somewhat better performance may now be possible, it is unlikely that significant changes will occur in the next few years because of the many factors affecting performance, e.g., photo-conductor spread function, electron source and beam diameter, field mesh period, etc.

The electron optic, which contains the components that deflect and focus the reading beam, is the most complex part of the electronic readout system in TV tubes. It must provide uniform beam focus over the format, uniform electron landing and low image distortion. These requirements tend to limit the useful format size possible with TV tubes. The largest photoconductor format size tested to date capable of the performance shown in Figure 6-8 is 50 mm (4.5" RBV). While format sizes up to 100 mm appear feasible with reasonable power requirements (Ref. 24), it seems unlikely that the development pace will make them available in the time frame considered here.

The geometric fidelity requirements outlined in Appendix D do not appear to be attainable with present or near term future TV technology. Factors contributing to this difficulty include small format size, sweep circuit non-linearity, target dimensional instability with time and environmental changes, and electron optic changes (Ref. 25).

Figure 6-7 Sine Wave Modulation Transfer Functions of Television Camera Components

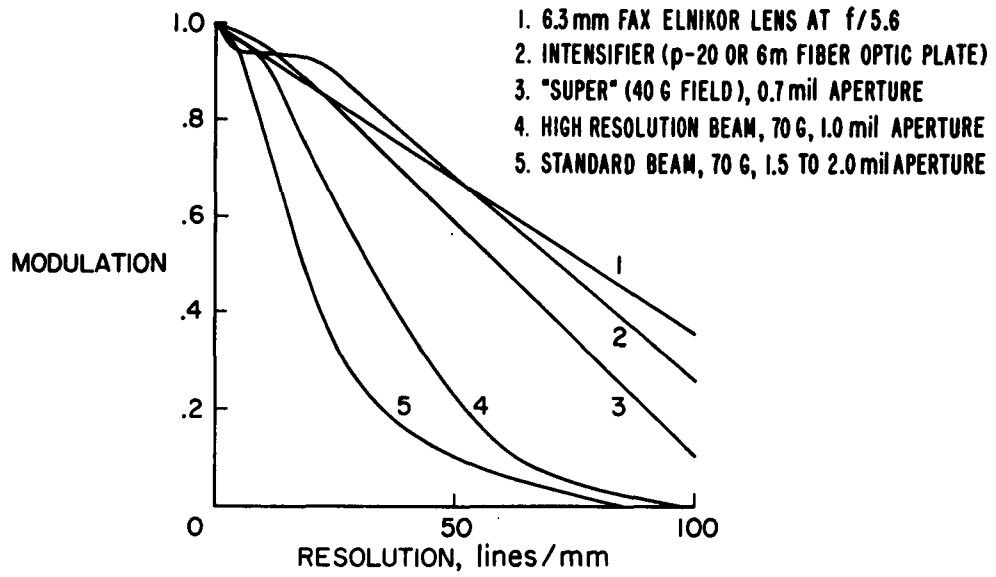
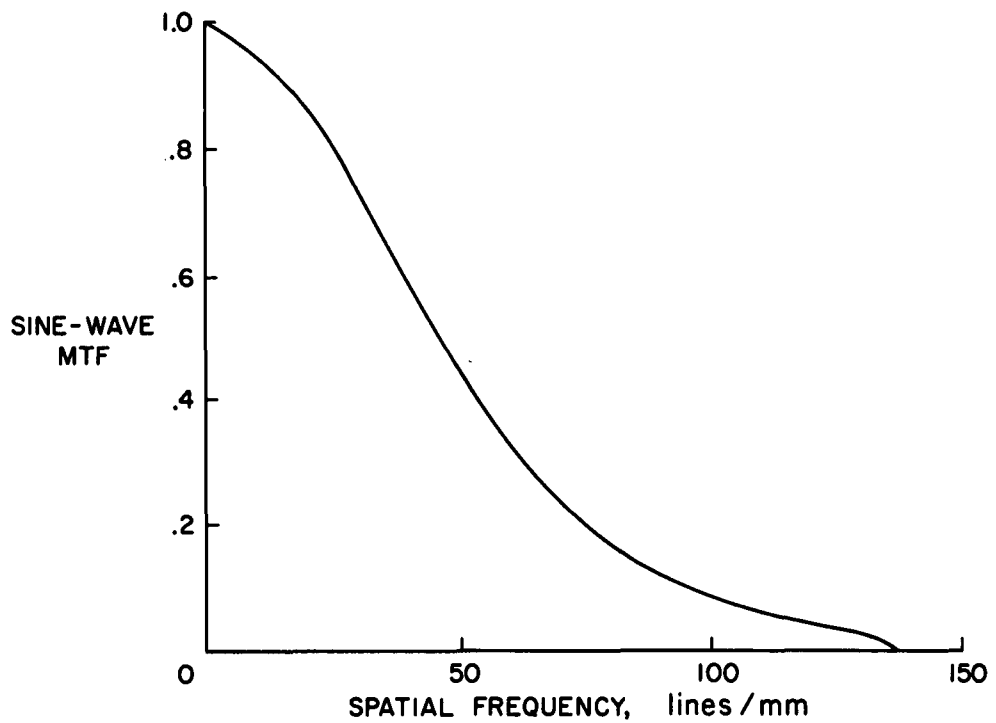


Figure 6-8 4.5" RBV Modulation Transfer Function (Without Lens)



Reseau marks on the target can be used to minimize these problems but location of a point in the image plane to much better than 1 percent of the format size seems unlikely.

Television Scaling Laws

The factors affecting the performance of a television system are much the same as those that affect the performance of a film camera system, e.g., scene brightness, contrast and content, atmospheric transmission and scattering, the lens, image motion, and the characteristics of the photo-mosaic. Similarly, the MTF approach is equally applicable to Vidicon systems. There are, however, two major differences. First of all, processing is not required for a Vidicon system since the electrical image is translated in near-real time to electronic signals where it can be either transmitted directly or stored for later transmission to ground stations; and secondly, the readout process is integral with the electro-optical sensor in contrast with the external flying spot scanner required for film systems.

If contrast-limited performance rather than noise-limited performance is assumed for the electro-optical sensor, then the product of the component MTF's for the system must equal or exceed about 0.04. (Taken as the visibility threshold under these conditions.) Based on a low contrast scene (1.3 to 1), the lens, the image motion characteristics, and the sensor must each display modulation transfers of 68 percent or more at the spatial frequency determined by the resolution requirements to achieve system response of 0.04 (see Appendix F). The ultimate capability of projected return beam Vidicons under these conditions, as shown in Figure 6-8, is about 30 line pairs per millimeter.

Referring again to the geometry shown in Figure 6-4, the ground size can be expressed as

$$S = 0.1 \frac{D}{F} H$$

The resolution is, as in the case of the film system, simply the ground size divided by the total line pairs or,

$$R = \frac{S \times 10^3}{30D} = 3.43 \frac{H}{F}$$

This expression is plotted in Figure 6-9 for values of $F \leq 635$ cm.

Under low contrast conditions, the best resolution for a system at a given state-of-the-art is

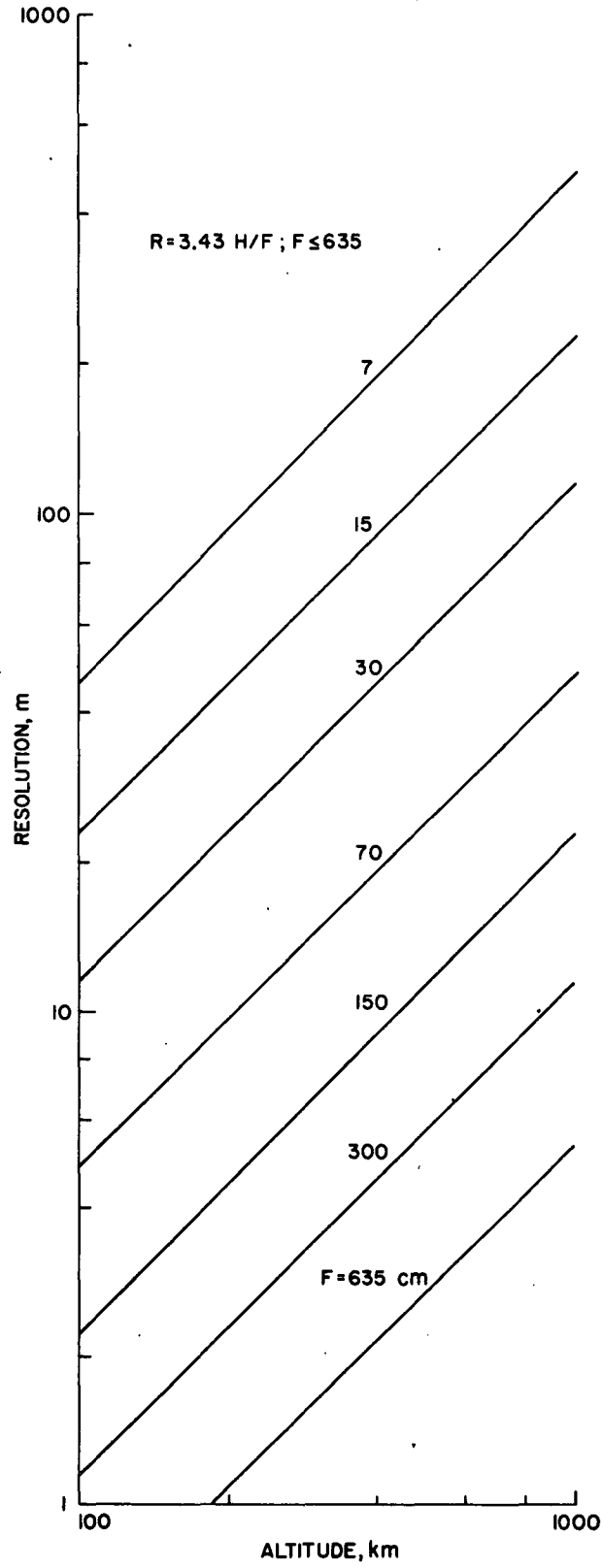
$$R_{\max} = \frac{S_{\min}}{LD} = \frac{8H}{1500} = 5.33 \times 10^{-3} H$$

The expressions above, for both the film camera and television systems, apply to both the spacecraft and aircraft case. Because of the different velocity/altitude circumstances in the two cases, however, exposures will be somewhat different as will the attitude control requirements.

Multispectral Scanner

The multispectral scanner is a device utilizing a series of point detectors in the image plane of a suitable optical system which has integral scanning capability. That is, the image is moved from side to side in the image plane in such a way that each point detector sees a line of the image for each scan. A series of such scans, closely spaced in time, provides a two dimensional view of the region encompassed by the optical system. Normally, the scanning motion transverse to the track of the spacecraft is provided by a scanning mirror or other similar device in the multispectral scanner itself, and the motion along the spacecraft track provides the necessary displacement in the other direction. The instantaneous field of view (IFOV) observed by any one detector in such a system determines the resolution capability of the device; and the scan angle, that is, the angle through which a point in the scene is

Figure 6-9 RBV Spatial Resolution



moved determines the swath width of the instrument. The field of view along the track, of course, is determined only by the length of the spacecraft track and the on-time of the device.

Typically, a number of detectors, each sensitive in a desired spectral band and appropriately filtered, is used with a multispectral scanner so that information of interest can be collected simultaneously in a number of narrow spectral bands. The actual selection of spectral bands depends on the scenes being imaged and the information desired from those scenes. For example, in imaging an agricultural scene for a particular kind of disease infestation, the combination of spectral bands that permits unique identification of that disease in that particular crop for that region of the country would be selected (if, indeed, a unique determination can be made on the basis of spectral data alone). This type of spectral signature analysis represents a potentially powerful means of obtaining information concerning details of distant scenes without the need for the high spatial resolution requirements normally associated with such data.

Besides the advantages of multispectral signature recognition associated with this type of sensor, there is also a distinct advantage associated with the fact that data in several spectral regions can be collected essentially simultaneously and in register. Consequently, the problems normally associated with rectification and registration are largely eliminated by this method of scanning. The gain is not made without disadvantages, however, the principal one being that the dwell time per element with a typical multispectral scanner is a small fraction of the dwell time per element with a frame imaging device like a camera or vidicon. For these latter devices, all of the resolution elements for the frame are exposed simultaneously for the same length of time making these devices, in effect, multichannel scanners with the number of channels equal to the number of resolution elements. Since, even under photon noise limited conditions, the required dwell time per element is not

vanishingly small, the spatial resolution capability of a typical channel of a multispectral scanner is not competitive with that of a frame-type device.

In this section of the report, the component state-of-the-art for multispectral scanners will be discussed followed by the development of scaling laws useful for estimating the performance characteristics of these systems.

Multispectral Scanner Component State-of-the-Art

A schematic diagram of a typical MSS is shown in Figure 6-10. The two components having a dominant effect on the performance of such systems are the collecting aperture (discussed earlier) and the detector element.

The size, sensitivity, and spectral characteristics of photomultiplier detectors useful for the visible and near IR channels of an MSS are shown in Figure 6-11. The performance of these devices is excellent in the near UV and visible bands but deteriorates badly (because of poor quantum efficiency) in the near IR portion of the spectrum, becoming virtually useless above about 1.1 μm . Quantum efficiencies can be improved by factors of 2 to 10 by optical enhancement techniques over the useful operating region (Ref. 26) and exotic photoemitters with unenhanced efficiencies on the order of one percent are on the horizon (Ref. 27). From about 0.6 μm to 1.1 μm , the silicon photodiode is becoming more popular because of its high (~75 percent) quantum efficiency but PM tubes probably still have a small advantage because of their high intrinsic gain. Generally, PM tube detectors are quantum noise limited while the photovoltaic/photoconductive types (silicon) are limited by self-generated or excess noise and amplifier noise. Consequently, even though PM tube quantum efficiencies are low in the near IR compared to silicon photodiodes, they still appear to have a small performance advantage for wide bandwidth systems. Size, weight and power supply considerations, however, favor the photodiode. The work here is based on the

Figure 6-10 Multispectral Scanner for ERTS

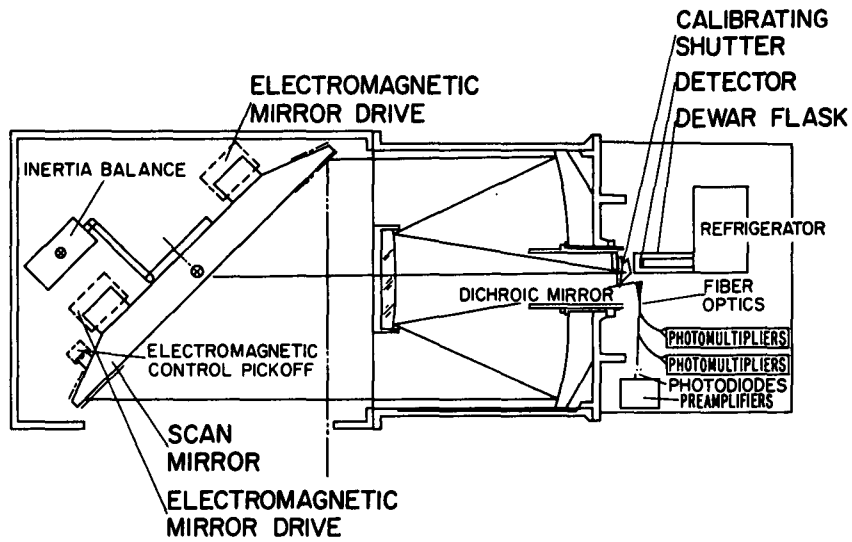
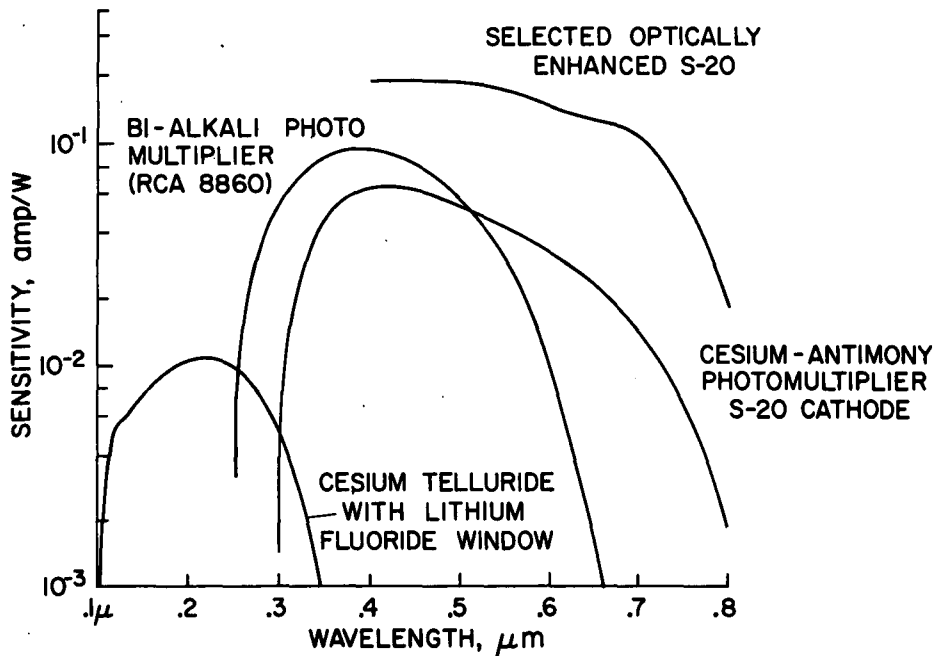


Figure 6-11 Spectral Response of Photomultipliers



use of PM tube detectors over the visible and near IR bands. Thermal IR detectors, suitable for the IR channels of an MSS, are covered in the following section.

Multispectral Scanner Scaling Laws

In the visible and near IR portions of the spectrum, the signal-to-noise ratio of a scanner exposed to a change in spectral radiance of a scene having an average spectral radiance N_λ is given by (see Appendix G):

$$S_n = \frac{\Delta\rho}{\rho} \left[\frac{N_\lambda AB^2 t \epsilon \bar{\lambda} \tau}{10^{-19}} \right]^{1/2}$$

The worst case conditions assumed here for the MSS correspond to a 50 degree (noon sun-synchronous orbit at 50 degrees north latitude, early spring) zenith angle for the sun in the 0.8-1.1 μm band. Taking the average reflectance for soils in this spectral range as 10 percent (Ref. 28), $N_\lambda \approx 1 \times 10^{-3}$ watts cm^{-2} ster $^{-1}$, and $\Delta\rho/\rho = 0.1$. With these values and a transmittance, t , of 0.5 and a quantum efficiency, ϵ , of 3×10^{-3} , the signal to noise ratio, S_n , becomes

$$S_n = 0.1 \left[\frac{10^{-3} AB^2 (0.5) 3 \times 10^{-3} (0.95) \tau}{10^{-19}} \right]^{1/2}$$

For a minimum S_n of 3 this reduces to

$$AB^2 \tau = 6.3 \times 10^{-11}$$

or $B^2 D^2 \tau = 8 \times 10^{-11}$

Since

$$\frac{nB^2 H}{\alpha V_s} = \tau \quad (S = \alpha H, R = 2BH)$$

or
$$\frac{nR^2H^2}{4H^2SV_s} = \frac{nR^2}{4SV_s} = \tau \quad (n = \text{no. of detectors})$$

Then
$$\frac{R^2}{4SV_s} = \frac{\tau}{10} \quad (\text{for } n = 10)$$

Spacecraft Summary

For $V_s = 7.8 \text{ km/sec,}$

$$\frac{R^2}{S} = 3\tau \text{ and } S = \frac{0.33 R^2}{\tau} \quad (R \text{ in km})$$

or
$$S = \frac{0.33 \times 10^{-6} R^2}{\tau} \quad (R \text{ in m})$$

This relationship is summarized in Figure 6-12.

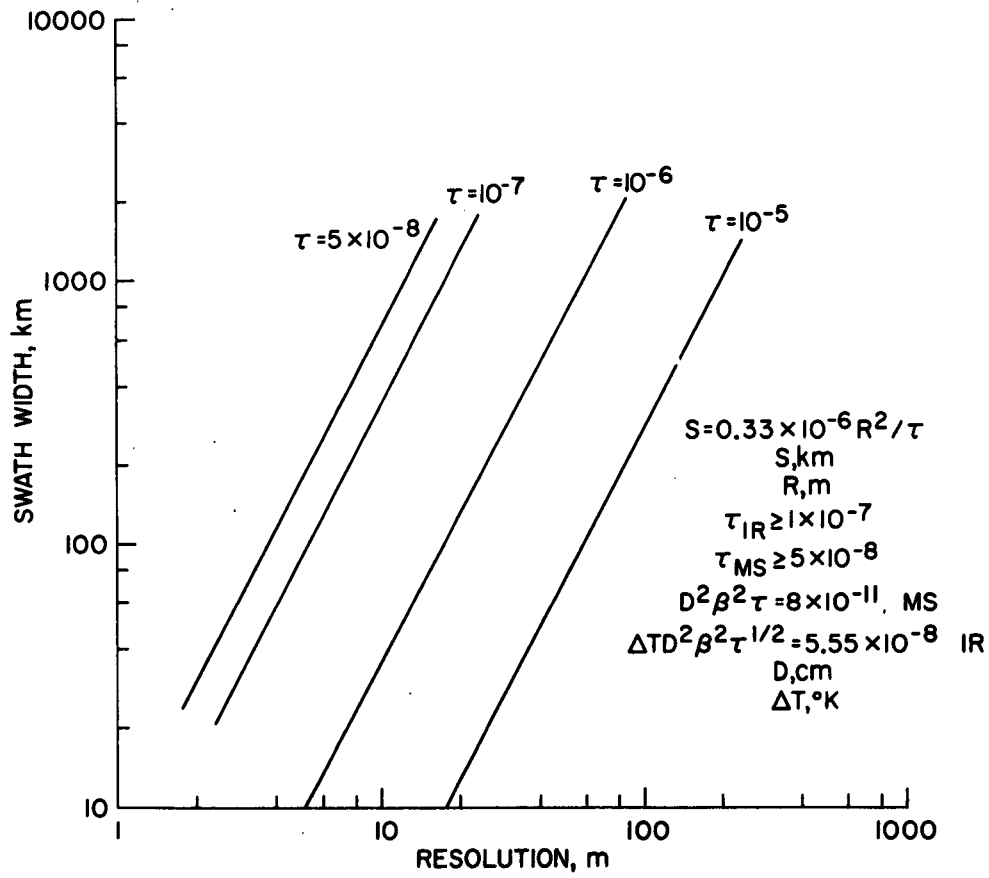
Aircraft Summary

For $V_s = 0.215, \quad S = \frac{46.5 B^2 H^2}{\tau}$

Infrared Scanner/Radiometer

The infrared scanner is identical in operation to the multispectral scanner just described and the radiometer is just a special case of the scanner for which $\alpha = 0$. In fact, it is common for one or more channels of a multispectral scanner to be located in the thermal infrared region. The performance characteristics for these channels would of course be dependent on the state-of-the-art for thermal infrared components. Because of these considerations, the material presented in this section will be equally appropriate for an infrared scanner per se, or for the thermal IR channels of a multispectral scanner. One special point needs to be made, however. When a thermal IR channel is included

Figure 6-12 Effect of Dwell Time on the Performance of Multispectral and Infrared Scanners



in the MSS, performance compromises are required. These compromises are discussed in the concluding parts of this section.

Infrared Scanner/Radiometer Component State-of-the-Art

The size, sensitivity, and spectral characteristics of detectors useful for infrared scanners are shown in Figure 6-13. It has been assumed here that the best detectivity values represent the state-of-the-art pertinent for the timeframe under consideration. While this may be somewhat conservative, it should be noted that the detectivity (D^*) approaches the theoretical value within a factor of 2 at the wavelength of peak response for most detectors. Consequently, for narrow band applications near the peak wavelength, little improvement in D^* can be expected. Also, losses in the optical system, the chopper used to convert the DC signal to AC, and the losses in the other electronic elements have been ignored. Consequently, some improvement in detectivity has been implicitly included in this data.

Infrared Scanner/Radiometer Scaling Laws

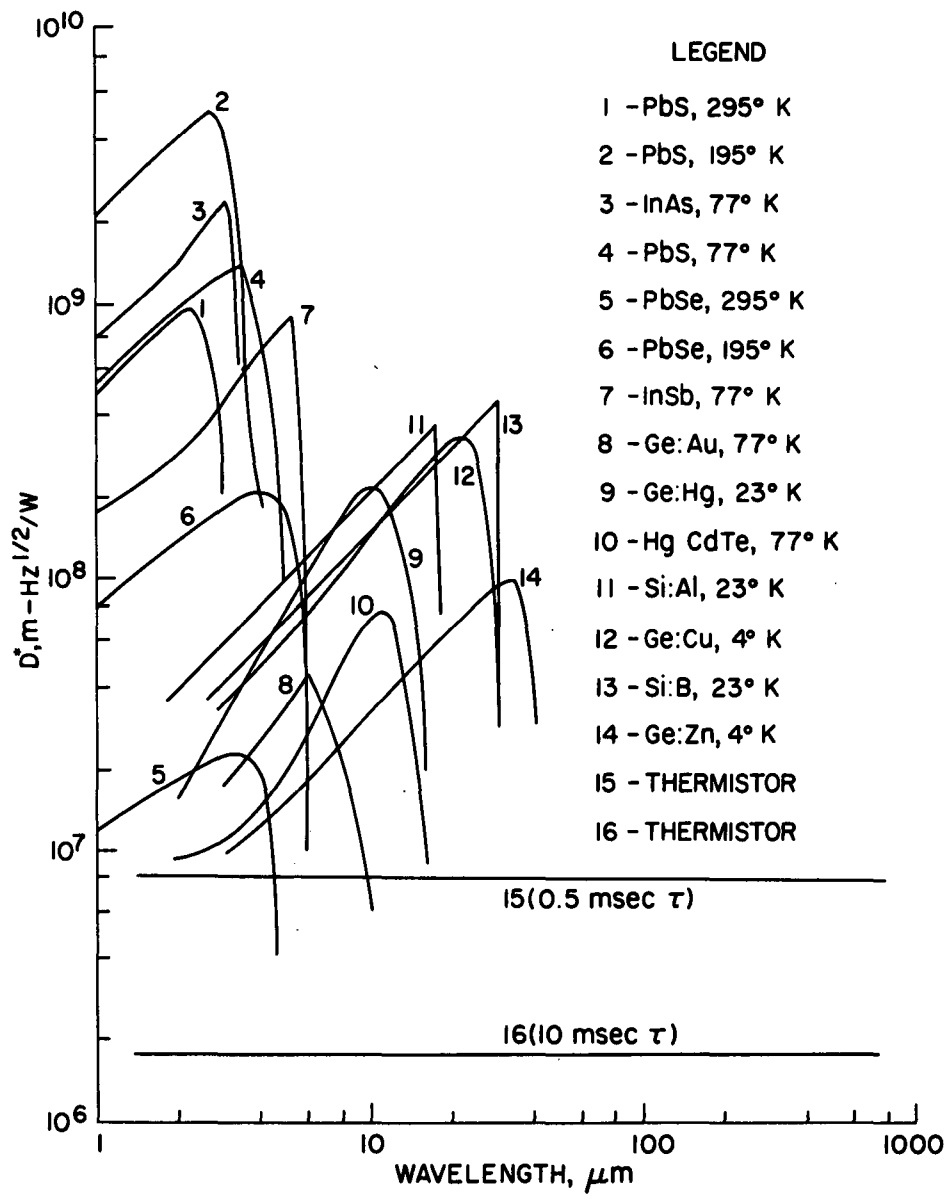
The signal-to-noise ratio of a scanner/radiometer operating in the thermal IR region of the spectrum is given by (see Appendix H):

$$S_n = \frac{14388 \Delta T N_\lambda AB^2 \tau D^*}{\lambda T^2 \sqrt{A_d \Delta f}}$$

When operating in the 10.4 to 12.6 μm band (ERTS band #5) at an average ground temperature of 283^oK (50^oF estimated as typical early spring, late fall ground temperature) with a Ge:Hg detector (the best available for this spectral range; $D^* = 5 \times 10^{10} \text{ cmHz}^{1/2}\text{W}^{-1}$) at an $S_n = 3$ and assuming a SOA limit of 0.1 mm for the detector dimension, we have

$$\frac{\Delta T 2.75 \times 10^{-5} AB^2 (0.5) 5 \times 10^{10} (\tau)^{1/2}}{0.1 \times 10^{-1}} = 3$$

Figure 6-13 Infrared Specific Detectivities



$$\Delta T AB^2 \tau^{1/2} = \frac{0.3 \times 10^{-1}}{6.0 \times 10^5} = 4.35 \times 10^{-8}$$

or $\Delta T B^2 D_c^2 \tau^{1/2} = 5.55 \times 10^{-8}$

Conditions $B > 1.6 \times 10^{-5}$ radians
 $\tau > 10^{-7}$
 $D_c < 100$ cm

Spacecraft Summary

The geometrical relationships discussed earlier for the MSS are also applicable here. Consequently,

$$S = \frac{0.33 R^2}{\tau}, \text{ (R in km) or } S = \frac{0.33 R^2 \times 10^{-6}}{\tau}, \text{ (R in m)}$$

Where $R = 2BH \times 10^3$ and $S = \alpha H$

and $\Delta T = \frac{22.2 \times 10^{-2} H^2}{K^2 D_c^2 \tau^{1/2}}$

Radiometer swath width versus altitude for various instantaneous fields of view are shown in Figure 6-14 and ΔT as a function of the ratio H/R with dwell time, τ , as a parameter is shown in Figure 6-15 for both scanners and radiometers. It should be mentioned that the only difference between the two devices is in the mechanization. Since radiometers do not scan, $\alpha = 0$ and $S = BH$.

Thermal IR Capability for MSS

As mentioned earlier, inclusion of a thermal IR capability in the multispectral scanner requires some performance compromises. This is primarily a consequence of the difference in detector sensitivities for the two spectral regions. Since high spatial resolution in the visible range is generally the overriding consideration, a large number of detectors is used to permit a relatively long dwell time per element. Because of the better performance of visible light detectors, the

Figure 6-14 Infrared Radiometer Swath Width

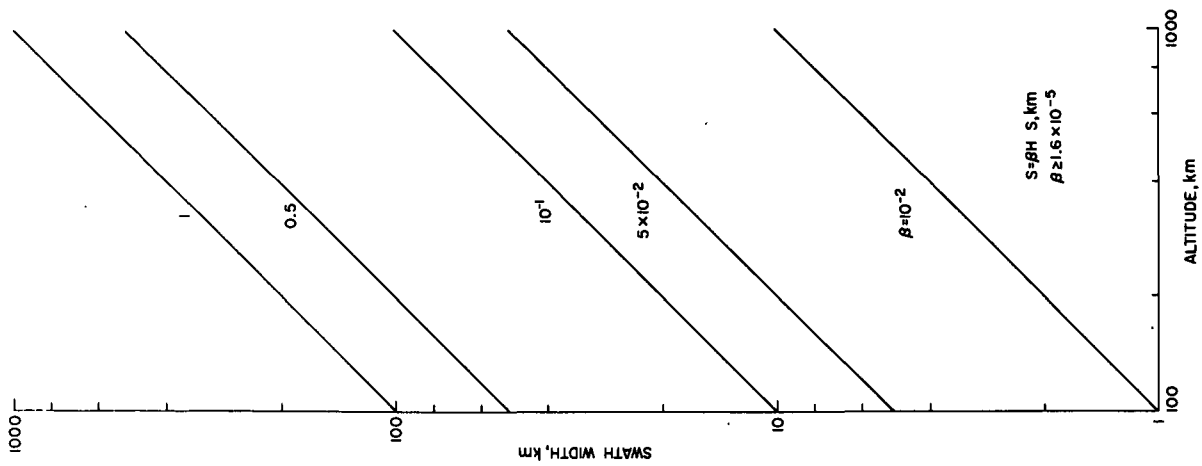
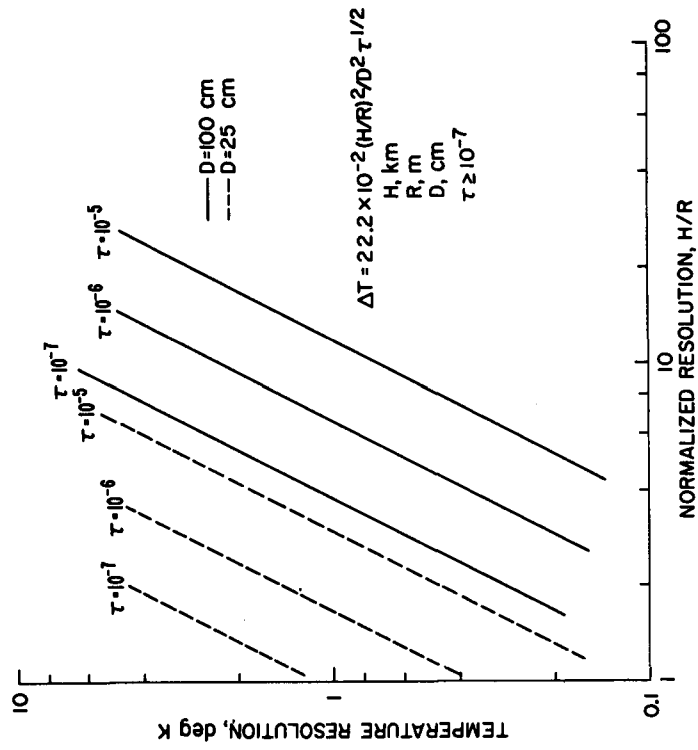


Figure 6-15 Effects of Dwell Time on the Performance of Infrared Scanners and Radiometers



instantaneous field of view in this spectral region can, therefore, be smaller for a given focal length than is the case in the thermal region. As a result, when the two spectral regions are combined in a single instrument, the instantaneous field of view for the visible range is generally better than the instantaneous field of view for the infrared range and, therefore, the infrared section requires fewer detectors. A relationship useful for combining the two spectral regions is given below (see Appendix I).

$$\Delta TB_2^2 D_c^2 \left(\frac{\tau_1 n_2}{n_1} \right)^{1/2} = 5.5 \times 10^{-8}$$

where subscript one pertains to the visible region and subscript two pertains to the IR region.

Microwave Scanner and Radiometer

Passive microwave systems sense radiation emitted within the instrument field of view. The amount of energy available depends on the operating frequency of the microwave device, the pass band around that frequency and the thermionic temperature and emissivity of the scene in the spectral region being measured. The method of operation of this type of device is entirely analogous to the operation of the thermal infrared radiometer/scanner. Differences lie in the types of components required because of the different spectral regimes and magnitude of the emitted radiation in the two regions. For a passive microwave system the collector consists of a microwave aperture, or antenna, which receives energy from the area under consideration. The antenna is coupled to a radio receiver that is capable (because of its inherently low noise characteristics) of sensing relatively small differences in the temperature produced radiation emitted from successive resolution elements (a resolution element is one IFOV). Hence, the device is intrinsically capable of sensing relatively small differences in temperature between adjacent resolution elements. As with the infrared scanner/radiometer, the radiation sensed is an average for the

overall instantaneous field of view. Consequently, a very small hotspot within the field is converted to a final reading proportional to the ratio of the hotspot area to the area encompassed by one IFOV.

Two basic types of microwave radiometers are in use. One is an unmodulated type normally used for imaging. The other, designed for rather accurate temperature resolution, is known as the Dicke radiometer, (Ref. 29) which alternately looks at the object field and a calibration source. This method of operation compensates for instrumental drifts by providing an output relative to the known calibrating source temperature.

Except for the possible difference outlined above, the radiometer and the scanner (or imager) are essentially identical in operation. Generally, the temperature sensitivity of a radiometer for a given size aperture can be much higher than a scanner because the effective dwell time per resolution element for a given spacecraft velocity is longer by the ratio of the scan angle to the instantaneous field of view.

Microwave Scanner/Radiometer State-of-the-Art Considerations

The two considerations having greatest impact on passive microwave system performance are current limitations on antenna size and receiver noise temperatures. Hiatt and Larson (Ref 30) have assessed the maximum antenna sizes expected to be feasible in the early 70's with results shown in Figure 6-16. Antennas of these sizes have not been achieved as yet for spacecraft use but appear to be within the state-of-the-art insofar as surface tolerance requirements are concerned. The larger sizes would generally be erectible, while the small size dishes would generally be fixed, accounting for the flattening of the curve at higher frequencies (shorter wavelengths). Figure 6-17 shows the attainable angular resolution for various antenna sizes for several wavelengths. The state-of-the-art boundary corresponding to Figure 6-16 is also shown on this figure. For this study, the simple linear relationships shown in Figure 6-18 were used. Over the range of interest, these curves approximate the more sophisticated data quite well.

Figure 6-16 Maximum Antenna Size for Microwave Systems

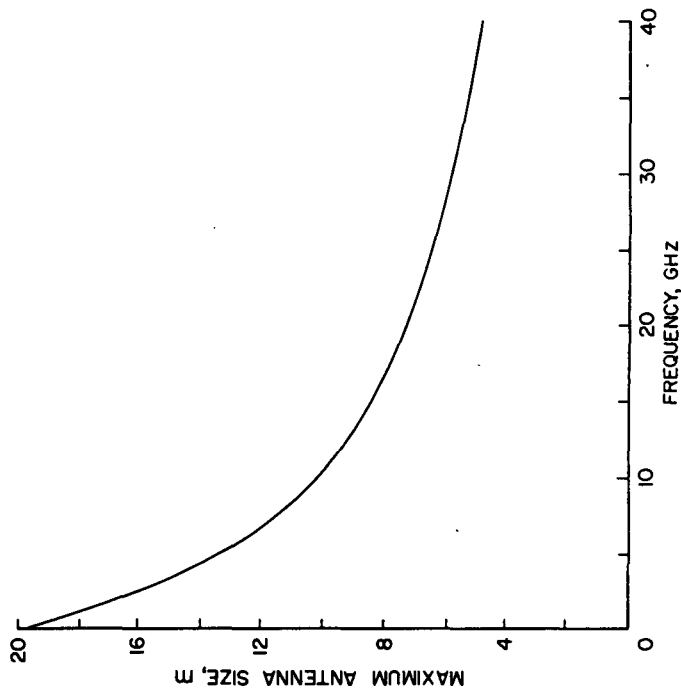


Figure 6-17 Attainable Angular Resolution for Parabolic Antennas

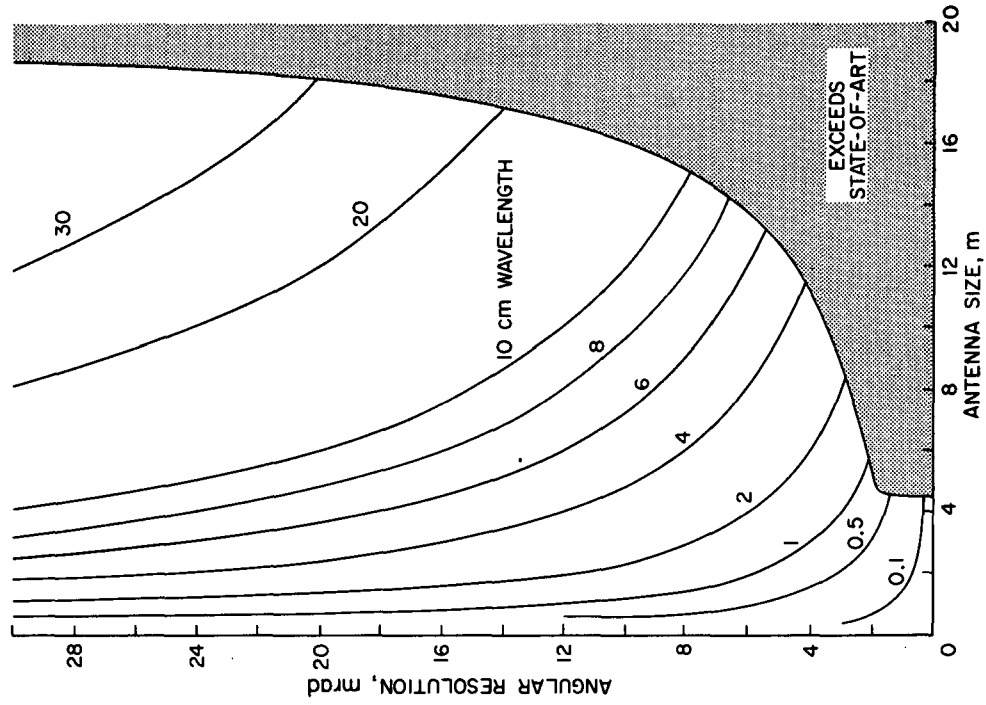
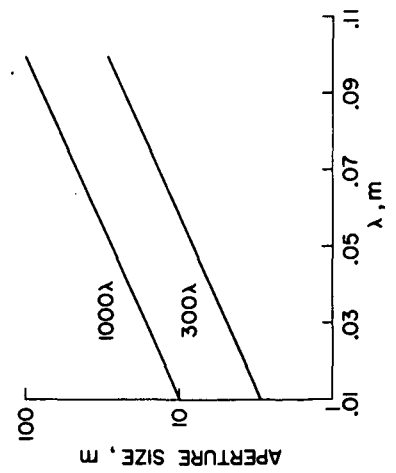


Figure 6-18 Limiting Aperture Size for Parabolic and Linear Antennas



Matthei (Ref. 31) has assessed the current technological capabilities of microwave receivers with the results shown in Figure 6-19. The solid line in the figure, representing the performance of tunnel diode amplifiers, is based on his data. The dashed extension in the figure is based on informal discussions with microwave receiver manufacturers. Lower noise temperatures can be obtained by using advanced equipment such as parametric amplifiers or traveling wave maser amplifiers, but these components are still in the development stages and cannot be regarded as approaching a space qualified status.

The factors outlined above affect the choice of operating frequency for these systems but atmospheric attenuation must also be considered before a selection can be made. The attenuation of the Earth's atmosphere through a vertical path is shown for wavelengths ranging from 3 cm to 0.1 cm in Figure 6-20. These data were obtained under low to moderate humidity conditions. The variable attenuation caused by fogs, clouds, and rain is not included. Experiments have shown, however, that only the most severe rainstorms have any serious effect on microwave propagation through the atmosphere at wavelengths greater than 1 cm (30 GHz). Statistical data indicates fifty percent reduction in transmission occurring less than 0.5 percent of the total time (Ref. 32).

Microwave Scanner/Radiometer Scaling Laws

A basic expression for the temperature sensitivity of a passive microwave radiometer is the following.

$$\Delta T = \frac{2}{\Delta f \tau}^{1/2} F_R T \quad (\text{Dicke}) \quad (1)$$

where

f is the bandwidth of the system in Hertz

τ is the time constant

F_R is the effective system noise figure

T is the reference temperature taken at 290°K.

Figure 6-19 Amplifier Noise Temperature

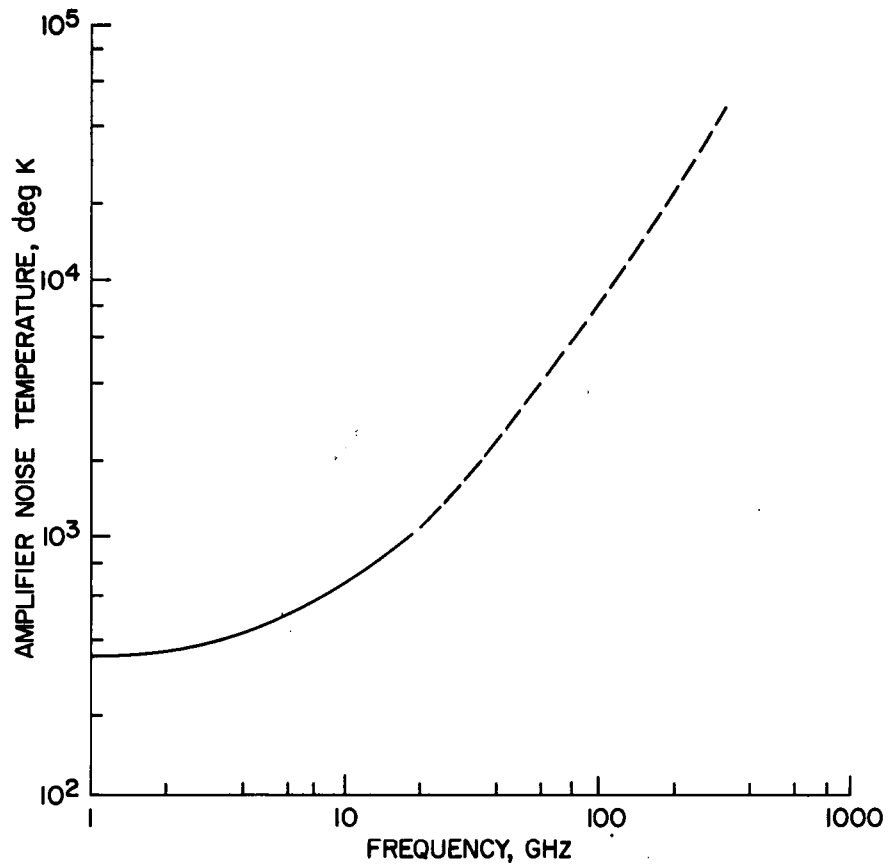
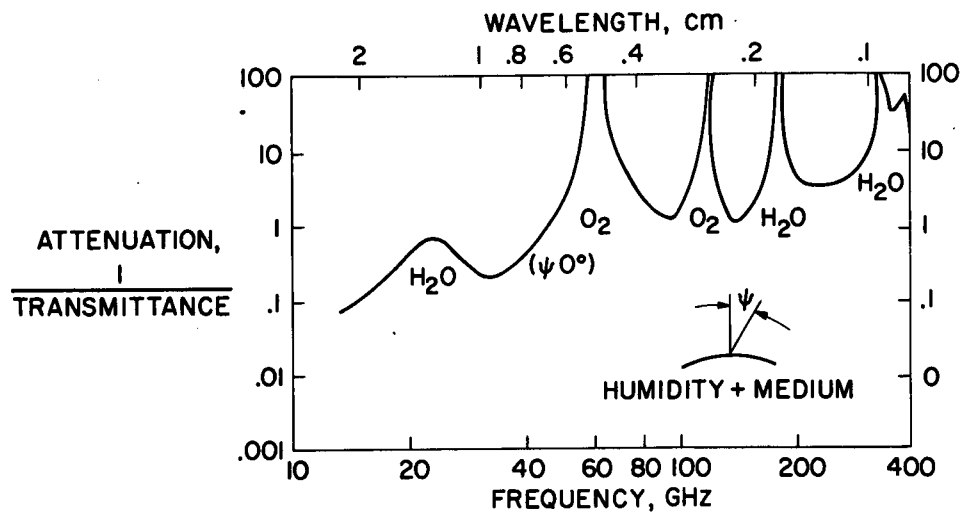


Figure 6-20 Atmospheric Attenuation in the Microwave and Millimeter Spectrum



State-of-the-art considerations limit f to a maximum value equal to 1/10 of the operating frequency. In the following material, that value has been used.

The effective system noise figure, F_R , is

$$F_R = \frac{T_A + T_N}{T}$$

where

T_N is the amplifier noise temperature

and

$$T_A = T'_A + T_L$$

where T'_A is the apparent antenna noise temperature within its field of view and T_L is the contribution to the temperature by system losses (taken here as 100°K). For a given operating frequency, all of the values in expression (1) except τ are defined by state-of-the-art considerations. Thus the expression can be rewritten as

$$\Delta T = \frac{C_m}{\tau} T / 2$$

For an operating frequency of about 90 GHz, the constant C_m for an Earth-looking system is about $6 \times 10^{-2} \text{ } ^\circ\text{K sec}^{1/2}$. The expression is plotted in Figure 6-21 using this constant.

The beamwidth of the receiving aperture, B , is

$$B = \frac{1.2 \lambda_r}{D_c}$$

Maintaining the line pair convention for resolution then results in the following expression which is shown in Figure 6-22:

$$R = \frac{2400 H}{D_c / \lambda_r}$$

Figure 6-22 Microwave Scanner and Radiometer Spatial Resolution

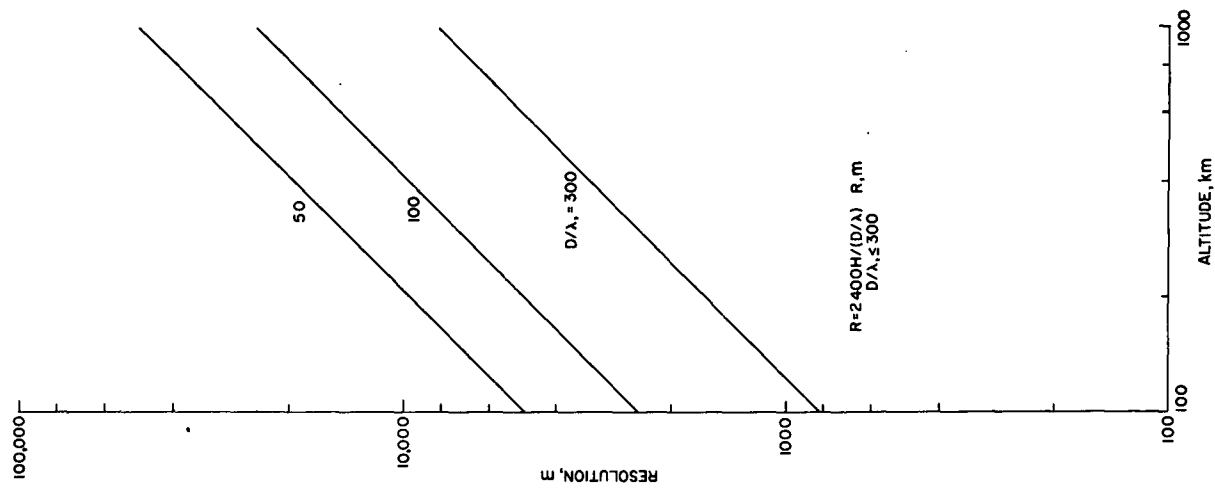
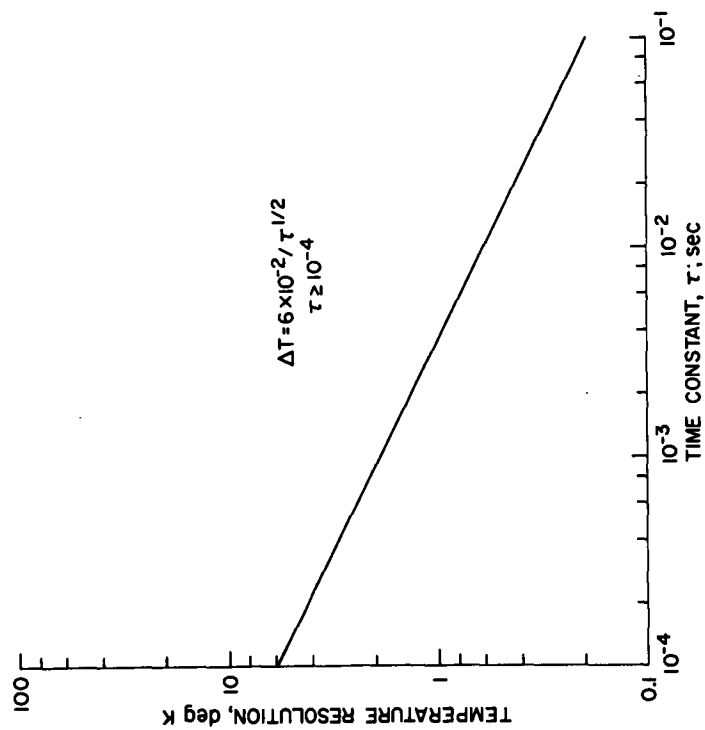


Figure 6-21 Temperature Resolution of Microwave Scanners and Radiometers



Since the state-of-the-art limits for D/λ_r are taken here as 300,

$$R > 8H$$

The dwell time (taking the time constant equal to the dwell time) determines the length of time that signal can be integrated from the ground patch encompassed within the antenna field of view. For a scanning radiometer,

$$\tau = \frac{R^2 \times 10^{-6}}{4 V_s S}$$

Spacecraft Summary

For the spacecraft the swath width is expressed as

$$S = \frac{0.32 \times 10^{-7} R^2}{\tau}$$

This expression is plotted in Figure 6-23.

Aircraft Summary

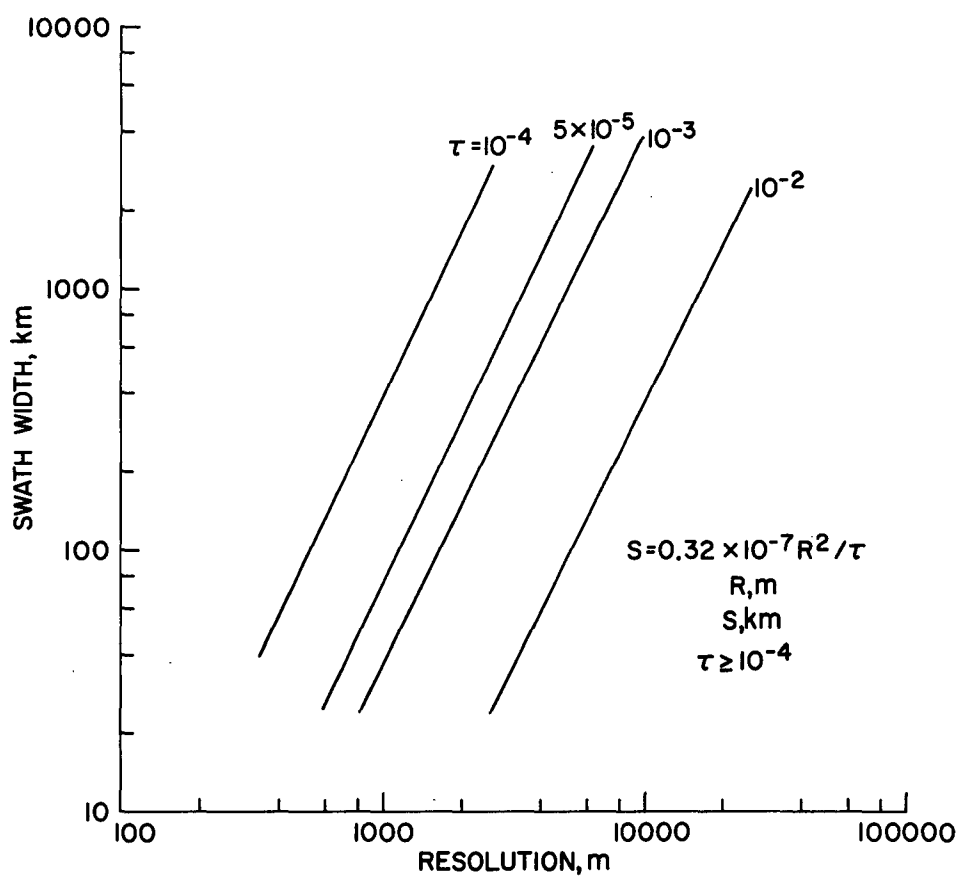
For aircraft useage, the swath width becomes

$$S = \frac{1.15 \times 10^{-6} R^2}{\tau}$$

Radar

This sensor, unlike the other devices discussed previously, is an active system in that it provides its own "illumination." Many variations of these systems are possible for use aboard moving vehicles but typically for spacecraft applications of the sort being discussed here, the antenna aperture would be "side looking," that is, looking at the terrain to the side of the spacecraft and perpendicular to the flight path. Also, because of the resolution requirements typical of Earth resources missions, a coherent synthetic aperture approach is required. Conventional or "brute force" radar has a

Figure 6-23 Effect of Dwell Time on the Performance of Microwave Scanners



3 ⊕

resolution capability inversely proportional to the physical aperture size. As a consequence, at practical operating wavelengths, extremely long (hundreds of meters) physical apertures would be required to achieve the needed resolution. Artificially creating a long aperture by collecting and synthesizing phase and amplitude data from many separate antenna positions is a practical alternative; therefore, our attention in this section will be limited to focused side-looking synthetic aperture radar systems.

Side-Looking Radar Component State-of-the-Art

Erectible linear antennas of the type used for side-looking radar systems are limited by state-of-the-art finish tolerances and mechanical considerations in space (thermal, torques, etc.) to a maximum dimension,

$$L_a < 1000 \lambda_r \quad (\text{see Figure 6-18})$$

Fortunately, for synthetic aperture systems, antennas approaching this limit will not normally be required. The pulse duration, which determines the range resolution, is limited by

$$\tau_a > 10^{-9} \text{ sec}$$

Because very short pulse durations tend to result in excessive peak power and bandwidth requirements, a technique known as pulse compression is now widely used to reduce peak power requirements for short pulses. Using this method, the transmitted pulse duration becomes

$$\tau_a = C \tau_c$$

where τ_c is the desired duration of the compressed pulse. The present state-of-the-art limits C to values of 400 or less. Values of C as high as 2000 appear to be attainable within the next decade. For surface mapping applications, the constraint on τ_a is not normally serious as far as range resolution is concerned since targets with

more than 0.6 of a meter separation in slant range can be resolved with a pulse duration of a nanosecond. The peak power limitation with short pulses, however, is a serious one and very often requires the use of pulse compression techniques as outlined above. The state-of-the-art peak power constraint is given by

$$P_t = 4 \times 10^8 \lambda_r$$

where λ is in meters. Receiver bandwidths are related to the pulse duration and are currently limited to about 10 percent or less of the operating frequency. Since the receiver bandwidth for a matched system is simply the reciprocal of the compressed pulse length, the pulse duration is

$$\tau_c \geq \frac{10}{f_0}$$

where f_0 is the operating frequency. The state-of-the-art constraint is often more stringent than that implied by a nanosecond uncompressed pulse length and a maximum compression ratio of 400.

The maximum pulse rate possible affects both the peak power requirement and also the antenna length required to eliminate azimuth ambiguities. The present state-of-the-art on radar pulsing systems limits this maximum rate to about 1 megacycle.

The signal to noise ratio is determined by the intensity of the received signal and by the system noise. Generally, an S_n of at least ten is desired. The current state-of-the-art for system noise is shown in Figure 6-24.

Side-Looking Radar Scaling Laws

The geometry for a coherent side-looking radar is shown in Figure 6-25. The maximum synthetic aperture length is given by the along-track dimension of the surface that is illuminated by the real physical antenna at any range. That is,

Figure 6-24 Radar System Noise

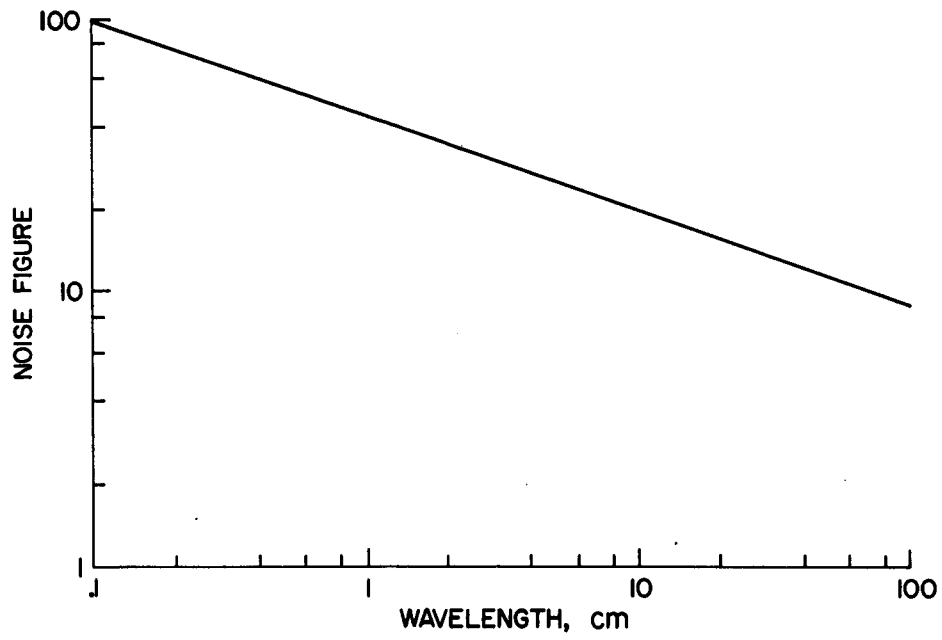
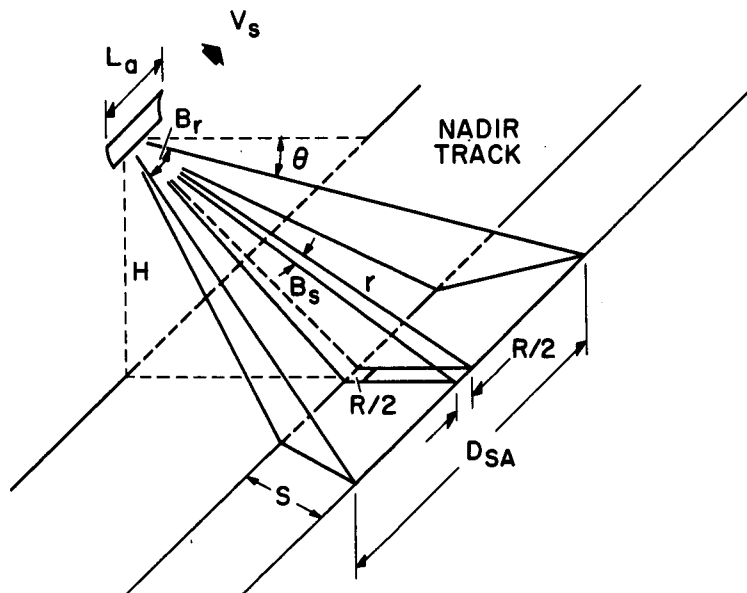


Figure 6-25 Focused Synthetic Aperture Radar Geometry



$$D_{SA} = 10^3 B_r r = \frac{1200 \lambda_r}{L_a} r$$

One would expect the expression for the beamwidth of the synthetic aperture thus generated to be analogous to the expression above with D_{SA} substituted for L_a in the denominator. Actually, however, the beam pattern produced by a synthetic aperture array is determined by the two-way phase shifts, that is, the phase shift occurring from the time the transmitted signal leaves the antenna until it reaches the ground, plus the phase shift occurring from reflection at the ground surface to reception at the antenna. In the physical array situation described by the equation above, the beam pattern is determined by the one-way phase shift because the antenna system has no way of "remembering" the transmitted phase but perceives only the difference in phase between the signals reflected from the surface. As a consequence, the effective length for a synthetic aperture antenna is twice the length actually generated. Thus, for the same real and synthetic aperture length,

$$B_r = 2 B_s$$

where B_s is the effective beamwidth of the synthetic aperture array. Because of these conditions, the ultimate resolution

$$R' = \frac{1200 \lambda_r r}{2 D_{SA}} = \frac{1200 r \lambda_r}{2(1200) \lambda_r r / L_a} = \frac{L_a}{2}$$

Again, recalling the convention used throughout (requiring two lines or a line pair per resolution element), $R \geq L_a$. Therefore, the ultimate resolution capability is determined only by the actual length of the physical aperture. Unfortunately though, there are constraints on the size of the physical antenna. The most important one is the azimuth ambiguity constraint which requires that

$$L_a \geq \frac{4 V_s \times 10^3}{p} \quad (2)$$

where V_s is the spacecraft ground velocity and p is the pulse rate of the radar. The unambiguous swath width, S , is determined by the roundtrip distance covered by a radar pulse during the interpulse period projected to the ground. Therefore,

$$S = \frac{c}{2p \cos \theta}$$

where c is the velocity of light and θ is the radar depression angle. Using this expression, equation (2) can be rewritten

$$L_a \geq \frac{8 V_s S \cos \theta}{c}$$

or

$$S < \frac{c L_a}{8 V_s \cos \theta}$$

Spacecraft Summary

For an orbital velocity of 7.8 km/sec,

$$S < \frac{5 L_a}{\cos \theta}$$

This relationship is plotted in Figure 6-26.

Aircraft Summary

For the aircraft case,

$$S < \frac{181 L_a}{\cos \theta}$$

Scatterometer

The scatterometer is essentially a radar system designed to determine scattering coefficient for a surface resolution element as a function of look angle. In some cases, a capability for measuring

Figure 6-26 Coherent Side Looking Radar Swath Width

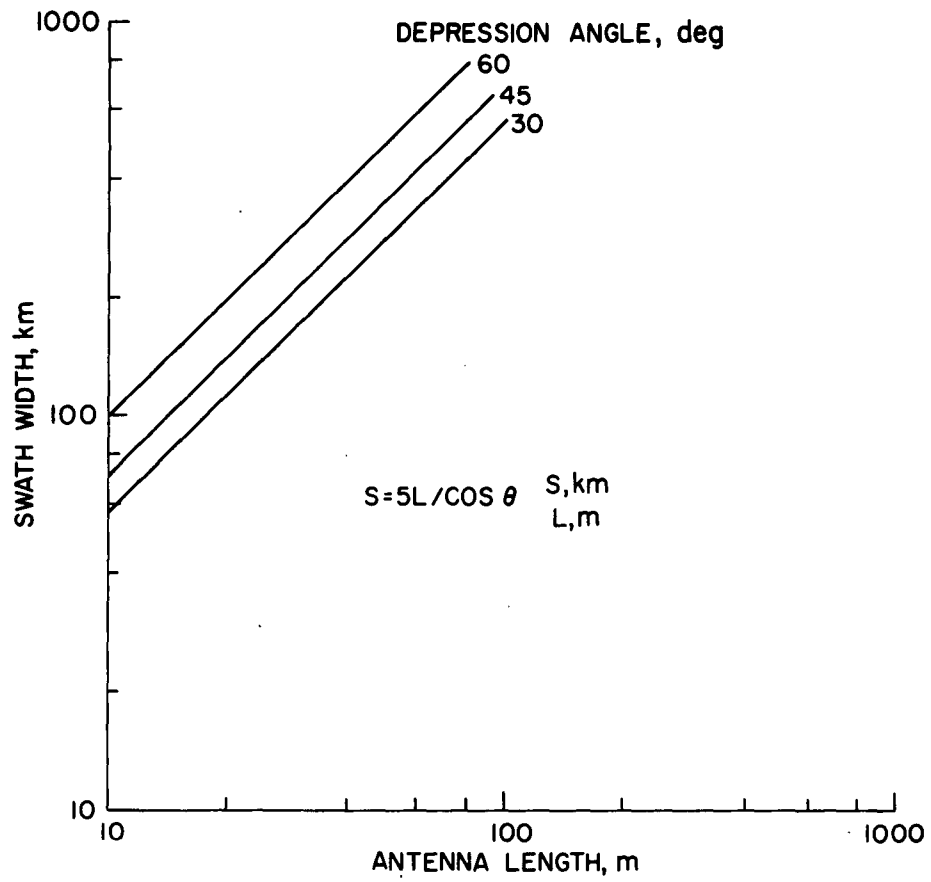
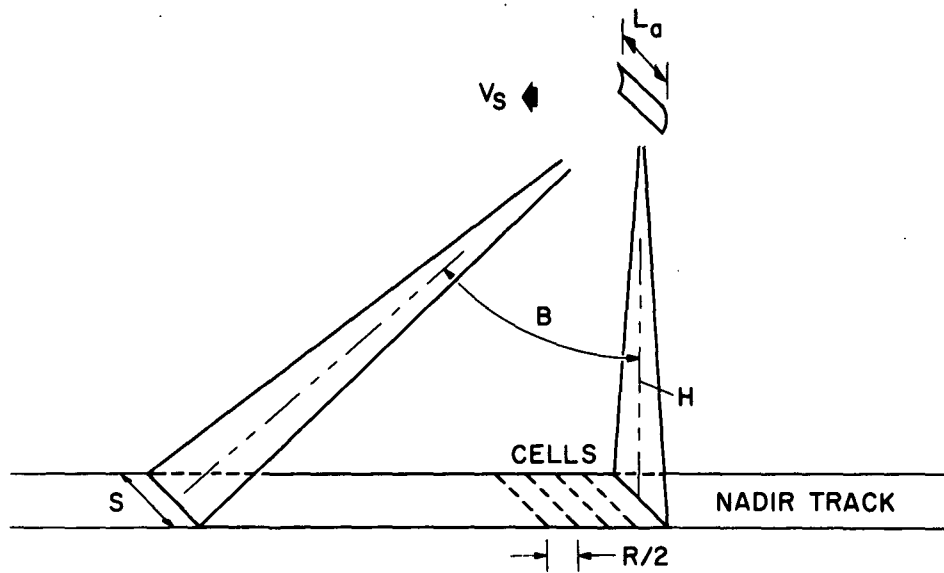


Figure 6-27 Scatterometer Geometry



scattering coefficients for different polarizations and at different wavelengths is also provided. The method of mechanization discussed here requires illumination of the surface region extending from the spacecraft nadir to a point 45 degrees ahead of the nadir (see Figure 6-27). The width of the beam and the number of elements in the 'along track' beam dimension depend on the resolution requirements imposed. In operation, the scattering coefficient for any one resolution element within the illuminated region is obtained for all depression angles from 45 to 90 degrees. Either data are acquired continuously or on a sampling basis along the track. The scaling laws presented here are predicated on a continuous system.

Scatterometer Component State-of-the-Art

The component data discussed in the preceding section for side-looking radar systems is generally applicable here also. Consequently, this material will not be repeated.

Scatterometer Scaling Laws

For a spacecraft flying at an altitude H above the surface, the illuminated region along the track is also H units long for a 45 degree look angle measured from the nadir. Consequently, the resolution along the track, R', is

$$R' = \frac{H \times 10^3}{N}$$

where N is the number of cells or resolution elements. Again, recalling our convention requiring two resolution elements for detection the actual resolution, R, becomes

$$R = \frac{2H \times 10^3}{N}$$

For any 'along track' beamwidth, B, this expression can be rewritten as

$$R = \frac{2H \tan B \times 10^3}{N}$$

The integration time, T_o , for each resolution element is then given by

$$T_o = \frac{H \tan B}{N V_s}$$

where V_s is the spacecraft velocity. The swath width for such a system (representing cross track resolution) is given by

$$S = \frac{H}{\cos B \left(\frac{L_a}{\lambda_r} \right)}$$

where L_a is the cross track antenna size and λ is the wavelength. Generally, such a system would be designed for a square resolution element. Thus, the swath width is related to resolution by

$$S = \frac{R}{2}$$

7. SENSOR SUPPORT REQUIREMENTS

The spacecraft support requirements for the sensor systems discussed in the previous section are presented here. They include essentially all of the factors that determine the performance requirements for the spacecraft subsystems, e.g., power, stability, weight, etc. The state-of-the-art limits discussed earlier have been used wherever they would simplify the relationships and at the same time provide meaningful results. The requirements for each sensor system are presented in the same order as the previous section, i.e., film camera, television, multispectral scanner, infrared scanner/radiometer, microwave scanner/radiometer, radar and scatterometer. Image motion considerations, pertinent for all of the passive devices, are discussed first.

Image Motion Considerations

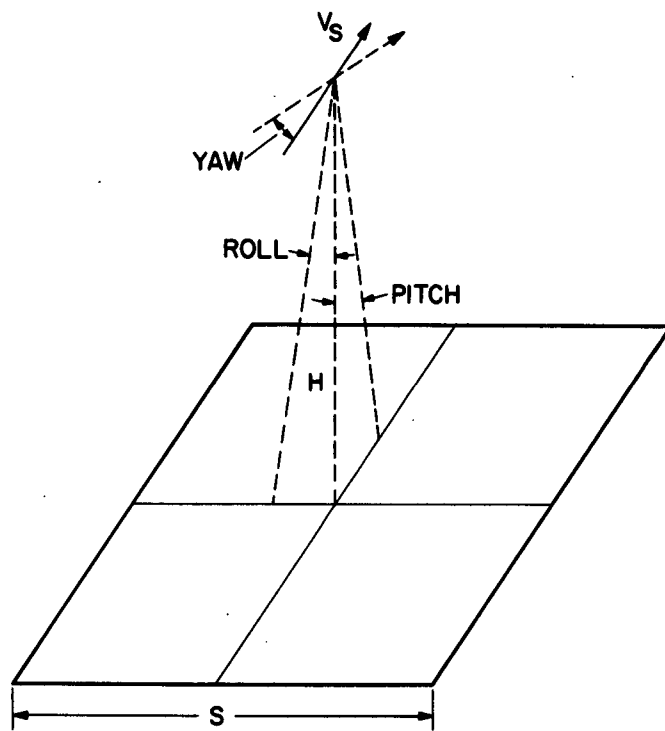
Relative motion between the sensor platform and the scene during imaging causes smear; that is, during the exposure or scan period, any uncompensated motion will result in scene or resolution element movement in the image plane. As a consequence, the effective system resolution is reduced. The extent of this reduction depends on the amount of movement. Image motion affects frame type devices (film cameras and vidicon) and scanning instruments differently.

The geometry for image motion is shown in Figure 7-1. This figure applies for both scanners and frame devices. Image motion compensation (IMC) corrects for the linear motion of the spacecraft relative to the scene. The angular rate, $\dot{\alpha}$, corresponding to this motion is

$$\dot{\alpha} = \frac{V_s}{H} \quad (\text{See Section 6 for nomenclature.})$$

Straightforward IMC systems consisting of a V/H sensor and associated electronics can compensate for about 95 percent of this type of motion. This type of IMC is only pertinent for frame devices.

Figure 7-1 Image Motion Geometry



Angular rates about the three spacecraft or aircraft axes produced by pitch, roll, and yaw motions affect both frame devices and scanners and can only be compensated by means of an inertially stabilized mount for the sensor. In this paper, it is assumed that such a mount is not employed.

For frame devices, the entire scene is exposed simultaneously. The pitch and yaw motions are at right angles to the roll motion and, in the worst case, are additive. The pitch motion at the image plane, m_p , is

$$m_p = 10F\dot{\phi}t_e \quad (\text{mm})$$

the yaw motion, m_y , is

$$m_y = \frac{D}{2} \dot{\phi}t_e$$

and the roll motion, m_r , is

$$m_r = 10F\dot{\phi}t_e$$

The total motion then becomes,

$$m_t = \sqrt{(m_p + m_y)^2 + m_r^2} \quad (\text{mm})$$

Permitting equal movement in all axes,

$$m_t = 2.24 m_{pyr}$$

or the maximum motion permitted for any one axis, m_i , is

$$m_i \leq \frac{m_t}{2.24}$$

For a scanner, the same considerations apply except for the fact that the exposure is made element by element. Since line overlap and picture element displacement line to line are the pertinent considerations here, the time to scan one complete line must be

used as the criterion. Also, the yaw motion expression should be modified to a more convenient form.

For a scanner, the effective format size, D , is

$$D = 20F \tan \alpha/2 \quad (\text{mm})$$

Thus,

$$m_y = 10F(\tan \alpha/2)\dot{\theta}t_e$$

Film Camera

Each of the major supporting areas for film camera systems is discussed briefly below.

Data Rate

The average data acquisition rate during a picture taking sequence is given by

$$D_R = \frac{(D)^2 G}{D_s t_c} = \frac{L^2 G}{t_c} \quad (\text{bits/sec})$$

where $t_c = \frac{S}{V_s}$

For a 9 inch film, a state-of-the-art scanning spot diameter of 5 micrometers, and a grey scale of 6 bits, this reduces to

$$D_R = \frac{(45700)^2 6(7.5)}{S} = \frac{9.45 \times 10^{10}}{S} \text{ bps}$$

For a 5 inch film,

$$D_R = \frac{2.88 \times 10^{10}}{S} \text{ bps}$$

Stability

The stability of the spacecraft during exposure determines the amount of smear and resulting loss that occurs due to smear. It was

shown in Section 6 that a modulation transfer of about 75 percent due to smear was tolerable and that under this and the other state-of-the-art conditions, the film resolving power was 72 1/mm.

Thus, the permitted pitch and roll motions become

$$\dot{\phi} = \frac{5.5 \times 10^{-4}}{2.24 F t_e} = \frac{2.5 \times 10^{-4}}{F t_e} \quad (\text{rad/sec})$$

and the tolerable yaw motion becomes

$$\dot{\theta} = \frac{2 \times 5.5 \times 10^{-3}}{2.24 D t_e} = \frac{4.9 \times 10^{-3}}{D t_e}$$

For the most difficult exposure situation anticipated (see Appendix J):

$$\dot{\phi} = \frac{2.5 \times 10^{-4}}{6.38 \times 10^{-4} f^2 F} = \frac{0.39}{f^2 F}$$

and

$$\dot{\theta} = \frac{4.9 \times 10^{-3}}{6.38 \times 10^{-4} f^2 D} = \frac{7.7}{f^2 D}$$

Size and Weight

Based on an analysis of existing film cameras, the following empirical expressions for the dimensions (with film and processing) of 5" and 9.5" cameras have been developed:

$$\begin{aligned} 5'' &: (0.102 + 0.01 F + 0.037 L_f^{1/2}) \times 0.25 \times (0.46 + 0.046 L_f^{1/2}) \quad (\text{m}) \\ 9.5'' &: (0.01 F + 0.037 L_f^{1/2}) \times 0.41 \times (0.51 + 0.046 L_f^{1/2}) \quad (\text{m}) \end{aligned}$$

With image motion compensation, additional volume is required for the sensor mechanism and the electronics. These dimensions are:

$$\begin{aligned} \text{Mechanism:} & \quad 0.15 \times 0.15 \times 0.15 \quad (\text{m}) \\ \text{Electronics:} & \quad 0.076 \times 0.15 \times 0.28 \quad (\text{m}) \end{aligned}$$

The weight of the film camera system including the processor but excluding shielding, scanning equipment, or the IMC sensor and electronics is:

$$5'' : M = 6.4k_1 + 0.082D_c^2 + L_f(k_2 + k_3) \quad (\text{kg})$$

$$9.5'' : M = 23.2 k_4 + 0.068D_c^2 + L_f(k_2 + K_3) \quad (\text{kg})$$

where

k_1 is 1.0 w/o IMC and 3.57 with IMC

D_c is lens diameter (cm)

L_f is film length (m)

k_2 is film weight (kg/m^2)

Thick tri-acetate base, $k_2 = 0.181 \text{ kg}/\text{m}^2$ ($w=0.014 \text{ cm}$)

Thin polyester base, $k_2 = 0.107 \text{ kg}/\text{m}^2$ ($w = 0.0069 \text{ cm}$)

k_3 is processing weight (kg/m^2)

$k_3 = 0.197 \text{ kg}/\text{m}^2$ ($w = 0.03 \text{ cm}$)

k_4 is 1.0 w/o IMC and 1.68 with IMC

The estimated weight of the V/H sensor and electronics is 4.6 kg and the flying spot scanner weight is also estimated at 4.6 kg.

The length of film required for a square format is given by:

$$L_f = \frac{(1 + g) A_c}{R^2 \Gamma^2 D} \times 10^6 \quad (\text{m})$$

The weight of a 9.5" film system with IMC and processor but excluding shielding is shown in Figure 7-2.

To estimate the shielding required, the area of the film spool must be determined and multiplied by the requisite shielding mass per unit area.

The film spool size is obtained by assuming the film to be wound on a spool of inner radius 1.27 cm and outer radius

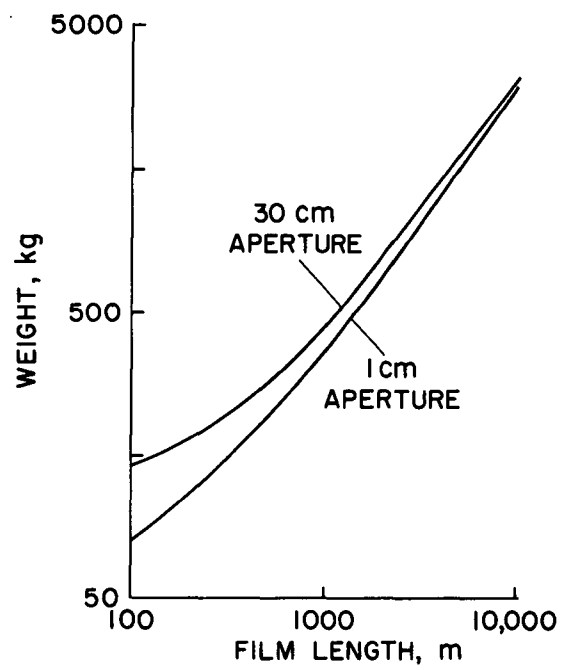
$$R_s = \left(1.27^2 + \frac{100WL_f}{\pi} \right)^{1/2}$$

where w = film thickness

and the surface area of the film spool is given by

$$A_f = 2\pi R_s (R_s + D/10) \quad (\text{cm}^2)$$

Figure 7-2 9.5" Film Shielding Weight with IMC and Processing (No Shielding)



The required shielding thickness depends on the orbit parameters and the type of film used. These factors are discussed in Appendix E. For SO-243 film and the nominal orbit considered here (Orbit No. 8 of Section 2), a shielding weight of 76 kg/m^2 is appropriate. Thus,

$$\begin{aligned} M_{sh} &= 76 A_f \times 10^{-4} && (\text{kg}) \\ &= .0478 R_s (R_s + D/10) && (\text{kg}) \end{aligned}$$

The shielding weight as a function of film length for a 9.5" film magazine is shown in Figure 7-3.

Power

Based on an analysis of the average power requirements for a number of aerial photographic systems and spaceborne designs including Lunar Orbiter, the estimated power for a spaceborne photographic system is,

$$\begin{aligned} P &= 29 + 5.6 D^2 && (\text{w/o IMC}) && (\text{W}) \\ P &= 47 + 16.8 D^2 && (\text{with IMC}) && (\text{W}) \end{aligned}$$

Television

The support requirements for television systems are covered below.

Data Rate

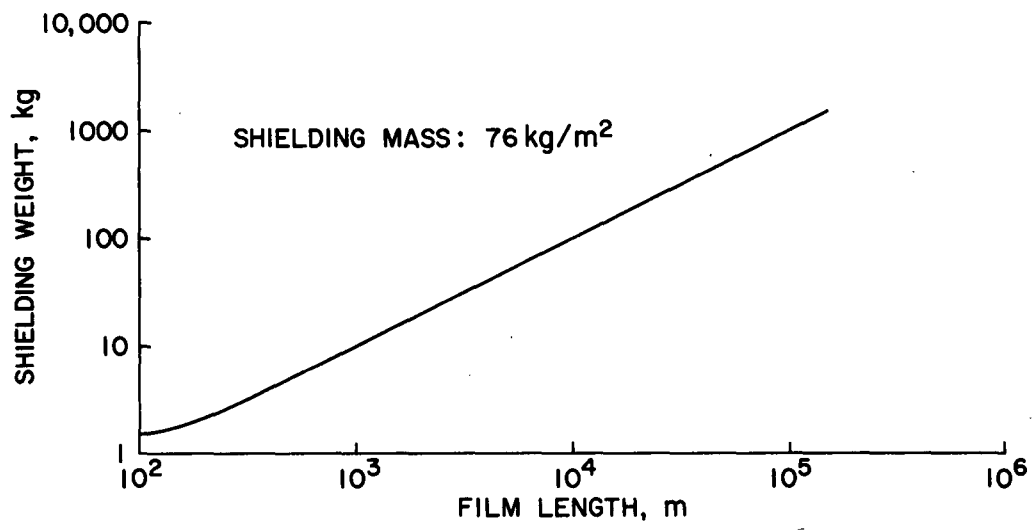
The average data acquisition rate, D_r , is

$$D_r = \frac{L^2 G}{t}$$

For the 4.5" Return Beam Vidicon,

$$D_r = \frac{(6500)^2 \times 6 \times (7.8)}{S} = \frac{1.98 \times 10^9}{S} \quad \text{bits/sec}$$

Figure 7-3 Radiation Shield Weight for 9.5" Film Magazine



Stability

To achieve a modulation transfer with linear image motion of 68 percent or more at a spatial frequency of 30 1/mm (see Section 6), the maximum image motion during exposure is 16.5 μm .

Thus, the tolerable pitch and roll motion, $\dot{\phi}$, are

$$\dot{\phi} = \frac{16.5 \times 10^{-4}}{2.24 F t_e} \quad \text{rad/sec}$$

and the yaw motion, $\dot{\theta}$, is

$$\dot{\theta} = \frac{2 \times 16.5 \times 10^{-3}}{2.24 D t_e}$$

For the anticipated worst case spacecraft exposure time (see Appendix J)

$$\dot{\phi} = \frac{7.4 \times 10^{-6}}{2.16 \times 10^{-5} f^2 F} = \frac{0.34}{f^2 F}$$

$$\text{and } \dot{\theta} = \frac{14.7 \times 10^{-6}}{2.16 \times 10^{-5} f^2 D} = \frac{0.68}{f^2 D}$$

Size and Weight

The dimensions for a vidicon camera are approximated by:

$$(L_t + F) \times 1.1D_T \times 1.1D_T \quad (\text{cm}) \quad (\text{no IMC})$$

where L_t is tube length (see Figure 7-4).

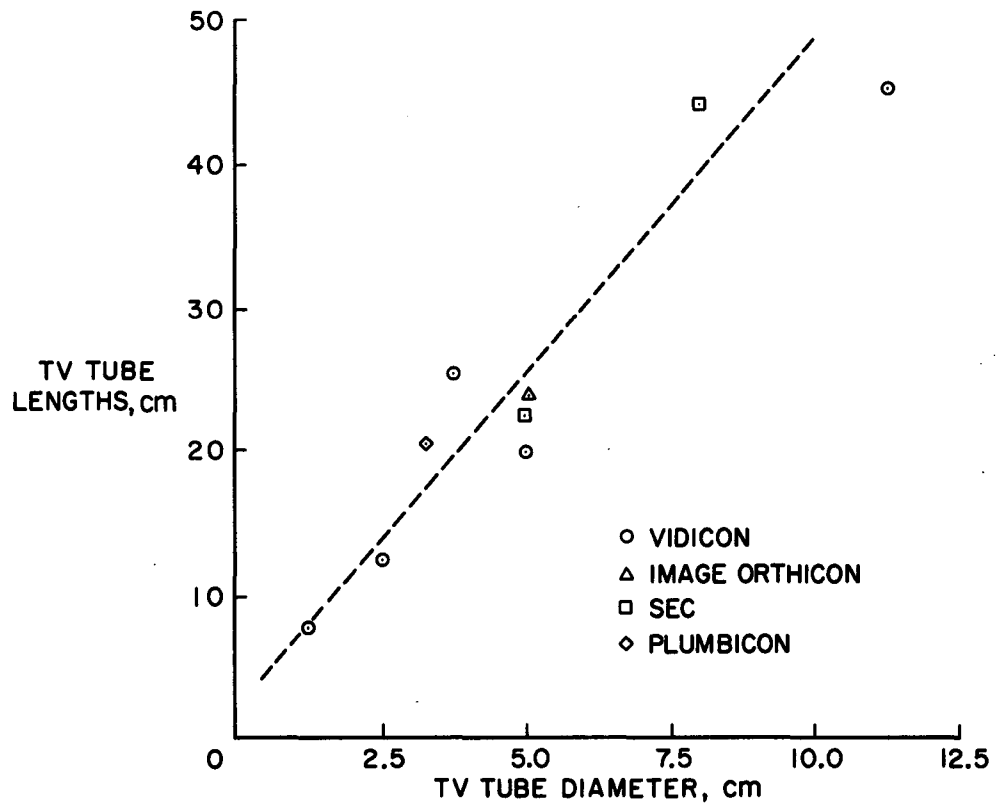
and D_T is tube diameter (assumes that $D_T > D_C$)

With IMC, an additional volume estimated at 0.013 m^3 is required for the mirror system and V/H sensor.

The weight, M , of a vidicon system is

$$M = 2.9 D_T + (.017 D_C^2) k_1 + 6.8 k_2 \quad (\text{kg})$$

Figure 7-4 TV Tube Lengths



where k_1 is zero if $D < 10$ and 1.0 if $D > 10$
 k_2 is zero without IMC, 1.0 with IMC

This expression is plotted in Figure 7-5 for a 4.5" vidicon.

Power

The system power required is

$$P = 6.3 D_T + 15 k_2 \quad (W)$$

Multispectral Scanner, IR Scanner and IR Radiometer

While there are significant differences in the sensitivity and spatial resolution capabilities of these three devices for a given level of support, all are basically similar and thus, with minor exceptions, one set of support requirements relationships suffices. These relationships are discussed below:

Data Rate

The data acquisition rate for these system is given by:

$$D_R = \frac{4SV_s G_n}{R^2} \quad (\text{bps})$$

where n is the number of detectors with resolution R

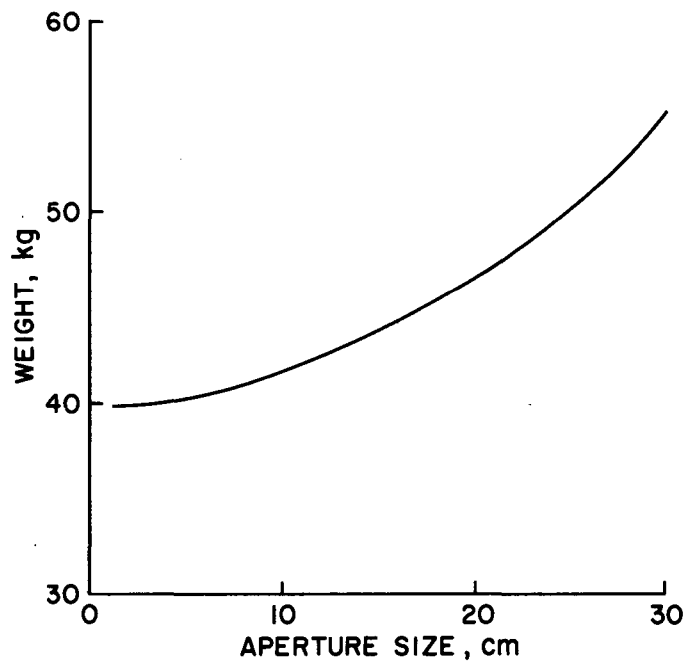
If the spatial resolution, R , varies for different spectral regions in an MSS, the total data rate must be found by summing the rates for all spectral channels.

Stability

For a total motion of one half scan line during the line scan time, the maximum image plane motion, m_t , is

$$m_t = \frac{10BF}{2} \quad (\text{mm})$$

Figure 7-5 4.5" Vidicon System Weight (With IMC)



Thus, the limiting pitch and roll motions, $\dot{\phi}$, are

$$\dot{\phi} = \frac{BF}{4.48 Ft_e} \quad (\text{rad/sec})$$

Since, for a scanner the line scan time, t_e , is expressed as

$$t_e = \frac{V_s \times 10^3}{R/2}$$

then
$$\dot{\phi} = \frac{BR}{4.48 \times 2V_s \times 10^3} = \frac{1.12 \times 10^{-4} BR}{V_s}$$

Similarly, the maximum yaw motion, $\dot{\theta}$, is

$$\dot{\theta} = \frac{2 BF}{2(2.24) F(\tan \alpha/2)t_e} = \frac{2.23 \times 10^{-4} BR}{V_s \tan \alpha/2}$$

For a radiometer looking at the nadir, the pitch and roll considerations are the same as above but there is no yaw motion stability requirement.

Size and Weight

The system volume, exclusive of the coolant subsystem for thermal IR, is

$$V = \frac{\pi D_c^2}{4} (0.73D_c + 0.61F) \quad (\text{cm}^3)$$

assuming the use of a singly folded optical system. The system diameter is approximately $1.1D_c$.

Based on the 80 deg. K closed cycle cooler designed by Hughes for the ERTS thermal IR channel, a volume of about 0.024 m^3 should be adequate per detector for such a device.

The system weight is

$$M = M_c + M_s + M_{sm} + M_m$$

where M_c is the primary mirror mass
 M_s is the secondary mirror mass
 M_{sm} is the scan mirror mass
and M_m is the structure mass

Scaling relations have been developed for each of these components. Assuming beryllium optical elements and an aluminum structure,

$$M = 230 \left[D_c^{5/2} - \left(\frac{0.5D_c}{f} \right)^{5/2} + 150 \left(\frac{D_c}{f} \right)^{5/2} + 230 D_c^{5/2} + 567 D_c^{5/2} \right] \text{ (kg)}$$

The structural weight could be reduced by the ratio of (1.85:2.7) by using beryllium but since large systems would normally be designed so that the spacecraft structure is the telescope housing, aluminum would appear to be a more likely choice. The telescope weight with and without structure is shown in Figure 7-6 for various aperture sizes. The weight of an 80°K cooler, if required, would add about 0.68 kg per detector to the system weight.

Power

The power needed for rotation of the scan mirror in large imaging systems is large compared to the other system power requirements. Thus, system power is approximated by:

$$P = 7.5 \times 10^{-3} D_c^2 M_{sm} \omega^3 \quad \text{(W)}$$

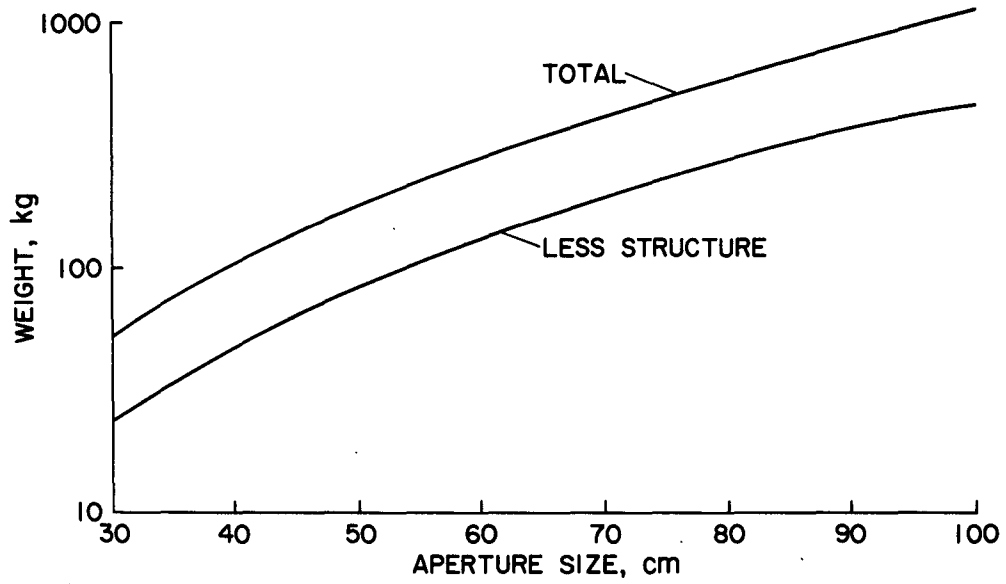
where ω is the mirror rotational speed (rad/sec).

For non-scanning systems the sensor and sensor electronics, reference source, and cooling system are the principal power users. The sensor/electronics power requirement, P , is

$$P = kn^{1/2}$$

where $k = 1.5$ for thermal detection
 $= 4$ for photo detection
 $n =$ number of detectors

Figure 7-6 Cassegranian Telescope Weight



The reference source requires about 5W. If a detector array is used, this should be increased to 10W. The cooling power for 80°K operation is estimated at 20W per detector.

Microwave Scanner/Radiometer

Microwave scanner/radiometer support requirements are discussed below.

Data Rate

The data acquisition rate for a scanning system is given by:

$$D_R = \frac{\alpha G V_s}{B^2 H} \quad (\text{bps})$$

where α is the scan angle
and B is the instantaneous field of view

Since $\alpha = S/H$ and $B = R/2H$,

$$D_R = \frac{4H^2 S G V_s}{R^2}$$

For non-scanning devices (radiometers), the same expression applies with $S = R/2$.

Stability

The considerations discussed in the preceding section apply here also.

Size and Weight

The receiver volume and weight for operation in the vicinity of 30 GHz are estimated at 4900 cm³ and 6.8 kg, respectively.

The form factor can be arranged to suit the aircraft or spacecraft configuration. The antenna volume, V_a , is

$$V_a = \frac{\pi D_c^2}{12}$$

The antenna weight, based on a density of 2.5 kg/m^2 , is

$$M_A = \frac{2.5\pi D_c^2}{4}$$

Antenna weight as a function of aperture area is shown in Figure 7-7. The drive mechanism, assumed to be hydraulic for large antennas, is estimated to weigh 4.6 kg.

Power

The receiver power requirement is estimated at 10W and the antenna drive power at 50W.

Radar

Support requirements for focused coherent side-looking radar systems are discussed below.

Data Rate

The raw data acquisition rate, D_R , for this type of radar system, is

$$D_R = \frac{pSG}{R/2} \quad (\text{bps})$$

Using the azimuth ambiguity constraint, the expression becomes,

$$D_R = \frac{8V_s SG}{L_a R}$$

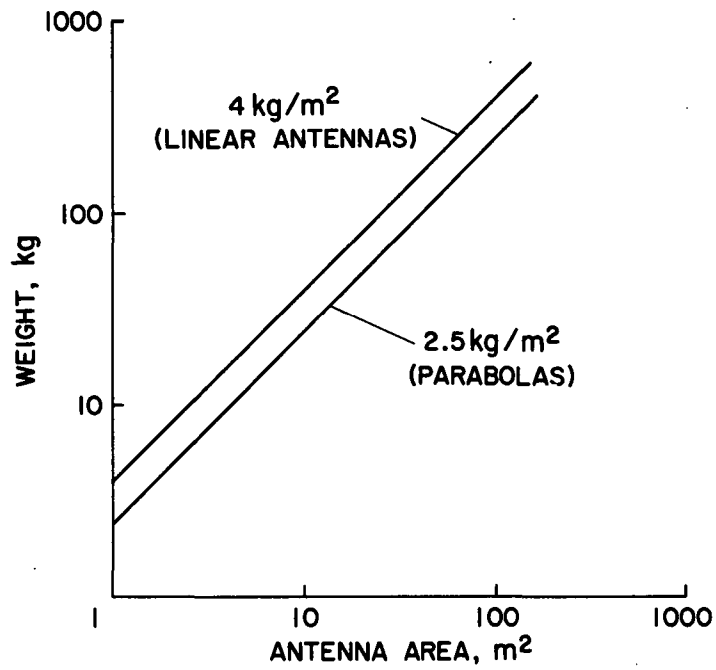
Onboard processing would result in a data rate given by

$$D'_R = \frac{4V_s SG}{R^2}$$

reducing the subsequent data handling and transmission load. The ratio, D'_R/D_R , is given by

$$\frac{D'_R}{D_R} = \frac{4V_s SG L_a R}{R^2 8V_s SG} = \frac{L_a}{2R} \quad (L_a \leq R)$$

Figure 7-7 Antenna Weights for Active and Passive Microwave Systems



Consequently, the processed data rate will be at least a factor of two smaller than the raw data rate. The feasibility of onboard processing has not yet been explored but the size, weight, and complexity of existing systems appear to make early achievement of this capability unlikely.

Stability

With a synthetic aperture system, all mapped elements must remain within the locus of the 3dB real antenna beam contour during the integration time associated with the generation of the synthetic aperture. This implies that the synthetic aperture beamwidth must move a distance less than the resolution size during the integration time. Taking a displacement of one half resolution element as acceptable, the allowable yaw rate, $\dot{\theta}$, becomes

$$\dot{\theta} = \frac{\lambda_r}{2 D_{SA} t_e} \quad (\text{rad/sec})$$

The equivalent 'frame time,' t_e , for the radar is

$$t_e = \frac{\lambda_r r}{L_a V_s}$$

Thus,
$$\dot{\theta} = \frac{L_a V_s}{2 D_{SA} r}$$

The maximum pitch rate, $\dot{\phi}$, is expressed by

$$\dot{\phi} = \frac{\cos^{-1} \left[\frac{\lambda_r / L_a - \lambda_r / 2 D_{SA}}{\lambda_r / L_a} \right]}{t_e}$$

$$= \frac{L_a V_s \cos^{-1} \left[L_a \left(\frac{1}{L_a} - \frac{1}{D_{SA}} \right) \right]}{\lambda_r r}$$

Since target position in range is determined by transit time, roll rate need not be controlled except that the entire mapped swath

must be illuminated during the integration period. Consequently, the elevation beamwidth must be adequate to account for the roll motion. Thus,

$$\dot{\phi} r t_e = \frac{A - S}{2}$$

or
$$\dot{\phi} = \frac{(A-S)L_a V_s}{2r^2 \lambda_r}$$

where A is the region illuminated by the elevation beam.

Size, Weight and Power

The weight of the radar (less antenna) is approximated by

$$M = \frac{P}{78 \sqrt{d_c}} \quad (\text{kg})$$

where P is the average power

and d_c , the transmitter duty cycle, is given by

$$d_c = p\tau = \frac{4V_s}{L_a} \frac{R \cos \theta}{c} \quad \text{without pulse compression}$$

or
$$d_c = pC\tau = \frac{4V_s}{L_a} \frac{C R \cos \theta}{c} \quad \text{with compression}$$

where τ is the pulse length required by the desired ground resolution

C is the compression factor (< 400)

The average power is expressed as

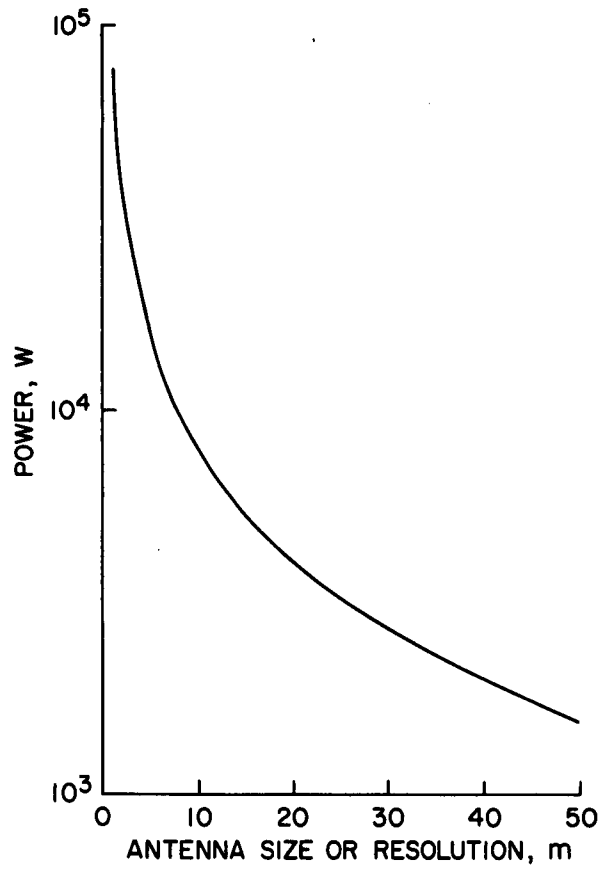
$$P = \frac{94H \sin \theta}{L_a \cos^2 \theta} \quad (\text{W})$$

(assuming 20 percent efficiency; $\lambda_r = 10$ cm, $L_a = R$, and $L_v = \frac{S \sin \theta}{1.2 \lambda_r r}$)

This expression is plotted in Figure 7-8.

Figure 7-8 Radar Total Input Power

20% EFFICIENCY $L_0 = R$ $H = 590\text{ km}$



Thus the weight can be expressed as

$$M = \frac{120 H \sin \theta}{L_a \cos^{5/2} \theta \sqrt{R}} \quad \text{no compression}$$

or

$$M = \frac{12 H \sin \theta}{L_a \cos^{5/2} \theta \sqrt{R}} \quad \text{compression of 100}$$

Radar transmitter weight as a function of antenna size, or resolution, for compression factors of 0 and 100 is shown in Figure 7-9.

The radar transmitter volume, V_R , is

$$V_R = \frac{M}{560} \quad (\text{m}^3)$$

The antenna weight (see Figure 7-7), based on a density of 4 kg/m^2 , is

$$M_A = 4L_a L_v \quad (\text{kg})$$

and the antenna volume is

$$V_A = \frac{L_a L_v}{3} \quad (\text{m}^3)$$

Scatterometer

These relationships are for a scatterometer with a fan-shaped beam extending from the nadir to 45 degrees in front of the spacecraft.

Data Rate

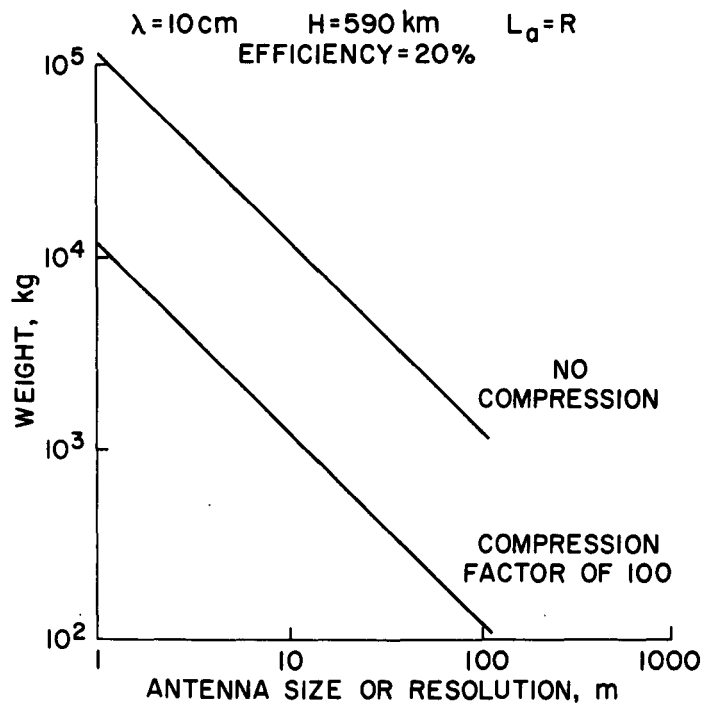
For the geometry outlined above, the cell size, R , on the surface is

$$R = \frac{2H \times 10^3}{N} \quad (\text{m})$$

where H is the altitude

and N is the number of cells (resolution elements)

Figure 7-9 Radar Transmitter Weight



The data collection period, t_e , becomes

$$t_e = \frac{H}{NV_s} = \frac{R \times 10^{-3}}{2V_s}$$

$$\text{Thus } D_R = \frac{NG}{t_e} = \frac{4HV_s G \times 10^6}{R^2} \quad (\text{bps})$$

For a dynamic range of 40 dB in 0.62 dB steps, $G = 6$. For two frequencies and two polarizations, G must be increased to eight. (It is assumed that one frequency and one polarization is used for any one collection period.)

Stability

Assuming that the yaw rate must not exceed the value that results in one half the cross track beamwidth at the far end of the swath,

$$10^3 \dot{\theta} t_e = \frac{R}{4}$$

$$\text{or } \dot{\theta} = \frac{R}{4Ht_e \times 10^3} = \frac{V_s}{2H} \quad (\text{rad/sec})$$

Using the same criterion for pitch and roll,

$$H\dot{\phi} t_e = \frac{R}{4}$$

$$\text{or } \dot{\phi} = \frac{V_s}{2H}$$

Size and Weight

The scaling laws discussed in the radar section apply here also.

Power

The average power is expressed as

$$P = 4.4 \times 10^{-10} \frac{H^2 V_s}{R^2} \quad (\text{W})$$

8. COMMUNICATIONS SYSTEMS ANALYSIS

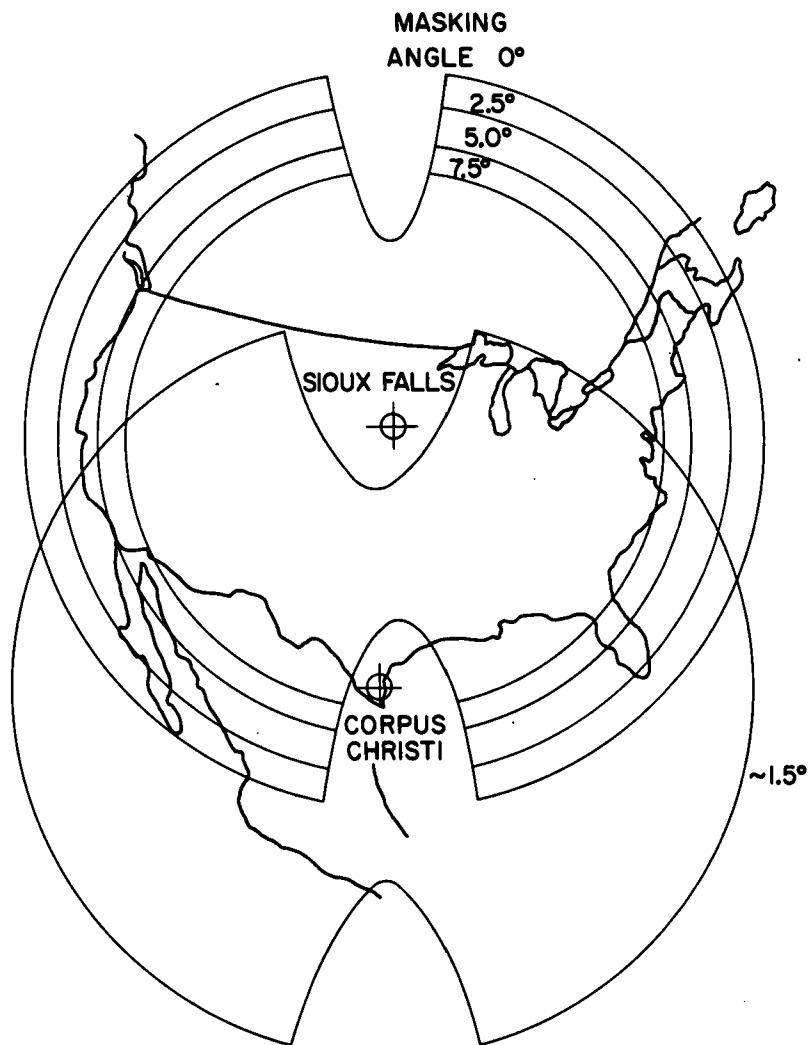
The purpose of this section is to address the fundamental questions of data transfer from a spaceborne observation system to a ground-based central facility. In keeping with the study constraints the emphasis is on transfer of data acquired over (or near) the continental United States. However, consideration is also given to data transfer from an acquisition system operated on a global basis. A review of possible sensors indicated that very high acquisition rates, up to several gigabits per second, might be necessary to satisfy resolution and coverage requirements for some applications. To provide the flexibility to satisfy these requirements should they materialize, the analysis is not limited to a review of current S-band transmission capability and possible modest extensions. Instead it includes, as well, investigations of the utility of geosynchronous relay satellites, the relative advantages of stored data transmission through the existing world-wide network, and postulated advanced communications systems compatible with higher data acquisition rates. Data transmission alternatives are examined without attempting to tailor any telemetry system to a particular sensor requirement other than, as indicated, to satisfy the spectrum of sensors under consideration.

The analysis is limited to downlink telemetry from the acquisition system since this imposes the most severe requirements on a communications link and may impact spacecraft design and restrict operational flexibility as well. The command or uplink, due to availability of high transmitter power and low data rate, is not critical and was not investigated.

Real Time Transmission

Figure 8-1 shows the nominal ground station coverage over the continental United States for a satellite altitude of 590 km (Orbit No. 8 of Section 2). The Manned Space Flight Network (MSFN) station at Corpus Christi, Texas, having a 30 ft. tracking antenna, is assumed available to this task as shown (Ref. 33). In addition, a portion of the Goddard facility and a Satellite Tracking and Data Acquisition Network (STADAN) site at Fairbanks may be allocated for additional coverage. A new site in the vicinity of Sioux Falls, South Dakota, is under consideration to supplement or supersede the

Figure 8-1 Nominal Station Coverage for Data Acquisition
System Altitude of 590 km



above coverage (Ref. 34). This latter site is also shown in Figure 8-1 for a range of possible masking angles. The cusps in each pattern are due to gimbal interference that limits low angle coverage.

It is clear from the figure that coverage of the continental United States from this altitude with real-time data transmission to these sites is feasible. It is also evident that using only these sites the incorporation of data storage aboard the spacecraft would not markedly enhance this capability since the coverage patterns do not extend significantly beyond the area of sensor activation. (It is assumed that the Alaskan site would be needed for real-time Alaskan data.)

Real-time data transmission performance is described in Table 8-1 for a ground station with a 30 ft. antenna and uncooled parametric amplifier receiver operating at S-band (2300 MHz). This is the most common station configuration in the NASA network. Other ground station configurations currently in operation are compared in Table 8-2. It is clear that for a satellite at this altitude the rate of data delivery is not limited by available satellite power. For the minimum capability system, 6 Mbps may be transmitted for each watt of RF power. It must be noted that Table 8-1 also suffices to describe performance at X-band (8450 MHz) since increased space loss would be compensated by increased ground antenna gain.

The ground network which receives the sensor telemetry consists mainly of dual stations at each site that have the capability of simultaneously demodulating four channels of data. With the anticipated receiver improvements (Refs. 36,37) an estimated total data rate limitation of approximately 50 to 60 Mbps to a dual site, or half of this to a single site, is possible in the 2200-2300 MHz band.

Provided improved receiving equipment were installed at each site, existing spectrum allocations could permit operation over a 2200-2450 MHz band. In this case it would be possible to transmit up to about 125 Mbps to a site. This would, however, mean possible interference from amateur radio service (Ref. 38).

As an alternative, a change in modulation method such as the use of quadriphase PSK rather than either biphase PSK or PCM/FM could increase the

Table 8-1
Downlink Telemetry
Power Budget at S-band, Altitude 590 km

Transmitter power (1 watt)	0 db
Transmitter antenna gain	4
Transmitter pointing loss	- 3
Transmission loss	- 1.5
Receiver loss	- 0.5
Free space loss (2300 MHz, 2500 km)	-167.7
Ground station antenna gain (30')	44
Receiver pointing loss	<u>- 0.5</u>
Received Power	-125.2
 <u>Carrier Channel</u>	
Modulation loss ($\Delta\phi = 1.1$ radian)	<u>- 7</u>
Carrier Power	-132.2
Noise spectral density (T = 130°K, uncooled paramp)	-207.5
Noise tracking bandwidth (700 Hz)	<u>28.5</u>
Noise Power	-179.0
C/N	46.8
C/N Threshold	- 12
Required margin for system tolerances	<u>- 3</u>
Margin	31.8
 <u>Data Channel</u>	
Modulation loss ($\Delta\phi = 1.1$ radian)	<u>- 1</u>
Signal Power	-126.2
Noise spectral density (T = 130°K)	-207.5
S/N ₀	81.3
Required ST/N ₀ (PSK (BT = 2), P _e = 10 ⁻⁵)	10.5
Required margin for system tolerances	<u>3.0</u>
Maximum Data Rate	67.8 db ≈ 6 Mbps

Table 8-2
MSFN Comparative Telemetry Performance

Ground System	Antenna Gain	Noise Temp. at 50° Elev.*	Maximum Data Rate at 1 Watt Trans. Power
30' uncooled parametric amplifier	44	130°K	6 Mbps
30' cooled parametric amplifier	44	65°K	12 Mbps
85' cooled parametric amplifier	52.5	65°K	85 Mbps

*Refs. 35,36

Table 8-3
Summary of Maximum Data Rate Capability
for Various Communications Systems

Present S-band capability

25-30 Mbps to a single station

50-60 Mbps to a dual station

Possible extensions of present system

125 Mbps biphase

250 Mbps quadriphase

Possible improved capability at X-band

250 Mbps biphase

500 Mbps quadriphase

Advanced systems

500-1000 Mbps, mm-band link

500-5000 Mbps or higher, laser link

data rate in the available bandwidth. For example in the 2200-2450 MHz band, 250 Mbps could be transmitted. Quadriphase PSK modems operating at X-band have been demonstrated with data rates of 450 Mbps (Ref.39).

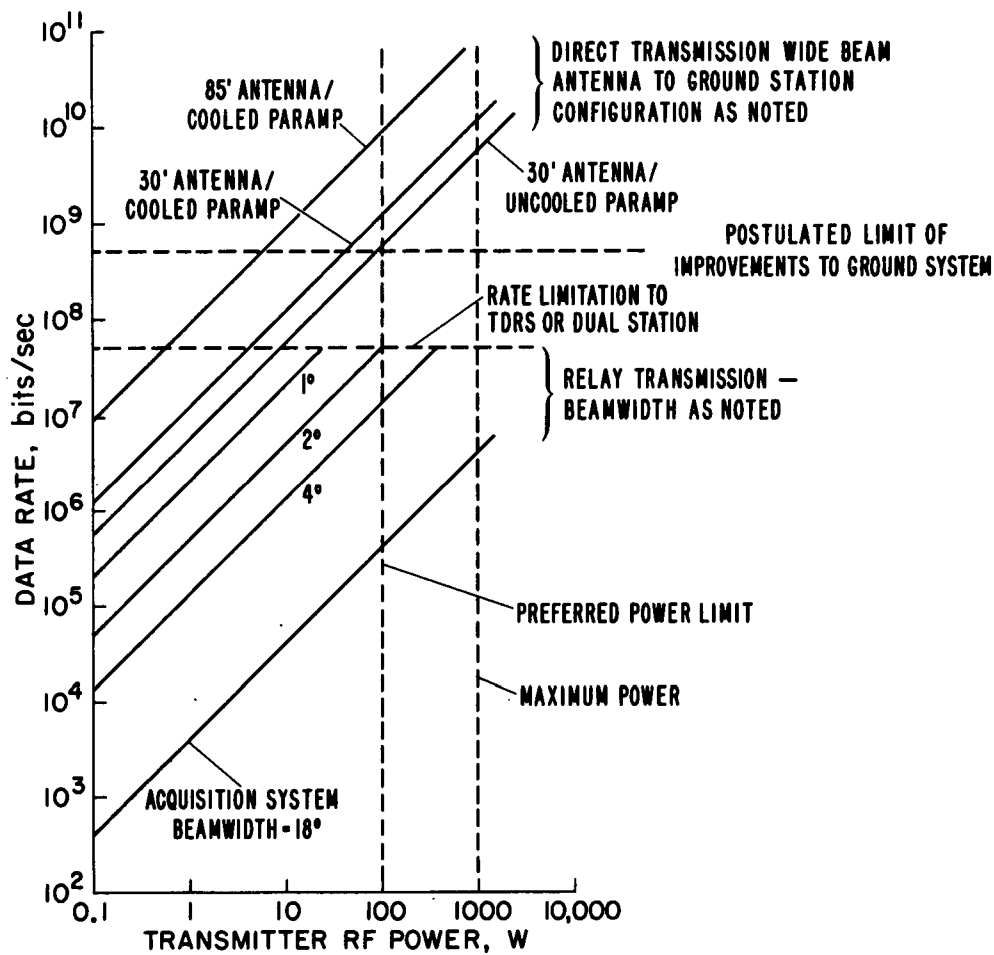
In order to further widen the available bandwidth it is also possible to transfer operations to a higher frequency. At X-band, 0.5 GHz channels have been allocated to communications satellite service. Provided agreements could be obtained and non-interference guaranteed, it would be possible to transmit up to 250 Mbps with biphase PSK or 500 Mbps with quadriphase.

A further extension of operating frequency into the mm region would require increased power due to atmospheric and other losses. Decreased transmitter efficiency would further increase the spacecraft auxiliary power system requirements. However this portion of the spectrum is not congested and rates up to 400 Mbps are under study (Ref.40). It appears that with continued development rates on the order of 1000 Mbps will be possible at radio frequencies. Laser links could be employed at higher rates, the final limitations of which are not yet known. These systems will be further explored in following sections. Table 8-3 summarizes the capability so far described.

Figure 8-2 depicts the limitations and zones of application of both direct and relay data transmission modes. Shown is the data rate versus RF power for direct transmission to the various ground stations of Table 8-2, and the performance utilizing a tracking and data relay satellite (TDRS) obtained from Ref. 41. The effect of acquisition system antenna beamwidth, which is directed toward the TDRS, is also shown. Since the TDRS is at synchronous altitude, an antenna with approximately an 18 degree beamwidth would keep it in view during acquisition system passage from limb to limb. As indicated in the figure this results in severely curtailed transmission which, nevertheless, may be adequate for many applications. To achieve higher data rates with reasonable power levels a narrow beam antenna would be required to track the TDRS. The direct link operates satisfactorily with a wide beam, low gain antenna aboard the spacecraft.

Also indicated on Figure 8-2 are suggested acquisition system

Figure 8-2 Data Link Performance and Limitations



transmitter power limits. While TWT's in the one kilowatt range are available, and multikilowatt tubes have been studied for TV broadcast satellites, the impact of such power demands upon the weight of the spacecraft tend to constrain transmitters to the 100 watt class.

The TDRS concept of Reference 41 considers the merits of various operating frequencies: Between the acquisition system/TDRS; VHF, S, X and K-bands: between TDRS/TDRS; X and K-bands: and between TDRS/ground; X-band. Both 4 foot and 8 foot TDRS antenna diameters are considered in the reference to be appropriate for this application. The configuration presented here employs either an S-band or X-band (7.9 GHz) link between acquisition system and relay satellite with an 8 foot antenna on the latter. This configuration performance is independent of whether S or X-band is used and permits a valid comparison of TDRS performance with that of the existing (S-band) or updated (X-band) ground network for direct transmission, which likewise is independent of frequency. (Higher frequency operations are compared in a later section.)

The proposed relay satellite design has an instantaneous bandwidth of 100 MHz which, for two-phase PSK, typically limits the telemetry channel capacity to 50 Mbps. As indicated in Figure 8-2, this is comparable to the current capacity of dual ground stations. From a review of this figure it is clear that for applications with moderate data rates either system would be satisfactory based on spacecraft power requirements. For higher rates, above 50 Mbps, only a direct link would be feasible since it offers the potential of much higher rates with reasonable power. The postulated extension in performance to about 500 Mbps by improvements to the ground network is also shown. Higher telemetry rates would likely necessitate the use of advanced systems.

Stored Data Transmission

With a given transmission channel capacity it is possible to accommodate higher sensor data acquisition rates by recording the data for delayed transmission at tolerable rates. Transmission may be either through a TDRS to a ground site in the United States, or "direct" to the worldwide NASA network as previously described. It is presumed here that

both STADAN and MSFN stations which are configured to receive high data rate S-band telemetry would be available, at least in part, to support an operational Earth observation program. The data, once received, would then require satellite relay or physical transport to a processing center in the United States.

The use of data storage aboard the acquisition system provides flexibility in that the acquisition rate need not be limited by the transmission rate. The maximum acquisition rate, R_a , provided there exists adequate total data storage capacity is given by

$$R_a = R_t (P/T) F$$

where

- R_t = available transmission rate
- P = orbital period (= 5800 sec. at 590 km)
- T = data acquisition period
- F = view fraction

The view fraction is the relative portion of each orbit in which data transmission is possible. For two TDRS stationed in synchronous orbit 132 degrees symmetrically from the longitude of Washington, D.C., communication is possible for approximately 93% of each orbit at this altitude (Ref. 42).

The view fraction for direct transmission is a function of site placement, site low angle coverage and masking patterns, and orbital altitude and inclination. For an altitude of 590 km and employing a typical masking angle of 5 deg., Table 8-4 indicates the duration of data acquisition periods for orbits which pass over the continental United States as well as the corresponding view fraction. The view fraction varies with the longitude of the ascending node and minimum and average values, which are of interest for communications, are shown. It should be mentioned that although the availability of a TDRS would result in the probable closing of several overseas sites, the entire network was included in arriving at these figures.

Table 8-4
Communications Parameters for Representative Orbits

Orbit Code	Inclination	Data Acquisition Period per Orbit (sec)		View Fraction per Orbit	
		<u>Maximum</u>	<u>Average</u>	<u>Minimum</u>	<u>Average</u>
4	50°	555	315	34%	49%
6	63°	390	310	10%	28%
8	97°	350	240	9%	21%
11	117°	390	310	10%	28%

For the above parameters the sensor rate, for a telemetry rate of 50 Mbps, is shown in Figure 8-3. For an inclination of 50° there is a clear advantage in transmitting the data (that which could not be sent to U.S. sites) to the overseas network. Sensor rates may be increased to 200 to 450 Mbps as compared to a real-time rate of 50 Mbps. At higher inclinations however, the lesser improvement may not justify the additional difficulty of collecting and merging data obtained by several sites.

The relay satellite performance is not shown in Figure 8-3 for clarity, but would extend the improvement to 93% contact in each case. The maximum sensor rate is then given in Table 8-5 below.

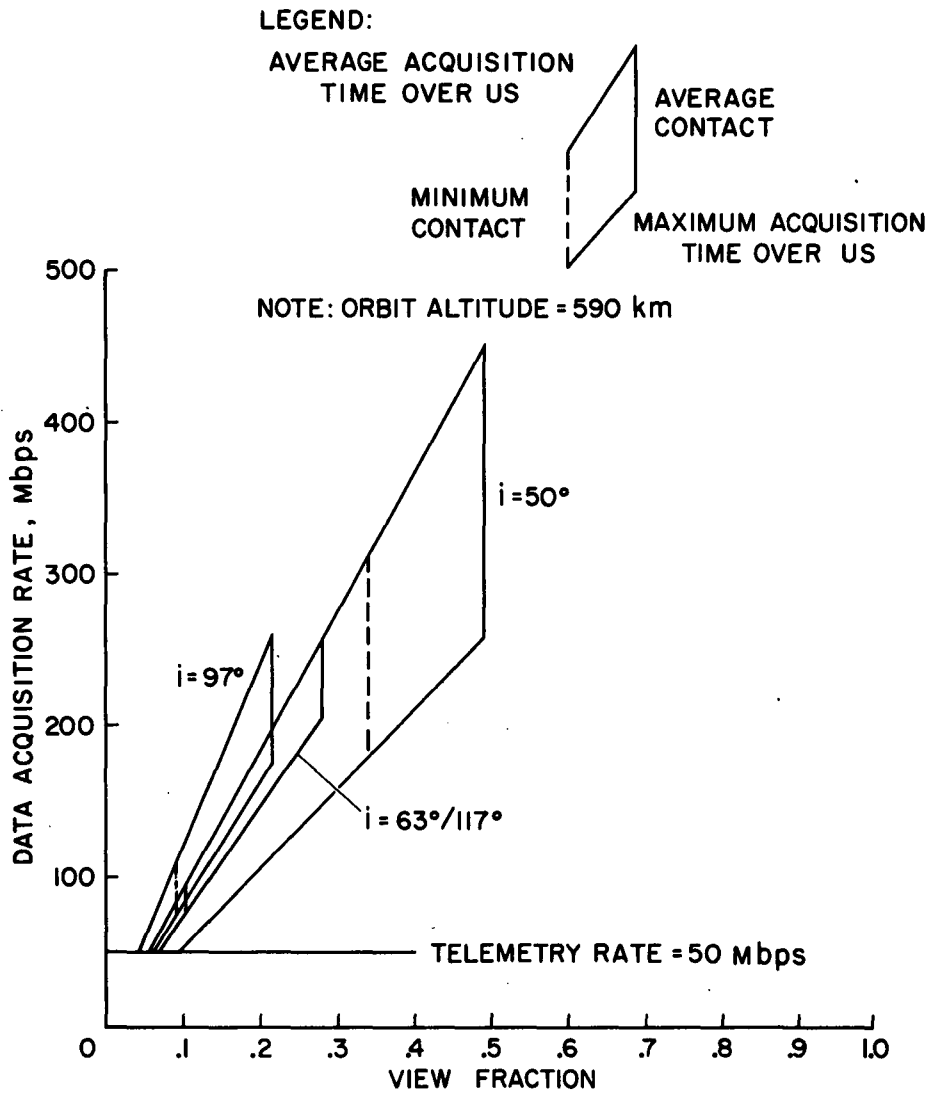
Table 8-5
Maximum Sensor Rate for 50 Mbps Telemetry
Through a Data Relay Satellite

Inclination	Acquisition Period over United States	
	<u>Maximum</u>	<u>Average</u>
50°	485 Mbps	857 Mbps
63°/117°	693	870
97°	770	1120

The relay satellite offers significantly higher sensor rates and the advantage of returning all the data to the same U.S. tracking station. The penalty for such operations is, as previously noted, in the higher transmitter power borne by the Earth observation system.

Recording system capability required for the applications discussed in this report is on the order of 10^{11} - 10^{12} . Recorder input rate is a

Figure 8-3 Data Acquisition Rate Over U. S. with Constant 50 Mbps Telemetry Rate Throughout Orbit



result of the sensor required for a given application; the highest value uncovered in this study is 290 Mbps (see Table 9-2) which is about an order of magnitude beyond current recorder band width capability. The camera systems (see Table 9-2), which have the highest data rate requirement, use film for storage. Continued effort to increase recorder capacity and reliability is needed as well as research to develop new methods of data storage. Since the recorder is often the weakest element in a data system, improvements to this device directly enhance mission effectiveness.

Advanced Systems

For sensors with very high rates, and there are only a few which exhibit this requirement, adequate telemetry capability may be provided by one of several means. The previous section described the sensor rates which could result from non real-time transmission. The magnification factor of 4 to 9 times the telemetry rate would also apply above 50 Mbps transmission capacity. Thus by relatively modest improvements in ground station capability, to several hundred Mbps, sensor rates in the Gbps range would be feasible. Alternatively, the use of higher carrier frequencies, either RF or optical, provides a means of telemetering in real-time sensor rates to several Gbps. This obviates the need for data storage or, alternatively, permits even greater resolution and/or coverage to be obtained. This section examines the penalties which accompany these improvements, in terms of increased transmitter power, operational complexity or spacecraft stabilization accuracy.

Millimeter Systems

Due to the inherently wider bandwidths of components and the relatively large blocks of unallocated or "government use" spectrum, millimeter wavelength transmissions may operate at rates of 500-1000 Mbps. Disadvantages lie in the increased link susceptibility to weather and, to some extent, the unavailability of components. This latter problem, however, is in the process of being rectified.

The present status of data links under study or development in the cm to mm region operate at 250-500 Mbps, and rates to 1000 Mbps are anticipated. It is not clear at this time whether higher rates will be preempted by laser links which are more suited to operations at several

Gbps. The acquisition system requirements given in Table 9-2 reach a maximum rate of 0.9 Gbps with the exception of one film system which requires 3.3 Gbps. Therefore this section will examine mm systems operating at a nominal of 1 Gbps, for both direct and relay transmission. As indicated in Table 8-3, this is the approximate limiting capability of mm systems.

In the mm and near-mm region are several frequencies with sufficient spectrum for wideband telemetry. Table 8-6 lists those which could be considered as candidates for direct communications to Earth (Ref. 38). Although higher frequency windows exist at about 94, 140 and 200-300 GHz, the effects of weather and the state of component development are such that the frequencies listed are preferable for this application. In the region between 20 and 27 GHz, atmospheric attenuation is more severe than at immediately higher or lower frequencies, and for this study those frequencies are not considered further. However with increased power this region could provide a viable telemetry band.

Table 8-6
Possible Bands for High Data Rate Telemetry

f (GHz)	Bandwidth (GHz)
13.4 - 14.0	0.6
14.4 - 15.35	0.95
15.7 - 17.7	2.0
19.7 - 21.0	1.3
22.0 - 24.25	2.25
25.25 - 27.52	2.25
31.5 - 31.8	0.3
33.4 - 38.6	5.2

For this application the 35 GHz window was employed since sufficient bandwidth is available for 1 Gbps telemetry, and it provides a more clear demonstration of mm capability than would lower frequencies. For relay links atmospheric attenuation is not a consideration and interference with Earth based systems is minimal. Thus far more flexibility is possible in the choice of frequency. The TDRS study previously mentioned did not

consider frequencies above 15 GHz due to present component limitations. In the 1980 time frame, however, projected technology improvements should permit operational links at 35 GHz with moderate power requirements. For a postulated relay satellite link at 35 GHz, Table 8-7 lists transmitter powers based on current technology as demonstrated on the ATS experiment and estimated improved receiver capability (Ref. 43).

Table 8-7
Acquisition System RF Power for 1 Gbps
Through Relay Satellite

	Receiver NF	Transmitter ERP	RF Power for Transmitter Antenna Diameters	
			4 foot	8 foot
ATS Technology	17 db	79.4 db	870 watts	220 watts
Improved Technology	9 db	71 db	126	31

As is evident from the above, lowered noise figures for spaceborne mm receivers is essential if relay links are to be used at very high rates. Transmitter power is presently limited to about 50 watts at this frequency, without elaborate cooling techniques.

The employment of large (8') antennas results in a reduction of the half-power beamwidth to 0.25 degrees as compared to 0.5 degrees with a 4 foot dish. A more sophisticated examination than can be performed here would be necessary to ascertain the minimum beamwidth for which acquisition time and satellite-to-satellite tracking is acceptable.

The alternative method of data retrieval is, as before, direct to ground stations. Since such a network does not presently operate in the mm band, one or several stations would need to be constructed for this application. Table 8-8 details the power budget with the assumed ground system characteristics of a 30' antenna followed by an uncooled parametric amplifier with a 400°K noise temperature. (Ref. 44). It is seen that in order to transmit the data at the assumed rate of 1 Gbps, a transmitter power of 2 W is needed to yield an adequate rain margin.

Table 8-9 compares performance of this link with some alternatives. From the power budget of Table 8-1 a transmitter power of 166 watts is required for 1 Gbps at either S or X-band. A link consisting, as in this

Table 8-8
Power Budget for 1 Gbps Spacecraft-to-Ground
Telemetry at 35 GHz

Transmitter power (2 watts)	3.0 db
Spacecraft antenna gain (6" diameter)	32
Transmitter pointing loss	- 1
Transmission loss	- 2
Atmospheric attenuation	- 0.5
Free space loss (1200 km)	-185.0
Ground station antenna (30')	67.8
Receiver pointing loss	<u>- 0.5</u>
	- 87.2
 <u>Carrier Channel</u>	
Modulation loss ($\Delta\phi = 1.1$ radian)	- 7
Carrier power	- 94.2
Noise spectral density (490°K)	-201.7
Noise tracking bandwidth	28.5
Noise power	-173.2
C/N	79.0
C/N Threshold	12
Required margin for equipment tolerance	<u>3</u>
Margin	64
 <u>Data Channel</u>	
Modulation loss ($\Delta\phi = 1.1$ radian)	- 1
Signal power	- 88.2
Noise spectral density	-201.7
S/No	113.5
Required ST/No ($P_e = 10^{-5}$)	10.5
Data rate (10^9 bps)	90
Required margin for equipment tolerance	<u>3</u>
Rain or fading margin	10 db

Table 8-9
Comparison of Direct Transmission Modes
for a Data Rate of 1 Gbps

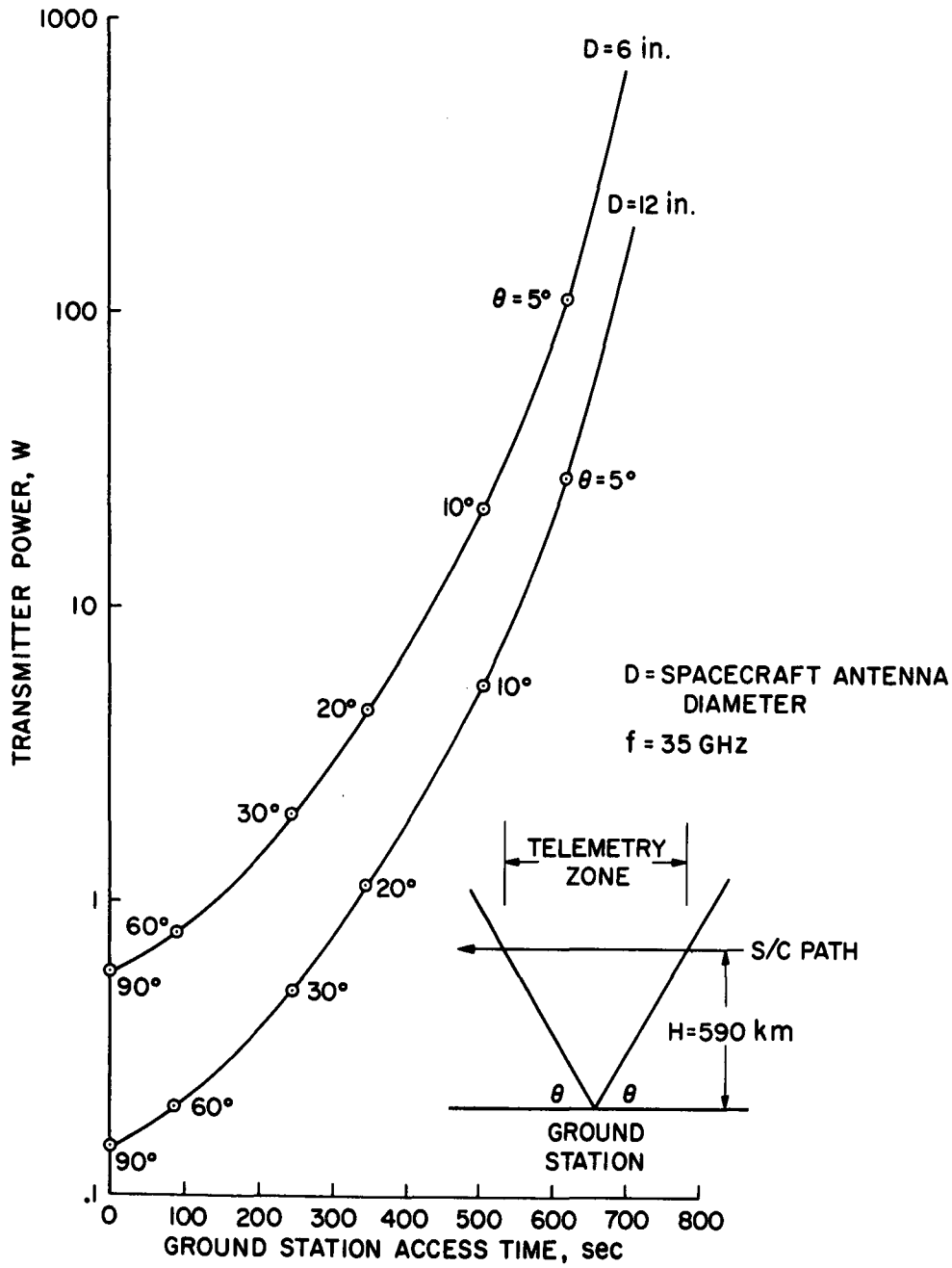
	Spacecraft Transmitter Power (watts)	Single-Station Communications Time per Pass
S, X-band broad beam	166	620 sec.
mm-band, broad beam	2000	240
mm-band, narrow beam	2	240

case, of a fixed gain transmitter antenna directed towards a fixed aperture receiving antenna is nominally independent of frequency. However, at 35 GHz the higher noise figure receiver and additional margin to compensate for rain attenuation result in a substantial increase in required power. It is evident from Table 8-9 that a fixed broad beam antenna, comparable to that used at lower frequencies, is not feasible in the mm region. A high gain trainable antenna must be used to reduce the power to a reasonable level. The angular tracking rates for direct transmission are about two orders of magnitude greater than for relay transmission and a much wider beam antenna must be used to ease tracking loop design. Thus, rather than the 4 to 8 foot antenna employed to track the relay satellite, a 6 inch parabolic dish is used. This is sufficient to supply three orders of magnitude increase in gain as shown in Table 8-9. This antenna produces a 4 degree beam which must be directed towards the ground receiver to an accuracy of about ± 1.2 degrees. This should not be excessive for an open loop control system. If needed, however, a low power signal could be transmitted from the ground station for closed loop tracking.

Table 8-9 also indicates a reduction in access time to the ground station. This is due to the requirement for restricting the ground system low angle coverage due to increased noise and attenuation at low angles at higher frequencies. At S or X-band tracking may be permitted down to 0° in many cases; but masking limits coverage to an average of 5° . In the mm-band, a 30° limitation is a reasonable limit. Figure 8-4 demonstrates the impact of elevation angle at signal acquisition upon both transmitter power and access time for this design. Increased telemetry time could be obtained as indicated by the employment of a 12 inch antenna on the spacecraft. Again a more extensive study would be necessary to balance these factors in an optimum design. Figure 8-4 does not include allowance for multipath fading at low angles. The rain margin of 10 db from Table 8-8 is used as a nominal value sufficient to maintain communications during approximately a 15 mm/hr rainfall at the ground station (Ref. 45).

It is concluded that mm links would be feasible with continued technology improvement and would provide a means of retrieving the data

Figure 8-4 Effects of Ground Station Access Time on Transmitter Power



in real time. In the case of direct transmission, implementation would be more difficult than at lower frequencies due to the necessity for mutual acquisition and tracking by the ground station and satellite.

Laser Systems

Table 9-2 lists only one sensor with a data rate which would be difficult to accommodate by means of mm links. Should that system, which is a film system requiring 3.3 Gbps, or another with comparable performance be implemented, laser links provide the only reasonable real-time means of retrieving the data. In addition, a growth potential for more advanced sensors is provided by laser communications development. Laser systems are undergoing very rapid progress. This section highlights the areas of required continued component development and discusses the feasibility of both direct and relay links.

A direct link from satellite to ground station must pass through the Earth's atmosphere and this influences several technical choices in the link design. Since clouds effectively block laser transmission, ground stations would preferably be located in regions with a low probability of cloud cover. In order to reduce the effects of a clear atmosphere, the path length is restricted by limiting transmission to a zone within 30° of zenith. This, as shown in Figure 8-4, results in a communications time of 90 sec. for a direct flyover of a single site. In order to reduce acquisition procedures to a minimum, non-coherent or direct detection is utilized.*

Table 8-10 details the power requirements for a laser link as well as providing a summary of the technical assumptions necessary to its design; these will be discussed in turn. A visible wavelength rather than infrared is used since wideband, sensitive direct detectors are not yet available at long wavelengths. A number of lasers have been developed which operate in the visible spectrum and which would be equally

* Coherent link performance has the further disadvantages of possible phase corruption by a turbulent atmosphere and a doppler-shifted signal which must be tracked. For a signaling rate much higher than the temporal phase change the former may not be critical, and by operation at infrared wavelength the doppler shift may be reduced to an acceptable level; however these factors must be more extensively investigated in future studies.

satisfactory. Efficiencies are very low (typically less than one percent), although possibly acceptable due to the lower power requirement of this direct link. Indeed, although laser emission levels of 100 watts have been demonstrated in the laboratory, their low efficiency is the factor which restricts transmitter power levels to less than a watt for a space-borne device. As indicated in Table 8-10, 0.1 watt radiated power is sufficient for a data rate of up to 5 Gbps. This rate, as indicated in Table 8-3, is representative of the upper range of rates obtainable with these devices and also is a significant improvement over that achievable by means of millimeter systems. Although this bit rate is not possible today, it should be possible in the early 1980s.

Referring back to Table 8-10, turbulence in the atmosphere results both in amplitude fluctuations in the signal and in a spreading of the laser beam which reduces the effective gain (Ref. 46). Propagation phenomena of this nature are not well defined. For this study, however, a $10 \overline{\text{sec}}$ standard deviation is assumed for this effect resulting in a beam divergence requirement of nominally $25 \overline{\text{sec}}$. A fading margin in excess of 10 db is necessary to ensure communications continuity; nearly 17 db margin is provided by this link. To reduce background noise an optical filter is used which also attenuates the signal by 7 db. A photomultiplier detector is assumed which has a responsivity of .05 amperes per watt (Ref. 47). The modulation method employed is PCM and could consist of amplitude or polarization modulation or pulse position modulation with a pulsed laser. No attempt has been made to determine the optimum method for this application; instead amplitude modulation has been used since this has been demonstrated to have a wideband capability (Ref. 48). An energy ratio of 10 db was used as a nominal value of E/N_0 in Table 8-10. This could be improved by the use of coding but at the cost of even higher bit rates. Pulse interval or position modulation would reduce the bit rate for a fixed data rate (ref. 49). Finally, a margin of 3 db to accommodate equipment degradations is provided. As is evident from Table 8-10, direct link performance is not limited by available transmitter power. The limiting factors are the non-availability of very wideband modulators and detectors, efficient wideband transmitters, (CW or pulsed,) and generally space-qualified laser components.

Table 8-10
Laser Direct Link Power Budget

Transmitter power (100 milliwatts)	- 10 db
Transmitter optical gain (25 sec)	89
Transmitter optical loss	- 3
Atmospheric Loss	- 1
$1/4\pi R^2$ (100° km)	-131.1
Receiver optical loss (including filter)	- 10
Receiver collecting area (10 M diameter)	<u>18.9</u>
Received Power (watts)	- 47.2
Noise spectral density, N_0	<u>-174</u>
S/N_0	126.8
Data rate 5 Gbps	97
Required E/N_0	<u>10</u>
	19.8
Equipment tolerance	<u>- 3</u>
Fading margin	16.8 db

A laser relay link consists of a relay spacecraft at synchronous altitude directing a laser transmitter toward a fixed ground station and a laser receiver toward the sensor spacecraft. The relay satellite is assumed to have sufficient power to accomplish its mission; the emphasis here is on the sensor spacecraft laser requirements.

A satellite-to-satellite link avoids the encumbrance of the Earth's atmosphere and has considerably more time for signal acquisition and data transmission, (in this case on the order of 25 to 30 times as long,) and a much lower doppler shift. On the other hand, the increased communications distance puts a premium on high power and high efficiency transmitters and sensitive receivers. As a result, heterodyne detection of infrared (10.6 microns) has been investigated. This permits the consideration of CO₂ lasers which currently have efficiencies up to 20% and high average powers. The optics are larger than at visible wavelengths and for this application are limited to 8 inch diameter (0.2m) at both sensor and relay satellites in order to restrict communications systems weight. As a result the beamwidth is 13.3 $\widehat{\text{sec}}$ which permits a pointing stability of several arc seconds. This is well within present capability and the critical operational phase will be the initial pointing and signal acquisition which may determine the beamwidth requirement.

The detection process operates within 6 db of the theoretical quantum limit with a detector quantum efficiency of 0.5 (ref. 47). This should be expected to improve before the contemplated operational period. Although a data rate of 1 Gbps was used in this instance, power requirements may be directly extrapolated to higher data rates. The required rate for relay operation may be much lower than for direct transmission due to the greater access time, and a 1 Gbps rate is consistent with the options of either a pure laser or mixed system with a mm link from relay satellite to ground station. An energy ratio of 10 db was assumed for heterodyne detection for $P_e = 10^{-5}$ without coding (Ref. 50).

Table 8-11 demonstrates that for this link a transmitter power of 10 watts is sufficient to provide a margin of 6.4 db to compensate for equipment tolerances and degradations. Carbon dioxide lasers are readily constructed with powers on the order of 100 watts or greater which could

provide a growth potential to 10 Gbps for this link. Laboratory models have operated with output powers as high as 9 kw but transmitter cooling and spacecraft power supply requirements limit the power level which may be considered as appropriate to this application. The technological effort again must concentrate on wideband techniques and components. Wideband heterodyne detectors have been undergoing development and have exceeded 1 GHz by cooling the mixer (Ref. 51). Modulators at present require excessive driving power and continued research is necessary (Ref. 52). The approach to be implemented will be determined by the extent of technological progress in these areas.

Table 8-11
Laser Relay Link Power Budget

Transmitter power (10 watts)	10
Transmitter optical gain ($D = 0.2M, 13.3 \text{ sec}$)	94.5
Transmitter optical loss	- 3.
$1/4 \pi R^2$ (50000 km)	-165.
Receiver area ($D = 0.2 \text{ m}$)	- 14.9
Modulation loss	- 3.
Receiving optical loss	<u>- 3.5</u>
Received power	- 84.9
Noise spectral density, N_0	-191.3
S/N_0	106.4
Data rate (1 Gbps)	90.
Required E/N_0	<u>10.</u>
Margin	6.4

9. REPRESENTATIVE ACQUISITION SYSTEMS

The purpose of this section is to identify, from the innumerable number that could be postulated, a small number of representative satellite and aircraft borne acquisition systems. These systems are identified by sensor type, capabilities, orbit, data acquisition rate, power requirements and gross weight of either the complete satellite or of the sensor/support package that would be flown aboard the aircraft.

These system definitions are preceded by charts that summarize in parametric fashion the capabilities of each satellite borne sensor type. The results are a straightforward application of the detailed sensor capability analysis presented in Section 6. Shown with the capability charts are figures that depict the data acquisition rates and the estimated gross weight of the sensor-carrying satellite. These parametric summary data can serve two purposes. First they will help identify the representative systems shown later in relation to the multitude of other choices that could have been made. Second it is hoped that these charts can be used jointly by representatives of the user community and NASA as part of the effort needed to arrive at the best compromise between requirements and capabilities.

These summary data are followed by a description of the analytical method used to select the representative systems. Since the method makes use of the user requirements it is appropriate that it be explained so that it might be employed by others using different requirements.

Sensor Capability Summary

The capabilities are summarized in Figures 9-1 through 9-9. Each figure is in three parts. Part (a) displays for each sensor the relationship between spatial and temperature resolution, swath width, time for complete coverage (at 40° latitude) and the percent coverage

during other coverage intervals.* All results are based on Orbit No. 8, namely the sun-synchronous circular orbit of approximately 590 km altitude. (Recall from Section 2 that this orbit yields nearly 15 orbits per day with the actual altitude being a weak function of the time required for complete coverage.) Certain other orbits (e.g., 14 orbits per day, elliptical, etc.) can be more advantageous for certain sensor types but the results shown here are typical of those for medium altitude orbits. Such orbits are included in the definition of the representative acquisition systems later in the section.

Other clarifying statements are needed for a better understanding of the summary charts. For instance the data for film camera and RBV systems represent only a single black and white imager. And, for the multispectral scanner, the data is predicated on imaging in the visual and near-IR spectrum only. The representative systems identified later in this section, however, are not necessarily subject to such simplification. Thus systems that make use of multiple cameras as a possible alternative to a multispectral scanner are shown, as are systems that employ a multispectral scanner that would operate from the visual through the far IR.

Part (b) of each figure shows the data acquisition rates. These results are based on the sensor support requirements discussed in Section 7. These rates may be compared with the data transmission capability summarized in Table 8-3. For seven of the nine applicable sensors, the S-band telemetry network presently utilized by NASA is adequate. For the remaining sensors, this network is satisfactory only for resolutions on the order of 50-100 meters. To accommodate resolutions down to a few meters improved capability is necessary, including the possible development of new communications systems as discussed in Section 8.

Part (c) shows the gross weight of each satellite system. Also shown are the payload weight capabilities of representative launch

* Time for complete coverage and percent coverage are shown in Figure 9-1(a) only. For a given orbit and swath width these measures of capability are independent of sensor capability.

vehicles from Section 3. The satellite weight estimates were made using a digital computer program, described in Reference 53, that was developed to estimate parametrically the weights of unmanned spacecraft. The program was developed for use primarily in the analysis of scientific, as opposed to applications oriented, spacecraft and was modified to make it more suited to the systems being considered here. This weight synthesis includes all subsystems normally included in unmanned vehicles and is predicated on the appropriate sensor design technology projections discussed in Section 7. Results are based on the use of solar arrays with storage batteries as required. Real-time data transmission is presumed (although this is not necessarily required nor, for certain combinations of sensors and communication systems, even possible) and consequently no onboard data storage systems are included (except that inherent to film systems). Similarly no provision is made for an onboard system to receive data from remote ground based sensors although an operational Earth observation system would likely include such a feature. The communications subsystem was sized for a direct transmission mode to S-band tracking stations. This tends to result in somewhat conservative weight estimates at very high data rates. Relay communications, as discussed in Section 8, provide greater operational flexibility in data readout but exact an additional weight penalty which was not evaluated. All satellite weights are predicated on a one year useful lifetime. Thus sufficient support system redundancy and attitude control gas is included as well as, for the film camera systems, the proper length of film and radiation shield weight. As a last point of clarification, no orbit adjust propulsion system is included.

The results shown here should not be taken literally but are felt to be sufficiently accurate to identify the class of launch vehicle required for the various sensor characteristics. History indicates, however, that early weight estimates are uniformly optimistic even after the equipment list has been agreed upon.

System Selection Technique

At first glance it would not seem possible to employ user requirements in a systematic process of identifying typical systems because, even taking the requirements as known, the requirements are not commensurable. For instance, suppose a system could meet either spatial resolution requirements or temperature resolution requirements but not both. Without the existence of some kind of value function that expresses both of these measures of resolution on a common "value" scale, we would not know which compromise would result in the optimum system. The development of techniques for arriving at value functions in general for this class of problem has been the subject of much research but the results to date do not lend themselves to the task at hand.

Thus attempts at removing the incommensurability of the various measures of requirements were not pursued and, as a consequence, the value of a system cannot be determined. However if the nominal requirements are assumed known it is nevertheless possible to arrive at some measure of the worthwhileness of a system by investigating its deviations from nominal. To do this a normalized error function, E, of the general form

$$E^2 = \left(\frac{R}{R_0} - 1\right)^2 + \left(\frac{1.2S_0}{S} - 1\right)^2 + \left(\frac{\Delta T}{\Delta T_0} - 1\right)^2 + \left(\frac{T}{nT_0} - 1\right)^2 + \left(\frac{P_0}{nP} - 1\right)^2$$

was constructed, where the variables are:

R = spatial resolution

S = swath width

ΔT = temperature resolution

T = time for total coverage

P_0 = percent of area viewed after T_0 days

n = number of properly oriented satellites

The subscript "o" refers to nominal requirements from Table C-1 where P_0 is taken to be 100 percent. Note also that the design swath width

is greater than the nominal value to yield a corresponding 20 percent overlap between adjacent ground tracks.

For a given sensor type, then, the sensor design variables and satellite orbits are varied and the combination that minimizes E is the preferred system. Although this approach does obviate the need for commensurability it contains three other inherent assumptions that should be mentioned here. First it implies that all five dimensions of capability are of equal importance, e.g., swath width is as important as temperature resolution. Second it implies that the change in value within each dimension is a linear function of the absolute measure of the capability. Thus a spatial resolution of $2R$ is presumed to result in a system that is exactly half as valuable (so far as resolution is concerned) as a system of resolution R . Finally it is assumed in using the error function that no additional value would accrue if the nominal requirements were to be exceeded. (Computationally each term in the expression is set to zero if the requirements are exceeded to avoid, as the expression might imply, penalizing a system with superior performance. This third assumption simply states that no additional credit is given such a system.)

In the actual computation of the error additional constraints are imposed for those systems (namely the film camera, vidicon, multispectral scanner and infrared scanner) whose performance depends on solar elevation angle and/or cloud cover. Define $L(n)$ to be the fraction of time during the year if n satellites are used that, for at least one satellite, (a) the solar elevation angle is greater than 20 degrees for circular orbits or (b) the elevation angle is greater than 20 degrees and simultaneously, for elliptical orbits, the altitude over the continental United States is less than the equivalent circular altitude. For a circular sun-synchronous orbit having (approximately) either 14 or 15 orbits per day $L(1) = 1$. For elliptical orbits with a non-stationary apsidal line and all orbits of

other inclinations $L(1) < 1$ and, in this way, it is possible to isolate the relative utility of such orbits.

To account for the presence of clouds the expected fractional time, $B(n)$, for unobstructed observations if n satellites are employed can be approximated from Section 5 as:

$$B(n) = 1 - C^{(nT_0/T)}$$

where C is the average cloud cover.

Thus the constraint on the area viewed in T_0 days, even for $T \leq T_0$, is

$$\frac{P_0}{nP} \leq \frac{1}{L(n) B(n)}$$

Table 9-1 summarizes the specific form of the error function for each sensor type and for each intermediate altitude orbit. The sensor technology constraints discussed earlier in Section 7 are also repeated for convenience.

It should be pointed out here that this approach for system definition was felt to be unnecessary for aircraft borne sensors. If the not unreasonable assumption is made that the resolution achievable from an aircraft is adequate one would simply design a system that yields the maximum practical swath width and accept the corresponding resolution. This is taken to be 25 km, based on a 90 degree field of view from an altitude of 40,000 feet. (See Section 4.)

Representative Systems

Tables 9-2 and 9-3 summarize the salient features of the systems chosen for investigation for satellite borne and aircraft borne sensors respectively. It should be apparent that none of the systems can necessarily be recommended at this time for more detailed study. They do, however, reflect the broad spectrum of capabilities that could be realized and the requirements thus imposed on the support subsystems.

For each satellite borne sensor type at least one system is shown as determined by using the normalized error function. Since the error function is intended only as an aid in the selection process, and since the minimum deviation sometimes remains nearly constant over a wide range of sensor design parameters and orbit types (hence capabilities), other systems are also shown as denoted by the asterisks. Included in this category are acquisition systems that would operate from geosynchronous orbit. A few of the user requirements (remembering the earlier caveat of Appendix C) dictate coverage frequencies on the order of one day or less. Such frequencies are difficult to achieve from the more traditional orbits. The essentially continuous coverage of the continental United States (and nearby waters) possible from synchronous altitudes make such orbits at least worthy of consideration.

With the possible exception of the six band multispectral scanner the entries in the table are self-explanatory. For this particular sensor the differences in radiant energy and detector performance between the thermal IR band and the visual bands require that different time constants and instantaneous fields of view be used.

Note that the majority of systems employ circular sun-synchronous orbits. All intermediate altitude orbits discussed earlier in Section 2 were investigated using the normalized error function. But the inability to meet solar elevation angle constraints or the higher altitudes encountered over the United States during certain times of the year tend to make them unattractive. The one possible exception to this general conclusion is the elliptical orbit with stationary apsidal lines. The low altitude that is maintained over the United States permits better resolution (and apparently an adequate swath width) for those sensors that do not require particular lighting conditions.

Insofar as the aircraft borne sensors are concerned the systems shown in Table 9-3 are predicated on a payload weight compatible with

the smaller twin engine jet aircraft. As noted in the table, two sensor/support package weights are shown. The first and lighter of the two (W_1) is based on the use of a gasoline powered generator to supply electrical power. The weight of the generator and fuel, of course, depends on the electrical power requirements but is typically about 25 kg. Such a system could be used aboard the aircraft of a special purpose fleet to provide a package totally independent of the aircraft subsystems for ease of installation and removal. Since the generator is so light, however, the weights shown are also representative of a system that would draw its power from the aircraft electrical power system.

The heavier, battery powered, systems (W_2) are representative of the package weights if flown aboard commercial air carriers. The basic premise adopted here is that there should be absolutely no dependence of the package (except for structural support) on the aircraft systems and that, moreover, the package itself should contain no combustibles or high pressure gases. In these examples all electrical power is presumed to be supplied by storage batteries. In keeping with this non-dependency philosophy it is also assumed that an independent inertial guidance system is made a part of the sensor/support package to act, not necessarily as a guidance system, but rather to record the route that was actually flown. Such an independent system was also assumed to be aboard the craft of a special purpose fleet.

Table 9-1 Normalized Error Functions

	Error Function	C ₁	C ₂	C ₃	Orbit Inclination, deg						D	β	τ	D/A
					50		63/117		97					
					C ₄	C ₅	C ₄	C ₅	C ₄	C ₅				
Flm Camera	$\epsilon^2 = \left[\frac{C_1 (H/F)}{R_0} - 1 \right]^2 + \left[\frac{C_2 S_0}{D} (H/F) - 1 \right]^2 + \left[\frac{C_4}{n_0^2 D} (H/F) - 1 \right]^2 + \left[\frac{C_5 P_0}{n_0^2 D} (H/F) - 1 \right]^2$	1.38	1.0	-	1220	12.2	1700	17.0	2150	21.5	<35	-	-	-
Vidicon	$\epsilon^2 = \left[\frac{C_1 (H/F)}{R_0} - 1 \right]^2 + \left[\frac{C_2 S_0}{D} (H/F) - 1 \right]^2 + \left[\frac{C_4}{n_0^2 D} (H/F) - 1 \right]^2 + \left[\frac{C_5 P_0}{n_0^2 D} (H/F) - 1 \right]^2$	3.43	1.0	-	1220	12.2	1700	17.0	2150	21.5	<35	-	-	-
Multispectral Scammer	$\epsilon^2 = \left[\frac{C_1 B H}{R_0} - 1 \right]^2 + \left[\frac{C_2 S_0}{D} - 1 \right]^2 + \left[\frac{C_4}{n_0^2 D} - 1 \right]^2 + \left[\frac{C_5 P_0}{n_0^2 D} - 1 \right]^2$ $D^2 \beta^2 \tau = 8 \times 10^{-11}$	2000	0.75	-	909	9.09	1260	12.6	1600	16.0	<100	>1.6 x 10 ⁻⁵	>5 x 10 ⁻⁸	-
Infrared Scammer	$\epsilon^2 = \left[\frac{C_1 B H}{R_0} - 1 \right]^2 + \left[\frac{C_2 S_0}{D} - 1 \right]^2 + \left[\frac{C_3}{D^2 \beta^2 \Delta T} - 1 \right]^2 + \left[\frac{C_4}{n_0^2 D} - 1 \right]^2 + \left[\frac{C_5 P_0}{n_0^2 D} - 1 \right]^2$ $D^2 \beta^2 \tau = 5.55 \times 10^{-11}$	2000	0.75	5.55 x 10 ⁻⁸	909	9.09	1260	12.6	1600	16.0	<100	>1.6 x 10 ⁻⁵	>1 x 10 ⁻⁷	-
Infrared Radiometer	$\epsilon^2 = \left[\frac{C_1 B H}{R_0} - 1 \right]^2 + \left[\frac{C_2 S_0}{D} - 1 \right]^2 + \left[\frac{C_3}{D^2 \beta^2 \Delta T} - 1 \right]^2 + \left[\frac{C_4}{n_0^2 D} - 1 \right]^2 + \left[\frac{C_5 P_0}{n_0^2 D} - 1 \right]^2$	2000	1.0	5.55 x 10 ⁻⁸	1220	12.2	1700	17.0	2150	21.5	-	>1.6 x 10 ⁻⁵	>1 x 10 ⁻⁷	-
Microwave Scammer	$\epsilon^2 = \left[\frac{C_1 H}{R_0 (D/\lambda)} - 1 \right]^2 + \left[\frac{C_2 S_0}{D} (D/\lambda) - 1 \right]^2 + \left[\frac{C_3}{D \Delta T} - 1 \right]^2 + \left[\frac{C_4}{n_0^2 D} (D/\lambda) - 1 \right]^2 + \left[\frac{C_5 P_0}{n_0^2 D} (D/\lambda) - 1 \right]^2$	2400	5.17	0.06	6350	63.5	8950	89.5	11400	114	-	-	>10 ⁻⁴	<300
Microwave Radiometer	$\epsilon^2 = \left[\frac{C_1 H}{R_0 (D/\lambda)} - 1 \right]^2 + \left[\frac{C_2 S_0}{D} (D/\lambda) - 1 \right]^2 + \left[\frac{C_3}{D \Delta T} - 1 \right]^2 + \left[\frac{C_4}{n_0^2 D} (D/\lambda) - 1 \right]^2 + \left[\frac{C_5 P_0}{n_0^2 D} (D/\lambda) - 1 \right]^2$	2400	0.84	0.06	1015	10.2	1410	14.1	1760	17.6	-	-	>10 ⁻⁴	<300
Cohesent Side-Looking Radar	$\epsilon^2 = \left[\frac{C_1 H \sin \theta}{R_0 P \cos^2 \theta} - 1 \right]^2 + \left[\frac{C_2 S_0 P \cos^3 \theta}{H \sin \theta} - 1 \right]^2 + \left[\frac{C_3}{D \Delta T} - 1 \right]^2 + \left[\frac{C_4}{n_0^2 H \sin \theta} - 1 \right]^2 + \left[\frac{C_5 P_0 \cos^3 \theta}{n_0^2 H \sin \theta} - 1 \right]^2$	94	2 x 10 ⁻³	-	2.6	0.026	3.63	0.036	4.59	0.045	-	-	-	-
Scatterometer	$\epsilon^2 = \left[\frac{C_1 H}{R_0 (D/\lambda)} - 1 \right]^2 + \left[\frac{C_2 S_0 (D/\lambda)}{D} - 1 \right]^2 + \left[\frac{C_4}{n_0^2 H} - 1 \right]^2 + \left[\frac{C_5 P_0 (D/\lambda)}{n_0^2 H} - 1 \right]^2$	2380	0.715	-	872	8.72	1220	12.2	1535	15.3	-	-	-	<300

θ = depression angle; P = output of spacecraft auxiliary power system



Reproduced from
best available copy.

Table 9-2 Representative Satellite Borne Acquisition Systems

System Description	Orbit Code No.	Sensor Design Parameters					Capabilities						Support Requirements				
		Focal Length, F, (cm)	Char. Size, D, (cm)	Instant. Field of View, β , (rad)	Dwell Time, T, (sec)	Ant. Toler. D/ λ	Spot. Res. R, (m)	Swath Width, S, (km)	Temp. Res; ΔT , ($^{\circ}K$)	Cover. Time, T, (days)	% Cover. ¹ in "Req." Interval	No. of Sat	Power ² (w)	Max. Att. Rate (mr/sec)	Data Acq. Rate (bits/sec)	S/C Weight (kg)	Smallest Compat. Launch Vehicle
single black & white 9" film camera; 1 yr film supply for continental U.S. & Alaska	8	124	23	-	-	-	6	108	-	23 12 8	62 86 95	1 2 3	145	(IMC)	9.1×10^8	1450	Titan IIIB/ Agena D
single black & white 5" film camera; 1 yr film supply for continental U.S. & Alaska	8	84	12.5	-	-	-	10	83	-	29 15 10	54 79 90	1 2 3	60	(IMC)	3.0×10^8	705	Delta (3 SRM)
five ganged 9" cameras for multispectral imaging; 1 yr film supply for continental U.S. only	8	89	23	-	-	-	9	150	-	17 8 6	56 80 91	1 2 3	585	(IMC)	3.3×10^9	3720	Titan IIID/ SCS
single camera; 6" x 9" format composed of five 70 mm frames for multispectral imaging; 1 yr film supply for continental U.S. only	8	43	7	-	-	-	19	86	-	28 14 9	29 62 77	1 2 3	290	(IMC)	8.0×10^8	1300	Delta (9 SRM)
single return beam vidicon; 2" format	7	131 143 143	5	-	-	-	24 22 22	37 34 34	-	69 38 23	13 45 63	1 2 3	85	(IMC)	5.8×10^7	250	Delta (3 SRM)
five ganged 2" vidicons for multispectral imaging	7	62 66 66	5	-	-	-	34 32 32	50 48 48	-	50 26 17	10 35 56	1 2 3	435	(IMC)	2.9×10^8	765	Delta (6 SRM)
multispectral scanner; five bands; visual through near IR	7	-	100	3.1×10^{-5}	8.1×10^{-6}	-	61	150	-	17 8 6	56 80 91	1 2 3	1000	4.2	4.3×10^7	2190	Titan IIIB/ Agena D
multispectral scanner; five bands; visual through near IR	8	-	100	3.9×10^{-5}	5.3×10^{-6}	-	48	150	-	17 8 6	56 80 91	1 2 3	1000	6.6	6.6×10^7	2190	Titan IIIB/ Agena D
multispectral scanner; five bands; visual through near IR	7	-	75	3.6×10^{-5}	1.1×10^{-5}	-	69	150	-	17 8 6	56 80 91	1 2 3	560	4.2	3.3×10^7	1190	Titan IIIB/ Agena D
multispectral scanner; five bands; visual through near IR	8	-	75	4.5×10^{-5}	6.9×10^{-6}	-	56	150	-	17 8 6	56 80 91	1 2 3	560	5.7	5.1×10^7	1190	Delta (9 SRM)
infrared scanner; thermal IR band	7	-	100	4.7×10^{-5}	1.8×10^{-5}	-	90	155	0.6	16	72 92	1 2	1200	6.8	3.4×10^6	2220	Titan IIIB/ Agena D
infrared scanner; thermal IR band	7	-	75	5.7×10^{-5}	2.6×10^{-5}	-	109	155	0.6	16	72 92	1 2	760	6.8	2.3×10^6	1230	Titan IIIB/ Agena D
infrared scanner; thermal IR band	9	-	100	5.5×10^{-5}	9.7×10^{-6}	-	67	155	0.6	16	72 92	1 2	1200	6.5	6.2×10^6	2220	Titan IIIB/ Agena D
infrared scanner; thermal IR band	11	-	75	8.2×10^{-5}	2.4×10^{-5}	-	57	155	0.6	16	72 92	1 2	760	12.0	1.0×10^7	1230	Titan IIIB/ Agena D
multispectral scanner; six bands; visual through thermal IR; design parameters optimized through near IR	8	-	75	4.5×10^{-5} 9.6×10^{-5}	6.9×10^{-6} 1.4×10^{-5}	-	56 120	150 150	0.6	17 8 6	56 80 91	1 2 3	760	5.7	5.2×10^7	1250	Delta (9 SRM)
*multispectral scanner; six bands; visual through thermal IR; altitude & swath selected for one day coverage interval	8	-	75	7.5×10^{-5} 1.1×10^{-4}	2.6×10^{-6} 3.9×10^{-6}	-	133 197	2580 2580	0.6	1	100	1	760	4.2	1.4×10^8	1300	Titan IIIB/ Agena D
microwave scanner	11	-	-	-	1.0×10^{-3}	300	2800	280	1.9	7 3 2	43 86 100	1 2 3	60	very large	7000	185	Delta (3 SRM)
*microwave scanner; dwell time selected to meet temperature resolution requirements	11	-	-	-	1.4×10^{-2}	300	2800	15	0.5	138 68 45	2 4 6	1 2 3	60	very large	500	185	Delta (3 SRM)
microwave radiometer	11	-	-	-	1.4×10^{-2}	36 50 55	24100 17300 15800	12 9 7	0.5	170 113 97	4 6 7	1 2 3	10	very large	40 60 70	115	Delta (3 SRM)
*microwave radiometer; selected for best spatial resolution	11	-	-	-	1.4×10^{-2}	300	2800	1.4	0.5	1460 730 480	0.5 1.0 1.5	1 2 3	10	very large	350	155	Delta (3 SRM)
coherent side-looking radar; 2300 watts of power; 45 deg. depression angle	11	-	$19/0.6^3$	-	-	-	19	141	-	15	100	1	2300	0.31	1.5×10^8	5900	Titan IIID/ SCS
coherent side-looking radar; 500 watts of power; minimum depression angle	11	-	$19/5^3$	-	-	-	19	104	-	20	100	1	500	0.05	1.1×10^8	1900	Titan IIIB/ Agena D
scatterometer	11	-	-	-	-	5 10 12	196000 98000 81500	98 47 42	-	21 21 16	1.2 1.2 1.6	1 2 3	50	very large	<1	110	Delta (3 SRM)
*scatterometer; selected for best spatial resolution	11	-	-	-	-	300	3260	1.6	-	1250 625 416	0.02 0.04 0.06	1 2 3	74	very large	<1	255	Delta (3 SRM)
*infrared scanner; thermal IR band; one pass per day over U.S.	3	-	75	3.6×10^{-5}	1.6×10^{-5}	-	465	5150	0.6	1	100	1	760	0.6	4.1×10^6	1250	Atlas/Centaur TE-364-4
*single camera; 6" x 9" format composed of five 70 mm frames for multispectral imaging; 1 yr film supply; 1 snapshot of U.S. per day	1	58	7	-	-	-	850	4300	-	1	100	1	290	(IMC)	$5.9 \times 10^{3(4)}$	650	Atlas/Centaur TE-364-4
*single camera; 6" x 9" format composed of five 70 mm frames for multispectral imaging; 1 yr film supply; camera programmed for 45 pictures per day; complete U.S. coverage; maximum resolution	2	635	7	-	-	-	114	395	-	1	100	1	320	(IMC)	$2.7 \times 10^{11(4)}$	2200	Titan IIID/ Centaur
*multispectral scanner; five bands; visual through near IR; 45 min. per scan; complete U.S. coverage each scan	1	-	50	1.6×10^{-5}	1.3×10^{-4}	-	1150	4300	-	1	100	1	250	0.05	2.4×10^7	580	Atlas/Centaur TE-364-4
*infrared scanner; thermal IR; 45 min. per scan; complete U.S. coverage each scan	1	-	50	3.7×10^{-5}	6.8×10^{-4}	-	2680	4300	0.6	1	100	1	450	0.05	8.7×10^4	615	Atlas/Centaur TE-364-4
*multispectral scanner; six bands; visual through thermal IR; 45 min. per scan; complete U.S. coverage each scan	1	-	50	1.6×10^{-5} 8.8×10^{-5}	1.3×10^{-4} 6.9×10^{-4}	-	1150 6350	4300	- 0.6	1	100	1	450	0.04	2.4×10^5	640	Atlas/Centaur TE-364-4

* System not based on normalized error function
 (1) See Table G-1 for required coverage interval; percent coverage shown above includes cloud cover effects for sensors operating in visual and IR bands
 (2) Electrical power output required of S/C power system for sensor support only
 (3) Antenna length/width (m)
 (4) Bits/day

Reproduced from best available copy.

PRECEDING PAGE BLANK NOT FILLED

Table 9-3 Representative Aircraft Borne Acquisition Systems

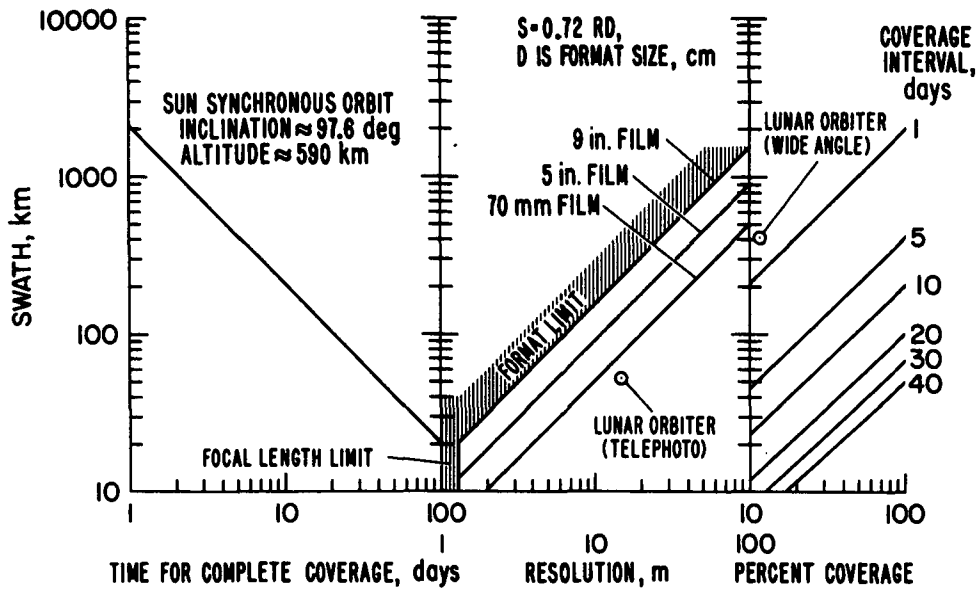
System	Sensor Design Parameters				Capabilities ¹			Support Requirements			
	Focal Length, F, (cm)	Char. Size, D, (cm)	Instant. Field of View, β , (rad)	Dwell Time, τ , (sec)	Spat. Res., R, (m)	Swath Width, S, (km)	Temp. Res; ΔT , ($^{\circ}K$)	Power (w)	Max. Att. Rate (mp/sec)	Platform Weight; Gen. Power, W_1 (kg)	Platform Weight; Batt. Power, W_2 (kg)
Five ganged 9" cameras for multispectral imaging	12	23	-	-	1.5	25	-	535	(IMC)	365	845
Infrared scanner; thermal IR band	-	50	8.8×10^{-5}	2.3×10^{-5}	2.2	25	0.6	500	8.7	325	800
Multispectral scanner; five bands; visual through near IR	-	50	5.7×10^{-5}	9.7×10^{-6}	1.4	25	-	250	8.7	300	645
Multispectral scanner; six bands; visual through thermal IR	-	50	5.7×10^{-5} 1.4×10^{-4}	9.7×10^{-6} 2.3×10^{-5}	1.4 3.4	25 25	- 0.6	500	8.7	325	800
Coherent side-looking radar	-	$1/1^3$	-	-	1.0	25	-	135	19.2	385	665

¹ Complete coverage of U.S. in 14 days with twelve twin jet aircraft (typical)

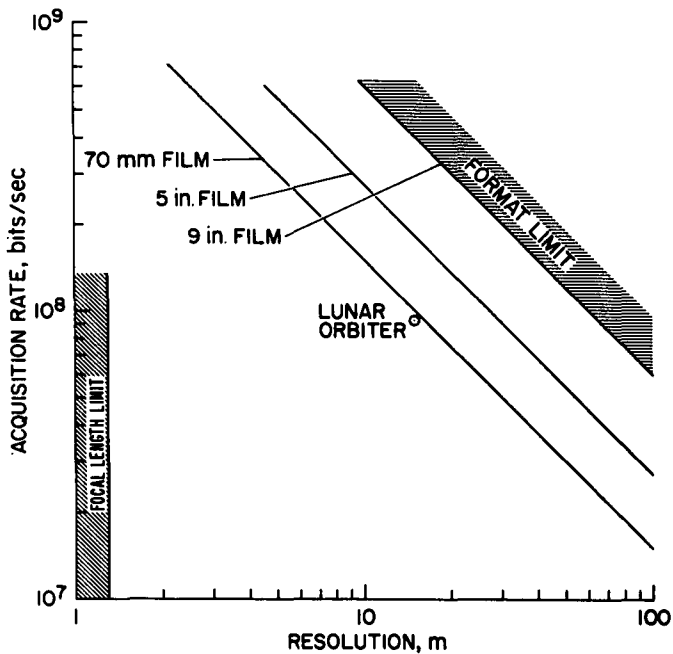
² For all systems except radar, resolution is twice as poor at edge of field of view as that shown

³ Antenna length/width (m)

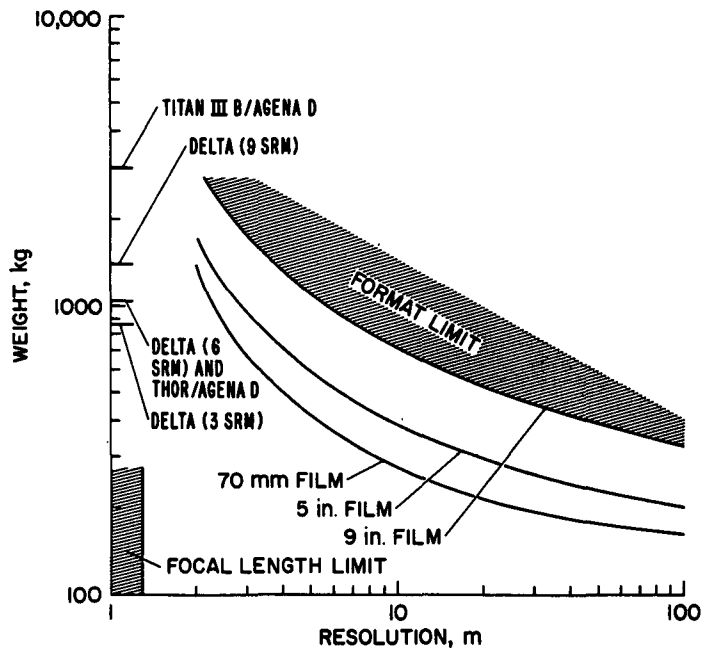
Figure 9-1 Film Camera Characteristics



a. Coverage Summary

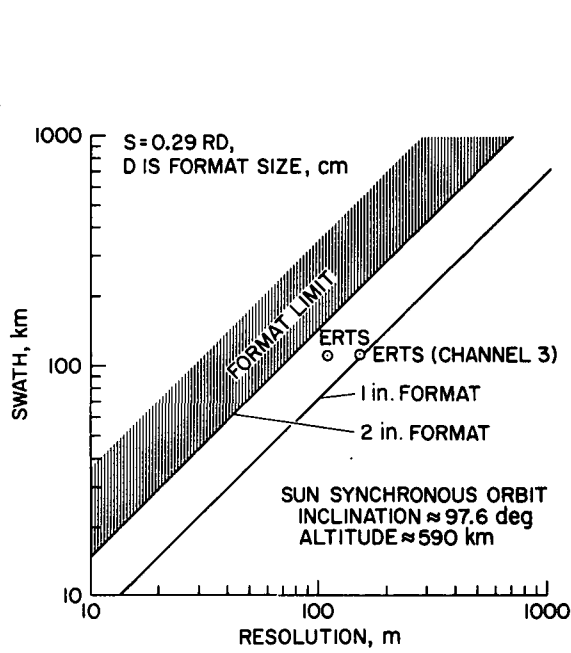


b. Data Production

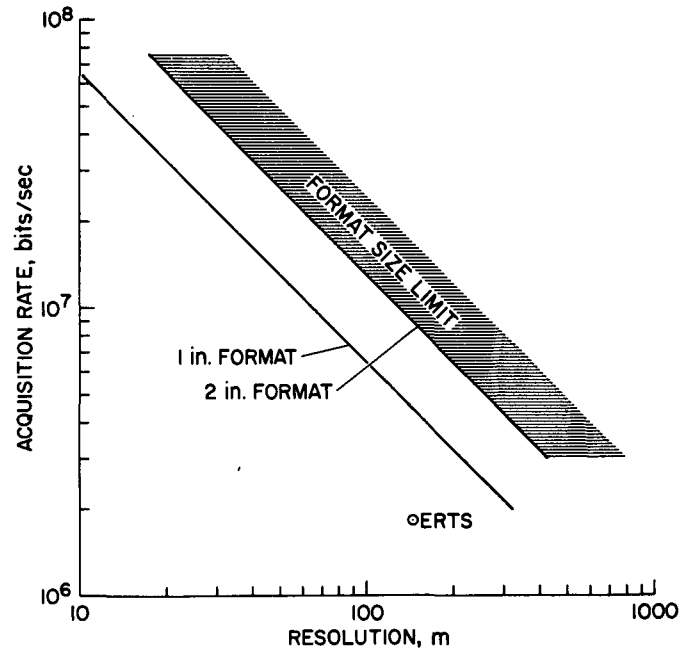


c. Satellite Weight

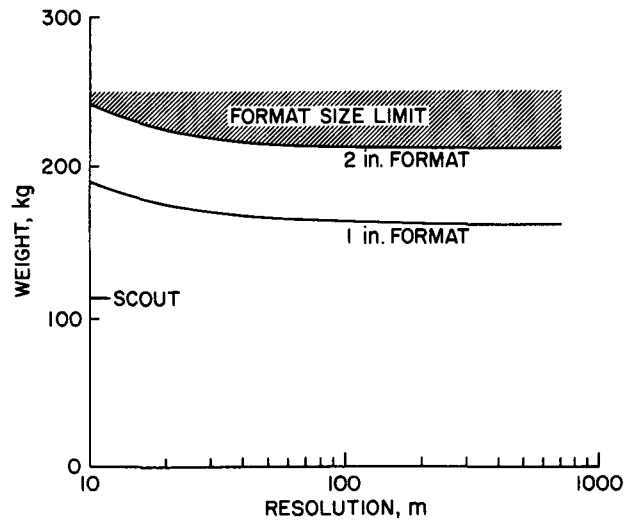
Figure 9-2 Return Beam Vidicon Characteristics



a. Capability Summary

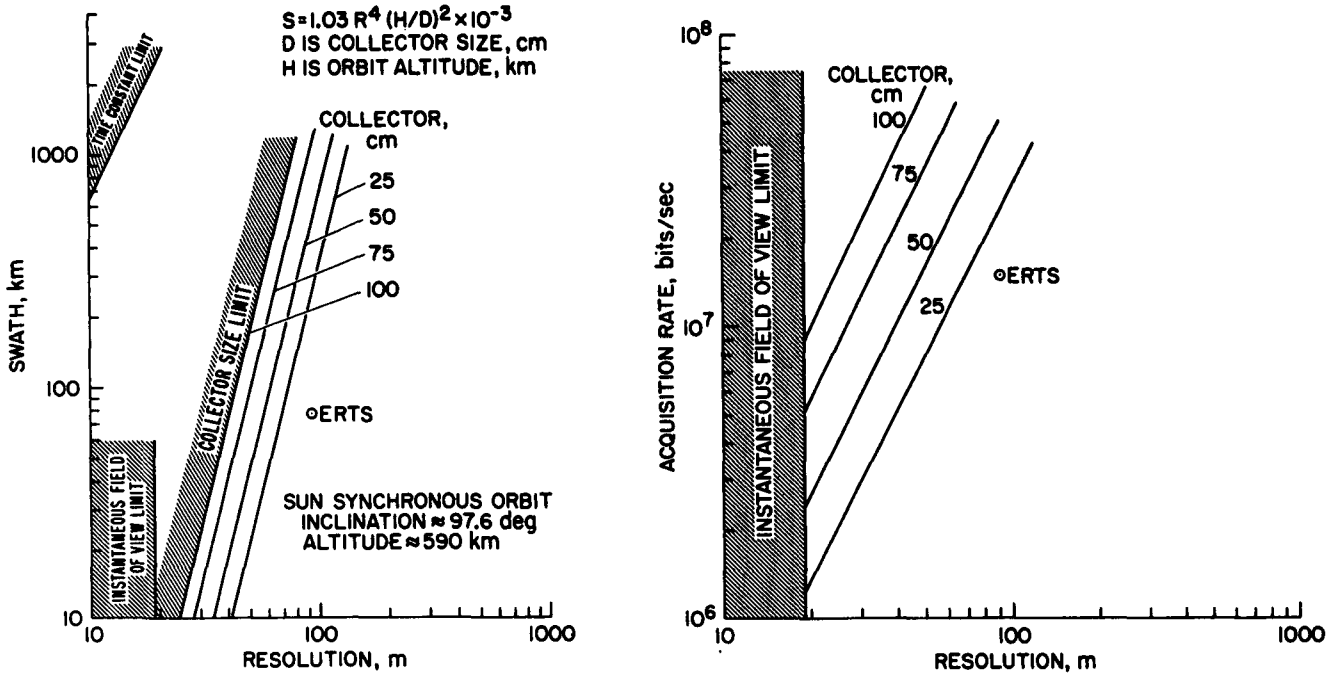


b. Data Production



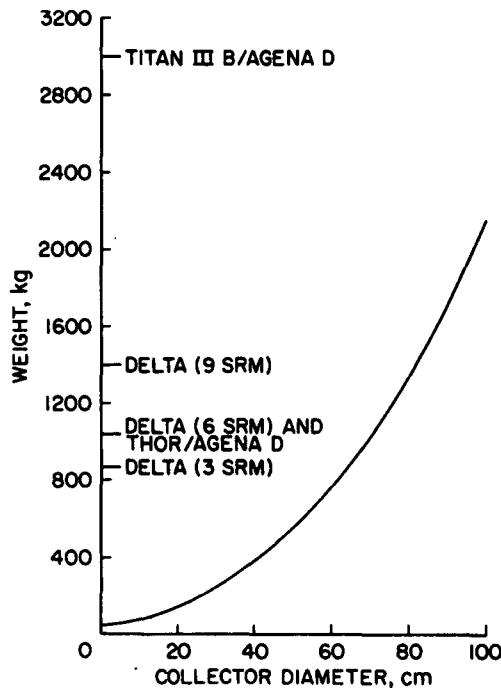
c. Satellite Weight

Figure 9-3 Multispectral Scanner Characteristics (5 Channels)



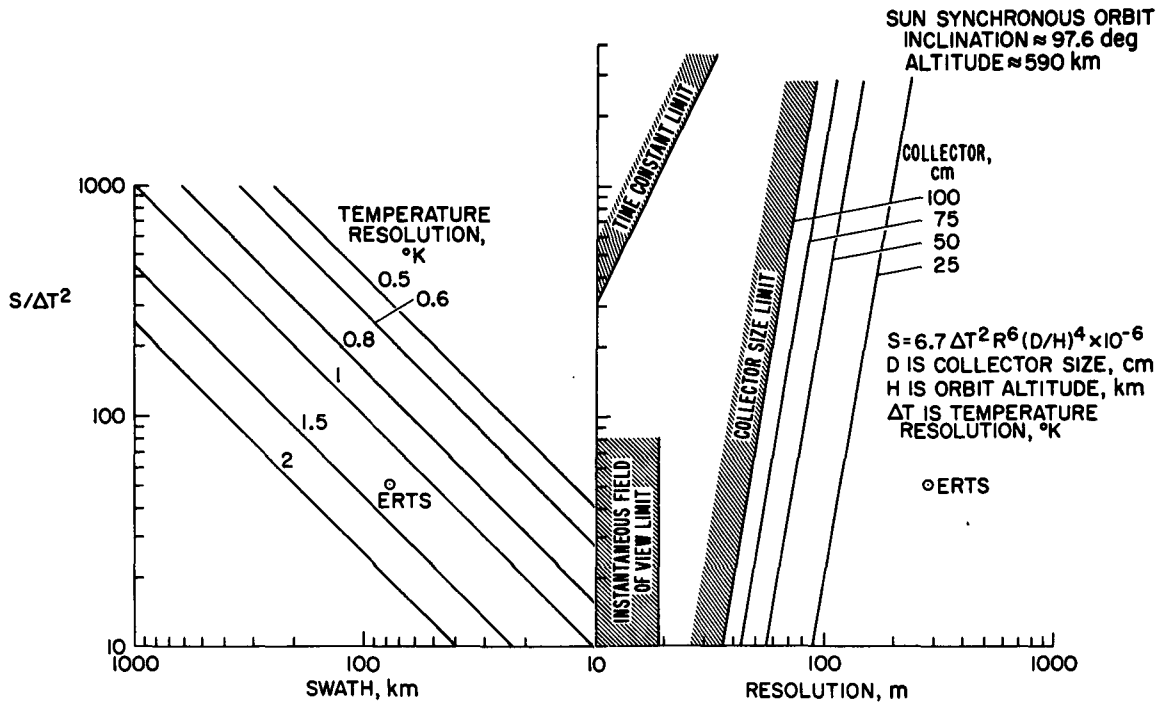
a. Capability Summary

b. Data Production

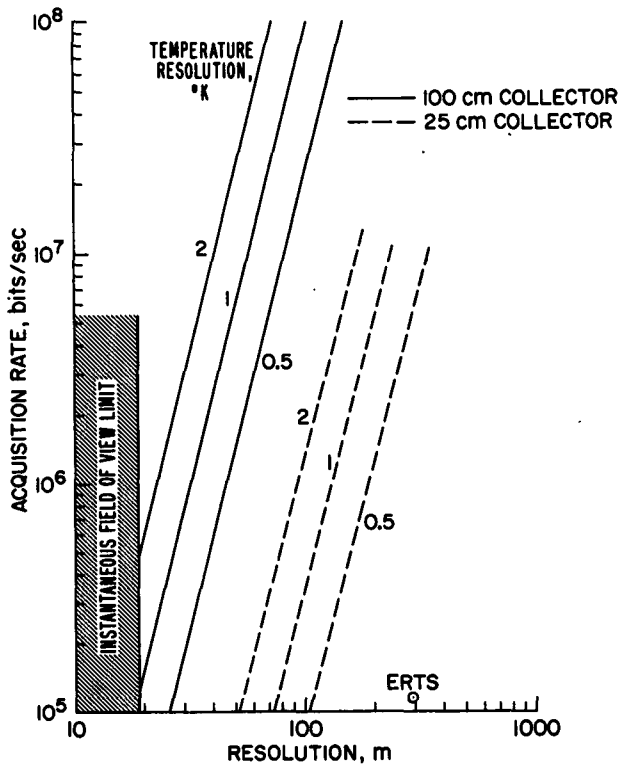


c. Satellite Weight

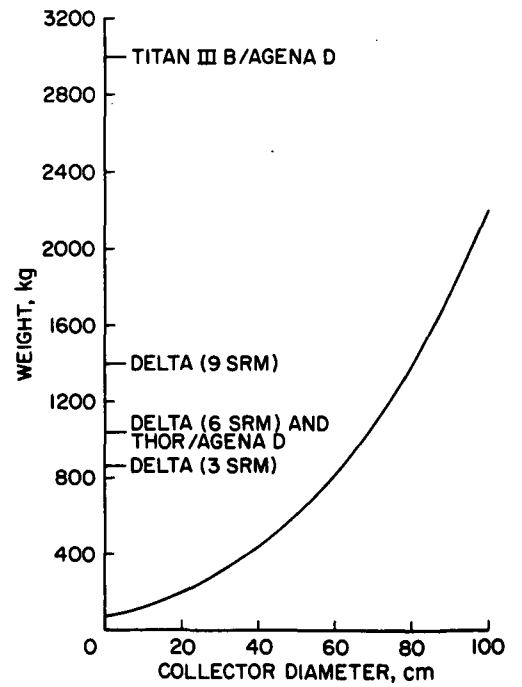
Figure 9-4 Infrared Scanner Characteristics



a. Capability Summary



b. Data Production



c. Satellite Weight

Figure 9-5 Infrared Radiometer Characteristics

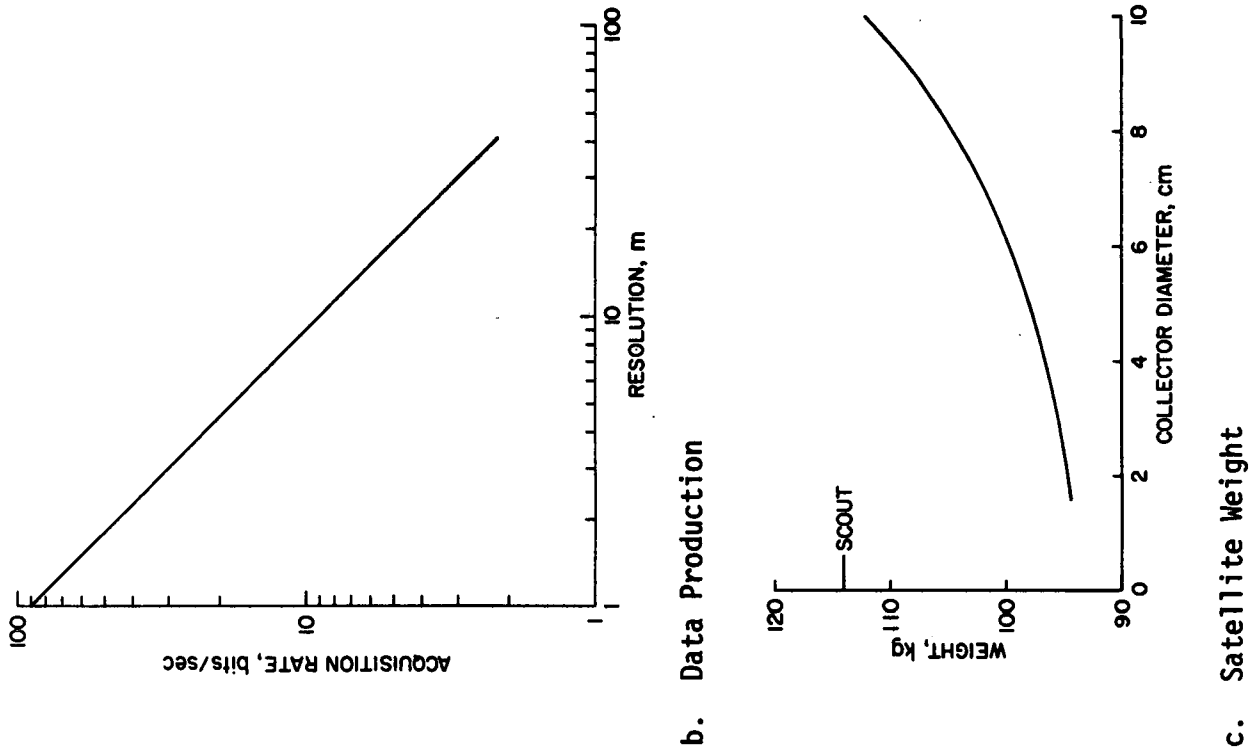
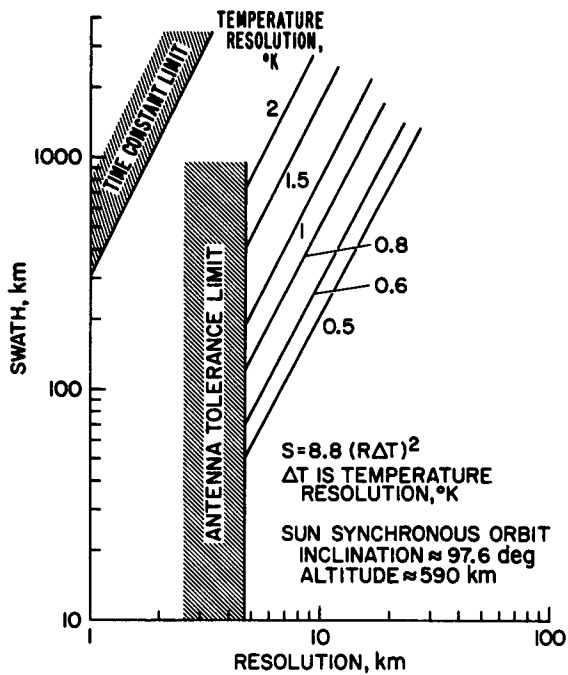
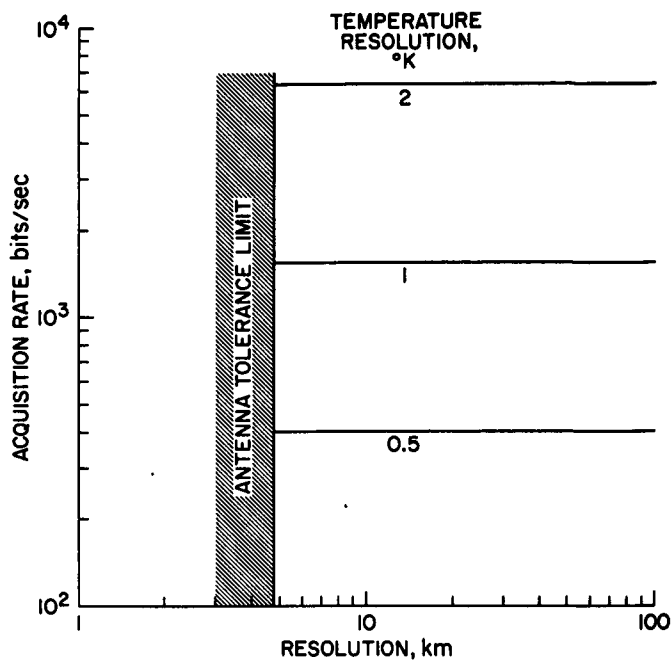


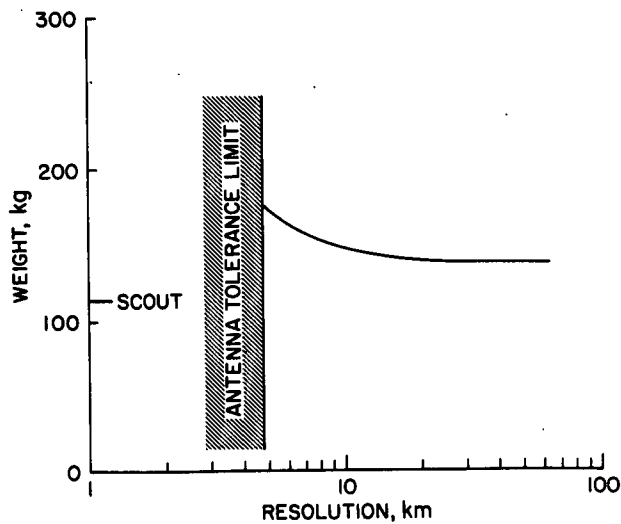
Figure 9-6 Microwave Scanner Characteristics



a. Capability Summary

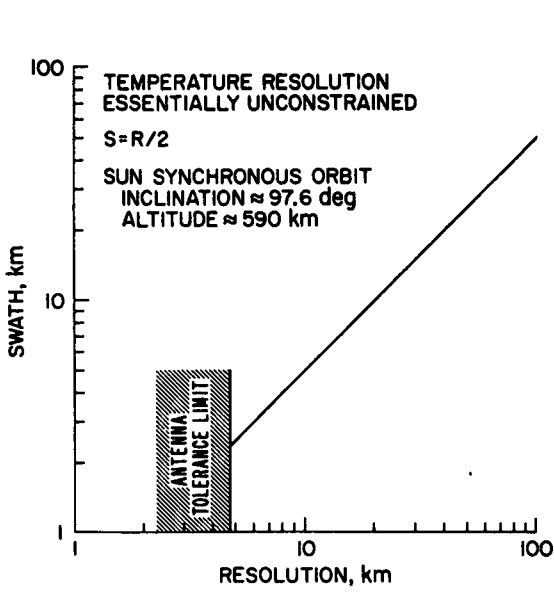


b. Data Production

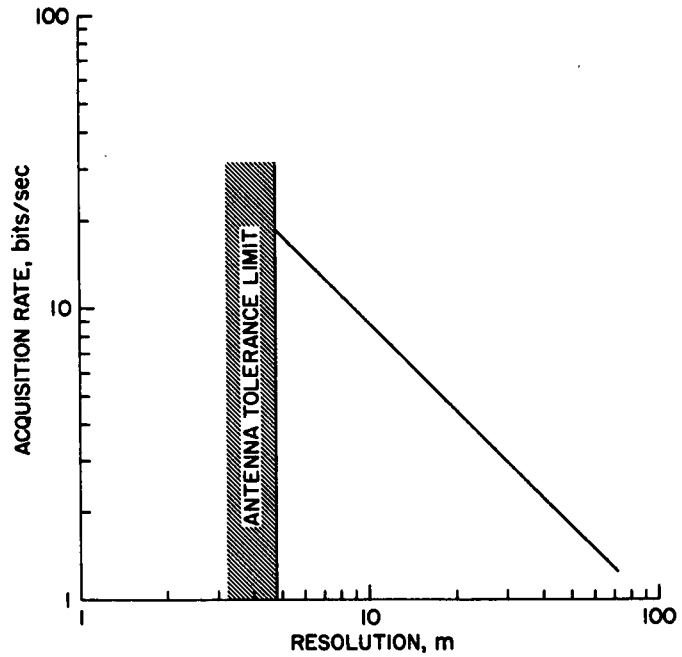


c. Satellite Weight

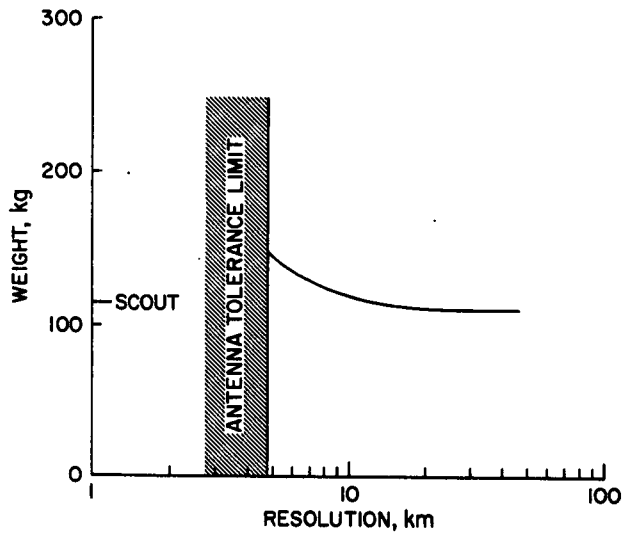
Figure 9-7 Microwave Radiometer Characteristics



a. Capability Summary

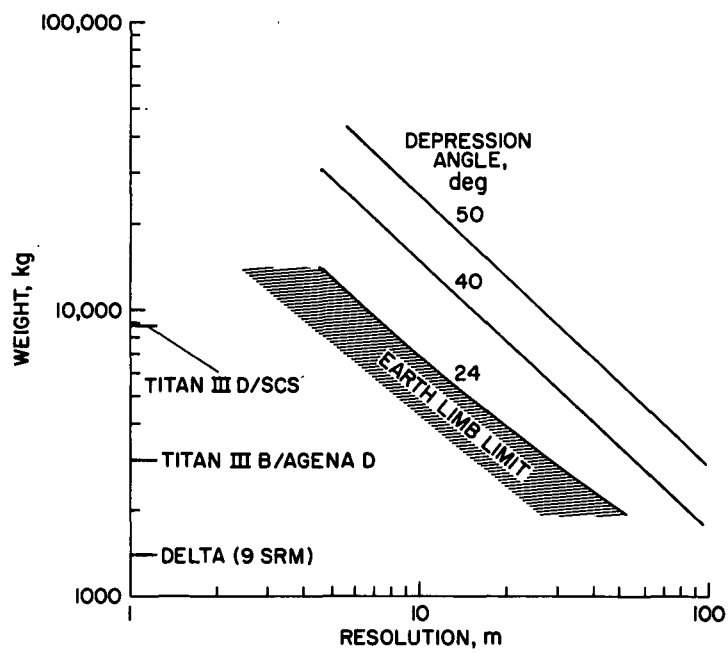
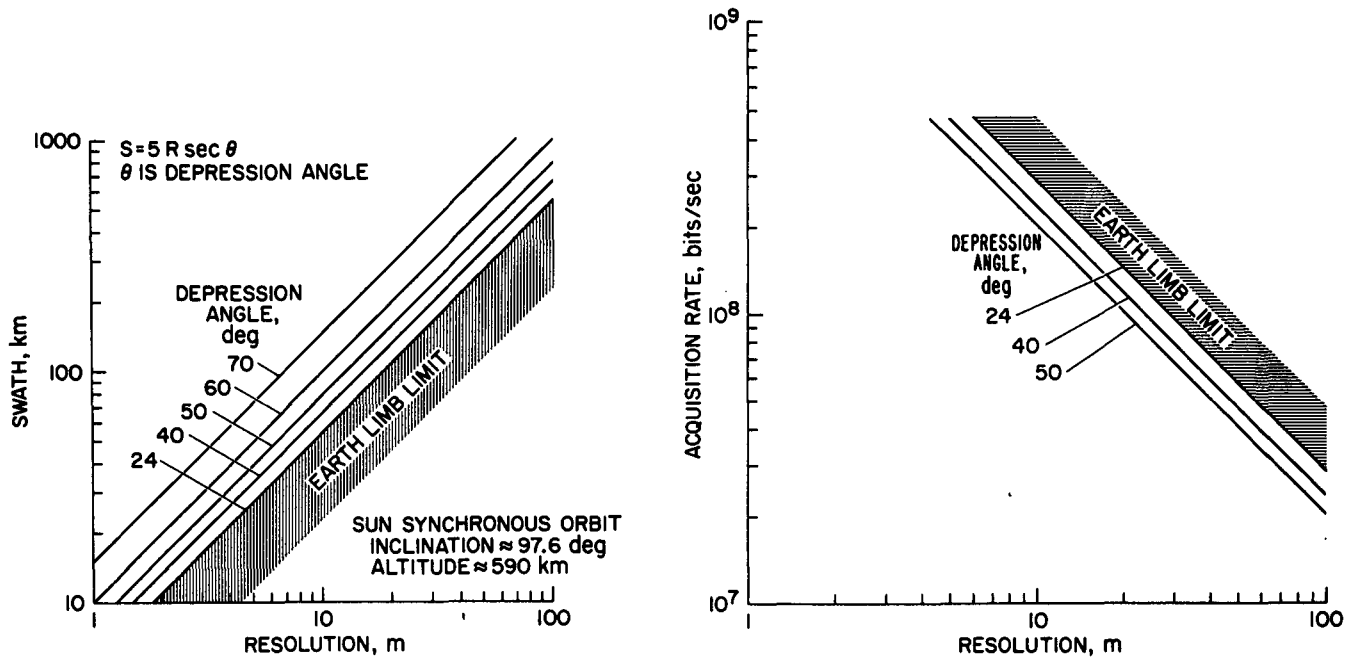


b. Data Production



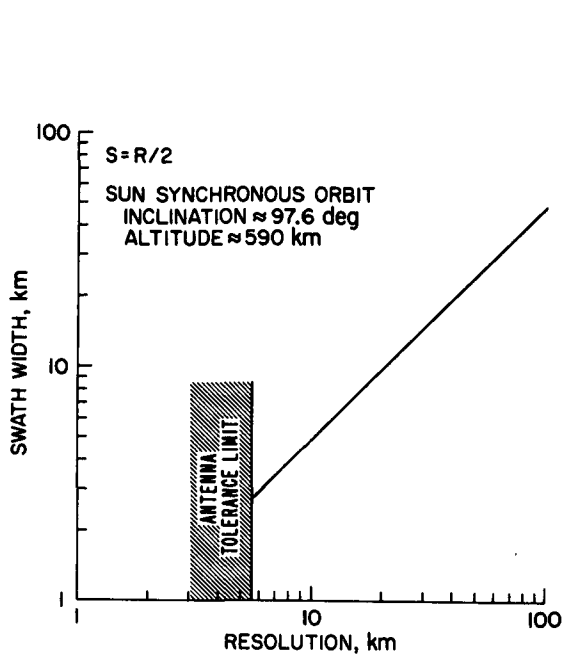
c. Satellite Weight

Figure 9-8 Coherent Side-Looking Radar Characteristics

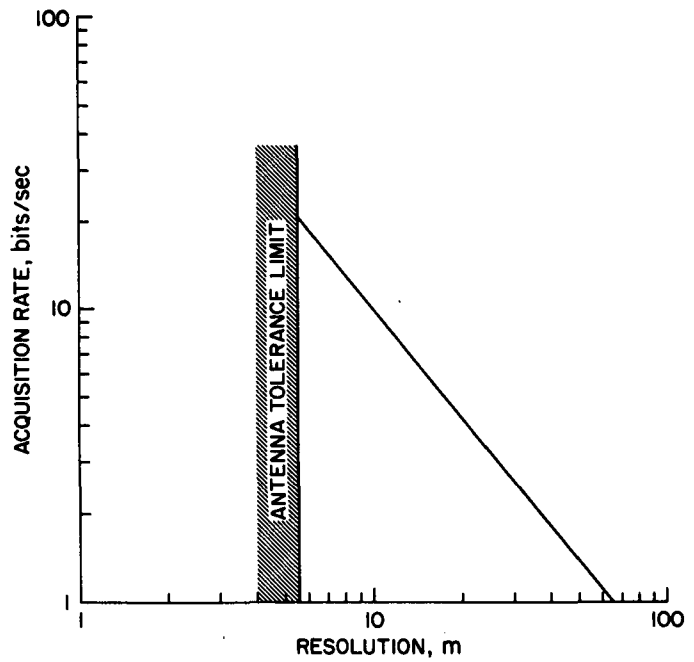


c. Satellite Weight

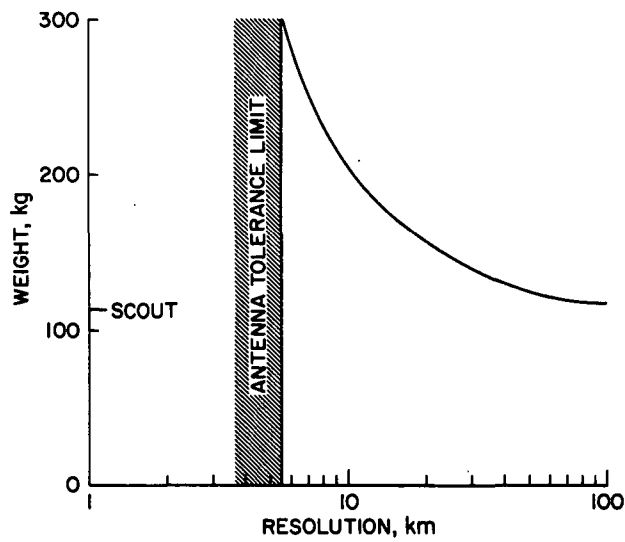
Figure 9-9 Scatterometer Characteristics



a. Capability Summary



b. Data Production



c. Satellite Weight

10. DATA HANDLING

As mentioned in Section 1, data handling systems have not been analyzed in detail but a study of data acquisition systems for operational Earth observation missions would be remiss if the subject were completely ignored. The purpose of this section is to help lay the groundwork for future study of this vitally important element of the total system by outlining some gross concepts for information extraction and by classifying user groups according to their information needs.

Concepts

It is convenient to envision the process that leads to extraction of information by (or for) the user to consist of five phases, the final three of which consist, as defined here, of the "data handling" system. These phases are outlined below but not necessarily in chronological order.

1. Data acquisition by the airborne or spaceborne sensors.
2. Transmission of this data, together with data received from remote Earth-based data collection sites, to the ground. The data receiving locations would, of course, be airports or tracking sites.
3. Preliminary data processing at one or more locations. The processing centers may or may not be co-located with the data receiving sites. Examples of functions performed in the preliminary processing phase include tape-to-film conversion; geometric and radiometric correction; image annotation; computer readable digital tape preparation; data cataloging and storage; and shipping or transmission of the processed data to the proper parties. Note that the functions described here are those that will be performed at GSFC as part of the ERTS program.
4. Data analysis. This is the step in the process that transforms adequate and timely data into information of direct utility to

the user in satisfying his objectives. To exploit acquired information an extensive data management system is required.

Historically, photography has been recognized as a highly efficient method for gathering and storing data about the physical world. More recently sensors sensitive to many other parts of the electromagnetic spectrum have come into use. Multispectral imaging has opened up a far more complex analysis situation. The extraction of data from this type of imagery to produce information in a format amenable to more direct applications is largely a human intellectual activity (Reference 54). Because of this, automation techniques have taken the form of man-machine systems in support of mensuration, image enhancement, graphic and map compilation, information retrieval, and signature analysis. Information extraction by imagery interpretation is now, and for the foreseeable future, an art which requires a human in at least four distinct activities requiring both physical and intellectual effort namely detection, identification, analysis, and communication. It should be noted that both the extraction and application aspects of data analysis will use other data, such as previous pictures, graphics, historical maps, statistics, and spectral scans. Important improvements in man-machine systems have helped speed the interpretation of imaging and thereby increase the productivity of each interpreter so increased quantities of data can be accommodated. Most significant has been the increase in amount of relative time that can be devoted to the task best performed by a human--that of analysis. Most of these techniques have not as yet been adapted to the Earth observation program. Operational systems will make the use of these and many more new techniques mandatory.

5. Data or information transfer to the user.

These five phases can occur in many sequences but the following five seem most likely:

- i. 1,2,3,4,5,
- ii. 1,2,3,5,4 (ERTS sequence)
- iii. 1,2,5,3,4
- iv. 1,(2,5),3,4
- v. 1,3,4,(2,5)

Each sequence has associated with it its own level of complexity, required technological advance, manpower requirements, cost, and usefulness. It is to be hoped that one such sequence, though not necessarily optimal, would at least be serviceable for all elements of the user community. But, because the users are such an amorphous group, this universal utility is not a foregone conclusion.

User Classification

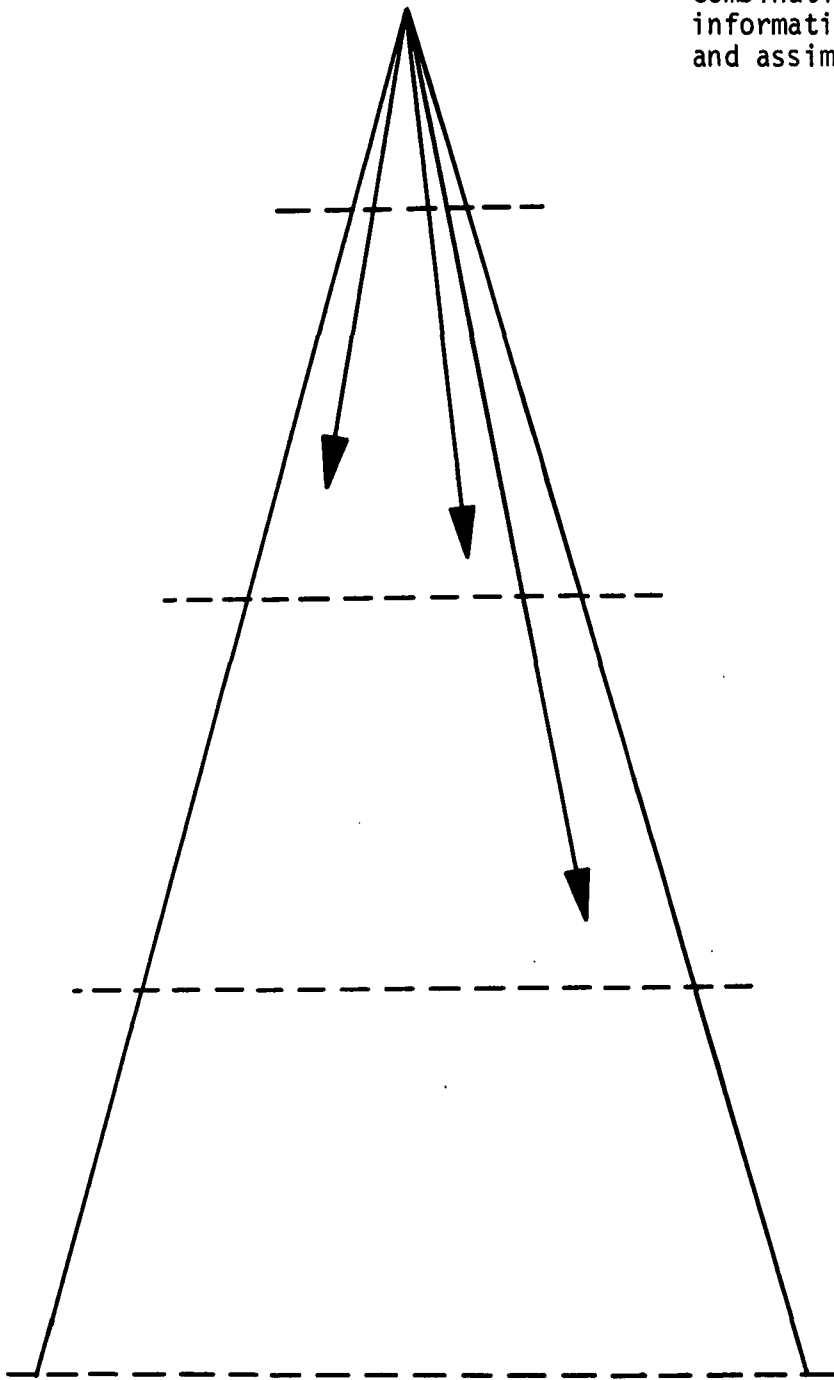
The identification of individual user groups is made difficult because of the myriad combinations of formal and informal channels employed in the data diffusion process. Whenever data are processed and transformed into information by a particular group, that information is filtered and usually changed to some degree before being projected to another user. Such a process may continue within and between levels almost indefinitely, subject only to the differing timeliness constraints of the various levels. A data/information diffusion model helpful in understanding the process is depicted in Figure 10-1. The general model, and much of the associated discussion, is based on Reference 55. For purposes of illustration, however, the following general descriptions of the individual levels are highlighted using the agricultural community as a specific example.

Level I

These users take the initiative in seeking data to satisfy their particular needs or desires. Because their numbers are small and their search behavior is highly focused, these users are usually

Figure 10-1 Basic Information Diffusion Model

Initial data which by itself or in combination with other data becomes information to a user when processed and assimilated.



Level I. - Initial consumer level: specific individuals, scientists, research laboratories, universities, institutes (strong vested or personal interest).

Level II. - Federal and State agencies, educational and commercial laboratories, specific professional societies and research organizations.

Level III. - Members of the general academic and professional communities, private industry, and related community interests; small businesses and related interests.

Level IV. - The general public, individuals and regional groups. The national and international public interests and organizations (little or no self-motivation to obtain or use information).

easily identifiable--quite often to the individual level. During an R&D program the principal investigator and his staff are typical users. Examples of users at this level in the context of an operational Earth observation program might be specific scientists at the Forestry Remote Sensing Laboratory of the University of California-Berkeley; the Remote Sensing Institute, South Dakota State University; and the LARS Laboratory at Purdue University. Specific individuals and small groups within NASA, the Department of Agriculture, and other Governmental agencies and instrumentation research organizations in private industry with a strong research or vested interest are also representative of Level I users.

Level II

At this level the distinction between those users who initiate requests for data and those who do not becomes apparent although the former are still by far the most numerous. The users at Level II can be characterized by having a sophistication of the content of the subject matter together with an increased awareness (compared with the lower levels) of the applications and generalizations that the data affords. Most of the information of potential use at the lower levels will be extracted from the data (i.e., data analysis) at this level. Specific sub-groups within Governmental agencies and commercial enterprises are likely to be at Level II and if proprietary information exists, it is unlikely to get below this level.

Examples of specific groups and individuals at this level include resource managers, planners, professional agriculturists at many levels of both Federal and state agencies. This might include the Agricultural Stabilization and Conservation Service which uses multi-spectral photography to annually measure acreage and determine crop condition and use of agricultural land. A second example might be the Soil Conservation Service, working with ESSA, to provide snow survey information from a combination of both in situ and spacecraft imagery.

Level III

Level III users are characterized by less subject matter sophistication and tend to serve as interpreters and relayers of data/information that had been identified and processed at Level II. At this level, an increased strain is imposed on the data handling system in terms of dissemination of recorded or otherwise documented materials since, by the time the data/information has reached this level, virtually all of the raw data has been processed and filtered by at least one other group or individual at a higher level. Thus, very little direct transfer of data/information is likely to occur.

Increasing attention is also paid at this third level to identification of users in terms of the techniques they employ to receive data/information. An increasing use of information bulletins and statistical or forecast summaries is characteristic of this level, as is a potential time lag between it and the prior levels. In the context of the agricultural community members of Level III would include the state agricultural extension services, the Statistical Reporting Service of the USDA, and the general agribusiness community. Nongovernmental users include farm equipment manufacturers, elevator operators, traders, brokers, millers, and fertilizer or pesticide manufacturers. The large corporation farmer and CO-OP's would of course be included. In general, Level III users are the agricultural producers; their suppliers; and purchasers, traders, and users of agricultural products.

Level IV

The Level IV users consist of a great number of diverse groups and are therefore potentially the most difficult to satisfy in terms of their real needs. Yet they are the recipients of data/information upon whose judgment of the usefulness of the data may rest the decision to commit public funds to enhancement (or even perpetuation) of the system.

A major complication for satisfying user needs at this last level is that the user is typically not self-motivated to seek the data. Traditionally, the user benefits only peripherally (and often unknowingly) from the data produced. The efforts to make information transfer beneficial for this level of user are therefore quite different than for users at the higher levels. Technological spin-off is hardly adequate, as witness the general lack of awareness of space program benefits by the general public. Unlike its behavior at the higher levels, at this final level the system must actively seek out the user and on his terms.

At this level, the key of the agricultural information system is, and will continue to be, the county agent. A popular scenario has it that when a farmer of the future visits or telephones his county agent for information the official in charge will be able to refer to, and interrogate, a data center file. Either pictorial or tabular data on a TV display system will review the status of the farmer's land (Reference 56). This scenario may be a realistic preview of the future but only insofar as the information transfer and retrieval system alluded to comes into being at least quasi-independently of any operational Earth observation program. It is most unlikely that such a system would be embraced simply because of the existence of the observation program. Again, the Level IV user must be sought on his own terms.

It should be apparent that the classification of users by levels as described above is not a mutually exclusive one. It is entirely possible that a given individual or group may be a user at more than one level. Nevertheless, the identification of data/information users by the levels described does provide a systematic way of examining the total user population of any applications discipline. Hopefully, the characteristics and needs of users can also be used to suggest appropriate techniques for establishing and managing a useful data handling system.

11. TECHNOLOGY IMPLICATIONS

Several technology requirements have been identified and are described below. No attempt is made in the listings to rank order the importance of all of these development efforts although the section does conclude with some implications for future OART planning. The technology requirements are organized into the three categories of sensors, onboard data handling, and communications systems. This discussion of technology implications should not be interpreted as a conclusion that developmental efforts be devoted necessarily to every sensor, or for that matter, that every sensor studied will be of real utility in an operational Earth observation program. The proper interpretation is that if a given sensor is to be employed in an operational sense then advances in the technologies enumerated could be of benefit. The technologies marked with an asterisk are critical, however, in that in order for the particular sensor to possess the capabilities and/or support requirements ascribed it in this study, the technology enumerated must be brought to fruition. The other technologies listed are not essential but whose availability, nonetheless, would contribute in a meaningful way to enhanced capabilities, greater operational flexibility, lighter weight, and the like.

Sensors

Technology requirements are discussed below for the following sensor categories: Film cameras, vidicon, scanners, and microwave devices.

Film Camera

* Thin Base Film Anti-Ferrotyping. Thin base (2.5 mil, of the type considered in this study) films with smooth emulsion surfaces have a tendency to ferrotypes, or stick together, and mottling of the processed image may result. This tendency is currently overcome by incorporating very small particles of translucent silicon into the backing. These particles provide enough separation between layers in the film roll to prevent ferrotyping. One disadvantage of these

particles is that they increase the noise level of the image. Another is that they increase the overall weight of the film. Thicker base films do not present such difficulties and need not be treated in this manner. Since the weight of film-carrying satellites can be quite heavy (see Table 9-2), use of the thick films seems out of the question. Thus, a more suitable means should be found to prevent ferrotyping without recourse to the thicker films. In addition, a dye backing is normally used on the thin base films to prevent halation but this backing is not removed by onboard (monobath) processing. Consequently, about 0.2 neutral density is added to the negative. Processing and/or anti-halation techniques that would eliminate this added density are desirable.

Onboard Color Processor. The processor envisioned here is of the type employed aboard Lunar Orbiter. This system processes black and white film only. In order to use such a system for multispectral applications, multiple cameras or lenses (each with an appropriate filter) must be used and, for each, a separate processor is required. This complexity could be avoided by employing color film if a suitable onboard processor were available.

Narrow Band Color Emulsions. If an onboard color processor becomes available, then certain advances in color film technology could become worthwhile. Color film is currently comprised of only three dyes since, to the eye, this is sufficient for color fidelity. For multispectral signature analysis, however, a larger number of dyes yielding finer spectral resolution and/or coverage would be desirable.

Black and White Film Sandwich with Integral Filters. As an alternative to either multiple lens/camera systems or color film one can envision a single film with "filters" integrated directly into the film. This would obviate the need for development of an onboard color processor (the color separation being performed on the ground) yet would result in images in as many spectral bands as there are filters.

Higher Radiation Tolerance Film. The S0-243 film is considered here only because of its high (300 rad) radiation tolerance. Higher radiation tolerance films would, at the least, reduce the shield weight. Of more importance faster film could then be considered.

* Return Beam Vidicon

The capability presumed to be available in the 1980 time period is represented by a two inch format and an operational resolution of 1500 lines (line pairs). To approach the capability of present film systems even larger formats and/or resolving power in lines/mm would be required. Under operational conditions, film systems have a maximum of about 16,400 lines to the frame. To achieve resolution/coverage characteristics similar to film systems, the vidicon must be improved by about a factor of ten in total lines (line pairs) per frame.

Multispectral and IR Scanner

* Mirror Technology. Large aperture, near-diffraction limited mirrors for spacecraft are heavy and, if made of metal, lacking in long term stability. The technology required to produce large, stable, lightweight mirrors is critical to the development of high resolution scanners for spacecraft applications. Work done at the University of Arizona, has demonstrated the feasibility of large mirrors (60 inch) made of the aluminum alloy Tenzalloy. However, other types of aluminum (notably 356-T6) were unsatisfactory because of instability. Large mirror technology using even lighter materials, such as beryllium, needs to be emphasized.

* Detector Cooling Systems. Sensitive thermal infrared detectors require cooling to the 23 to 77 degree K range depending on detector type and operating wavelength. Much research has been done on cooling systems for such detectors but practical, long life cooling systems of the closed cycle type are not available except as postulated developments. Three companies* have built working models of 77-80 degree K closed cycle coolers. These devices appear to have the

* Arthur D. Little Corp., Cambridge, Mass.; Airesearch Corp., Los Angeles, Calif.; and Hughes Aircraft Co.

characteristics necessary for long term continuous operation. However, the operating power required for the least efficient design is about 500 W for 2 W of cooling at 77 degrees K and about one kilowatt at 30 degrees K. The second model is expected to require about 200 W per watt of cooling at 30 degrees K. The most efficient design of the three requires about 40 W at 80 degrees K for 600 mW of cooling. This latter device has been flight tested and has an expected lifetime of 3,000 hours but it is claimed that only minor modification would be required to extend the life to 10,000 hours. Lower temperature systems of the latter type have not been designed.

Solidified gas cooling is another possible approach. Laboratory studies have shown that a solid methane system could provide cooling to 77 degrees K, a neon system to about 23 degrees K, and a solid hydrogen system to about 13 degrees K. For a heat load of 0.1 W, an outer container temperature of 300 degrees K and an operating life of one year, these systems would require coolant and insulation weights of 12, 54, and 30 kg, respectively. Total system weights are projected to be about 35 percent greater than these figures.

While it appears that modest additional development should result in a satisfactory 77-80 degree K system, lower temperature units with reasonable power, size, and weight characteristics appear to require significant developmental emphasis.

Detector Arrays. Multi-element detector arrays would make it possible to reduce mirror size for the same sensitivity since the dwell time for a given swath width/resolution capability would be increased in direct proportion to the size of the array. Two configurations are attractive. The first, using a limited number of detectors (say, 50-100) in the image plane and arranged parallel to the flight path would increase the line scan time (and, hence, the dwell time per element) directly with the number of detectors. The cost of this approach is an increase in image rectification problems. With this configuration, a scan mirror is required to provide cross track coverage. The second method uses a large number of detectors

(several thousand) in the image plane and arranged perpendicular to the flight path. This approach, known as a push-broom scanner, results in a very large increase in dwell time and eliminates the need for a scan mirror since cross-track scanning is not required. Key problems in developing these approaches are detector uniformity and high speed multiplexing/encoding capability together with light weight, reliability, and power requirement characteristics suitable for long term operation on unmanned spacecraft.

* Microwave

Large, lightweight erectible antennas suitable for spacecraft use are required for microwave radiometry and radar. Forthcoming (1973) ATS experiments using a large erectible antenna (~10 meters) should provide much data but the general technology associated with such antennas, capable of operating at wavelengths from 5 mm to several meters, should be emphasized.

Onboard Data Handling

* Recorders

There is a need for wide band (up to 1000 Mbps) recording capability with a total storage capacity approaching 10^{12} bits. The technique desired should have a reusable substrate and, ideally, involve no mechanical motion. The lifetime of the system including the recording medium should be in excess of one year. The need for such a recorder is based on a 50 Mbps communications capability; higher rates, as shown below, would modify or eliminate the requirement.

Multiplexer/Encoder

A multiplexer/encoder system capable of operating at sampling rates in the 10^7 - 10^8 per second region and encoding to six or eight bits is needed for advanced multi-detector scanning systems.

Communications

The technology requirements for communications systems are a result of the telemetry rate to be accomplished, which ultimately depends upon the sensors utilized by the data acquisition system. For moderate rates (approximately 50 Mbps or less), existing communications technology is adequate. For higher rates several options are available to provide adequate capability. The application of imaging sensors, except for film camera systems, results in data generation rates up to about 300 Mbps. By using existing overseas STADAN and MSFN data reception stations for non realtime transmission at 50 Mbps, coupled with a spaceborne recorder of nominally 10^{11} bits capacity, the data acquired over the U. S. at 300 Mbps can be retrieved. Alternatively, U. S. ground station capability could be sufficiently improved to satisfy such a requirement by incorporation of wideband components and systems. This could entail a shift in operating frequency to X-band.

For camera systems much higher rates of data generation can result, up to a maximum of 3000 Mbps. Three options could provide satisfactory capability depending upon the ultimate data rate requirement. By using the existing ground capability with a data relay satellite and non realtime transmission, sensor rates of 500 to 1000 Mbps could be accommodated. Alternatively, the development of mm wavelength space and ground system, preferably at 45 GHz, would provide realtime channel capacity for up to 1000 Mbps. This would require primarily efforts to increase bandwidth of all components, improved noise figure receivers, and spaceborne transmitters of 10 watts for a direct transmission or up to about 250 watts for a relay mode.

The third alternative would be the development of laser telemetry systems which could satisfy realtime transmission requirements of 1000 Mbps and higher. This would encompass continued development of all elements of such links including transmitter efficiency, size, weight and lifetime, receiver sensitivity, modulator efficiency, reduced optical losses and efforts to increase bandwidths of all components.

APPENDIX A

INTEGER ORBITS

This analysis of integer orbits is an extension of Reference 1. The following variables are defined as follows:

- a = semi major axis
- e = eccentricity
- $J_2 = .001082$
- R = radius of the Earth
- I = inclination
- $\Delta\Omega$ = angular change in the longitude of the ascending node per orbit
- n = mean motion
- μ = Earth's gravitational parameter
- τ = orbital period
- N = number of orbits per day
- T = number of days until the ground track repeats
- p = semi latus rectum

First, we have that

$$p = a (1 - e^2)$$

$$a = a_0 \left[1 - \frac{3}{2} J_2 \left(\frac{R}{p} \right)^2 (1 - \frac{3}{2} \sin^2 I) \sqrt{1 - e^2} \right]$$

$$\Delta\Omega = 3\pi J_2 \left(\frac{R}{p} \right)^2 \cos I$$

$$n^2 a^3 = \mu \left[1 - \frac{3}{2} J_2 \left(\frac{R}{p} \right)^2 (1 - \frac{3}{2} \sin^2 I) \sqrt{1 - e^2} \right]$$

Using

$$\tau = 2\pi \sqrt{\frac{a_0^3}{\mu}} \text{ and solving for } \tau \text{ in terms of } a_0$$

$$\tau = 2\pi \left[1 - \frac{3}{2} J_2 \left(\frac{R}{p} \right)^2 (1 - \frac{3}{2} \sin^2 I) \sqrt{1 - e^2} \right]^{3/2} \sqrt{\frac{a_0^3}{\mu}}$$

In the above equation the subscript $_0$ denotes initial values while non-subscripted variables indicate average values of the orbit elements.

The time of rotation of the Earth in $(N - \frac{1}{T})$ days and the total regression of the node in this time are equal for integer orbits. Therefore we have

$$(N - \frac{1}{T}) \tau = \frac{\kappa}{2\pi} [2\pi - (N - \frac{1}{T}) \Delta\Omega] \text{ where } \kappa = 86164.1 \text{ sec/day.}$$

Equivalently

$$(N - \frac{1}{T}) 2\pi \sqrt{\frac{a^3}{\mu}} [1 - \frac{3}{2} J_2 (\frac{R}{p})^2 (1 - \frac{3}{2} \sin^2 I) \sqrt{1 - e^2}]^{3/2} =$$

$$\frac{\kappa}{2\pi} [2\pi - (N - \frac{1}{T}) 3\pi J_2 (\frac{R}{p})^2 \cos I]$$

This is a transcendental equation and cannot be solved algebraically. However, iterative methods on the computer converge rapidly. A first guess is obtained by setting $J_2 = 0$.

APPENDIX B

CLOUD COVER DISTRIBUTION

Table B-1 contains distributions of various continental U. S. resources by area percentages that lie within the predefined global cloud regions (Figure B-1) established in Ref. 16. Table B-2 and Figure B-2 provide analogous distribution of continental U. S. resources versus cloud regions for aircraft observation data derived from Ref. 18.

Table B-3 provides an example of the method employed to arrive at the continental U. S. cloud cover statistics shown earlier [Figure 5-1(a)]. Using the predefined geographic cloud regions as a grid, the continental U. S. land area encompassed by each cloud region was calculated as a percent of the total land area. Next, by multiplying these percent land distribution factors by the seasonal percent cloud cover observed for that geographic region, and summing the results, four seasonal average cloud cover values, C , were derived for the continental United States as a whole: winter 63.2 percent, spring 60.5 percent, summer 44.9 percent and fall 47.0 percent. The annual average cloud cover, using these seasonal averages, is 53.9 percent.

Table B-1

Resource Distribution (% Total Area by Global Cloud Region)*

	<u>01</u>	<u>02</u>	<u>04</u>	<u>05</u>	<u>07</u>	<u>08</u>	<u>09</u>	<u>10</u>	<u>11</u>	<u>12</u>	<u>13</u>	<u>14</u>	<u>18</u>	<u>19</u>	<u>20</u>
<u>Global Cloud Region</u>															
Crops:															
Wheat		21.3				11.7			53.1					13.9	
Corn									87.4					12.6	
Delta (Rice)			5.0											95.0	
Forests		10.0	1.6	0.1		13.7			30.7	5.2			2.1	36.7	
Minerals	3.1	21.8				27.6			23.3	5.4			5.1	13.7	
Fish:															
Gulf			63.0												37.0
Pacific				8.5	3.4					4.3	48.7	19.3			15.8
Snow Cover		13.6				62.4			4.1		13.6		6.3		
Icebergs:															
Observed											57.5	42.5			
Formation								46.0				53.5			
Alaskan Resources							69.0								30.4

* See Figure B-1 for global region identification.

Table B-2

Resource Distribution (% Total Area by Aircraft 10° Latitude/Longitude Sectors)*

	<u>1</u>	<u>2</u>	<u>3</u>	<u>4</u>	<u>5</u>	<u>6</u>	<u>7</u>	<u>8</u>	<u>9</u>	<u>10</u>	<u>11</u>	<u>12</u>	<u>13</u>	<u>14</u>	<u>15</u>
	<u>10° Latitude/Longitude Region</u>														
Crops:															
Wheat							16.7	15.1	36.5	26.2	5.5				
Corn					15.0	14.4	48.3	22.2							
Delta (Rice)								100.0							
Forests	1.5	7.6	7.7	5.7	6.2	23.6	7.3	14.2	4.2	8.1	9.0	5.1	6.1	1.5	
Minerals	1.7	7.7	7.7	2.7	1.4	5.7	7.8	3.9	5.1	13.1	19.9	18.7	9.0	3.2	
Snow Cover									12.7	16.8	43.6	7.3	15.0	4.6	
Alaskan (All)															100.0

* See Figure B-2 for 10° latitude/longitude sector identification.

Table B-3

Continental United States Cloud Cover Statistics

<u>Cloud Region</u>	<u>% Area of U.S.</u>
01	1.2
02	16.8
04	1.6
05	.1
08	17.6
11	32.8
13	2.5
19	27.2
20	<u>.2</u>
	100.0

% Cloud Cover (1300 LST)

<u>Region</u>	<u>%</u>	<u>Winter</u>	<u>Wtd C</u>	<u>Spring</u>	<u>Wtd C</u>	<u>Summer</u>	<u>Wtd C</u>	<u>Fall</u>	<u>Wtd C</u>
01	1.2	.36	.004	.37	.004	.14	.002	.12	.001
02	16.8	.50	.084	.44	.074	.16	.027	.40	.067
04	1.6	.52	.008	.51	.008	.62	.010	.52	.008
05	.1	.48	- -	.52	- -	.54	- -	.48	- -
08	17.6	.71	.125	.63	.111	.34	.060	.45	.079
11	32.8	.66	.216	.65	.213	.57	.187	.50	.164
13	2.5	.80	.020	.80	.020	.74	.018	.76	.019
19	27.2	.64	.174	.64	.174	.53	.144	.48	.131
20	<u>.2</u>	.70	<u>.001</u>	.77	<u>.001</u>	.74	<u>.001</u>	.66	<u>.001</u>
Tot.	100.0		.632		.605		.449		.470

Figure B-1 Global Cloud Cover Regions

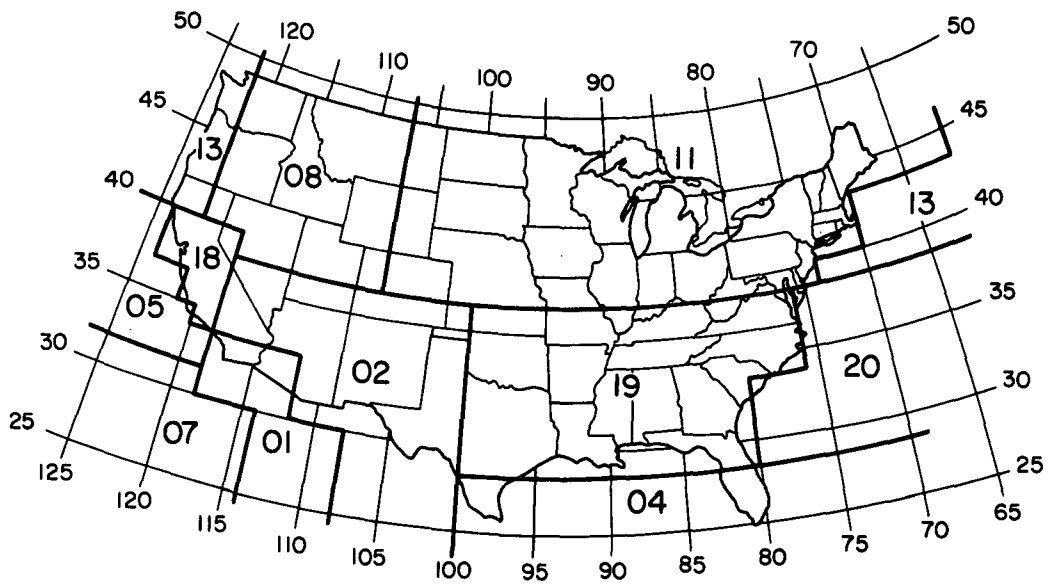
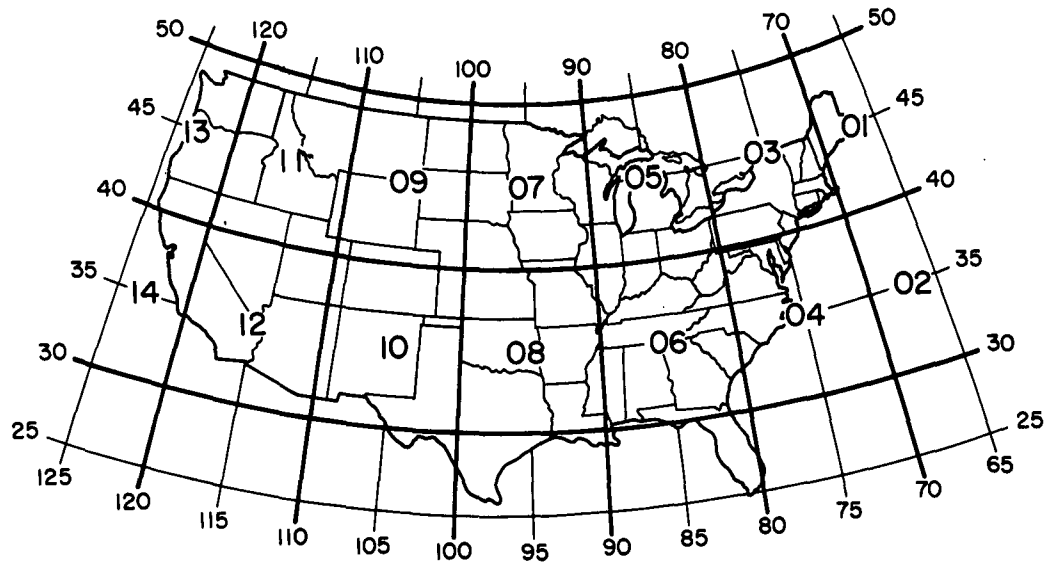


Figure B-2 Ten Degree Latitude/Longitude Regions



APPENDIX C

GENERALIZED USER REQUIREMENTS

Since it is the purpose of this study to postulate typical operational acquisition systems for Earth observations and because of the uncertainties surrounding the real nature of the user requirements, it might seem prudent to ignore requirements in the process of defining capabilities. To be sure, the relationships between various dimensions of capabilities (spatial resolution, temperature resolution, swath width) and sensor component design features can be displayed parametrically without any knowledge whatever of the requirements. Such a parametric summary was shown in Section 9.

To take the next step of defining a few representative systems, however, it was felt necessary to consider the requirements as we understand them. One could, of course, establish typical systems for example, by merely defining systems whose sensor components are presumed to operate at the limits of their respective technologies. Although such an approach would have been possible in this study it was never seriously considered. Rather, this study takes advantage of earlier studies that provide a summary of user requirements for each sensor type. These summary requirements then became design goals for the representative systems. The method by which these requirements were employed in the system selection process was also discussed in Section 9.

Requirements Summary

The requirements are summarized in Table C-1 and, without exception, are based on information from Ref. 8. This reference, in turn, is a quite detailed compilation of requirements in the various disciplines (e.g. forestry, geology, agriculture, etc.) and was based on a review of about sixty other user-oriented documents. Sources consulted during its preparation included NASA contractor reports, reports of other government agencies and their contractors, journals and symposia articles, representatives of some of the major cooperating agencies, and contacts with some of the principals associated with developmental Earth observation programs.

Table C-1
User Requirements Summary

Sensor	Spatial Resolution (m)	Temperature Resolution (°K)	Swath Width (km)	Coverage Interval (Days)	Solar-Elevation Angle (deg)	Representative Uses
Film Camera & Vidicon	7	-	90	36	20-90	Geographic & Geologic Mapping; Mineral & Oil Exploration; Snow Cover Survey; "Act of God" Damage Assessment; Urban Environment Changes
Multispectral Scanner	10	-	125	22	60-90	Crop Inventory & Forecast; Forest Mapping & Timber Inventory; Rangeland Forage Potential
Infrared Scanner	60	0.6	130	33	-	Ocean Current Mapping & Fish Location; Geothermal Power Sources; Volcanic Belt Reconnaissance; Forest Fire Detection; Ground Water Discharge
Infrared Radiometer						(No Requirements Stated)
Microwave Scanner	20	0.5	160	3	-	Iceberg Detection & Surveillance; Ocean Current Mapping & Fish Location
Microwave Radiometer	1000	0.5	-	7	-	Sea State Determination; Snow Cover Survey
Radar	15	-	112	27	-	Iceberg Detection & Surveillance; Geologic Mapping; Earthquake Belt Reconnaissance; River & Lake Ice Formation; Storm & Flood Damage Assessment
Scatterometer	1000	-	-	1/4	-	Sea State Determination

Since requirements are not the subject of this study and are used only to provide general guidance in the selection of representative systems, it is not necessary to consider each discipline (let alone specific tasks within each discipline) separately. Specifically, in the terminology of Ref. 8, the entries in the table are simply the numerical averages of the "desired" capabilities for all tasks that would be best performed if the given sensor were the "primary" means of data collection. Thus the summary includes no capabilities that are merely "acceptable" nor does it include those requirements for which a sensor is envisioned to be either a "supplementary" or an "alternate" mode of data collection. This policy naturally results in the most stringent (average) requirements but seems justified since our intent is to identify systems that might truly meet the needs of the user community about ten years hence. Should subsequent iterations between user needs and system capabilities lead to requirements that are less severe than those summarized here (and, in our judgment, this is likely to occur), the parametric results and the method used to define the typical systems will remain valid. But conclusions that are influenced by requirements must, of course, be reassessed.

Note that spectral resolution and spectral coverage requirements are not shown in Table C-1. This is simply because of the very meager documentation of requirements that is at hand--not because of any intent to disparage the utility of spectral information. That essentially no spectral requirements are available reflects an uncertainty of the users' needs even greater than the uncertainties surrounding the other requirements. This situation will exist until data becomes available from aircraft and ERTS flights (another facet of the requirements/capability iteration alluded to earlier). In fact, one would hope that such continuing efforts will result not only in the spectral requirements but also in the mutual influences between spectral and spatial requirements.

A Caveat

Throughout this report the numerical values assigned to requirements are those shown in Table C-1 and the word "requirements" is used as if they were known with certainty. The proper qualifying phrases ("as we understand them", "presumed to be...", etc.) are not used only to avoid repetition.

APPENDIX D

METRIC ACCURACY REQUIREMENTS

The following information summarizes "metric" accuracy requirements for map-making, i.e., the accuracy with which maps are required to represent the locations and elevations of features which they portray.

Significant excerpts of the U. S. National Map Accuracy Standards, which apply to planimetric and topographic maps, are repeated below from Ref. 57:

"With a view to the utmost economy and expedition in producing maps which fulfill not only the broad needs for standard or principal maps, but also the reasonable particular needs of individual agencies, standards of accuracy for published maps are defined as follows:

1. Horizontal accuracy. For maps on publication scales larger than 1:20,000, not more than 10 percent of the points tested shall be in error by more than 1/30 inch, measured on the publication scale; for maps on publication scales of 1:20,000 or smaller, 1/50 inch. These limits of accuracy shall apply in all cases to positions of well defined points only. "Well defined" points are those that are easily visible or recoverable on the ground, such as the following: monuments or markers, such as bench marks, property boundary monuments; intersections of roads, railroads, etc.; corners of large buildings or structures (or center points of small buildings); etc. In general what is "well defined" will also be determined by what is plottable on the scale of the map within 1/100 inch. Thus while the intersection of two road or property lines meeting at right angles would come within a sensible interpretation, identification of the intersection of such lines meeting at an acute angle would obviously not be practicable within 1/100 inch. Similarly, features not identifiable upon the ground within close limits are not considered as test points within the limits quoted, even though their positions may be scaled closely upon the map. In this class would come timber lines, soil boundaries, etc., etc.

2. Vertical accuracy, as applied to contour maps on all publication scales, shall be such that not more than 10 percent of the elevations tested shall be in error more than one-half the contour interval. In checking elevations taken from the map, the apparent vertical error may be decreased

by assuming a horizontal displacement with the permissible horizontal error for a map of that scale.

3. The accuracy of any map may be tested by comparing the positions of points whose locations or elevations are shown upon it with corresponding positions as determined by surveys of a higher accuracy. Tests shall be made by the producing agency, which shall also determine which of its maps are to be tested, and the extent of such testing."

Another statement of map accuracy requirements which is generally consistent with, although somewhat more stringent than, the above was provided by Doyle (Ref. 58). These requirements are listed below in Table D-1.

TABLE D-1

Map Accuracy Requirements

<u>Map Scale</u>	<u>Std. Error Position</u>	<u>Ground Resolution</u>	<u>Contour Interval</u>	<u>Std. Error Elevation</u>
1,000,000	300 m.	50 m.	500 m.	150 m.
250,000	75	12.5	100	30
100,000	30	5.0	50	15
50,000	15	2.5	25	8
25,000	7.5	1.3	10	3

APPENDIX E

RADIATION SHIELDING CONSIDERATIONS FOR FILM

Film must be protected against trapped Van Allen radiation as well as against high energy protons associated with solar events. The trapped radiation consists of electrons and protons whose flux increases monotonically with altitudes up to about 2000 km. The flux is also dependent upon latitude and for all practical purposes vanishes at the geomagnetic poles. Thus, for a given altitude, the trapped radiation dosage tends to decrease with orbit inclination. Although the Van Allen belts provide considerable inherent shielding against solar protons up to middle latitudes this reduced flux near the geomagnetic poles gives rise to a solar proton "window" that renders the solar proton flux important for the higher inclination orbits of interest here.

The radiation dosage due to trapped protons and electrons is shown in Figure E-1. The figure is taken from Ref. 59 and is predicated on an arbitrary shield density of 1 gm/cm^2 of aluminum. Figure E-2, based on data from Refs. 59 and 60, is used to determine the dose attenuation for the higher shield densities of interest. The discontinuity in the electron dose curve is due to the dominance of the bremsstrahlung effect for shield densities greater than about 4 gm/cm^2 .

Solar events occur sporadically and vary greatly in proton fluxes and energy spectra. The dose received during a mission depends on the number of events encountered, their fluxes and spectra and, of course, the radiation protection available. Because of the irregular variations in flux, spectrum and frequency, the only reliable method of predicting the solar radiation environment for long duration missions is by statistical evaluation of past data on solar proton events to produce distribution functions of the critical quantities. Such a statistical study was carried out in Reference 61 and the shield weight requirements determined for various times within the 11 year solar cycle.

Figure E-1 Trapped Radiation Dose

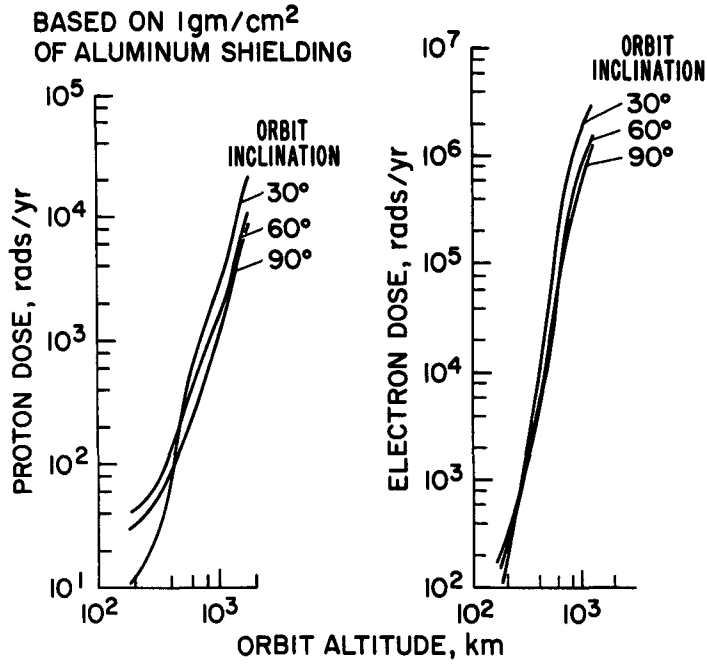
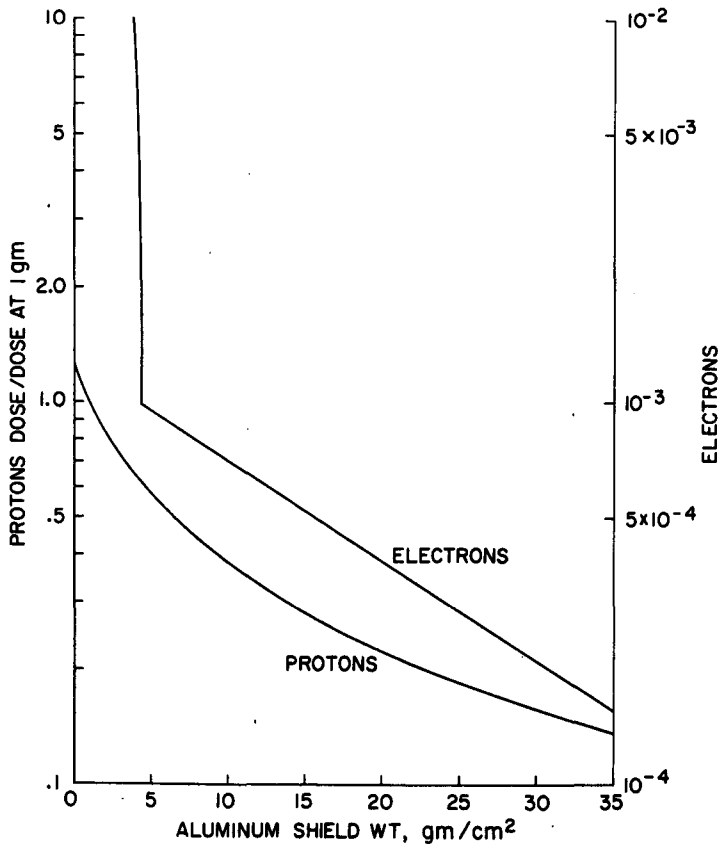


Figure E-2 Radiation Shield Effectiveness



The results are shown as the "free space" (i.e., unattenuated by trapped radiation) curve in Figure E-3 and are based on the average maximum solar activity defined in Ref. 61. Also shown in the figure are estimated doses as attenuated by the trapped radiation for the three orbit inclinations of interest. These curves were derived by assuming that on the average, from Reference 62, the radiation windows lie within minor circles of approximately 30 degrees radii centered at each geomagnetic pole. The fraction of time, on the average, that the satellite spends outside of these windows was then taken to be the attenuation factor.

The total radiation dose is shown in Figure E-4 for each orbit defined earlier in Table 2-1. The dose is plotted against "structure plus shield weight" since the basic spacecraft structure itself and subsystems act as a radiation shield. This inherent shielding is of minor importance, however, since typical values are only about 2 gm/cm². These results were obtained by employing the data from the figures previously described based on the time-average altitude of each orbit. For Orbit Numbers 1-3, however, (recall that these are very high altitude orbits essentially beyond the Van Allen belts) the total dose is in reality the unattenuated solar proton dose.

Data compiled by MSFC in connection with the ATM mission (circular orbit, 30° inclination, 245 nm) show the following proton dose sensitivities:

<u>Film Type</u>	<u>Tolerable Dose*</u>
3401	10 rads
3400	40

* Based on a fog level of 0.6 net density.

Figure E-3 Solar Proton Dose in Earth Orbit

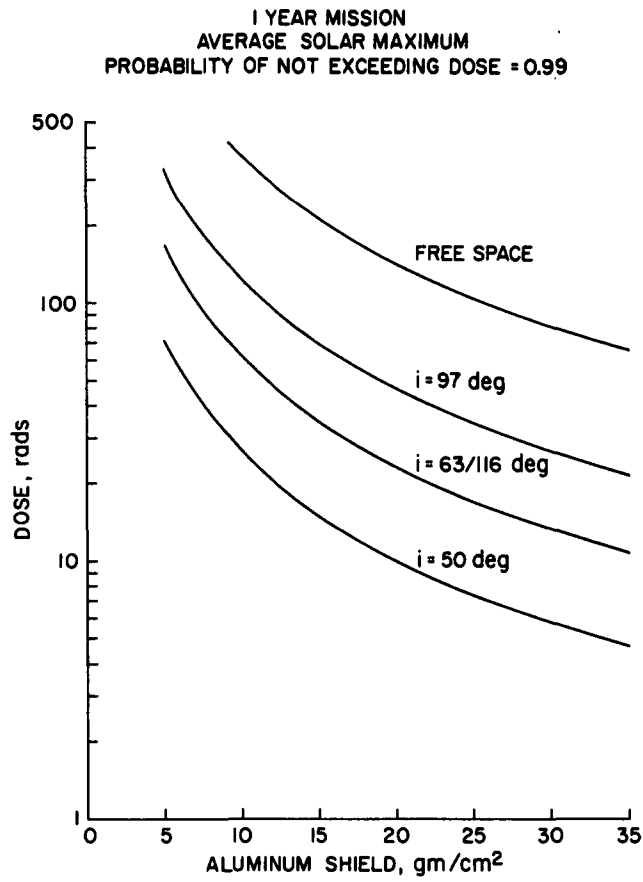
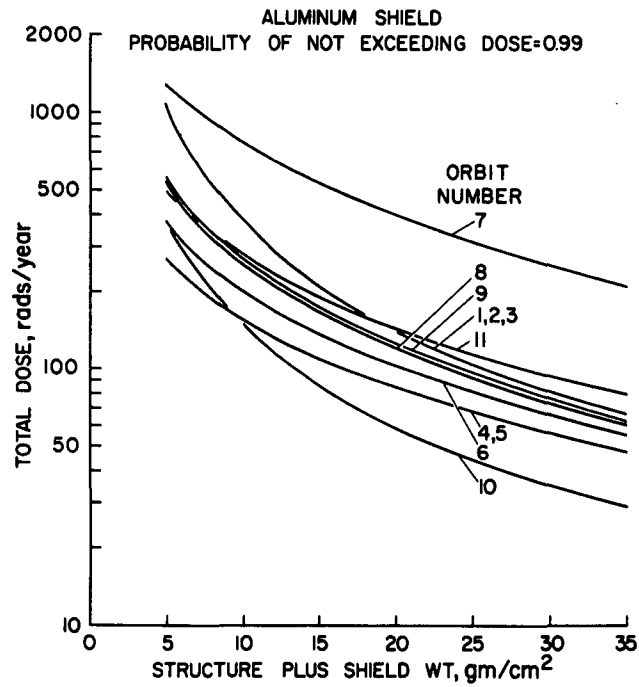


Figure E-4 Total Radiation Dosage



Assuming that film speed is directly related to proton dose sensitivity, type 243 film should tolerate a total dose 6-10 times larger than type 3400 film.

The fog level used for these dose values is probably near the limit for satisfactory performance. Some experts (Ref. 23) cite 0.4 net density as the maximum acceptable fog level.

Appendix F

MODULATION TRANSFER FUNCTION ANALYSIS FOR FILM CAMERA AND TELEVISION

The MTF is a measure of contrast transfer by an imaging system component or the entire system. It is defined as the ratio of the output to the input modulation intensity of a sinusoidal pattern at a given spatial frequency. Thus, a value of 1.0 corresponds to a faithful reproduction of the input pattern and a value of zero represents no signal transfer. A complete system, or each of the components of a system, has a unique MTF. The system modulation transfer is given by the product of the individual component transfers. Thus, for a TV system

$$T_o = T_c T_v T_a T_m T_s$$

where T_o = overall system MTF
 T_c = contrast
 T_v = sensor (includes readout for TV)
 T_a = lens
 T_m = image motion
 T_s = other elements

To visually detect a contrast change in some part of an imaged scene, the overall system transfer, T_o , at the pertinent spatial frequency must equal or exceed the visibility threshold, taken here as 0.04. This figure assumes a signal-to-noise ratio high enough so that performance is contrast limited. Since a spaceborne imaging system generally must record a wide variety of scenes, a conservative contrast value should be used to insure the required minimum system performance level under worst case conditions. Typically, contrasts in the range of 1.3:1 to 2:1 are observed from high altitudes. Consequently, a value of 1.3:1 is used here. Then, the contrast, T_c , is:

$$T_c = \frac{1.3-1}{1.3+1} = 0.13$$

Consequently, assuming the product of the transfer functions of the other elements, T_s , equals one (since these elements can generally be made as good as desired), the product

$$T_v T_a T_m \geq 0.31$$

The value T_v is determined in each case by the image plane resolution required to satisfy the measurement task. Therefore, the transfer function associated with the lens and the image motion must be given by:

$$T_a T_m \geq \frac{0.31}{T_v}$$

or the required image plane resolution cannot be realized.

For a film system, the same considerations apply except that the performance of the readout system and the type of film used must be taken into account as discussed later.

In preliminary mission studies, a useful estimate of the component requirements can be obtained by assuming that each component of the system, except for T_s which is assumed equal to one, contributes equally to the system contrast transfer loss. On this basis, a TV system consists of three components, i.e., the lens, sensor and image motion. Thus, each component of a TV system must have a modulation transfer of at least 0.68 at the spatial frequency required by ground resolution considerations to provide an overall system transfer, T_o , equal to 0.04 for a minimum contrast, T_c , of 0.13. Obviously, equal allocation of loss is not mandatory but if any one element is degraded significantly below the levels indicated, the requirements on the remaining system elements tend to become completely unrealistic except for low resolution systems.

A film camera system consists of four components, i.e., the lens, film, scanner, and image motion. Using an argument similar to that above requires each component of a film system to have a transfer of at least 0.75.

Appendix G

MULTISPECTRAL SCANNER SIGNAL AND NOISE CONSIDERATIONS

The output produced by a scanner when exposed to a scene producing a spectral radiance, N_λ , at the detector is given by

$$S_1 = N_\lambda AB^2 t \epsilon \quad \text{watts}$$

where A is the collector area
 B is the instantaneous field of view (IFOV)
 t is the transmittance of the optical system
 ϵ is the quantum efficiency of the PM tube

The signal caused by a change in the spectral radiance of the scene is given by

$$S_2 = \frac{\Delta \rho}{\rho} S_1$$

where ρ is the reflectance associated with N_λ
and $\Delta \rho$ is the change in reflectance

Detection of the signal, S_2 , requires that the system signal to noise ratio be high enough to permit unambiguous identification of the change. Since the noise in a system of this type (with photomultiplier detectors) is related to the statistical nature of photon emission from the imaged scene, it is useful to convert the energy flow in watts to a photon rate. This can be accomplished by determining the energy per quanta at the wavelength of interest. Thus,

$$E_\lambda = \frac{2 \times 10^{-19}}{\bar{\lambda} (\mu\text{m})} \quad \text{watt sec.}$$

Converting S_1 to a photon rate, we have

$$S_1' = \frac{N_\lambda AB^2 t \epsilon \bar{\lambda}}{2 \times 10^{-19}} \quad \text{Photons/sec}$$

and $S_2' = \frac{\Delta\rho}{\rho} S_1'$

The one sigma (or standard deviation) noise is given by

$$n_s = \frac{1}{t_e} \sqrt{S_1' t_e}$$

where t_e is the effective integrating time in seconds.

For a count rate integrator using resistance and capacitance elements, the effective integrating time,

$$t_e = 2RC = 2\tau$$

Thus, $n_s = \sqrt{S_1'/2\tau}$

and the signal-to-noise ratio,

$$S_n = \frac{S_2'}{n_s} = \frac{\Delta\rho}{\rho} \left[\frac{N_\lambda AB^2 t_e \bar{\lambda} 2\tau}{2 \times 10^{-19}} \right]^{1/2}$$

Appendix H

IR SCANNER/RADIOMETER SIGNAL AND NOISE CONSIDERATIONS

The power flow into a thermal IR scanner or radiometer is given by:

$$P = N_{\lambda} AB^2 t$$

where N_{λ} is the spectral radiance
 A is collector area
 B is instantaneous field of view (IFOV)
and t is the overall transmittance

For a change in temperature (emissivity constant), the change in power flow,

$$\Delta P = \frac{\Delta N_{\lambda}}{N_{\lambda}} P$$

where $\frac{\Delta N_{\lambda}}{N_{\lambda}} \approx \frac{14388}{\lambda T^2} \Delta T$

The noise equivalent power for a photon sensitive thermal detector.

$$NEP = \frac{\sqrt{A_d \Delta f}}{D^*}$$

where Δf = bandwidth
 D^* = detector detectivity
 A_d = detector area

Again, requiring a signal-to-noise (S_n) ratio of 3

$$S_n = \frac{14388 \Delta T N_{\lambda} AB^2 t D^*}{\lambda T^2 \sqrt{A_d \Delta f}} = 3$$

APPENDIX J

FILM CAMERA AND TELEVISION EXPOSURE AND IMAGE MOTION CONSIDERATIONS

Film Camera

The desired density change in the film for low contrast scenes and the available illumination under worst case conditions determine the suitability of film types, lens shutter speed, and image motion compensation characteristics required to properly record those scenes.

Assuming that the integrated proton dose will not exceed 300 rad, the maximum estimated background density on S0-243 film is 0.6. Under these conditions, the film exposure should be adjusted to provide some density increment above 0.6 for scene lowlights. Taking this gross density as 1.0, the relative log exposure required for S0-243 film is 1.35. Since the base absolute log exposure for S0-243 is $\bar{2}.52$ or 3.32×10^{-2} meter candle seconds, the exposure required to achieve a density of 1.0 is 0.74 meter candle seconds.

The luminance available to produce this exposure depends on the solar illumination, the lowlight reflectance and atmospheric losses. For a sun synchronous orbit at noon local time, the lowest solar elevation angle for agricultural observations (3/15 - 11/1) at 40 degrees north latitude is about 40 degrees, providing a solar horizontal plane illumination, I_s , of about 6000 ft. candles. Assuming a lowlight reflectance, R_q , of 2 percent; an atmospheric luminance, B_a , of 680 ft lamberts (40 degrees solar elevation, clear weather, minus blue filter); and an atmospheric transmission, T_a , of 0.7, the luminance at the camera, B_o , is:

$$B_o = I_q R_q T_a + B_a$$

or $B_o = 764$ ft lamberts

With this amount of light available at the camera, the shutter speed, t_e , is expressed as follows:

$$t_e = \frac{E_f^2 F_f}{2.7 B_o T_L}$$

where E is the required exposure (0.74 meter candle sec.)
 f is the lens stop used
 F_f is the filter factor
and T_L is the lens transmittance

Assuming use of a Wratten 12 minus blue filter (500 m μ m cutoff) to reduce haze, the filter factor for S0-243 film is 1.6. For a moderate focal length lens, the transmittance is taken as 0.9. Using these values, and those previously computed.

$$t_e = 6.38 \times 10^{-4} f^2$$

With no image motion compensation (IMC), the aperture stop, f , used must be large enough to provide a shutter speed that restricts smear to tolerable levels. The tolerable image plane motion during exposure for a modulation transfer of 75 percent is 5.5 μ m at 72 lines/mm. The shutter speed, t_2 , limiting the motion to this value is

$$t_2 = \frac{5.5 H}{F V_s} \times 10^{-9}$$

For example, for the first data acquisition system shown in Table 9-2,

$$t_2 = \frac{4.67 \times 10^5 \times 5.5}{7.8} \times 10^{-9}$$

$$= 3.29 \times 10^{-4} \text{ sec,}$$

Since $t_e > t_2$ for any reasonable aperture, IMC is required but since only about 50 percent correction is needed no problem is anticipated.

Based on the considerations outlined, S0-243 film appears to be satisfactory for black and white photography. Additional analyses are required to determine performance when using narrow band filters for multispectral applications.

Television

The exposure time, t_e , is

$$t_e = \frac{4 E_v (f)^2 F_f}{n B_o}$$

where E_v = required energy at RBV (ft. candle sec.)
 f = relative aperture
 F_f = filter factor (3.7 for 500 μm cutoff)
 n = optical efficiency (taken as 0.9)
 B_o = scene luminance at camera (ft. lamberts)

Using the illumination data for film systems, $B_o = 764$ ft. lamberts, and a value of 1×10^{-3} ft. candle sec for E_v ,

$$t_e = 2.16 \times 10^{-5} (f)^2 \text{ sec}$$

The tolerable image plane motion (no IMC) for 75 percent transfer at 31 1/mm is 16.5 μm . Thus, the shutter speed limiting motion to this value is,

$$t_2 = \frac{16.5 H}{F V_s} \times 10^{-9}$$

If a shutter speed slower than this value is required to obtain sufficient energy, then IMC must be employed.

REFERENCES

1. Swenson, B. L.: Orbit Selection Considerations for Earth Resources Observations. NASA TM X-2156, June 1970.
2. Landerback, P. W.: An Analysis of Low Orbital Drag Constraints of Orbit and Sun-Oriented Arrays. 1967 Intersociety Energy Conversion Engineering Conference, Miami Beach, Florida, August 1967.
3. Anon.: Flight Performance Manual for Orbital Operations. Northrop Corporation Norair Division Report NOR.61-208, 1961. (Contract No. NAS8-861)
4. Anon.: Space Planners Guide. U. S. Air Force, 1965.
5. Teeter, R. R., et al: Launch Vehicle Performance File, Battelle Memorial Institute Report BMI-NLVP-DD-70-1, March 1970. (Contract NAS2-2018)
6. Anon.: Launch Vehicle Estimating Factors. Prepared by NASA/OSSA, Code SV, January 1970.
7. Anon.: Titan III - Building Blocks to Space. Martin Marietta Corporation, 1970.
8. Stratton, A. J., et al: Earth Resources Objectives and Measurement Requirements. NASA/OART Mission Analysis Division Working Paper MS 70-1, April 1970.
9. Anon.: General Aviation Operating Costs. COT-FAA, February 1969.
10. Anon.: Business and Commercial Aviation. Volume 26, No. 4, April 1969.
11. Anon.: Enroute High Altitude U. S. Airway Maps. H-1, H-2, H-3, H-4;
12. Anon.: DMS World Aircraft Forecast 1969-1978.
13. Anon.: Enroute IFR Air Traffic Survey - Peak Day 1969. DOT-FAA,
14. Anon.: FAA Air Traffic Activity - FY 1970. DOT-FAA,
15. Anon.: Enroute IFR Peak Day Charts - FY 1970. DOT-FAA
16. Sherr, P., et al: World Wide Cloud Cover Distribution for Use in Computer Simulations. Allied Research Associates, NASA CR-61226, June 1968.

50

17. Brown, S. C.: Simulating the Consequence of Cloud Cover on Earth-Viewing Space Missions. American Meteorological Society, 51, No. 2, 126-131, February 1970.
18. Bertoni, E. A.: Clear Lines-of-sight from Aircraft. AFCRL, Aerospace Instrumentation Laboratory Report 67-0435, AF Survey in Geophysics, No. 196, Project 3624, August 1967.
19. Klopp, D., et al: Imaging Sensor System Scaling Laws. NASA CR-73453, September 1969.
20. Jones, A. C., et al: Remote Sensor Systems for Unmanned Planetary Missions. Space Division, North American Rockwell, Sept. 1970, NASA CR 114371.
21. Elle, B. L., et al: The Lunar Orbiter Photographic System. Journal of the Society of Motion Picture and Television Engineers, Vol. 76, No. 8, August 1967.
22. Bashe, R. and Schwartz, I: Planetary Film Reconnaissance System. NASA CR-1358, June 1969.
23. Brock, G. C., et al: Photographic Considerations for Aerospace. Itek Corporation, 1966.
24. Biberman, L. M. and Nudelman, S.: Photoelectronic Imaging Devices. Volume 2, Plenum Press, New York, 1971.
25. Wong, K. W.: Geometric Calibration of Television Systems for Photogrammetric Applications. American Society of Photogrammetry Annual Meeting, March 10-15, 1968.
26. Gunter, W. D., Grant, G. R., and Shaw, S. A.: Optical Devices to Increase Photocathode Quantum Efficiency. Applied Optics 9, 251, February 1970.
27. Sonnenberg, H.: InAsP-Cs₂O a High Efficiency Infrared Photocathode. Applied Phys. Letter 16, pp 355-357, November 1968.
28. Remote Multispectral Sensing in Agriculture. Res. Bulletin No. 844, Purdue University, Agriculture Exp. Station, Sept. 1968.
29. Dicke, R. H.: The Measurement of Thermal Radiation at Microwave Frequencies. Rev. Sci. Inst. 17, 268-275, 1946.
30. Hiatt, R. and Larson, R. W.: Survey of High Gain, Broadband, Passive Deployable Antennas with Scanning Capabilities for Installation in a Manned Satellite. Memo 6734-502-M, University of Michigan, 1964.

31. Matthei, W. G.: Recent Developments in Solid State Microwave Devices. Tech Report ECOM-2676, U. S. Army Electronics Command, Fort Monmouth, New Jersey, 1966.
32. Pascalar, H. G.: Microwave Radiometric Instrumentation for Remote Sensing Applications. Aerojet General Corp.
33. Underwood, T. C.: Manned Spaceflight Network Telemetry System. ITC Proceedings, Vol. 6, 1970, pp 502-527.
34. Gurk, H., et al: Ground Data Handling System Study for the Earth Resources Observation Satellite. AED R-3537, January 27, 1970.
35. Anon.: Communications Systems Performance and Coverage Analysis for Apollo II (G Type Mission). Vol. IV, MSC Internal Note No. E13-12-R-09-7, June 26, 1969.
36. Spearing, R. E.: Manned Spaceflight Network Unified S-Band System 1970. ITC Proc. Vol. 6, 1970, pp 491-501.
37. Anon.: Manned Space Flight Network, Network User's Guide. MSFN No. 101.1, July 1970.
38. Anon.: Frequency Allocations 10 KC/S-90Gc/S. RCA Frequency Bureau, RCA, September 1, 1969.
39. Polson, J. H. and Kerrigan, M.: Report on a 400 Megabit/second Digital Modem. IEEE International Conference on Communications, June 1969, pp 29/1-14.
40. Anon.: Study of Efficient Transmission and Reception of Image-Type Data Using Millimeter Waves. Philco TR-DA 2180, March 1970.
41. Anon.: GSFC Mark 1 Tracking and Data Relay Satellite (TDRS) System Concept, Phase A Study Final Report, November 1969.
42. Barritt, P. F. and Habib, E. J.: Tracking and Data Relay Satellite System: An Overview. AIAA Paper No. 70-1305, October 1970.
43. Vammen, C. M. and McCormick, F. L.: ATS-5 Millimeter Wave Propagation Experiment. IEEE Transaction AES-6, November 1970, pp 825-831.
44. Getsinger, W. J.: Paramps Beyond X-band. Microwave Journal, November 1970, pp 49-55.
45. Ippolito, Louis J.: Effects of Precipitation on 15.3 and 31.65 GHz Earth Space Transmissions with the ATS-V Satellite. IEEE Proceedings, February 1971, pp 189-205.

46. Pratt, William K.: Laser Communications Systems. John Wiley & Sons, 1969.
47. Melchior, Hans, et al: Photodetectors for Optical Communications Systems. IEEE Proceedings, October 1970, pp 1466-1486.
48. Paoli, Thomas L., Ripper, Jose E.: Direct Modulation of Semiconductor Lasers. IEEE Proceedings, October 1970, pp 1457-65.
49. Ross, Monte: Jupiter Calling. Laser Focus, October 1969, pp 32-38.
50. Anon.: Deep Space Communications and Navigation Study. Bell Telephone Laboratories Final Report, Vol. 3, May 1968, p 32.
51. Arams, F. R.: Infrared 10.6-Micron Heterodyne Detection with Gigahertz IF Capability. IEEE J. Quantum Electronics, November 1967, pp 484-492.
52. McElroy, John H.: Carbon Dioxide Laser Systems for Space Communications. IEEE International Conference on Communications, Proceedings Vol 1, 1970, pp 22.27-22.36.
53. Edsinger, L. E.: Parametric Sizing of Unmanned Spacecraft. NASA/OART Mission Analysis Division Working Paper MS 70-3, April 1970.
54. Mumbower, Leonard E.: Ground Data Processing Considerations for Earth Resource Information. The Princeton University Conference on Aerospace Methods for Revealing and Evaluating Earth Resources, June 1970.
55. Vachon, R. I., et al: User Network for Information Storage, Transfer, Acquisition and Retrieval. NASA-Auburn-ASEE Summer Faculty Fellowship Program in Engineering Systems Design, NASA CR-61333, October 1970 (Contract No. NGT 01-003-044).
56. Lorsch, Harold G.: Agricultural Resource Information Requirements of Nongovernmental Users. The Princeton University Conference on Aerospace Methods for Revealing and Evaluating Earth Resources, June 1970.
57. Thompson, Morris M., et al: Manual of Photogrammetry. Vol. 2, American Society of Photogrammetry, 1966.
58. Doyle, F. J.: Mapping of the Land from Space. Vol. 23, Advances in the Astronautical Sciences, 1968.

59. Parametric Study of Logistics-Type Entry Vehicles, Volume III - Parametric Data and Discussions, Book 1; Douglas Aircraft Company Missile and Space Systems Division Report No. SM-48785, September 1965, Contract NAS2-2461.
60. Second Symposium on Protection Against Radiations in Space. NASA SP-71, October 1964.
61. Snyder, J. W.: Radiation Hazard to Man from Solar Proton Events. Journal of Spacecraft and Rockets, Vol. 4, No. 6, June 1967.
62. Space Station Definition Study, Volume II Mission Analysis. McDonnell Douglas Astronautics Company Report MDCG0605, July 1970, Contract NAS8-25140.